MODULATION OF THE CYCLOOXYGENASE BRANCH OF THE ARACHIDONIC ACID CASCADE BY POLYPHENOLS

Dissertation

to obtain the academic degree

Doctor rerum naturalium

(Dr. rer. nat.)

Faculty of Mathematics and Natural Sciences

of the

Bergische Universität Wuppertal

by

Ina Willenberg

Minden

- 2015 -

Die Dissertation kann wie folgt zitiert werden:

urn:nbn:de:hbz:468-20150724-111634-7
[http://nbn-resolving.de/urn/resolver.pl?urn=urn%3Anbn%3Ade%3Ahbz%3A468-20150724-111634-7]

Erster Gutachter: ..... PD Dr. Nils Helge Schebb

Zweiter Gutachter: ..... Prof. Dr. Pablo Steinberg

Tag der mündlichen Prüfung: ..... _____. _____. 2015

Tag der Promotion: ..... _____. _____. 2015

Für meine Eltern

Table of Contents

Chapter 1

Introduction and Scope

1.1 Introduction

A diet rich in fruits and vegetables is associated with a long healthy life. Epidemiological data suggest that the dietary intake of fruits and vegetables has beneficial effects on a variety of diseases, such as different types of cancer, cardiovascular diseases, diabetes and the prevention of osteoporosis [1-4]. A large number of studies suggest that these protective effects are elicited by polyphenols present in fruits and vegetables [1-3].

Polyphenols are naturally occurring phytochemicals found in plant-based food, such as fruits, vegetables, legumes, whole grains, tea, coffee, wine and nuts and several thousand different polyphenolic compounds have been identified [2]. Based on their chemical structure polyphenols can be classified in phenolic acids (e. g. hydroxybenzoic or hydroxycinnamic acids), flavonoids, stilbenes, chalcones and lignanes [5]. Flavonoids are characterized by a 2-phenylchromane basic structure. Depending on the degree of oxidation of the carbon atom at position C-2, -3 and -4, flavonoids are further divided in different subgroups: flavanols, anthocyanidines, flavanones, flavons, flavonols and isoflavones [6]. Stilbenes are characterized by an ethylene group substituted with two phenyl groups [5]. One stilbene derivate and exemplary chemical structures of flavonoids are shown in Fig. 1.1.

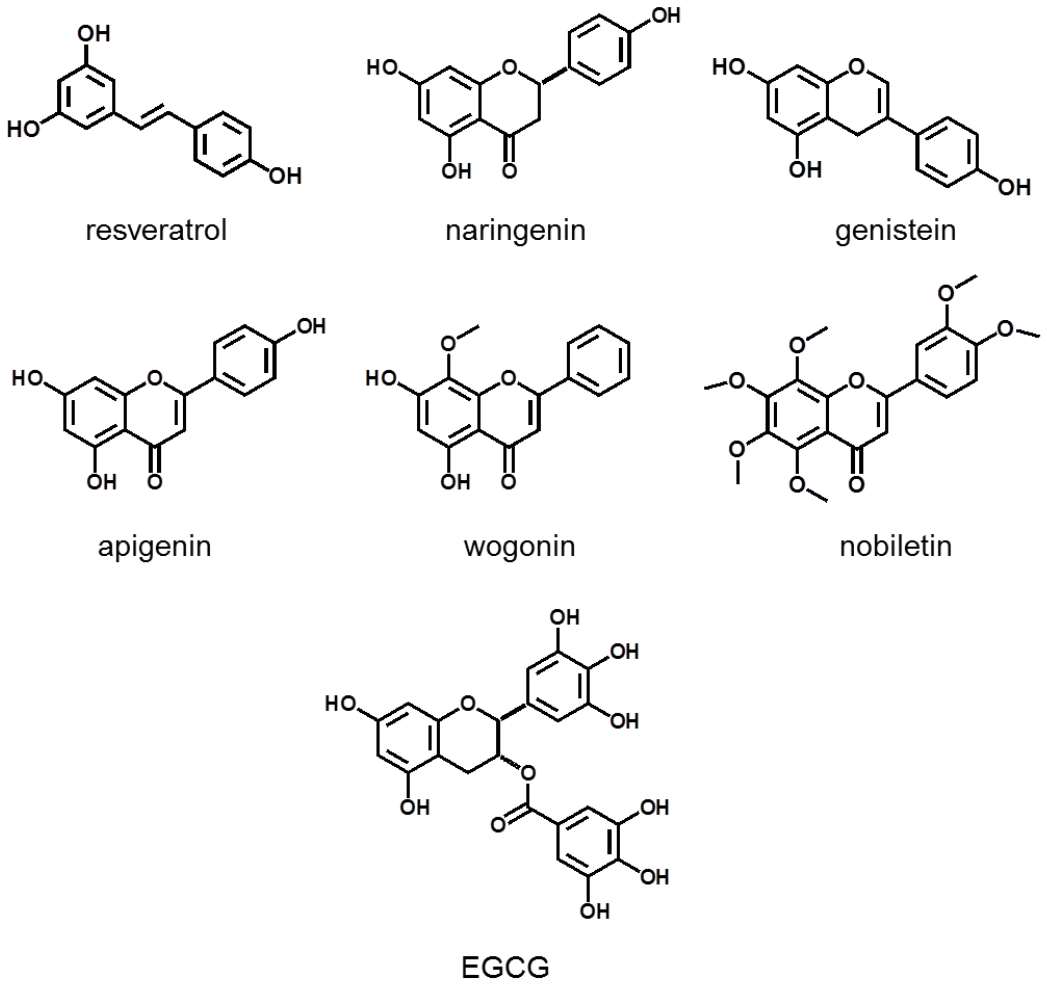

Fig. 1.1: Chemical structures of selected compounds investigated in this thesis. For the structures of the resveratrol oligomers please refer to Fig. 2.1.

Dietary sources of the most extensively studied stilbene resveratrol are grapes, berries, peanuts and red wine. The average concentration of *trans*-resveratrol in red wine is reported to be 1.9 mg/L, ranging from non-detectable levels to 14.3 mg/L [7]. In addition to the monomer, grapes and their products contain resveratrol oligomers, e. g. the dimer ε-viniferin or the tetramer hopeaphenol with concentrations up to 1.2 or 3.8 mg/L in red wines from North Africa [8].

Main sources of the isoflavone and phytoestrogen genistein are soybeans (442 mg/kg) and soy-products, e. g. soymilk (18 mg/kg) [5]. Epigallocatechingallat (EGCG) is the gallic acid ester of the flavan-3-ol

epigallocatechin and can be found in the leaves of *Camellia sinensis* [5]. The concentration of EGCG in tea ranges between 3 and 48 mg/ 100 mL for black tea infusions and between 5 and 190 mg/ 100 mL for green tea infusions, respectively [9]. In plants, flavones and flavonols are mainly found as glycosides [10]. Apiin is the glycosylated form of the flavon apigenin occurring in parsley and celery [11, 12]. After hydrolysis, concentrations between < 1 and 191 µg/g fresh weight are reported for the aglycone apigenin (flavone) in celery [11]. The flavanone naringenin and its glycoside naringin can be found in citrus fruits [5]. Grapefruit juice contains 4.8 to 120 mg/ 100 mL naringin and < 0.2 to 15.8 mg/ 100 mL of the aglycone [13], whereas the concentration in orange juice is considerably lower and ranges between 0.01 and 0.3 mg/ 100 g for naringin and between 0.1 and 0.17 mg/ 100 g for naringenin [14]. Nobiletin is a polymethoxylated flavon present in citrus peel [15]. Large amounts of peel are byproducts of juice productions and affords are made to process the peel to polyphenol-rich products [15]. Molasses are intermediate products of this process with a nobiletin concentration range of between 2200 and 71100 mg/ 100 mL [15]. Several other polyphenols only occur in medical plants, for example wogonin, a monomethoxylated flavone, found in the root of *Scutellaria baicalensis* Georgi. The dried root is widely used in traditional Chinese medicine to treat liver diseases (jaundice), as well as hyperlipidemia, atherosclerosis and inflammatory diseases [16].

A large number of studies report a variety of biological actions elicited by these polyphenols including cardioprotective effects, anti-inflammatory actions and cancer preventive effects [3, 15-21].

A compound can only elicit a biological effect if it reaches the target cell or tissue in a sufficiently high concentration. Thus, the bioavailability plays a major role regarding the potential health effects of the dietary intake of polyphenols. In addition to distribution and excretion, the intestinal absorption and metabolic processes determine the systemically available amount of each polyphenol after the ingestion of polyphenol containing food [22]. Although there are exceptions

for some glycosides, polyphenols are in general believed to be only intestinally absorbed as aglycones [22, 23]. Therefore, glycosylated compounds have to be hydrolyzed by intestinal enzymes or colonic microflora prior to absorption [22]. Once absorbed, the polyphenols are metabolized by intestinal or liver phase II enzymes: Common conjugation reactions include methylation, sulfonation, and glucuronidation [22]. Despite an extensive metabolism upon absorption, polyphenol plasma concentrations in the µM range were detected after ingestion of polyphenolic compounds. Consumption of a black tea infusion containing 80-105 mg of EGCG resulted in maximal plasma concentrations of 0.13-0.33 µM [24]. The bioavailability of flavanones and isoflavones seems to be better: The ingestion of grapefruit juice (199 mg total naringenin, sum of free and conjugated form) resulted in a plasma peak level of 6 µM for the flavanone after conjugate cleavage [25]. After consumption of a single soy meal containing 3.6 µmol total genistein/kg bodyweight, maximal plasma concentrations of 4 µM after conjugate cleavage were observed 8 h after the meal [26]. However, due to extensive metabolic processes the majority of the bioavailable polyphenol is present in its metabolized form, dominantly as O-glucuronides [27]. Information about the biological activity of most metabolites is scarce and it cannot be assumed that it has the same biological activity as the parent compound [27]. Therefore, absorption and metabolism may be a limiting factor for the polyphenols to elicit their biological effects. Thus, the potency *in vitro* cannot be easily translated to the *in vivo* situation [27].

Several modes of action have been described for the anti-inflammatory effects of polyphenols: antioxidative and radical scavenging properties, a modulation of the gene expression of pro-inflammatory mediators and a modulation of the activity of enzymes of the arachidonic acid (AA) cascade [28]. The AA cascade comprises the formation of a multitude of biologically active lipid mediators, also referred to as oxylipins, from AA and other polyunsaturated fatty acids (PUFAs). Fig. 1.2 gives a simplified overview of the enzymatic and autoxidation pathways of the AA cascade and highlights selected metabolites and their physiological actions.

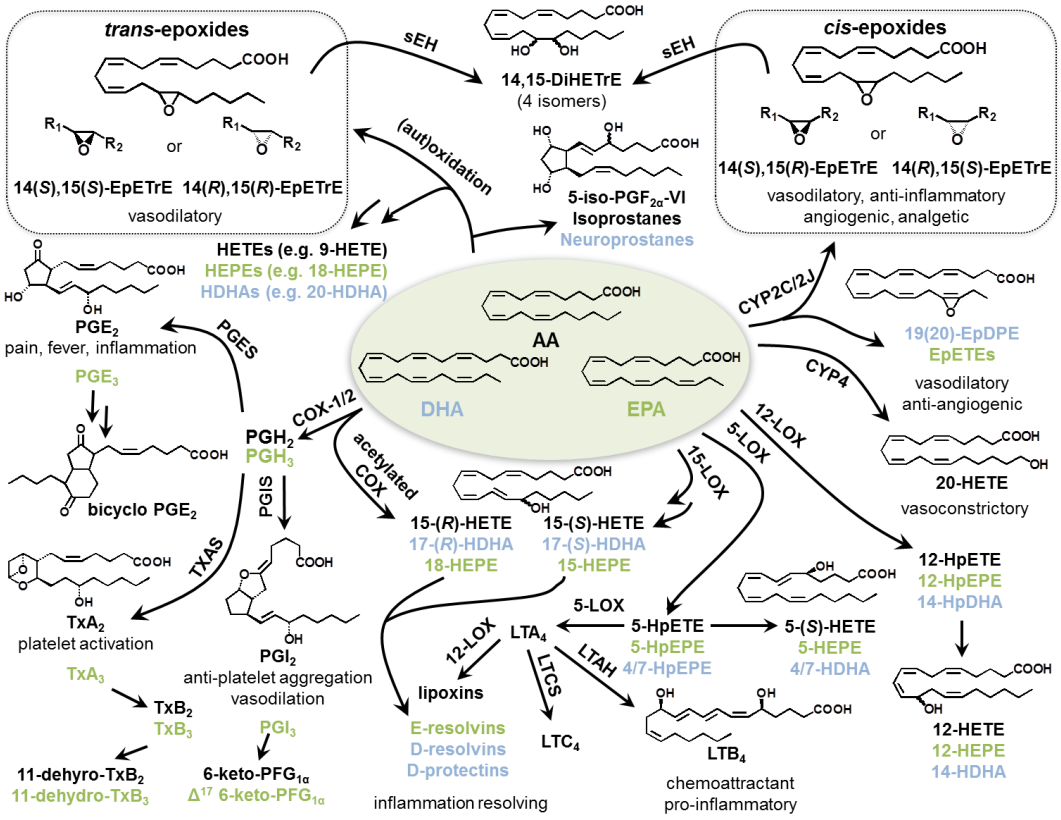

Fig. 1.2: Overview of the AA cascade. It should be noted that only few products are shown of the complex oxylipin pattern and the biological effects are summarized in a simplified fashion.

The enzymatically formation of oxylipins in the AA cascade can be divided into three pathways: the cyclooxygenase (COX), the lipoxygenase (LOX) and the cytochrome-P-450 (CYP) branch [29]. Conversion of AA by COXs results in the formation of PGH_2 which is subsequently processed by different prostaglandin synthases or thromboxane A synthase (TXAS) [29]. Prostaglandin-E-synthase (PGES) yields PGE_2, a lipid mediator with a multitude of physiological actions, such as the mediation of pain, fever and inflammation (Fig. 1.2) [30]. PGI_2, formed by prostacyclin synthase (PGIS), acts vasodilatory and inhibits platelet aggregation and is therefore an important regulator of vascular homeostasis and thrombosis [30]. Conversion of PGH_2 by prostaglandin D synthase gives rise to PGD_2, a bronchoconstrictor [31]. Prostaglandin F synthase catalyzes the reaction of PGH_2 to $PGF_{2\alpha}$ which plays, among others, a role in luteolysis, ovarian function, acute and chronic inflammation and cardiovascular diseases

[32, 33]. TxA_2 formed by TXAS is the main COX product of platelets and acts platelet aggregating and as a vasoconstrictor [30]. The fate of the initially formed PGH_2 depends on the enzymatic environment at the side of formation. COXs exist in different isoforms: COX-1 is a constitutively expressed isoform involved in the maintenance of physiological homeostasis, such as stomach acidity control and renal function [29]. The expression of COX-2 is inducible and increased in response to inflammatory mediators, such as the cytokines IL-1α/β or TNF-α [34].

Conversion of AA or other PUFAs by 5-,12- or 15-LOXs results in the formation of hydroperoxides, e. g. 5-HpETE, 12-HpETE and 15-HpETE, which can be reduced to the corresponding hydroxy-FAs (5-HETE, 12-HETE, 15-HETE) [35]. The 5-LOX product LTA_4 is a precursor for the formation of the chemoattractant LTB_4, anti-inflammatory lipoxins or cysteinyl-leukotriens (e. g. LTC_4) which are potent contractors of airway smooth muscles and increased during acute asthma and rhinitis (Fig. 1.2) [35, 36]. Conversion of eicosapentaenoic acid (EPA) by acetylated COX-2 or CYP gives rise to 18-HEPE [37]. 15-LOX forms 17-HDHA from docosahexaenoic acid (DHA) [37]. These and other hydroxy-FAs can be further converted to a series of multiple hydroxylated FAs called resolvins and protectins which are believed to take part in the resolution of inflammation [37].

The third branch of the AA cascade includes the oxidation of PUFAs by CYPs. A product of the ω-hydroxylation by members of the CYP4 family is the vasoconstrictor 20-HETE [38]. R,S- and S,R-epoxy-FAs formed by members of the CYP2J and CYP2C families possess vasodilatory, anti-inflammatory and analgetic properties and are hydrolysed by the soluble epoxide hydrolase (sEH) to the corresponding dihydroxy-FAs [39, 40].

Products of autoxidative processes are hydroperoxy-FAs which react further to hydroxy-FAs, isoprostanes and *R,R*- and *S,S*-epoxy-FAs among other products (Fig. 1.2) [41-43]. In contrast to the enzymatic oxidation which is stereoselective, autoxidative products are formed in racemic mixtures.

1.2 Aim and Scope

The central role in the physiological regulation of inflammation, blood pressure, coagulation, and pain makes the enzymes of the AA cascade a major target of pharmaceuticals [29]. COX-2 is the target of non-steroidal anti-inflammatory drugs (NSAIDs) and COX-2 selective inhibitors [30]. A large number of studies indicate that polyphenols also inhibit COX and influence the endogenous PG formation *in vitro* and it is suggested that some polyphenols mediate their anti-inflammatory effects – in part – via this mechanism [21, 28, 44]. The differences between the *in vitro* test systems used make it hard to compare the efficacies of polyphenols obtained in the different studies. Most of these studies lack the direct comparison of the COX-2 inhibitory potency of the polyphenols with a well characterized COX-2 inhibitor. Therefore, it is difficult to estimate the biological relevance of the observed effects. Moreover, the *in vitro* potency of polyphenols cannot easily be transferred to the *in vivo* situation [27]. Thus, the relevance of *in vitro* activities has to be tested *in vivo*. Regarding the bioavailability of polyphenols, it is important to further improve the knowledge about absorption and metabolism. This may help to evaluate the *in vivo* relevance and to identify metabolites which may contribute to the biological action of the parent compound.

Most studies investigating the biological actions of polyphenols present in grapes and wine mainly focus on resveratrol. Recent studies additionally included resveratrol oligomers, such as the dimer ε-viniferin and the tetramer hopeaphenol. These studies demonstrated that both oligomers act antioxidative and anti-inflammatory [19, 45, 46] and inhibit the growth of tumor cell lines [18, 47, 48]. If the dietary intake of these compounds can elicit these actions, depends on their bioavailability. No information about the intestinal absorption and metabolism of resveratrol oligomers was available. Therefore, *Chapter 2 and 3* address these questions. In *Chapter 2* a rapid LC-UV method for the quantification of resveratrol and its oligomers ε-viniferin, hopeaphenol, r2-viniferin and r-viniferin has been developed. This method was used as read-

out for the investigation of the chemical and metabolic stability of these compounds. Glucuronidation is a major metabolic pathway for resveratrol and many other polyphenols [22]. The metabolic stability of ε-viniferin and hopeaphenol towards glucuronidation was studied and compared to that of resveratrol (*Chapter 2*). *Chapter 3* aimed to investigate the intestinal absorption of ε-viniferin and hopeaphenol. The Caco-2 model, which is a commonly applied model to study intestinal absorption *in vitro*, was used to test if the oligomers can pass the intestinal gut barrier in a similar manner as resveratrol.

Reliable analytical tools for the quantification of oxylipins in biological matrices are needed to elucidate if the dietary intake of polyphenols results in changes of oxylipin levels. Liquid-chromatography coupled to mass-spectrometry (LC-MS) is today's most frequently used approach for the quantification of oxylipins. In addition to the instrumental analysis, sample preparation is an important parameter for the reliable quantification of oxylipins. *Chapter 4* highlights the challenges of LC-MS based targeted metabolomics of the AA cascade, including new information about the effects of sample preparation on the oxylipin pattern.

Oxylipins regulate several physiological processes and are known to be involved in the onset and progression of different diseases. PGs for example are elevated during inflammation and play, among others, a role in the pathogenesis of cancer, inflammatory bowel disease, sepsis and cardiovascular diseases [49-51]. A comprehensive analysis of oxylipins in animal models of diseases may help to better understand their role in health and disease and to identify potential drug targets. Although a large number of oxylipins are formed and there is a crosstalk between the different branches of the AA cascade [52, 53], current studies investigating the role of oxylipins in animal models focus only on single analytes or pathways of the AA cascade. Moreover, if animal models are used to study effects of polyphenols on the activity of enzymes of the AA cascade, it has to be ensured that the selected model is characterized by changes in the oxylipin pattern. Accordingly, a model which aims to study

effects on COX-2 has to be characterized by increased PG levels. Otherwise, an inhibitory potential cannot be detected. For these reasons *Chapter 5 and 6* apply a targeted metabolomics approach (*Chapter 4)* to give comprehensive insights in oxylipin levels during different animal models of inflammatory diseases. *Chapter 5* characterizes the time course of systemic lipid mediator levels during the development of chronic colitis in the DSS rat model. Moreover, changes in plasma and colonic tissue oxylipin levels were correlated with classical clinical and histopathological endpoints of inflammation. In *Chapter 6* two commonly used murine models of sepsis, the lipopolysaccharide (LPS) induced sepsis model and the cecal ligation and puncture (CLP) model, were comprehensively characterized and compared regarding their plasma and tissue oxylipin levels.

Rapid analysis with an automated sample preparation is preferable for the investigation of the activity of single enzymes of the AA cascade. *Chapter 7* presents the development and characterization of a fast online-solid phase extraction-LC-MS method for the quantification of the COX products (TxB_2, PGE_2, and PGD_2). This method was applied as read-out for three different *in vitro* test systems for the determination of COX-2 inhibitory effects. These test systems comprise an enzyme assay, the constitutively COX-2 expressing human cancer cell line HCA-7 and primary human monocytes stimulated with LPS. The COX-2 modulating drugs, celecoxib, indomethacin and dexamethasone, were used to characterize the assays.

A large number of studies suggest a COX-2 inhibitory effect of polyphenols [20, 21, 28]. Most of the studies were carried out in different *in vitro* test systems, making a comparison of compounds difficult. Moreover, most of the studies did not include a known COX-2 inhibitor as positive control, further complicating the evaluation of the potency of the observed effects. In *Chapter 8* the COX-2 inhibitory effects of a small library of polyphenols, including potent COX-2 modulating polyphenols described so far as well as hopeaphenol and ε-viniferin, were studied for their effects on COX-2. The polyphenols were tested in a tiered

approach starting from a cell free enzyme assay to cellular systems. In all steps, the potency was directly compared with pharmaceuticals. Finally, the *in vivo* relevance was studied for the most potent polyphenols. LPS-induced murine sepsis was chosen as *in vivo* model of inflammation because among the inflammation models tested (*Chapter 5 and 6*), the increase in PG levels was most pronounced in this model.

General conclusions, future perspectives and limitations of the presented studies are discussed in *Chapter 9*.

1.3 References

[1] Arts I. C. W., Hollman P. C. H. *Am J Clin Nutr* (2005) 81, 317S-325S

[2] Bahadoran Z., Mirmiran P., Azizi F. *J diabetes Metab Disord* (2013) 12, 43

[3] Nijveldt R. J., van Nood E., van Hoorn D. E. C., Boelens P. G., van Norren K., van Leeuwen P. A. M. *Am J Clin Nutr* (2001) 74, 418-425

[4] Riboli E., Norat T. *Am J Clin Nutr* (2003) 78, 559S-569S

[5] Belitz H. D., Grosch W., Schieberle P. Lehrbuch der Lebensmittelchemie (2008). Springer-Verlag, Heidelberg

[6] Habermehl G., Hammann P. E., Krebs H. C., Ternes W. Naturstoffchemie (2008). Springer-Verlag, Heidelberg

[7] Stervbo U., Vang O., Bonnesen C. *Food Chem* (2007) 101, 449-457

[8] Guebailia H. A., Chira K., Richard T., Mabrouk T., Furiga A., Vitrac X., Monti J.-P., Delaunay J.-C., Mérillon J.-M. *J Agr Food Chem* (2006) 54, 9559-9564

[9] Bronner W. E., Beecher G. R. *J Chromatogr A* (1998) 805, 137-142

[10] Hollman P. C. H., Arts I. C. W. *J Sci Food Agr* (2000) 80, 1081-1093

[11] Crozier A., Lean M. E. J., McDonald M. S., Black C. *J Agr Food Chem* (1997) 45, 590-595

[12] Nielsen S. E., Young J. F., Daneshvar B., Lauridsen S. T., Knuthsen P., Sandström B., Dragsted L. O. *Br J Nutr* (1999) 81, 447-455

[13] Ho P. C., Saville D. J., Coville P. F., Wanwimolruk S. *Pharm Acta Helv* (2000) 74, 379-385

[14] Cerqueira e Silva L. C. R., David J. M., Borges R. S. Q., Ferreira S. L., David J. P., Reis P. S., Bruns R. E. *J Anal Methods Chem* (2014) 2014, 5

[15] Manthey J. A., Grohmann K. *J Agr Food Chem* (2001) 49, 3268-3273

[16] Tai M. C., Tsang S. Y., Chang L. Y. F., Xue H. *CNS Drug Rev* (2005) 11, 141-150

[17] Aggarwal B. B., Bhardwaj A., Aggarwal R. S., Seeram N. P., Shishodia S., Takada Y. *Anticancer Res* (2004) 24, 2783-2840

[18] Empl M. T., Macke S., Winterhalter P., Puff C., Lapp S., Stoica G., Baumgärtner W., Steinberg P. *Vet Comp Oncol* (2014) 12, 149-159

[19] Ha D. T., Kim H., Thuong P. T., Ngoc T. M., Lee I., Hung N. D., Bae K. *J Ethnopharmacol* (2009) 125, 304-309

[20] Murakami A., Ohigashi H. *Int J Cancer* (2007) 121, 2357-2363

[21] Pan M.-H., Lai C.-S., Ho C.-T. *Food Funct* (2010) 1, 15-31

[22] Manach C., Scalbert A., Morand C., Remesy C., Jimenez L. *Am J Clin Nutr* (2004) 79, 727-747

[23] Hollman P. C., de Vries J. H., van Leeuwen S. D., Mengelers M. J., Katan M. B. *Am J Clin Nutr* (1995) 62, 1276-1282

[24] Scalbert A., Williamson G. *Am J Clin Nutr* (2000) 130, 2073S-2085S

[25] Erlund I., Meririnne E., Alfthan G., Aro A. *J Nutr* (2001) 131, 235-241

[26] King R. A., Bursill D. B. *Am J Clin Nutr* (1998) 67, 867-872

[27] González R., Ballester I., López-Posadas R., Suárez M. D., Zarzuelo A., Martínez-Augustin O., Medina F. S. D. *Crit Rev Food Sci Nutr* (2011) 51, 331-362

[28] Garcia-Lafuente A., Guillamon E., Villares A., Rostagno M. A., Martinez J. A. *Inflamm Res* (2009) 58, 537-552

[29] Buczynski M. W., Dumlao D. S., Dennis E. A. *J Lipid Res* (2009) 50, 1015-1038

[30] Simmons D. L., Botting R. M., Hla T. *Pharmacol Rev* (2004) 56, 387-437

[31] Hardy C. C., Robinson C., Tattersfield A. E., Holgate S. T. *N Engl J Med* (1984) 311, 209-213

[32] Basu S. *Med Res Rev* (2007) 27, 435-468

[33] Samuelsson B., Goldyne M., Granstrom E., Hamberg M., Hammarstrom S., Malmsten C. *Annu Rev Biochem* (1978) 47, 997-1029

[34] Morita I. *Prostag Oth Lipid M* (2002) 68-69, 165-175

[35] Haeggström J. Z., Funk C. D. *Chem Rev* (2011) 111, 5866-5898

[36] Holgate S. T., Polosa R. *Nat Rev Immunol* (2008) 8, 218-230

[37] Serhan C. N., Petasis N. A. *Chem Rev* (2011) 111, 5922-5943

[38] Kroetz D. L., Xu F. *Annu Rev Pharmacol Toxicol* (2005) 45, 413-438

[39] Imig J. D. *Physiol Rev* (2012) 92, 101-130

[40] Morisseau C., Inceoglu B., Schmelzer K., Tsai H.-J., Jinks S. L., Hegedus C. M., Hammock B. D. *J Lipid Res* (2010) 51, 3481-3490

[41] Milne G. L., Musiek E. S., Morrow J. D. *Biomarkers* (2005) 10, 10-23

[42] Nakamura T., Bratton D. L., Murphy R. C. *J Mass Spectrom* (1997) 32, 888-896

[43] Yin H., Brooks J. D., Gao L., Porter N. A., Morrow J. D. *J Biol Chem* (2007) 282, 29890-29901

[44] González-Gallego J., García-Mediavilla M. V., Sánchez-Campos S., Tunón M. J. *Br J Nutr* (2010) 104, S15-S27

[45] He S., Lu Y., Jiang L., Wu B., Zhang F., Pan Y. *J Sep Sci* (2009) 32, 2339-2345

[46] Huang K.-S., Lin M., Cheng G.-F. *Phytochemistry* (2001) 58, 357-362

[47] Kang J. H., Park Y. H., Choi S. W., Yang E. K., Lee W. J. *Exp Mol Med* (2003) 35, 467-474

[48] Kim H., Chang E., Bae S., Shim S., Park H., Rhee C., Park J., Choi S. *Arch Pharm Res* (2002) 25, 293-299

[49] Cohen J. *Nature* (2002) 420, 885-891

[50] Ricciotti E., Fitzgerald G. A. *Arterioscler Thromb Casc Biol* (2011) 31, 986-1000

[51] Stenson W. F. *Scand J Gastroenterol Suppl* (1990) 25, 13-18

[52] Meirer K., Steinhilber D., Proschak E. *Basic Clin Pharmacol Toxicol*

(2013) 114, 83-91

[53] Peri K. G., Varma D. R., Chemtob S. *FEBS Letters* (1997) 416, 269-272

Chapter 2

Development of a Rapid LC-UV Method for the Investigation of Chemical and Metabolic Stability of Resveratrol Oligomers *

Resveratrol, piceatannol, ε-viniferin, r-viniferin, r2-viniferin and hopeaphenol are naturally occurring polyphenols, associated with potentially beneficial health effects. We developed a rapid LC–UV-method allowing the simultaneous determination of these six compounds in biological samples in less than 2.5 minutes with standard LC equipment. Utilizing this method for the assessment of the stability of the six analytes, we demonstrated that all stilbene polyphenols disappear rapidly in Dulbecco's Modified Eagle Medium (half life piceatannol: 0.4 h, resveratrol: 1 h). By contrast the tetramer hopeaphenol was stable over the maximum incubation time of 72 hours. In incubations with liver microsomes, ε-viniferin was rapidly glucuronidated, although to a lower extent than resveratrol. Hopeaphenol was not glucuronidated at all. Given that glucuronidation is the major metabolic pathway for polyphenols, hopeaphenol might exhibit significantly different pharmacokinetic properties than other polyphenols. Taking together chemical and metabolic stability and biological activity of hopeaphenol, these findings warrants further investigation of this polyphenol.

* Reprinted with permission from Willenberg I., Brauer W., Empl M. T., Schebb N. H. *J Agr Food Chem* (2012) 60 (32), 7844-7850.

Author contributions: IW: Contributed to research design, performed experiments and wrote the manuscript; WB: Performed stability experiments; MTE: Contributed to research design and manuscript writing; NHS: Designed research, performed experiments and wrote the manuscript.

2.1 Introduction

The polyphenols resveratrol (*trans*-3,5,4'-trihydroxystilbene), piceatannol (*trans*-3',4',3,5-tetrahydroxystilbene), ε-viniferin, r-viniferin, r2-viniferin and hopeaphenol are secondary metabolites occurring in grapes and various plant species, especially in the Vitaceae but also in the Dipterocarpaceae family [1-3]. The structures of the compounds are depicted in Fig. 2.1.

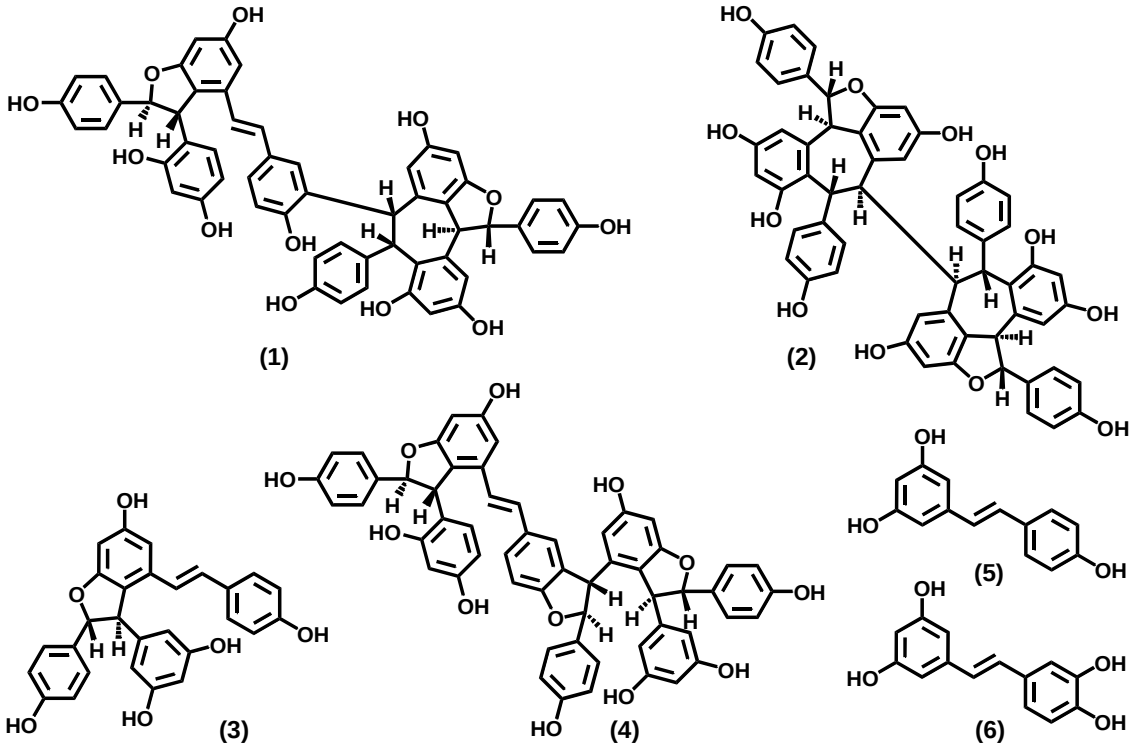

Fig. 2.1: Structures of the analytes: r2-viniferin (**1**), hopeaphenol (**2**), ε-viniferin (**3**), r-viniferin (**4**), *trans*-resveratrol (**5**) and *trans*-piceatannol (**6**). Shown is the conformation as previously reported.

With the exception of r-viniferin and r2-viniferin all of them have been detected in red wine. For example, the mean stilbene polyphenol concentration in different wines from northern Africa was found to be 26 mg/mL, with a mean of 1.7 mg/L resveratrol, 0.2 mg/L ε-viniferin and 1.4 mg/L hopeaphenol [4]. In recent years many studies reported a variety of biological effects exhibited by these substances [5, 6]. In particular resveratrol has been extensively studied and is known to exert antioxidative, cardioprotective and anticarcinogenic

effects [7]. The potential health-promoting effects of piceatannol include antioxidant and cell cycle modulatory activities [8]. Only limited information about the biological activity of the resveratrol oligomers, ε-viniferin, r-viniferin, r2-viniferin and hopeaphenol is available. Few studies report, aside from antioxidant and anti-inflammatory properties, effects on the growth and proliferation of different tumour cell lines (i. e. leukaemia, colon, breast and prostate cancer cells) [2, 5, 6]. Due to their potency to drastically inhibit the growth of human tumor cell lines, the resveratrol oligomers may represent a new class of natural anti-carcinogens [9]. In order to study these biological effects and their underlying molecular mechanisms in more detail, cell culture experiments are indispensable. However, several studies demonstrate that polyphenols, including resveratrol, rapidly degrade under cell culture conditions [10, 11]. Therefore, it is necessary to evaluate the stability of resveratrol oligomers in cell culture medium before biological endpoints can be further investigated using cell culture systems. For the assessment of the chemical stability, analytical methods are needed, allowing the quantitation of resveratrol and its oligomers. Numerous methods are described for the quantitation of resveratrol by liquid chromatography (LC) [12, 13], but only a few methods for the quantitation of resveratrol oligomers have been published [1, 14, 15]. Furthermore, these methods have a limited spectrum with regard to the compounds detected, e. g. none of the methods allows the quantitation of r-viniferin and r2-viniferin. For that reason we developed a rapid LC-UV method for the fast simultaneous quantitation of resveratrol, piceatannol, ε-viniferin, r-viniferin, r2-viniferin and hopeaphenol in biological samples. This method was used to assess the chemical stability of resveratrol and its oligomers in cell culture medium under different conditions. As a second application, we employed the developed method to investigate the metabolic stability of the resveratrol-oligomers towards conjugation with glucuronic acid *in vitro*.

2.2 Experimental

2.2.1 Chemicals and biological materials

Trans-piceatannol (99%) and *trans*-resveratrol (99%) were purchased from Sigma-Aldrich (Schnelldorf, Germany). The dimer ε-viniferin (90%) and the tetramer hopeaphenol (95%) were obtained from Actichem SA (Montauban, France). The two other tetramers, namely r-viniferin and r2-viniferin with a purity level of at least 90%, were a kind gift from the laboratory of Dr. Winterhalter of the University of Braunschweig, Germany. The chemical structures of the analytes are displayed in Fig. 2.1. Dulbecco's Modified Eagle Medium (DMEM) was purchased from Biochrom AG (Berlin, Germany) and all other chemicals from Sigma-Aldrich (Schnelldorf, Germany). The ingredients of the DMEM were in accordance with the suggestion of the American Type Culture Collection (ATCC). Microsomes were obtained from BD Biosciences (Woburn, MA, USA). Preparations of pooled human liver microsomes (HLM) from 25 mixed gender donors and pooled rat liver microsomes (RLM) from 150 male Sprague Dawley rats at a concentration of 20 mg protein/mL were used. The activity of the microsomal preparations was characterized by monitoring their ability to conjugate the standard UGT substrate 4-(trifluoromethyl)-umbelliferone (TFMU) as previously described [16]. HLM showed an activity of 56 ± 4 nmol/min/mg and RLM an activity of 71 nmol/min/mg.

2.2.2 LC-UV analysis

LC-UV analysis was performed on an Agilent 1100 system (Waldbronn, Germany). Separation was carried out on a 75 mm x 4.6 mm i.d., 2.7 µm, HALO RP-18 with "fused core" particles. The analytes (injection volume 10 µL) were separated by a binary gradient at a flow rate of 2.0 mL/min of 0.1% acetic acid (HAc) as solvent A and 95/5 acetonitrile (ACN)/water (v/v) acidified with 0.1% HAc as solvent B. The following gradient was used: 0.0-0.2 min isocratic 30% B, 0.2-1.8 min linear 30-70% B, 1.8-1.9 min linear 70-100% B, 1.9-2.5 min

isocratic 100% B, 2.51 min return to initial conditions of 30% B. The column was reconditioned during the next injection cycle of the autosampler (about 1 min). The analytes were detected by a photodiode array (PDA) detector operating at a detection frequency of 5 Hz with a slit of 4 nm. Piceatannol, hopeaphenol and r2-viniferin were detected at a wavelength of 283 nm, resveratrol at 305 nm and the signal of ε-viniferin und r-viniferin was detected at 325 nm.

Quantitation was performed by external calibration of the LC-UV signal of standards utilizing one of the resveratrol oligomeres as internal standard (IS). For the determination of resveratrol, piceatannol, ε-viniferin and r-viniferin, hopeaphenol (2 µM) was used as IS. For the quantitation of hopeaphenol and r2-viniferin the closely eluting ε-viniferin (1 µM) was used as IS. For calibration, the polyphenols were sequentially diluted (0.3, 0.5, 1, 2, 3, 5, 8, 10 µM) in 50/50 ACN/water containing IS and 0.1% acetic acid. The acid was added to ensure the stability of IS and analytes. The analyte to IS area ratios were fitted in a linear way reciprocally weighted by concentration.

Sample preparation was carried out by mixing equal volumes of IS solution (4 µM hopeaphenol or 2 µM ε-viniferin, in ACN with 0.2% HAc) and incubation samples. The resulting mixtures were gently vortexed and centrifuged at 21,000 x g for 10 min at 4 °C. The supernatant was transferred to brown glass vials and immediately analyzed by LC-UV. Recovery rates were determined in DMEM spiked with 3 µM, 5 µM and 10 µM of the polyphenols. These samples were analyzed within the same day as the other samples. All analyses were carried out as triplicates and results are presented as mean with the standard deviation (SD).

2.2.3 Determination of chemical stability during incubation in cell culture medium

The stability of the stilbene polyphenols was determined in DMEM (pH 7.4) in a Polysterol 96-well plate (Techno Plastic Products, Trasadingen, Switzerland) to mimic cell culture experimental conditions. Each well was filled with 100 µL of

polyphenol solution (10 µM) in DMEM and the plate was incubated in four different conditions: i) at 4 °C in the dark, ii) at 23 °C in the dark, iii) at 37 °C in a cell culture incubator (5% CO_2) in the dark, iv) at 23 °C on a laboratory bench at room light (2 m away from a commercial fluorescent tube). In addition, experiments were also carried out at 23 °C in the dark in DMEM medium adjusted to pH 4.0 with HAc and pH 9.0 with 1 M tris(hydroxymethyl)-aminomethane. After 0.25, 0.5, 1, 3, 6, 9, 24, 48 and 72 h, 75 µL were sampled per well and analyzed by LC-UV. For the unstable piceatannol, sampling was performed additionally after 2.5, 5, 10, 15, 20, 25, 30 and 60 min. In order to generate *cis*-isomers for the characterisation of degradation products the stilbene polyphenols were subjected to daylight for 10 min (piceatannol) to 30 min (resveratrol, ε-viniferin, r-viniferin, and r2-viniferin) as previously described [17].

2.2.4 Glucuronidation assays

The glucuronidation assay was carried out as previously described [16]. In brief resveratrol, ε-viniferin, and hopeaphenol were incubated with microsomes in a total volume of 200 µL of 100 mM potassium phosphate buffer (pH 6.9). In a generic scheme, 10 µL of microsome solution containing 12.5 µg protein were mixed with 96 µL buffer and 40 µL of alamethicin solution (125 µg/mL) and placed on ice for 15 min. Alamethicin forms pores in the microsomal membrane and therefore increases the substrate accessibility of the uridine 5'-diphosphate-glucuronosyltransferases (UGTs) [18]. Subsequently 4 µL of the substrate (concentration in the assay: 20 µM), 20 µL magnesium chloride and 10 µL of the β-glucuronidase inhibitor saccharolactone (concentration in the assay: both 10 mM) were added and the mixture pre-incubated for 5 min at 37 °C on a heated shaker. The reaction was initiated by the addition of 20 µL of uridine 5'-diphosphoglucuronic acid (UDPGA, 20 mM) and the reaction tubes incubated for further 40 min. The reaction was then stopped by the addition of 200 µL of IS solution (4 µM hopeaphenol for ε-viniferin; 2 µM ε-viniferin for hopeaphenol and resveratrol in ACN acidified with 0.2% HAc) followed by a centrifugation step

and LC-UV analysis. For control incubations buffer was added instead of UDPGA solution.

2.3 Results and Discussion

2.3.1 LC-UV method

A new ultra fast LC-UV method was developed, to enable rapid analysis of resveratrol and its analogs and oligomers in biological samples. The separation was carried out on a 2.7 µm “core-shell” particle reversed-phase column. In addition to the advantages of sub-2.7 µm particle size, the not entirely porous stationary phase allows a more efficient mass transfer between stationary and mobile phase because of a shorter diffusion path in the shell type particles [19]. The flow rate was set to 2.0 mL/min to compensate for the large void volume of the standard LC equipment used. As shown in Fig. 2.2, this setup led to a very high chromatographic resolution in an analysis time of less than 2.5 minutes.

The mobile phase gradient was optimized to fully separate analytes from the void volume (22 s, 0.7 mL) of the system, where polar matrix compounds elute. Applying a shallow gradient from initial 30% to 70% organic solvent in 1.6 min allows the baseline separation of all six analytes (Fig. 2.2). Piceatannol and resveratrol eluted first in narrow peaks, followed by the tetramer hopeaphenol which showed a relatively broad peak. Finally ε-viniferin, r2-viniferin and r-viniferin eluted in very narrow peaks (for retention times see Tab. 2.1). Thereafter, the column was washed with two void volumes of organic solvent and reconditioned with three void volumes during the autosampler injection cycle of the next sample (about 1 min).

The polyphenols were detected close to their absorbance maxima as determined in the LC solvent using the PDA detector. Piceatannol, hopeaphenol and r2-viniferin were monitored at a wavelength of 283 nm, resveratrol at 305 nm and ε-viniferin and r-viniferin at 325 nm.

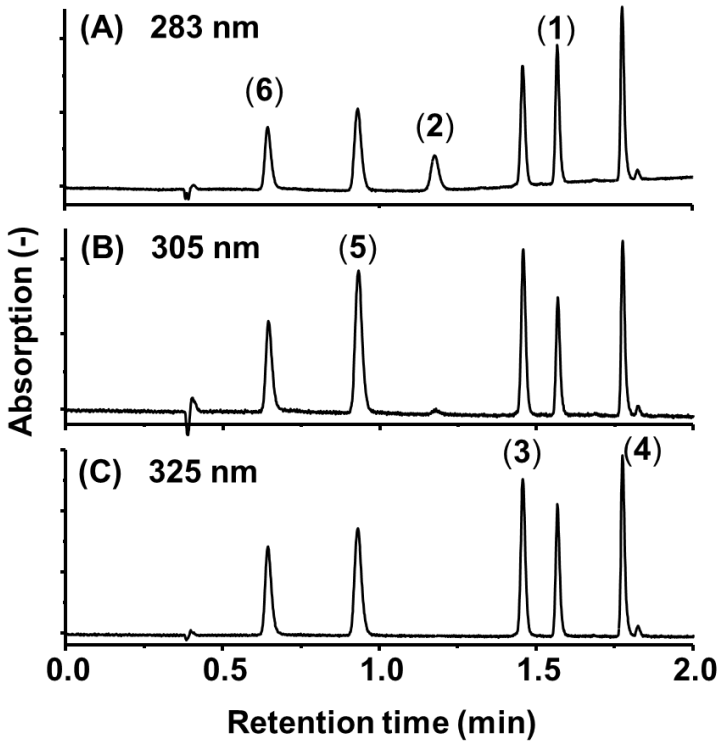

Fig. 2.2: Typical chromatographic separation of a standard solution of resveratrol (**5**), piceatannol (**6**) and four resveratrol-oligomers (**1-4**). Shown are the chromatograms at 283 nm (A), 305 nm (B) and 325 nm (C) used for quantitation of an injection (10 µL) of a 3 µM standard solution.

With this setup, a limit of detection (LOD) of 0.03 µM (0.3 pmol on the column) was determined for r2-viniferin and r-viniferin eluting in very narrow peaks with a full width at half maximum (FWHM) around 0.5 s (Tab. 2.1). With a broader peak width the LOD increased to 0.1 µM (1 pmol) for resveratrol and ε-viniferin and 0.3 µM (3 pmol) for hopeaphenol. This sensitivity is almost comparable to a recent LC-UV method for resveratrol-oligomers utilizing sub-2 µm particle-filled columns and a high pressure LC system, leading to LOD values between 5-50 µg/mL (0.2-0.55 pmol) [1]. With an analysis time of 2.5 min (about 3.5 min total running time) our method is more than twice as fast, while only using standard equipment (max pressure <250 bar). Moreover this method is the first for the quantitative measurement of r-viniferin and r2-viniferin described so far.

Tab. 2.1: Performance of the new LC-UV method. The observed retention times (t_R) , peak width at half maximum height ($w_{0.5}$), the resulting number of theoretical plates (N), the limit of detection (LOD) and the dynamic range for each analyte are shown.

Analyte	t_R (min)[a]	$W_{0.5}$ (s)[b]	N (-)	LOD (µM)[c]	Dynamic range (µM)[d]	r^2	Slope (1/µM)	Inter-cept (-)
Piceatannol	0.60 ± 0.03	1.32 ± 0.48	$4.2 \cdot 10^3$	0.3	1-10	0.999	0.63	-0.06
Resveratrol	0.89 ± 0.03	1.38 ± 0.48	$8.2 \cdot 10^3$	0.1	0.3-10	0.999	1.21	-0.02
Hopeaphenol	1.11 ± 0.06	1.98 ± 0.84	$6.3 \cdot 10^3$	0.3	1-10	0.999	0.49	0.03
ε-viniferin	1.43 ± 0.02	0.78 ± 0.18	$6.7 \cdot 10^4$	0.1	0.3-10	0.999	2.56	-0.03
r2-viniferin	1.55 ± 0.01	0.60 ± 0.06	$1.3 \cdot 10^5$	0.03	0.1-10	0.998	3.71	-0.10
r-viniferin	1.77 ± 0.03	0.48 ± 0.06	$2.5 \cdot 10^5$	0.03	0.1-10	0.994	0.85	0.04

[a] Mean of the 3 µM standard solution over 6 months (n = 6)
[b] Injection of 3 µM standard solution (n = 3)
[c] Signal-to-noise-ratio of at least 3:1
[d] 10 µM was the highest concentration tested; linear range >10 µM

In order to test the influence of matrix compounds on the separation and detection, DMEM was spiked with the polyphenols and analyzed after mixing with the internal standard and a centrifugation step. For all analytes the present method shows a good accuracy, with a mean recovery rate of 98 ± 6%. Moreover, the method precision was acceptable with an inter-sample variation of below 6.5% (Tab. 2.2). These results clearly demonstrate that increased analysis speed is not detrimental to analytical performance. Allowing the analysis of more than 400 samples in a single day, the developed LC-UV

method is ideally suited for stability studies, which require the analysis of large sets of samples.

Tab. 2.2: Recovery rates determined in spiked DMEM. The mean of the recovery rate (rec.) and the intra-day RSD of the analysis of 3 independent spiked samples are shown.

	Spiked content					
	3 µM		5 µM		10 µM	
	Rec. (%)	RSD (%)	Rec. (%)	RSD (%)	Rec. (%)	RSD (%)
Piceatannol [b]	103	5.2	91.6	1.2	84.4	1.8
Resveratrol	97.1 [a] 97.8 [b]	3.9 [a] 9.9 [b]	103 [a] 107 [b]	2.7 [a] 6.3 [b]	101 [a] 103 [b]	8.1 [a] 2.2 [b]
Hopeaphenol [a]	96.9	0.40	94.7	5.0	94.3	4.7
ε-viniferin [b]	97.1	5.8	106	5.8	101	2.4
r2-viniferin [b]	n.d. [c]	n.d. [c]	n.d. [c]	n.d. [c]	97.9	6.8
r-viniferin	116 [a] 98.9 [b]	9.6 [a] 6.5 [b]	114 [a] 107 [b]	6.9 [a] 6.3 [b]	118 [a] 102 [b]	4.8 [a] 3.6 [b]

[a] Internal Standard ε-viniferin (1 µM) [b] Internal Standard hopeaphenol (2 µM)
[c] not determined (limited amount of reference compound available)

2.3.2 Chemical stability of resveratrol, analogs and oligomers in cell culture medium

The stability of piceatannol, resveratrol, hopeaphenol, ε-viniferin, r-viniferin and r2-viniferin was analyzed in DMEM, a standard medium used to culture various cell lines. The compounds were incubated for up to 72 h under different conditions and their stability was assessed by LC-UV. As shown in Fig. 2.3 A, piceatannol, resveratrol, ε-viniferin, r-viniferin and r2-viniferin were rapidly degraded in the dark at a pH of 7.4 and a temperature of 23 °C. With a half life ($t_{1/2}$) of about 25 min piceatannol was the most unstable compound, followed by

resveratrol with a $t_{1/2}$ of about 1 h. Among the oligomers, r-viniferin showed the shortest half life ($t_{1/2}$ ~5 h), whereas the tetramer r2-viniferin was as stable as the dimer ε-viniferin with a half life of about 15 h.

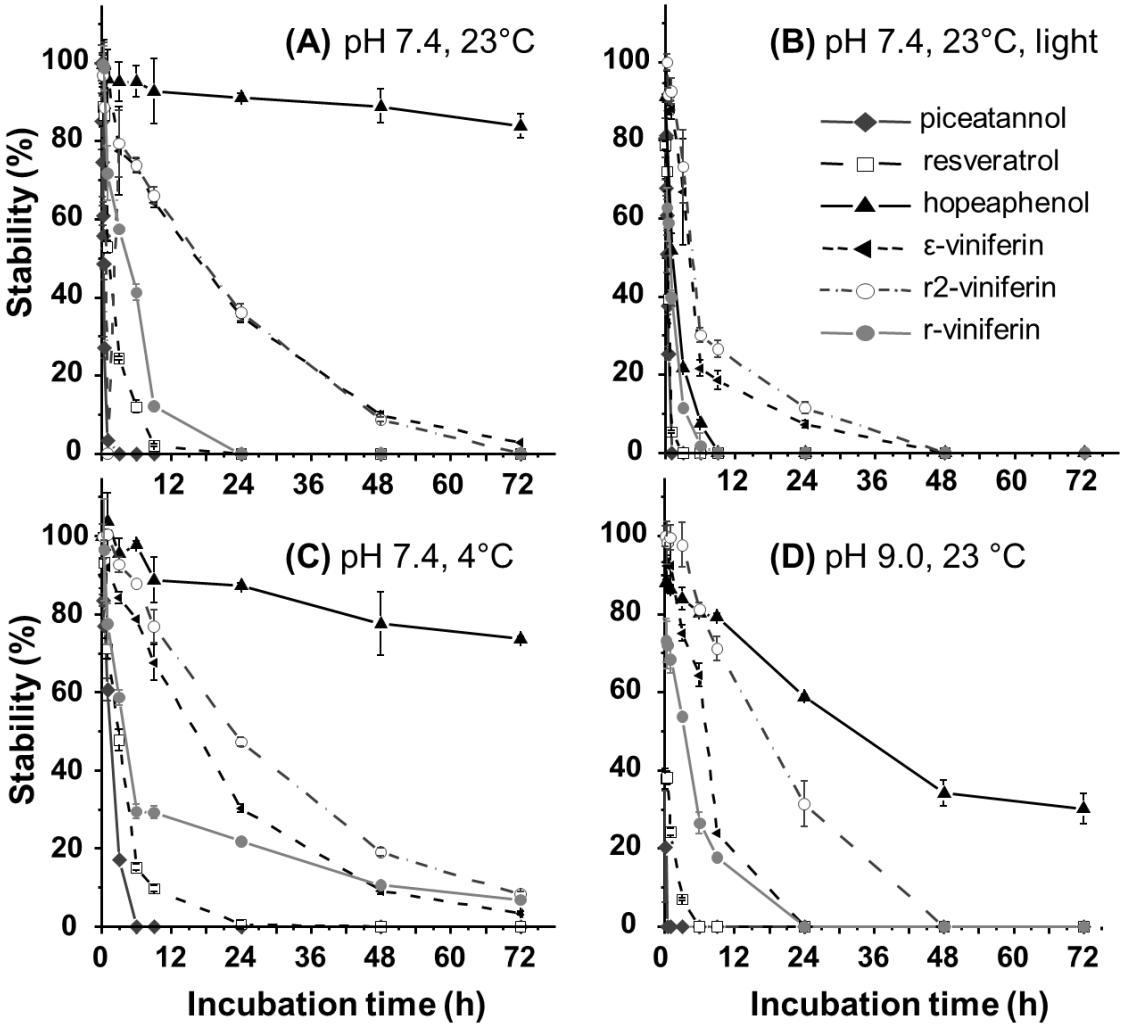

Fig. 2.3: Stability of the analytes during incubation in DMEM medium. At room temperature, pH 7.4 (**A**), at room temperature under room light, pH 7.4 (**B**), at 4°C in the dark (fridge), pH 7.4 (**C**) and in DMEM medium adjusted to pH 9.0 (**D**). Shown is the mean and SD of three incubations.

By contrast, the concentration of the tetramer hopeaphenol was virtually unchanged. Even after an incubation time of 72 h, 84 ± 3% of the initial concentration were detected. When incubated at a higher temperature of 37 °C in a cell incubator under a 5% CO_2 atmosphere, a similar stability pattern of the

compounds was observed ($t_{1/2}$ piceatannol ~20 min; $t_{1/2}$ resveratrol ~2.5 h; $t_{1/2}$ r-viniferin ~5 h; $t_{1/2}$ ε-viniferin ~19 h; $t_{1/2}$ r2-viniferin ~21 h; $t_{1/2}$ hopeaphenol >72 h). In accordance to these findings, a decrease in the temperature had only minor effects on the stability of the polyphenols (Fig. 2.3 C). Interestingly, the stability of r2-viniferin was markedly increased at low temperatures ($t_{1/2}$ ~24 h) when compared to the other polyphenols, which disappeared at a similar rate as higher temperatures (Fig. 2.3 C). Based on these results, one could conclude, that temperature only slightly influences the stability of resveratrol and its analogs and oligomers in DMEM. In contrast to that, the pH strongly influences the stability of the test substances. As already known for many other polyphenolic compounds [20, 21], the stability of piceatannol, resveratrol, ε-viniferin, and hopeaphenol decreased at a pH of 9 (Fig. 2.3 D). Although hopeaphenol was still the most stable compound among the analytes, with a half life of about 30 h, it nevertheless was subjected to a significant degradation under alkaline conditions. A decrease in pH to a value of 4.0 increased the stability of all compounds, and ≥90% of the initial concentration of all polyphenols was recovered after 72 h.

A faster loss of the compounds was observed at a pH of 7.4 and a temperature of 23 °C when the DMEM was subjected to room light (fluorescent tube) radiation during incubation. In this case, none of the polyphenols had a half life of longer than 4 h (Fig. 2.3 B), a finding which is consistent with previous results showing that *trans*-stilbene derivatives degrade under light [7, 22]. It is interesting to note, that under these conditions, r2-viniferin was the most stable compound, followed by ε-viniferin.

Despite the complete disappearance of the peaks of the test compounds during incubations at different conditions in the dark, no new peaks of degradation products could be observed for piceatannol, resveratrol, ε-viniferin and r2-viniferin at the monitored wavelengths (283 nm, 305 nm and 325 nm). Only r-viniferin gave rise to a new peak at a retention time of 1.56 + 0.01 min. The area of this peak increased between 0.5 and 9 hours during incubation at pH

7.4. At pH 9 the peak already appeared after 0.25 hours of incubation. In both cases longer incubation led to a decrease of the peak area, and after 48 hours it disappeared completely similar to its precursor r-viniferin (Fig. 2.4).

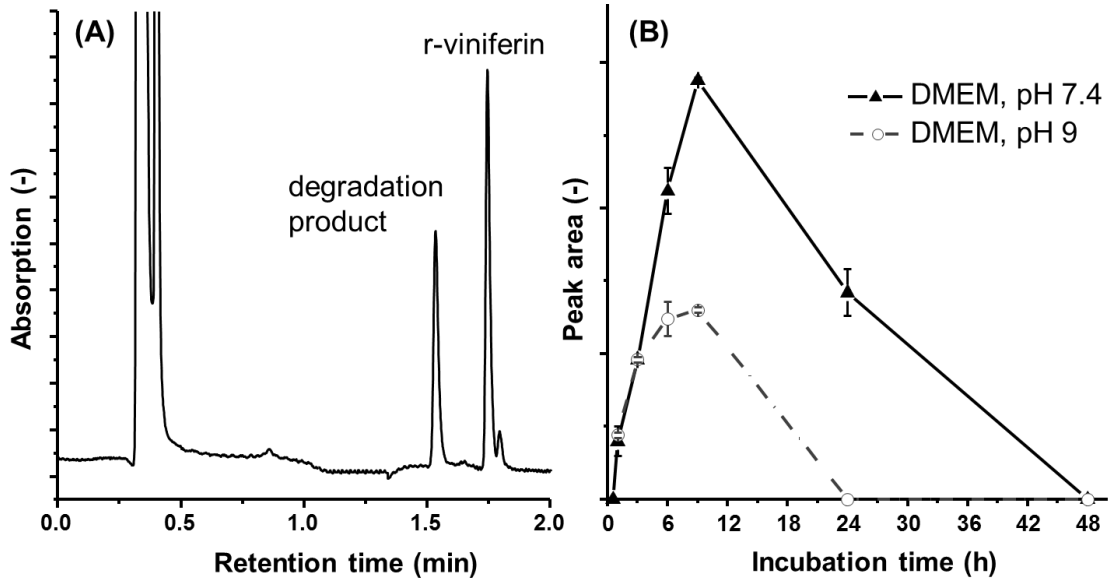

Fig. 2.4: Formation of degradation product of r-viniferin at a retention time of 1.56 min. (**A**) Chromatogramm (285 nm) of a 6 h incubation of r-viniferin at room temperature at the dark at pH 9. (**B**) Area of the newly formed compound peak over the incubation time at pH 7.4 and pH 9.

It is well known, that *trans*-stilbene polyphenols are converted to their *cis*-isomers in the light [7, 22]. In order to generate *cis*-isomers, light radiation was used as previously described for resveratrol [17]. All stilbene polyphenols were converted in the light, yielding a single product peak in LC-UV. The retention times of the products were: resveratrol 1.21 ± 0.01 min, piceatannol 0.82 ± 0.01 min, ε-viniferin 1.30 ± 0.01 min and r-viniferin 1.65 ± 0.01 min. Peaks of these tentatively identified *cis*-isomers of resveratrol, ε-viniferin and r-viniferin were detected during incubation in DMEM medium in the light, but vanished rapidly during further incubation. Thus, it is unlikely that even under light exposure the observed disappearance of the polyphenols in DMEM medium is driven by *cis*-*trans*-isomerization.

Recently Yang et al. [11] reported a complete degradation of resveratrol by auto-oxidative processes at 37 °C in the dark. They showed that after a 24 h incubation of 200 µM resveratrol in Base Modified Eagle Medium at 37 °C, 96% of the compound was degraded, with a considerable hydrogen peroxide formation. Consistent with our results no degradation products could be detected by LC-UV. This may be explained by the complexity of polyphenol auto-oxidation, leading to various products and adducts [7, 10, 20, 22, 23]. Among the stilbene monomers piceatannol is more susceptible to auto-oxidation than resveratrol, as is to be expected for a polyphenol with a catechol moiety [21]. By contrast, dimerization has a stabilizing effect, and ε-viniferin shows a significantly slower degradation than its monomer resveratrol (Fig. 2.3). Among the tetramers bearing one *trans*-stilbene moiety (Fig. 2.1), r2-viniferin is significantly more stable towards auto-oxidation than r-viniferin. The stilbene moiety seems to be a key factor for the instability in DMEM. Hopeaphenol, the only substance tested which does not exhibit this structural feature, is stable under physiological conditions (Fig. 2.3 A-C). Only prolonged incubation under alkaline conditions (Fig. 2.3 D) and light radiation causes a degradation of this compound. When taking this chemical stability into account, hopeaphenol holds a unique place among resveratrol and its oligomers.

Regardless of the nature of the underlying degradation processes in DMEM, the half life of stilbene polyphenols particularly that of resveratrol and piceatannol, is short. Therefore, care should be taken in the design of cell culture experiments investigating biological effects of polyphenols utilizing different cell culture media. In particular, the concentration of the stilbene polyphenols should be monitored in the medium throughout the incubation period.

In vivo, considerable amounts of resveratrol are detected as conjugates in serum and urine, suggesting that chemical degradation of stilbene polyphenols seems to be less relevant in the living organism. The difference of the degradation behavior of the test compounds in the cell culture medium used in our study when compared to the *in vivo* situation may be explained by a

stabilization of the stilbene polyphenols by extensive protein binding [7, 24]. This assumption is substantiated by the finding, that only about 50% resveratrol were degraded when incubated for 24 hours in DMEM containing 10% fetal calf serum [10], whereas in our experiments it disappeared completely.

2.3.3 Metabolic stability of resveratrol and its oligomers

To date, no information about the metabolism of resveratrol oligomers is available. Glucuronidation is the major metabolic pathway of resveratrol and many other polyphenols. Therefore, we applied the new rapid LC-UV method, to characterize the metabolic stability of ε-viniferin and hopeaphenol, and compare it to that of resveratrol. The polyphenols were incubated with rat liver microsomes (RLM) and human liver microsomes (HLM) at a substrate concentration of 20 µM. The conjugation rate was determined based on substrate consumption (Fig. 2.5). At a reduced pH of 6.9, all polyphenols were sufficiently stable over the incubation time of 40 minutes in phosphate buffer. More than 77 ± 2% of resveratrol, 95 ± 2% of ε-viniferin and 97 ± 1% of hopeaphenol of the initial amount was recovered in control incubations without UDPGA (Fig. 2.5). As described previously, resveratrol was quickly conjugated by both RLM and HLM [25, 26]. After 40 min incubation with RLM, less than 1% unconjugated substrate remained, and HLM conjugated 65% of resveratrol (remaining substrate 35 ± 2%). The dimer ε-viniferin was also significantly glucuronidated by both RLM and HLM, albeit to a lesser extent than resveratrol. After 40 min incubation with the same amount of microsomal protein, 15 ± 4% (RLM) and 54 ± 2% (HLM) of ε-viniferin remained unconjugated. To our surprise, the tetramer hopeaphenol was, under identical conditions, not glucuronidated at all. With a recovery rate of the unchanged substrate of 94 ± 1% compared to 97 ± 2% for incubations with RLM and HLM, respectively, almost the same amount of hopeaphenol was detected as in control incubations without UDPGA (Fig. 2.5).

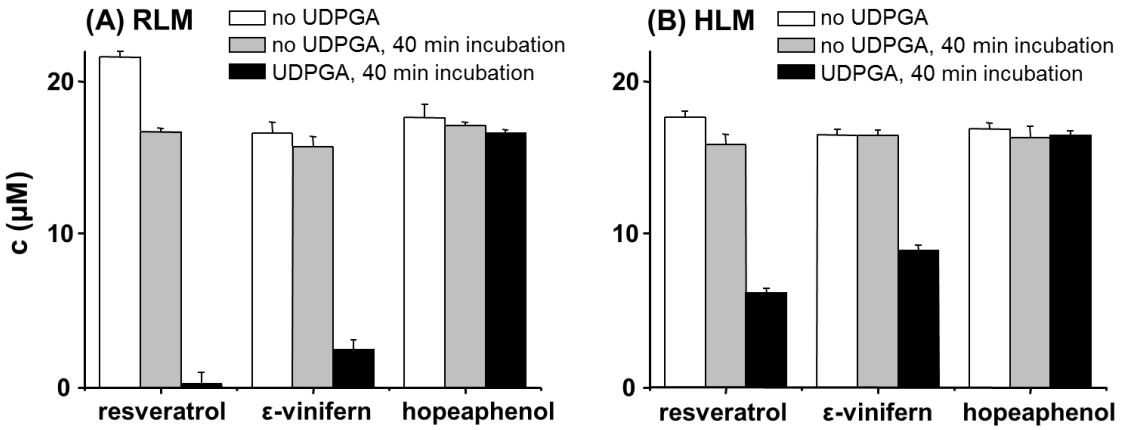

Fig. 2.5: Glucuronidation of resveratrol, ε-viniferin and hopeaphenol (each 20 µM) by human liver microsomes (HLM) and rat liver microsomes (RLM). Shown is the remaining concentration of the substrate after 40 min incubation with 0.25 mg/mL microsomal protein in presence and absence of the co-substrate UDPGA. Shown is the mean and SD of three independent experiments.

In spite of a high absorption rate, the bioavailability of resveratrol is very low [27, 28]. Extensive intestinal and hepatic metabolism of resveratrol by sulfonation and glucuronidation leads to a rapid conjugation of this polyphenol [7, 22, 27]. For instance, only trace amounts of free resveratrol (<5 ng/mL) is detectable in the plasma after a dietary relevant single oral dose of 25 mg in humans [28]. Even an ultra high single dose of 5 g resveratrol to human volunteers led only to a plasma concentration of 533 ng/mL (2.5 µM) [29]. In contrast to that, the plasma concentration of glucuronide and sulfate conjugates exceeded the concentration of the unchanged compound by a high order of magnitude [27, 28]. Although few studies describe a biological activity of the conjugates [7, 22, 27], the vast majority of potentially beneficial effects on the regulation of cellular pathways have been exclusively described for the parent compound. Poor oral bioavailability and thus a lack of effectiveness, is a common phenomenon described for many biologically active polyphenols [30]. Our finding that hopeaphenol is barely glucuronidated by human and rat liver enzymes sets it clearly apart from most naturally occurring polyphenols. Upon absorption, its slow phase II metabolism might lead to an improved bioavailability in comparison to other stilbene-derivatives and polyphenols.

However, it is questionable if a compound with a molecular weight of 907 g/mol is efficiently absorbed in mammals after oral intake.

Except for hopeaphenol, the tested polyphenols disappear rapidly in DMEM medium under cell culture conditions, probably caused by degradation through auto-oxidation. These findings demonstrate the necessity of cell culture experiments with polyphenols being always accompanied by a monitoring of the stability of the test compounds under assay conditions. Only if the polyphenol is stable for a given incubation time, a reliable correlation between observed biological effects and the substance can be deduced. With the new ultra fast LC-UV method, using only basic LC equipment, we developed a tool for the rapid assessment of the stability of resveratrol its analogs and oligomers.

2.4 Conclusions

Our findings show for the first time, that oligomerisation stabilizes stilbene polyphenols in cell culture medium. Among all tested compounds, the tetramer hopeaphenol has a unique stability with almost all of the initial concentration beeing recovered after a 72 h incubation period. Our initial investigation of the glucuronidation of the resveratrol-oligomers demonstrates that ε-viniferin, similar to resveratrol and many other polyphenols, is rapidly conjugated. Surprisingly, the tetramer hopeaphenol was not glucuronidated by liver UGTs, which might lead to an improved bioavailability upon absorption. If one takes the chemical and metabolic stability, as well as the high potency of hopeaphenol on inhibiting tumor cell growth into account, it is apparent, that especially this compound qualifies for further investigation. Current data clearly implies that hopeaphenol could be a promising natural anti-carcinogen, which also might contribute to the beneficial effects associated with moderate wine consumption.

2.5 References

[1] Boutegrabet L., Fekete A., Hertkorn N., Papastamoulis Y., Waffo-Teguo P., Merillon J. M., Jeandet P., Gougeon R. D., Schmitt-Kopplin P. *Anal Bioanal Chem* (2011) 401, 1513-1521

[2] Ha D. T., Kim H., Thuong P. T., Ngoc T. M., Lee I., Hung N. D., Bae K. J *Ethnopharmacol* (2009) 125, 304-309

[3] Sotheeswaran S., Pasupathy V. *Phytochemistry* (1993) 32, 1083-1092

[4] Guebailia H. A., Chira K., Richard T., Mabrouk T., Furiga A., Vitrac X., Monti J. P., Delaunay J. C., Merillon J. M. *J Agric Food Chem* (2006) 54, 9559-9564

[5] Huang K. S., Lin M., Cheng G. F. *Phytochemistry* (2001) 58, 357-362

[6] Ito T., Akao Y., Yi H., Ohguchi K., Matsumoto K., Tanaka T., Iinuma M., Nozawa Y. *Carcinogenesis* (2003) 24, 1489-1497

[7] Delmas D., Aires V., Limagne E., Dutartre P., Mazue F., Ghiringhelli F., Latruffe N. Resveratrol and Health (2011) 1215, 48-59

[8] Piotrowska H., Kucinska M., Murias M. *Mutat Res-Rev Mutat* (2012) 750, 60-82

[9] Steinberg P. *Ernahrungs Umschau* (2011) 58, 366-371

[10] Long L. H., Hoi A., Halliwell B. *Arch Biochem Biophys* (2010) 501, 162-169

[11] Yang N. C., Lee C. H., Song T. Y. *Biosci Biotechnol Biochem* (2010) 74, 63-68

[12] Andres-Lacueva C., Macarulla M. T., Rotches-Ribalta M., Boto-Ordonez M., Urpi-Sarda M., Rodriguez V. M., Portillo M. P. *J Agric Food Chem* (2012) 60, 4833-4840

[13] Boocock D. J., Patel K. R., Faust G. E. S., Normolle D. P., Marczylo T. H., Crowell J. A., Brenner D. E., Booth T. D., Gescher A., Steward W. P. *J Chromatogr B* (2007) 848, 182-187

[14] Amalfitano C., Agrelli D., Arrigo A., Mugnai L., Surico G., Evidente A. *Phytopathologia Mediterranea* (2011) 50, S224-S235

[15] Vergara C., von Baer D., Mardones C., Wilkens A., Wernekinck K., Damm A., Macke S., Gorena T., Winterhalter P. *J Agric Food Chem* (2012) 60, 929-933

[16] Schebb N. H., Franze B., Maul R., Ranganathan A., Hammock B. D. *Drug Metab Dispos* (2011) 40, 25-31

[17] Camont L., Cottart C. H., Rhayem Y., Nivet-Antoine V., Djelidi R., Collin F., Beaudeux J. L., Bonnefont-Rousselot D. *Anal Chim Acta* (2009) 634, 121-128

[18] Fisher M. B., Campanale K., Ackermann B. L., VandenBranden M., Wrighton S. A. *Drug Metab Dispos* (2000) 28, 560-566

[19] Gritti F., Guiochon G. *J Chromatogr A* (2010) 1217, 1604-1615

[20] Jhoo J. W., Lo C. Y., Li S. M., Sang S. M., Ang C. Y. W., Heinze T. M., Ho C. T. *J Agric Food Chem* (2005) 53, 6146-6150

[21] Gao S., Hu M. Mini *Rev Med Chem* (2010) 10, 550-567

[22] Amri A., Chaumeil J. C., C S., Charrueau C. *J Controll Rel* (2012) 158, 182-193

[23] Heinrich T., Willenberg I., Glomb M. A. *J Agric Food Chem* (2012) 60, 5221-5228

[24] Bourassa P., Kanakis C. D., Tarantilis P., Pollissiou M. G., Tajmir-Riahi H. A. *J Phys Chem B* (2010) 114, 3348-3354

[25] Brill S. S., Furimsky A. M., Ho M. N., Furniss M. J., Li Y., Green A. G., Bradford W. W., Green C. E., Kapetanovic I. M., Iyer L. V. *J Pharm Pharmacol* (2006) 58, 469-479

[26] Maier-Salamon A., Bohmdorfer M., Thalhammer T., Szekeres T., Jaeger W. *Drug Metab Pharmacokinet* (2011) 26, 364-373

[27] Scott E., Steward W. P., Gescher A. J., Brown K. *Mol Nutr Food Res* (2012) 56, 7-13

[28] Walle T., Hsieh F., DeLegge M. H., Oatis J. E., Walle U. K. *Drug Metab Dispos* (2004) 32, 1377-1382

[29] Boocock D. J., Faust G. E. S., Patel K. R., Schinas A. M., Brown V. A., Ducharme M. P., Booth T. D., Crowell J. A., Perloff M., Gescher A. J., Steward W. P., Brenner D. E. *Cancer Epidem Biomar* (2007) 16, 1246-1252

[30] Wu B., Kulkarni K., Basu S., Zhang S., Hu M. *J Pharm Sci* (2011) 100, 3655-3681

Chapter 3

Investigation of the Absorption of Resveratrol Oligomers in the Caco-2 Cellular Model of Intestinal Absorption *

Resveratrol oligomers are biologically active polyphenols found in wine. No information about the bioavailability of these polyphenols is available. In order to elucidate if the reseveratrol oligomers can pass the intestinal barrier, the transport of the dimer ε-viniferin and the tetramer hopeaphenol was studied in the Caco-2 transwell system. A flux through the cell monolayer could neither be observed for ε-viniferin nor for hopeaphenol (apparent permeability coefficient (P_{app}) <1 x 10^{-6} cm/s). In contrast, resveratrol showed a P_{app} of 11.9 x 10^{-6} cm/s. Nevertheless, about 16-30 % of the oligomers were found in the lysed cellular fraction. This leads to the conclusion that the intestinal absorption rate of the two resveratrol oligomers ε-viniferin and hopeaphenol is low and negligible when compared to resveratrol. Therefore, it is unlikely that the oligomers could elicit a systemic biological effect after dietary intake. However, the compounds may act locally on the intestinal epithelium.

* Reprinted from *Food Chemistry*, vol. 167, Willenberg I., Michael M., Wonik J., Bartel L. C., Empl M. T., Schebb N. H., Investigation of the Absorption of Resveratrol Oligomers in the Caco-2 Cellular Model of Intestinal Absorption, pp. 245-250, Copyright (2015), with permission from Elsevier.

Author contributions: IW: Designed research, performed experiments and wrote the manuscript; MM: Developed online-SPE-LC-MS method and performed transport experiment as part of her master thesis under the supervision of IW; JW: Helped with the stability experiments; LCB: Helped with the cell culture experiments; MTE: Contributed to research design and manuscript writing; NHS: Designed research and wrote the manuscript.

3.1 Introduction

Resveratrol oligomers are stilbenoid polyphenols consisting of two to eight subunits of resveratrol (Fig. 2.1) [1]. The structural characteristics of resveratrol oligomers are diverse and they are synthesized by many plant species, with the families of Dipterocarpaceae and Vitaceae producing the biggest diversity of molecules [1, 2]. Just like resveratrol [3], some resveratrol oligomers seem to be synthesized, at least in grapevine plants (Vitaceae family), following contact with pathogens and might therefore act as phytoalexins [4]. Grapevine plants and edible products derived therefrom (e.g. wine) act as the major dietary source for resveratrol derivatives as well as resveratrol itself [5-7]. The resveratrol dimer ε-viniferin (Fig. 2.1) and the tetramer hopeaphenol (Fig. 2.1) are found in wine at concentrations of 0.58-4.3 mg/L [8] and 0.3-3.1 mg/L [6], respectively. Similar to many other polyphenols in the diet, hopeaphenol and ε-viniferin show antioxidative and anti-inflammatory properties [9-12]. Moreover, they have strong effects on the viability and proliferation of mammalian tumor cells *in vitro*. The potency of ε-viniferin to inhibit the growth of tumor cells depends on the used cellular model and is comparable to that of resveratrol [13-15]. In contrast to that, hopeaphenol is much more potent than both the monomer and the dimer [16-18], with for instance IC_{50} values of 1.8 µM and 8.8 µM in various canine tumor cell lines [19]. Similar to resveratrol [5], the antiproliferative effects of both oligomers involve the activation of apoptotic signaling cascades and the induction of a cell cycle arrest in the case of hopeaphenol [14, 18-20]. Because of their high biological activity, resveratrol oligomers are discussed as a potential new class of natural anticarcinogens and chemopreventive compounds [18, 21]. However, no information about the bioavailability of these molecules is available. Since dietary compounds can only elicit biological effects upon intestinal absorption, information about such processes is crucial for the evaluation of their potential impact on human health. We therefore investigated the absorption of ε-viniferin as an example of a resveratrol dimer as well as hopeaphenol as a paradigm of a tetramer and

compared it to that of resveratrol in the Caco-2 transwell system, a widely used *in vitro* model for human intestinal drug absorption.

3.2 Experimental

3.2.1 Chemicals and biological materials

Caco-2 cells were purchased from the American Type Culture Collection (ATCC; distribution by LCG, Wesel, Germany). *trans*-resveratrol (≥99% purity) was purchased from Sigma-Aldrich (Schnelldorf, Germany) and the dimer ε-viniferin (≥90% purity) as well as the tetramer hopeaphenol (≥95% purity) were obtained from Actichem SA (Montauban, France). The chemical structures of the analytes are displayed in Fig. 2.1. Acetonitrile (HPLC grade) and acetic acid were obtained from Carl Roth (Karlsruhe, Germany). Dulbecco's Modified Eagle Medium (DMEM), fetal bovine serum (FBS) and all cell culture reagents were purchased from Biochrom (Berlin, Germany). β-glucuronidase (GUS) from Helix pomatia (HP-2 specific activity: GUS ≥100.000 u/mL, sulfatase: ≤7.500 u/mL), formononetin and all other chemicals were obtained from Sigma-Aldrich.

3.2.2 LC-UV analysis and sample preparation

Quantification was carried out by liquid chromatography with ultraviolet absorbance detection (LC-UV) with automated sample preparation by online-solid phase extraction (SPE) in backflush mode [22, 23]. The LC system included a SIL-10-ADVP autosampler (Shimadzu, Langenfeld, Germany), a Spectra System P4000 pump (Thermo Fisher, Bremen, Germany) as gradient pump 1, two LC-10-ADvp LC pumps (Shimadzu) as gradient pump 2, a high-pressure two-position "Cheminert" six-port valve (VICI, Schenkon, Switzerland), a CTO-10ASvp column oven (Shimadzu) set to 40 °C and a SPD-10ADVP dual channel UV-detector (Shimadzu). Separation was carried out on a 125 x 4.6

mm “Sphere Clone” C18-reversed phase column (Phenomenex, Torrance, CA, USA) filled with 3 µm particles and equipped with a C-18 4 x 3 mm pre-column (Phenomenex). The same type of pre-column was used as stationary phase for the online-SPE. An aqueous solution of 0.1% (vol) acetic acid was used as solvent A and 95/5 acetonitril/water (*v*/*v*) acidified with 0.1% acetic acid was used as solvent B. At the beginning of each analysis 10 µL of sample were transferred to the SPE column with a flow of 1.5 mL/min of solvent A. During this procedure, the polyphenols were extracted, while salts and proteins were washed to waste. After 0.5 min the six-port valve was switched and the analytes were eluted in the reverse direction (backflush) onto the separation column with the flow of pump 2 (1.0 mL/min). After 2.5 min, the analytes were transferred completely to the analytical column and the six-port valve was switched back to loading position. This allowed flushing the SPE column with solvent B (1.0-4.0 min) and its equilibration for the next run, while the polyphenols were separated by the gradient delivered by pump 2. The following solvent gradient was used: 0.0-4.0 min isocratic 25% B, 4.0-8.0 min linear from 25-70% B, 8.1-12.0 min isocratic 100% B and re-equilibration for 4 min at 25% B. Resveratrol, ε-viniferin and formononetin were detected at a wavelength of 305 nm and hopeaphenol at a wavelength of 285 nm as previously described [24].

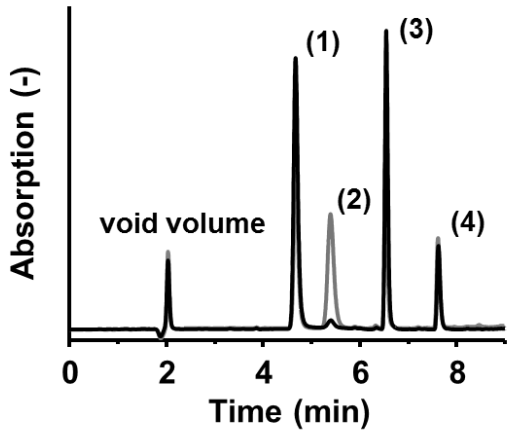

Fig. 3.1: Typical online-SPE-LC-UV chromatogram of a separation of resveratrol (**1**), hopeaphenol (**2**), ε-viniferin (**3**) and the IS (**4**). Black: signal at 305 nm; gray: signal at 285 nm.

Quantification was performed by an external calibration using formononetin as internal standard (IS). For calibration, the analyte to IS area ratios were linearly fitted, quadratic-reciprocally weighted by concentration. Instrument controlling and data analysis was performed with Excalibur 2.0 (Thermo Fisher). Under these conditions, all analytes as well as the IS were baseline separated (Fig. 3.1) and the limit of detection (LOD) for the polyphenols ranged from 0.05 to 0.2 µM with a linear range of more than three orders of magnitude (Tab. 3.1).

Tab. 3.1: Performance of the online-SPE-LC-UV method. The observed retention times (t_R), the limit of detection (LOD) and the dynamic range for each analyte are shown.

Analyte	t_R[a] (min)	LOD (µM)	Dynamic range[b] (µM)	r^2	Slope[c] (1/µM)	Intercept[c]
Resveratrol	4.66 ± 0.02	0.12	0.23-30	>0.99	0.44	0.009
Hopeaphenol	5.28 ± 0.04	0.23	0.47-30	>0.99	0.23	-0.005
ε-viniferin	6.25 ± 0.01	0.05	0.12-30	>0.99	0.33	-0.010
Formononetin (IS)	7.40 ± 0.24	-	-	-	-	-

[a] mean ± SD of the 3 µM standard solution over 2 months (n = 4).
[b] 30 µM was the highest concentration tested; linear range ≥30 µM.
[c] mean of 3 calibrations over 2 months.

The only necessary preparation step was mixing equal volumes of the biological samples with 10 µM IS solution in acetonitrile. As shown in Tab. 3.2, the accuracy for the quantification in different cell culture media was excellent (100 ± 10%). Only in spiked medium treated overnight with 10 000 u GUS, the recovery rate was barely acceptable (about 70%), probably caused by degradation of the analytes during incubation with the crude enzyme preparation. With the sensitivity, dynamic range and accuracy in biological

samples depicted in Tab. 3.1 and Tab. 3.2, the online-SPE-LC-UV method is ideally suited for the quantification of resveratrol, ε-viniferin and hopeaphenol in cell culture experiments.

Tab. 3.2: Recovery rates of resveratrol, hopeaphenol and ε-viniferin in cell culture media.

	Recovery[a] (%)		
	TRIS-buffered medium	**CO_3^{2-}-buffered medium, 10% FBS**	**TRIS medium after GUS treatment**
Resveratrol	103 ± 4.5	97.0 ± 5.6	73.1 ± 13
Hopeaphenol	104 ± 2.8	96.3 ± 1.8	65.3 ± 5.0
ε-viniferin	95.0 ± 1.5	92.9 ± 5.4	75.2 ± 5.0

[a] mean ± SD of 3 experiments, analyte concentration: 10 µM

3.2.3 Investigation of chemical stability of the polyphenols

The stability of the polyphenols was determined in different DMEM preparations (pH 7.4) in a 96 well plate (TPP, Trasadingen, Switzerland) to mimic the conditions of the transport experiments *in vitro*. Each well was filled with 100 µL of DMEM containing 10 µM resveratrol, ε-viniferin and hopeaphenol and the plate was incubated at 37 °C in a humidified incubator (5% CO_2). After 0, 1, 3, 6, 8, 24 and 48 h, 75 µL of each well were sampled and analyzed by the online-SPE-LC-UV method described above. The experiments were carried out in standard DMEM supplemented with 10% FBS as well as in DMEM without FBS and phenol red containing 50 mM TRIS buffer adjusted to pH 7.4 as a replacement for the usual carbonate buffer.

3.2.4 Cell culture

Caco-2 cells were cultured in DMEM supplemented with 10% FBS, 1% non-essential amino acids, 2 mM glutamine and 100 IU/mL penicillin and 100 µg/mL

streptomycin. Cultures were maintained in a humidified incubator at 37 °C, with an atmosphere containing 5% CO_2. Stock cultures were split at subconfluent densities (70-80%) by using trypsin/EDTA and seeded at a density of 13 x 10^5 cells/cm^2 into new culture vessels. For the transport experiment the subconfluent cells were seeded at a density of 1 x 10^5 cells/well in inserts ("ThinCerts", Greiner Bio One, Frickenhausen, Germany) with a permeable membrane, a pore size of 0.4 µm and a growth area of 1.13 cm^2. The inserts were placed in 12-well tissue culture plates with 0.5 mL of medium in the apical compartment and 1.5 mL medium in the basolateral compartment. The medium was changed 3 times a week.

3.2.5 Transport experiments

The transport experiments were performed 23-27 days post seeding in DMEM medium adjusted to pH 7.4 containing 50 mM TRIS buffer and without added phenol red or FCS. The integrity of the Caco-2 cell monolayer was characterized by trans-epithelial electrical resistance (TEER) measurements performed with an epithelial volt-ohm-meter ("EVOM^2", WPI, Berlin, Germany). Moreover, lucifer yellow (LY; 100 µM in the apical compartment) was used as a marker for paracellular diffusion. In order to investigate the integrity of the cell layer, the cells were incubated for 6 h with 100 µM LY in the apical chamber. Thereafter, 15 µL medium of the basolateral chamber were mixed with 85 µL fresh medium and the fluorescence was measured with a microplate reader (Tecan, Crailsheim, Germany) at an excitation wavelength of 427 nm and an emission wavelength of 535 nm. The limit of quantification was 0.02 µM LY, which corresponds to an apparent permeability coefficient (P_{app}) of 8.00 x 10^{-8} cm/s. No LY could be detected in the basolateral chamber 21 days post seeding and in the following days. The time course of the TEER and the permeability of LY are depicted in Fig. 3.2. For the experiment, only inserts which exceeded a resistance of 300 Ω/cm^2 were used and all transport experiments were carried out with a concentration of 20 µM of the polyphenols (resveratrol, ε-viniferin or hopeaphenol) in the apical chamber.

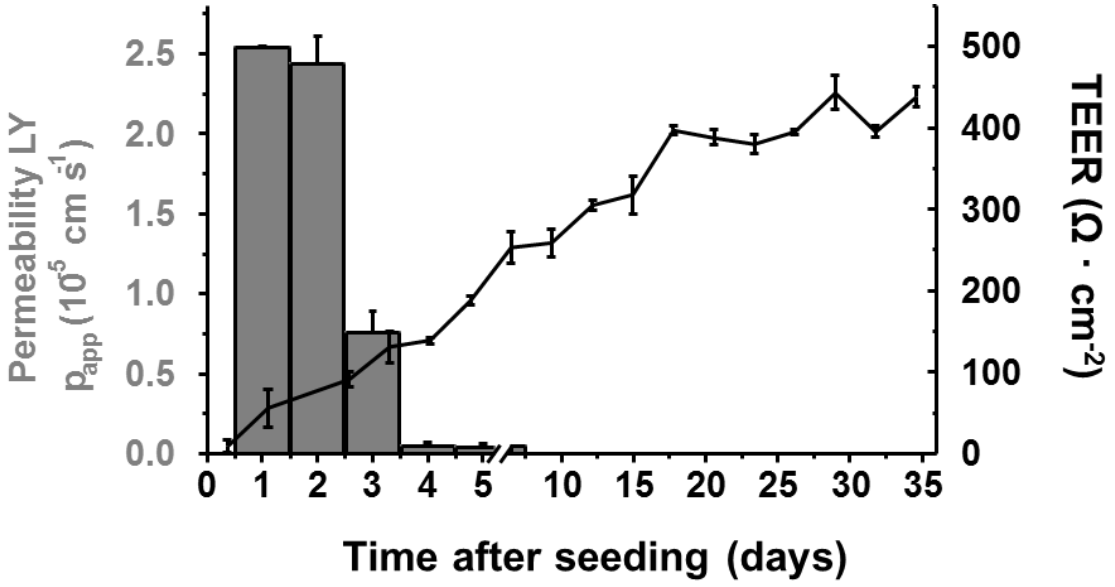

Fig. 3.2 Characterization of the Caco-2 cultivation on permeable membranes. Shown is the time course of the trans-epithelial electrical resistance (TEER, black line, right axis) and the apparent permeability coefficient (P_{app}) of the paracellular diffusion marker Lucifer Yellow (LY, gray bars, left axis). After day 21 no LY was detected in the basolateral chamber ($p_{app} \leq 1.00 \times 10^{-8}$ cm/s). Values represent the mean and SD of three independent determinations.

After 0, 1, 3 and 6 h, 60 µL of each well were taken as samples from the basolateral side and 20 µL from the apical side. After the last sampling point (6 h), the whole medium was collected from both chambers and the cells were lysed by incubation with 1% Triton X-100 solution for 10 min. In order to liberate polyphenols bound as conjugates, sample medium collected of both compartments was additionally incubated over night with 1000 u/mL GUS. All solutions were kept at -20 °C until analysis by online-SPE-LC-UV. The apparent permeability coefficient (P_{app}) was calculated according to Formula 1.

Formula 1: Calculation of the apparent permeability coefficient

$$P_{app} = \frac{\Delta c \cdot V}{\Delta t \cdot c_0 \cdot A} \left[\frac{cm}{s}\right]$$

Δc is the concentration (µM) in the receiver compartment, V is the volume of the receiver compartment, Δt is the duration of the transport experiment (s), c_0 is

the initial concentration in the donor compartment (µM) and A is the surface area of the membrane (cm^2) [25].

In order to assure that the integrity of the monolayer is not affected by resveratrol, ε-viniferin and hopeaphenol, the transport experiments were performed additionally in the presence of LY (100 µM in the apical compartment). After 6 h of incubation no LY could be detected in the basolateral chamber, indicating that the polyphenols did not comprise the integrity of the monolayer.

3.3 Results and Discussion

3.3.1 Stability of the polyphenols

The central aim of our study was to investigate the intestinal absorption of resveratrol, ε-viniferin and hopeaphenol *in vitro*. For these kinds of studies, it is a necessary prerequisite that the compounds are chemically stable during the whole duration of incubation. However, previous studies show that particularly resveratrol is not stable in standard DMEM, with a half-life of less than one hour [24, 26, 27]. In order to increase the stability of the polyphenols in the used cell culture environment, we followed two strategies. In the first approach, FBS was added to the cell culture medium. Similar to non-covalent binding of compounds to plasma proteins *in vivo*, the formation of polyphenol protein adducts could improve stability in cell culture medium [24]. Secondly, TRIS-buffered medium was used since bicarbonate ions are postulated to play a key role in the degradation of resveratrol [27]. As shown in Fig. 3.3, resveratrol, ε-viniferin and hopeaphenol were stable in both media, with a recovery of more than 90% after 48 h incubation.

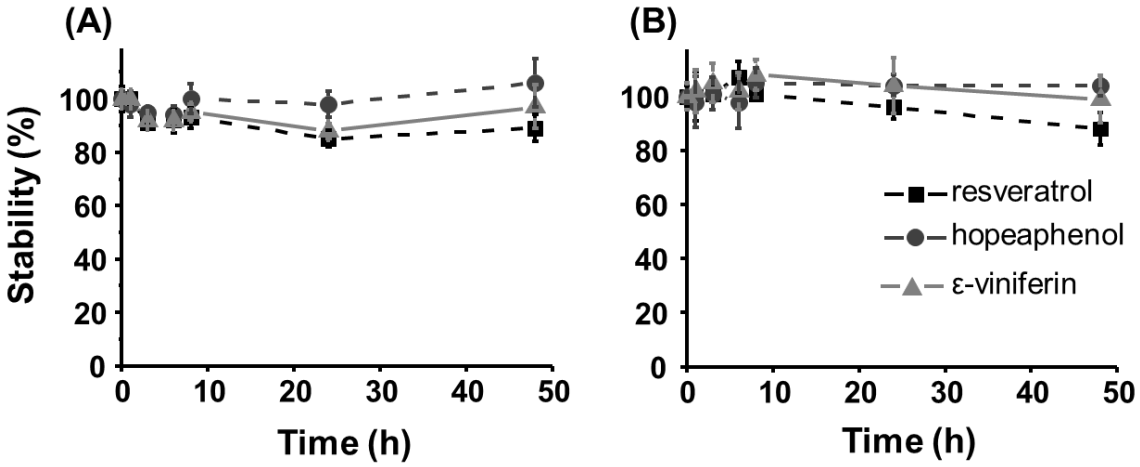

Fig. 3.3: Stability of resveratrol, hopeaphenol, ε-viniferin in cell culture media under cell culture conditions (37 °C, 5% CO_2). (**A**) TRIS-buffered DMEM (**B**) DMEM (CO_3^{2-}-buffered) with 10% FBS.

This is more than sufficient to perform studies on the absorption of these compounds. For the transport studies only FBS-free medium was used, because the non-covalent FBS adducts might hamper the diffusion of the compounds into the cells.

3.3.2 Intestinal absorption of resveratrol, ε-viniferin and hopeaphenol

The intestinal absorption of resveratrol and its oligomers was investigated for each compound individually using the Caco-2 transwell system. Long-term cell cultures of the human colorectal adenocarcinoma cell line Caco-2 show phenotypical similarities to small intestinal epithelium of man. Confluent Caco-2 monolayers grown on permeable membranes have become the standard model for the *in vitro* investigation of the intestinal absorption of xenobiotics [28]. For this reason we used the Caco-2 transwell system to evaluate the bioavailability of resveratrol oligomers in our experiments.

The incubation of resveratrol in the Caco-2 transwell system showed that the compound rapidly crossed the Caco-2 monolayer (Tab. 3.3).

Tab. 3.3: Distribution of 20 µM of each polyphenol after 1, 3 and 6 h incubation in the apical chamber of the Caco-2 transwell system. The table show the absolute amounts (nmol) detected in the apical and basolateral chamber and those of the cell lysates. For the cell culture medium, the amount of the free compound (n=6) and its conjugated form (amount after cleavage-free amount, n=3) is presented. All results are presented as mean ± SD. Moreover, the total recovery of the initially added amount of 10 nmol is calculated.

compartment		**resveratrol**	**ε-viniferin**	**hopeaphenol**
			1 h	
apical	free	4.3 ± 0.26	7.3 ± 0.80	7.5 ± 0.47
	conjugate	0.71 ± 0.50	n.d.	n.d.
basolateral	free	0.99 ± 0.17	n.d.	n.d.
	conjugate	1.2 ± 0.21	n.d.	n.d.
cell lysate	free	0.58 ± 0.01	0.68 ± 0.12	1.1 ± 0.22
	conjugate	0.16 ± 0.03	n.d.	n.d.
Recovery (%)		80 ± 12	80 ± 9.2	86 ± 6.9
			3 h	
apical	free	0.74 ± 0.06	6.1 ± 0.70	6.4 ± 0.36
	conjugate	2.3 ± 0.30	n.d.	n.d.
basolateral	free	1.3 ± 0.14	n.d.	n.d.
	conjugate	4.2 ± 0.45	n.d.	n.d.
cell lysate	free	0.10 ± 0.01	0.86 ± 1.6	2.4 ± 0.64
	conjugate	0.20 ± 0.06	n.d.	n.d.
Recovery (%)		88 ± 10	70 ± 8.3	88 ± 10
			6 h	
apical	free	n.d.	5.6 ± 0.39	5.5 ± 0.47
	conjugate	4.2 ± 0.15	n.d.	n.d.
basolateral	free	0.59 ± 0.08	n.d.	n.d.
	conjugate	4.3 ± 0.16	n.d.	n.d.
cell lysate	free	n.d.	1.6 ± 0.14	3.0 ± 0.13
	conjugate	n.d.	n.d.	n.d.
Recovery (%)		91 ± 3.9	72 ± 5.2	85 ± 6.0

After 1 h incubation 0.99 ± 0.17 nmol of free resveratrol were detected on the basolateral side corresponding to an apparent transport rate of 11.9 ± 0.2 x 10^{-6} cm/s. This rapid and high flux of resveratrol through the cell layer is consistent with earlier studies describing a P_{app} of 11.3-11.9 x 10^{-6} cm/s [29-31]. After three hours of incubation, a slightly higher amount of free resveratrol (1.3 ± 0.14 nmol) was detected, which, after 6 h, decreased to 0.59 ± 0.08 nmol free resveratrol on the basolateral side (Tab. 3.3). This can be explained by the rapid phase II metabolism of resveratrol by the Caco-2 cells. Consistent with this finding, a high amount of resveratrol glucuronides and sulfonates (4.3 nmol ± 0.08) was detected on the basolateral side after 6 h incubation time. This translates to 49% of the added amount of resveratrol passing through the Caco-2 monolayer after 6 h. By contrast, ε-viniferin and hopeaphenol could not be detected on the basolateral side, neither in their free form nor after conjugate cleavage (Tab. 3.3). Taking the limit of detection of the method into account, this corresponds to a P_{app} of lower than 0.3 x 10^{-6} cm/s for ε-viniferin and 1.4 x 10^{-6} cm/s for hopeaphenol. Compounds which are completely absorbed in the human intestine typically exhibit P_{app}-values of >70 x 10^{-6} cm/s in the Caco-2 transwell system, whereas compounds with poor absorption (<20%) have P_{app} values of < 10 x 10^{-6} cm/s [32]. It therefore has to be concluded, that it is unlikely that either resveratrol oligomer will be absorbed from the human intestinal epithelium after dietary intake. Nevertheless, it is impossible to exclude that a low portion of the ingested amount might cross the intestinal barrier, since an extrapolation from the Caco-2 model to the actual *in vivo* situation is not entirely accurate [25].

After 6 h of incubation 43 ± 2% of resveratrol were detected in form of its conjugates in the basolateral chamber, while 42 ± 2% were found conjugated in the apical chamber (Tab. 3.3, Fig. 3.4).

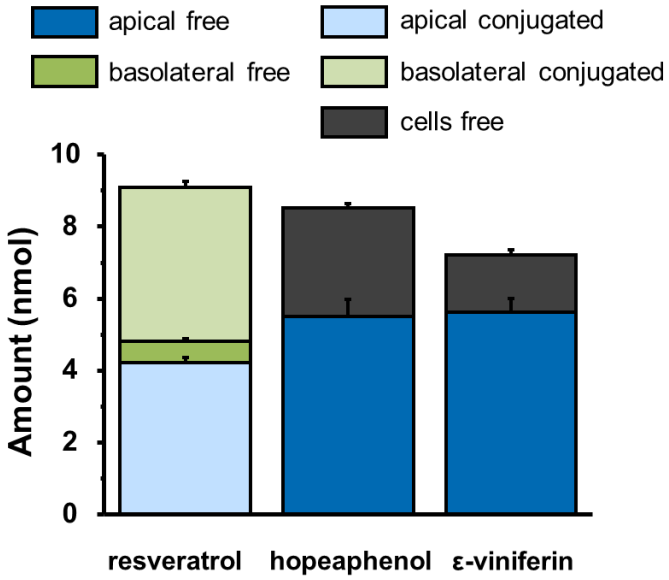

Fig. 3.4: Distribution of the total amount (10 nmol added to the apical chamber) of either free or conjugated polyphenols after 6 h of incubation time in the apical and basolateral chamber as well as in the cell lysate.

Since phase II enzymes are located intracellularly, the resveratrol conjugates detected in the apical compartment must have been released from the Caco-2 cells. It is somewhat striking that the whole amount of resveratrol recovered after 6 h (91%) has been absorbed at least once into the cells. However, no resveratrol or conjugated resveratrol was detected in the cells, indicating an efficient outward transport. This mechanism might be mediated by MRP2 on the apical side and MRP3 on the basolateral side [33, 34].

After 6 h of incubation, a significant portion of the added amount of ε-viniferin and hopeaphenol was found in the cellular fraction (Fig. 3.4). 16 ± 1% of ε-viniferin were found in or on the cell surface and 56 ± 1% could be recovered in the medium on the apical side. An even higher amount of hopeaphenol was found to be in or non-covalently bound on the cells (30 ± 1%), with 55 ± 5% being found in the medium. For both compounds, the cellular levels increased during the incubation period in a time-dependent manner (Tab. 3.3).

The amount of detected resveratrol oligomeres did not increase after conjugate cleavage. Thus, neither ε-viniferin nor hopeaphenol seem to be a substrate for the glucuronosyltransferases and sulfotransferases expressed by Caco-2 cells [35]. This finding supports the high metabolic stability of hopeaphenol towards glucuronidation and the low conjugation rate of ε-viniferin [24]. Slow phase II metabolism may provide a mechanistical explanation why such high amounts of ε-viniferin and hopeaphenol are found in or on the cells. On the contrary, resveratrol, which is an excellent substrate for human glucuronosyl- and sulfotransferases [36, 37] is rapidly conjugated and transported out of the cells.

3.4 Conclusions

Neither ε-viniferin nor hopeaphenol passed the Caco-2 cell monolayer in significant amounts. Together with low concentration in grapes and, wine and other foodstuff, it seems unlikely that a biological relevant amount of these two resveratrol oligomers would cross the human intestinal barrier. As is the case with other fairly large polyphenols such as proanthocyanidins [38, 39], the bioavailability of ε-viniferin and hopeaphenol after dietary intake has to be regarded as low. Since compounds can only elicit biological effects when they reach the cells in their target tissue in sufficiently high concentrations, the overall relevance of the described health-promoting effects of resveratrol oligomers *in vitro* may seem rather limited. However, the high levels of ε-viniferin and hopeaphenol found in or on the Caco-2 cells indicate that the compounds could possibly reach high concentrations in the intestinal epithelium after ingestion of dietary supplements enriched in resveratrol oligomers e.g. extracts from grapevine-shoots. Assuming that these compounds reach the intestine unchanged, one could therefore postulate a potential but locally confined biological activity in the gastrointestinal tract.

3.5 References

[1] Shen T., Wang X.-N., Lou H.-X. *Nat Prod Rep* (2009) 26, 916-935

[2] Sotheeswaran S., Pasupathy V. *Phytochemistry* (1993) 32, 1083-1092

[3] Langcake P., Pryce R. J. *Physio. Plant Pathol* (1976) 9, 77-86

[4] Langcake P., Pryce R. J. *Experientia* (1977) 33, 151-152

[5] Aggarwal B. B., Bhardwaj A., Aggarwal R. S., Seeram N. P., Shishodia S., Takada Y. *Anticancer Res* (2004) 24, 2783-2840

[6] Guebailia H. A., Chira K., Richard T., Mabrouk T., Furiga A., Vitrac X., Monti J. P., Delaunay J. C., Merillon J. M. *J Agric Food Chem* (2006) 54, 9559-9564

[7] Jeandet P., Douillet-Breuil A.-C., Bessis R., Debord S., Sbaghi M., Adrian M. *J Agric Food Chem* (2002) 50, 2731-2741

[8] Vitrac X., Bornet A., Vanderlinde R., Valls J., Richard T., Delaunay J.-C., Merillon J.-M., Teissedre P.-L. *J Agric Food Chem* (2005) 53, 5664-5669

[9] Ha D. T., Kim H., Thuong P. T., Ngoc T. M., Lee I., Hung N. D., Bae K. *J Ethnopharmacol* (2009) 125, 304-309

[10] He S., Lu Y. B., Jiang L. Y., Wu B., Zhang F. Y., Pan Y. J. *J Sep Sci* (2009) 32, 2339-2345

[11] Huang K. S., Lin M., Cheng G. F. *Phytochemistry* (2001) 58, 357-362

[12] Privat C., Telo J. P., Bernardes-Genisson V., Vieira A., Souchard J.-P., Nepveu F. *J Agric Food Chem* (2002) 50, 1213-1217

[13] Ito T., Akao Y., Yi H., Ohguchi K., Matsumoto K., Tanaka T., Iinuma M., Nozawa Y. *Carcinogenesis* (2003) 24, 1489-1497

[14] Kang J. H., Park Y. H., Choi S. W., Yang E. K., Lee W. *J Exp Mol Med* (2003) 35, 467-474

[15] Kim H. J., Chang E. J., Bae S. J., Shim S. M., Park H. D., Rhee C. H., Park J. H., Choi S. W. *Arch Pharm Res* (2002) 25, 293-299

[16] Ohyama M., Tanaka T., Ito T., Iinuma M., Bastow K. F., Lee K.-H. *Bioorg Med Chem Lett* (1999) 9, 3057-3060

[17] Rohaiza S., Yaacob W. A., Din L. B., Nazlina I. Afr. *J Pharm Pharmacol* (2011) 5, 1272-1277

[18] Steinberg P. *Ernährungs-Umschau* (2011) 58, 366-371

[19] Empl M. T., Macke S., Winterhalter P., Puff C., Lapp S., Stoica G., Baumgartner W., Steinberg P. *Vet Comp Oncol* (2012) 9999,

[20] Billard C., Izard J.-C., Roman V., Kern C., Mathiot C., Mentz F., Kolb J.-P. *Leuk Lymphoma* (2002) 43, 1991-2002

[21] Gonzalez-Sarrias A., Gromek S., Niesen D., Seeram N. P., Henry G. E. *J Agric Food Chem* (2011) 59, 8632-8638

[22] Schebb N. H., Huby M., Morisseau C., Hwang S. H., Hammock B. D. *Anal Bioanal Chem* (2011) 400, 1359-1366

[23] Schebb N. H., Inceoglu B., Rose T., Wagner K., Hammock B. D. *Anal Methods* (2011) 3, 420-428

[24] Willenberg I., Brauer W., Empl M. T., Schebb N. H. *J Agric Food Chem* (2012) 60, 7844-7850

[25] Artursson P., Karlsson J. *Biochem Biophys Res Commun* (1991) 175, 880-885

[26] Long L. H., Hoi A., Halliwell B. *Arch Biochem Biophys* (2010) 501, 162-169

[27] Yang N. C., Lee C. H., Song T. Y. *Biosci Biotechnol Biochem* (2010) 74, 63-68

[28] Hubatsch I., Ragnarsson E. G. E., Artursson P. *Nat Prot* (2007) 2, 2111-2119

[29] Kaldas M. I., Walle U. K., Walle T*. J Pharm Pharmacol* (2003) 55, 307-312

[30] Maier-Salamon A., Hagenauer B., Wirth M., Gabor F., Szekeres T., Jager W. *Pharm Res* (2006) 23, 2107-2115

[31] Teng Z. H., Yuan C. J., Zhang F., Huan M. L., Cao W. D., Li K. C., Yang J. Y., Cao D. Y., Zhou S. Y., Mei Q. B. *Plos One* (2012) 7,

[32] Rubas W., Jezyk N., Grass G. *Pharm Res* (1993) 10, 113-118

[33] Kaldas M. I., Walle U. K., Walle T. *J Pharm Pharmacol* (2003) 55, 307-312

[34] Henry C., Vitrac X., Decendit A., Ennamany R., Krisa S., Merillon J.-M. *J. Agric. Food Chem*. (2005) 53, 798-803

[35] van Breemen R. B., Li Y. Expert Opin. *Drug Metab. Toxicol*. (2005) 1, 175-185

[36] Delmas D., Aires V., Limagne E., Dutartre P., Mazue F., Ghiringhelli F., Latruffe N. Transport, stability, and biological activity of resveratrol. In: Resveratrol and Health (2011), pp. 48-59

[37] Saiko P., Szakmary A., Jaeger W., Szekeres T. *Mutat. Res*. (2008) 658, 68-94

[38] Deprez S., Mila I., Huneau J. F., Tome D., Scalbert A. *Antioxid Redox Signal* (2001) 3, 957-967

[39] Zumdick S., Deters A., Hensel A. *Fitoterapia* (2012) 83, 1210-1217

.

Chapter 4

Targeted Metabolomics of the Arachidonic Acid Cascade – Current State and Challenges of LC-MS Analysis of Oxylipins *

Quantification of eicosanoids and oxylipins derived from other polyunsaturated fatty acids in biological samples is crucial for a better understanding of the biology of these lipid mediators. Moreover, a robust and reliable quantification is necessary to monitor the effects of pharmaceutical intervention and diet on the arachidonic acid (AA) cascade, one of today's most relevant drug targets. Low (sub-nanomolar) concentrations and a large number of structurally similar analytes, including regioisomers, require high chromatographic resolution and selective and sensitive mass spectrometry analysis. Currently, reversed phase liquid chromatography in combination with detection on sensitive triple quadrupole instruments, operating in selected reaction monitoring mode, is the main method of quantitative oxylipin analysis. A lack of standardized sample collection, handling and preparation procedures, degradation of the analytes during sample preparation and purity and availability of standards (internal standards) are the major problems of targeted metabolomics approaches of the AA cascade. Major challenges for instrumental analytical methods are the detection of esterified oxylipins and separation and individual detection of oxylipin-isomers. Solving these problems would help to further knowledge of the biology of lipid mediators and is an important task for bio-analytical research.

* Reprinted from *Analytical and Bioanalytical Chemistry*, vol. 407, issue 10, 2015, pp. 2675-2683, Targeted Metabolomics of the Arachidonic Acid Cascade – Current State and Challenges of LC-MS Analysis of Oxylipins, Willenberg I., Ostermann A.I., Schebb N.H., with kind permission from Springer Science and Business Media.

Author contributions: IW: Designed research, performed experiments and wrote manuscript; AIO: Designed research performed experiment, and wrote manuscript; NHS: Designed research and wrote the manuscript.

4.1 Introduction

Lipid mediators have an important function in biology. In particular, eicosanoids (C20) and oxidative products of other long chain polyunsaturated fatty acids (PUFAs) regulate a large variety of cellular and physiological functions [1]. In mammals, these oxylipins are formed enzymatically via three pathways: i) constitutively expressed cyclooxygenase 1 (COX-1) and inducible COX-2, ii) 5-, 12- and 15-lipoxygenases (LOX) and iii) cytochrome P450 monooxygenases (CYP), particularly CYP2J and CYP2C. They are also formed non-enzymatically by (aut)oxidation. The products initially formed can be further converted by several other enzymes, for example by microsomal prostaglandin E synthase (mPGES) or by soluble epoxide hydrolase (sEH) leading to a pleiotropy of oxylipins formed in the arachidonic acid (AA) cascade (Fig. 1.2). In several cases, the product pattern of the four processes overlaps. For example, 15-HETE is not only generated by 15-LOX, but also by COXs and autoxidation, with distinct differences in stereochemistry [2]. Moreover, the route of formation of several mediators has not yet been discoverd, e.g. that of 18-HEPE, being the major hydroxy-FA metabolite in several cultured cells incubated with EPA [3].

More than half of the currently sold pharmaceuticals directly target the AA cascade [4], for example non-steroidal anti-inflammatory drugs (NSAIDs), including aspirin and selective COX-2 inhibitors (e.g. celecoxib), and 5-LOX inhibitors and leukotriene (LT) antagonists. Approximately 30 years after the Nobel Prize to J. Vane, S. Bergström and B. Samuelsson for the discovery of the importance of prostaglandins (PGs), the biological functions of non-classical eicosanoids and oxylipins other than PGs and LT are becoming clearer. For example, multiple hydroxylated docosahexaenoic acids (DHA) and EPAs have been discovered as a new class of inflammation resolving lipid mediators [5, 6]. The vasodilatory action of epoxy-FAs (Fig. 1.2) on endothelial cells is well established and a large number of studies describe anti-inflammatory and analgesic effects, although an epoxy-FA receptor has not been discovered.

Although AA, DHA and EPA-derived epoxides have similar biological activity, the effects in cancer are different, with AA derived epoxy eicosatrienoic acids (EpETrEs) promoting angiogenesis, whereas n3-PUFA derived epoxides suppress tumor growth [7].

To investigate and understand the function of the many different oxylipins in physiology, analytical methods are needed to quantify their levels in biological samples. The most promising strategy is the parallel quantification of a comprehensive pattern of products of the AA cascade derived from both n6-PUFAs, for example AA, and n3-PUFAs, for example EPA and DHA. By monitoring the activity of an enzyme or pathway of the cascade using several products instead of only one main product, the up and down regulation of distinct pathways can be deduced with higher certainty. Moreover, routes of formation and crosstalk between the branches of the AA cascade can be determined [8]. Because many pharmaceuticals modulate the AA cascade, quantification of oxylipins is also crucial for the determination of *in vivo* target engagement of established drugs, for example aspirin, and new experimental drugs, for example sEH inhibitors. This article briefly summarizes the current state of LC-MS based targeted metabolomics of the AA cascade and focusses on the challenges of the quantification of oxylipins in biological matrices.

4.2 Current state of oxylipin analysis

4.2.1 Instrumental analysis

Current targeted metabolomics LC-MS approaches for the AA cascade have impressive characteristics: One method enables parallel analysis of 141 lipid mediators derived from different n6- and n3-FAs. Of these, 102 can be quantified against standards using 30 stable isotope labelled internal standards (IS) in a run time of only 25 min with high sensitivity (limit of detection (LOD) 0.1-1 pg on column) [9]. Several other approaches have similar performance,

e.g. parallel quantification of 104 oxylipins with the use of 11 IS in 26 min and LODs between 1.8 and 340 pg on column [10], or quantification of 88 analytes (6 IS) in 21 min and LOQs between 0.06 and 15.96 pg on column [4, 11, 12]. For methods established in other labs the total number of covered analytes is not clear because the articles are focused on groups of analytes, e.g. resolvins, or only report oxylipins above the LOQ [5, 13, 14]. However, analysis times (of about 25 minutes) and sensitivities (LODs between 0.01 and 0.21 pg on column) are comparable [5, 13, 14].

All of these methods use reversed phase (RP) LC coupled to a highly sensitive triple-quadrupole (QqQ) MS instrument using negative electrospray ionization (ESI) of the slightly acidic analytes (fatty acid derivatives). For the analysis of oxylipins in biological samples the following challenges have to be addressed by the LC-MS method: (i) low (< nM) concentration of the analytes, (ii) huge concentration differences between the least and the most abundant oxylipin within a single sample (>103-fold), requiring a broad linear detector response [15, 16], (iii) correct identification of the LC-MS peaks and (iv) simultaneous quantification of a multitude of chemically and structurally similar analytes with numerous isomers present in all samples, e.g. regioisomers of hydroxy-FAs or PGE_2 and PGD_2 (Fig. 1.2). Although the sensitivity and linear detector response of modern QqQ-MS fulfill the demands of i-ii, confirming the identity of the analytes (iii) requires meaningful fragment spectra to be obtained [14, 17]. Because all oxylipins can occur in form of several isomers, identification only by retention time and selected reaction monitoring (SRM) of the analyte's transition can lead to false conclusions. Therefore, many groups use QTRAP instruments for oxylipin analysis, enabling operating the second analytical quadrupole to be operated as a linear ion trap to obtain high quality fragment spectra. Selective detection (iv) requires both, a highly efficient chromatographic separation and detection in SRM mode. This can be observed for the analysis of 8-, 9- and 12-HETE (Fig. 1.2, Fig. 4.1). Despite high chromatographic resolution using a modern <2µm particle filled column, 8- and 12-HETE coelute. In consequence, quantification can only be achieved by detecting unique fragment ions in SRM.

For 9- and 12-HETE the opposite is true: The MS/MS spectra of both compounds are very similar and provide no specific SRM transitions. Therefore, these hydroxy-FAs have to be separated chromatographically.

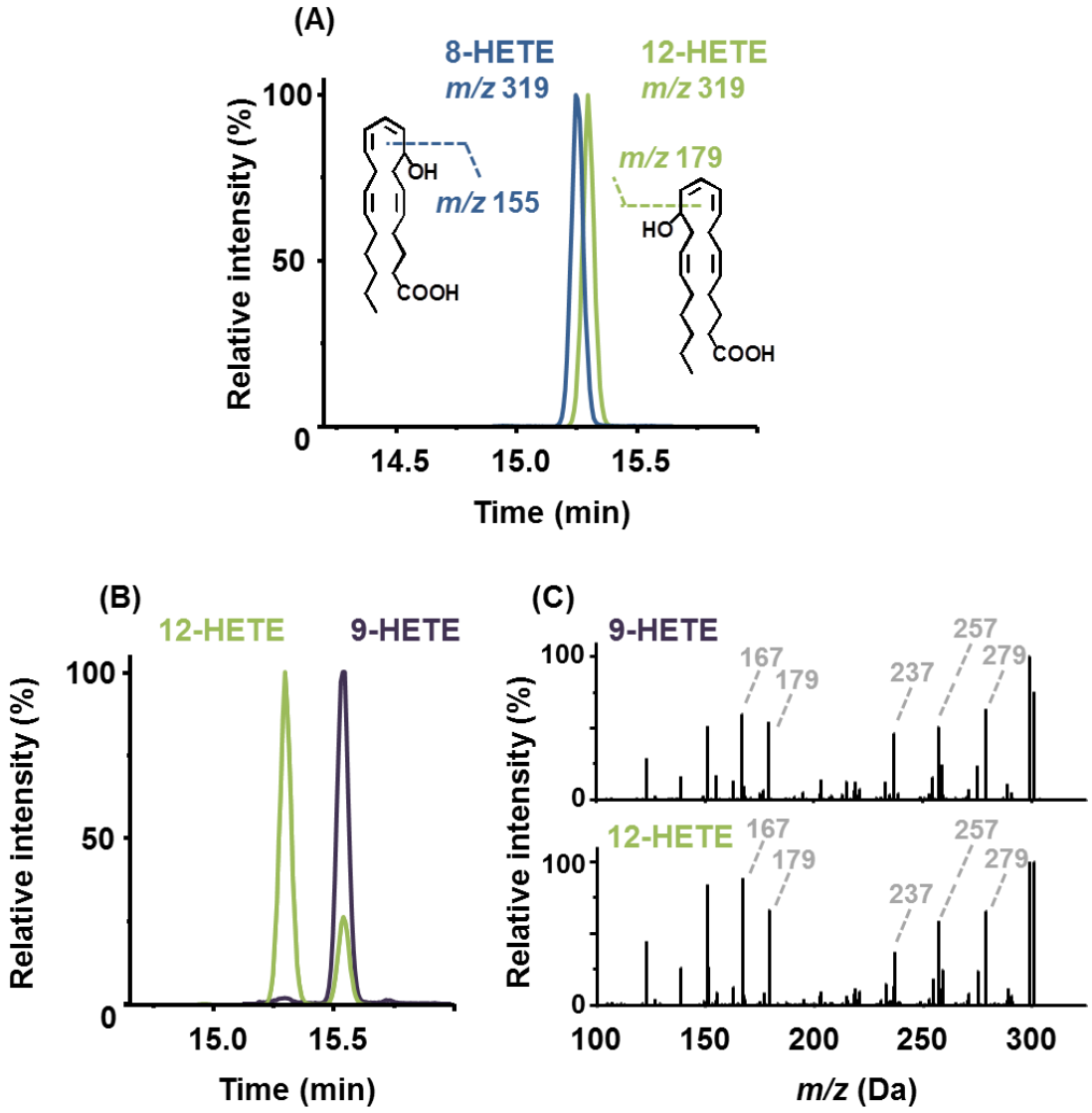

Fig. 4.1: Separation of regioisomers of hydroxy-AA (8-, 9- and 12-HETE) by means of RP-18 LC and ESI-MS/MS. (**A**) Co-elution of 8- and 12-HETE which can be detected independently, based on specific SRM transitions. (**B**) Chromatographic separation of 9- and 12-HETE. Both show interfering SRM transitions because of almost identical collision induced dissociation MS/MS spectra of their $[M\text{-}H^{+}]^{-}$ ions (**C**).

The narrow oxylipin peaks resulting from modern LC-methods require rapid switching times and sensitivity at short dwell times of the MS. To keep cycle

times of the MS short, but simultaneously providing enough data points per peak, all current methods use software assisted features for example scheduled or dynamic multiple reaction monitoring (MRM). Nevertheless, the narrow elution windows of a large number of analytes still require dwell times of less than 10 ms. It will be interesting if other MS detector types become available for targeted oxylipin analysis. High resolution MS (HRMS) could improve signal to noise ratio, but does not enable the numerous constitution isomers to be distinguished, meaning detection in SRM mode is mandatory for this analysis. It will be interesting to determine whether modern qTOF instruments can provide sufficient sensitivity and linear detector response. For orbitrap instruments, the major question is whether the cycle time for SRM detection could be short enough for quantification of the narrow LC peaks. The first report of oxylipin analysis using an orbitrap instrument is promising: The comparison of the quantitative performance between the orbitrap and a QqQ-MS showed similar results with respect to linear detection ranges, with LODs for the orbitrap ranging between 10 and 30 pg of the oxylipins [18]. If these instruments proof able to match the rapid, sensitive and robust quantification of QqQ-MS, the combination of quantification with HRMS and continous detection of fragment spectra would greatly enhance instrumental oxylipin analysis.

As well as improvements to LC-MS instruments, derivatization could lead to better separation efficacy and particularly improved MS detection. Gelb and coworkers introduced a derivatization strategy which converts the carboxy moiety of the oxylipins to an amide with positively charged N-(4-aminomethyl-phenyl) pyridinium (AMPP) [19], enabling detection in positive ESI mode. This strategy could also improve sensitivity on today´s instruments, although they have a more efficient ion transmission in negative ESI than the instruments used by Gelb and coworkers.

Derivatization to pentafluorobenzyl (PFB) esters was used by Blair and Coworkers allowing efficient normal phase chiral separation of oxylipins (see below). Furthermore, dedicated ion formation by electron capture atmospheric

pressure chemical ionization (APCI) increased both selectivity and sensitivity through decreasing background signals [2]. APCI is generally acknowledged to be less prone to matrix effects compared to ESI. Hence, a similar derivatization is promising to circumvent the massive problems resulting from ion suppression in RP-LC-ESI(-)-MS of oxylipins in biological samples [12]. New derivatization agents with specific ionization, e.g. electrochemistry-assisted ionization [20], or novel ionization techniques, for example dielectric barrier discharge ionization-MS [21], could further improve selectivity, sensitivity and robustness of oxylipin detection by mass spectrometry.

4.2.2 Sample preparation

Extraction of free oxylipins from a biological matrix, like plasma or tissues, is not trivial. The analytes have a broad polarity range and are prone to degradation by autoxidation (all oxylipins) and by base (PGs) or acid (epoxy-FAs) treatment. When analyte concentrations are well above the LOQ of the instrument – which is rarely the case – it is possible to directly inject the sample after dilution and/or protein precipitation with or by organic solvents. However, most analyses require pre-concentration. For this purpose liquid-liquid extractions (LLE) [22] or most frequently solid phase extractions (SPE) [4, 9, 10, 13, 14] are used. In contrast to similar instrumental analyses of oxylipins, SPE procedures differ substantially from lab to lab. Stationary phases range from RP-18 [14] and mixed mode phases with RP-8 and anion exchange properties [13] to polymeric phases [4, 9, 10]. As might be expected, these methods have a dissimilar performance leading to different oxylipin patterns for the same sample, particularly for epoxy-FAs (Fig. 4.2) [12]. The ESI-interfering matrix in plasma is most efficiently removed by specific SPE procedures using anion exchange stationary phases [13] (carboxy acid moiety of the oxylipins) or polar and non-polar washing steps (water and *n*-hexane) before elution of the medium to non-polar oxylipins with methyl formate on the tC-18 column [14]. The latter procedure on classical RP material overall outperforms the other procedures,

with respect to recovery of IS, reduction of ion suppressing matrix and extraction efficacy of oxylipins from the biological matrix (Fig. 4.2).

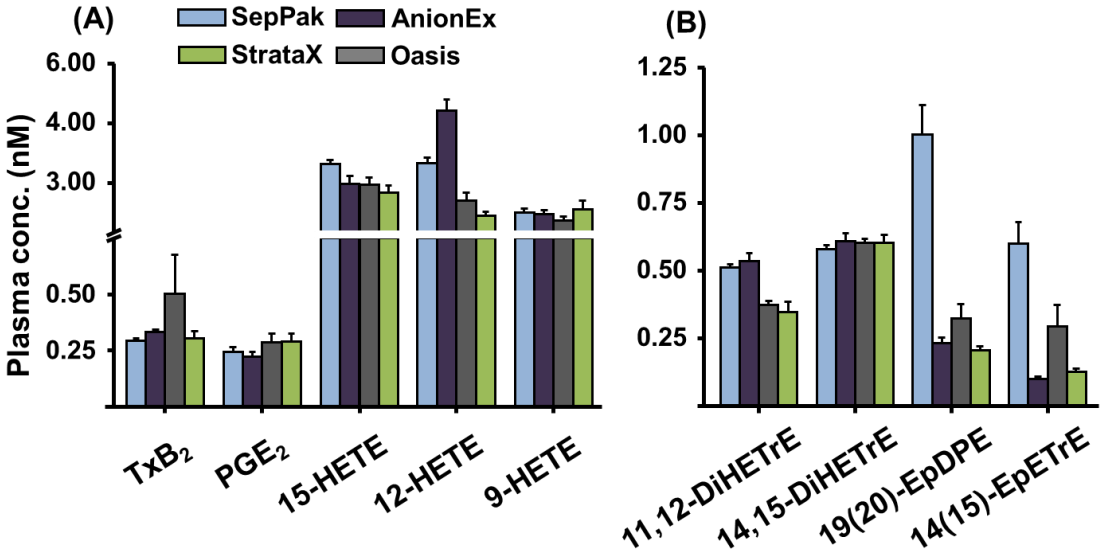

Fig. 4.2: Concentrations of selected oxylipins in pooled human EDTA plasma using different well established solid phase extraction (SPE) methods for sample preparation: (**A**) prostanoides and hydroxy-FA of AA and (**B**) dihydroxy-FAs and epoxy-FAs of AA and DHA. All results are shown as mean ± SD (n=5). The following protocols were used: SepPak – tC18 phase, washing with water and n-hexane, elution with methyl formiate [14]; AnionEx – C8 phase with anion exchange properties, washing with methanol/water (v:v, 1:1), elution with ethyl acetate/n-hexane (75:25) acidified with 1% acetic acid [13]; StrataX – polymeric phase with polar groups washing with 10% methanol, elution with methanol [9]; Oasis – polymeric phase with polar groups, washing with 5% methanol acidified with 0.1% acetic acid, subsequent elution with methanol and ethyl acetate [4].Instrumental analysis was carried out as described [4, 11]. The complete evaluation of the performance of the procedures can be found in [12].

An adequate sample preparation which eliminates as much matrix as possible is essential because insufficient removal of interfering matrix compounds is highly problematic for quantitative oxylipin analysis: In all methods, a single internal standard (IS) is used for a whole group of structurally similar analytes eluting at different retention times. Thus, the IS cannot compensate for all matrix effects, leading to matrix dependent over- and under-calculations of the oxylipin concentration. In addition to further optimization of the sample preparation procedures, the availability and use of more heavy isotope labeled

IS would much improve robustness, accuracy and precision of oxylipin analysis in biological samples.

4.3 Pitfalls and Limitations

4.3.1 (Biological) variation of oxylipin concentration

Reports on human serum and plasma oxylipin concentrations document strong (interindividual) variations between samples from different subjects [15, 23]. These variations impede the recognition of biologically significant differences in lipid mediator levels between groups of different (patho)physiological conditions. Moreover, significant effects of pharmacological or nutritional intervention can vanish within high standard deviations and/or standard errors. Part of the variation is obviously based on biological differences, e.g. different habits of human subjects. For example physical exercise elicits change in the systemic levels of epoxy- and dihydroxy-FAs [24]. Little is known about the changes in oxylipins during the circadian rhythm; however it is clear that the nutritional status strongly affects the levels of circulating lipids and lipid mediators. Even a single moderate dose of n3-PUFA causes changes in plasma hydroxy-, epoxy- and dihydroxy-FA levels [25]. Thus, sample collection from human subjects should be as standardized as possible (e.g. fixed fasting period, day time, physical activity).

Another major problem contributing to poor precision in the analysis of biological samples is the formation and degradation of oxylipins after sample collection. Even short storage of blood before further processing has massive effects on the plasma concentration of several oxylipins (Fig. 4.3). Moreover, if the sample sits for few minutes in the centrifuge, after centrifugation and before the plasma is collected and frozen, the levels of some oxylipins are significantly reduced (appendix Fig. 11.4).

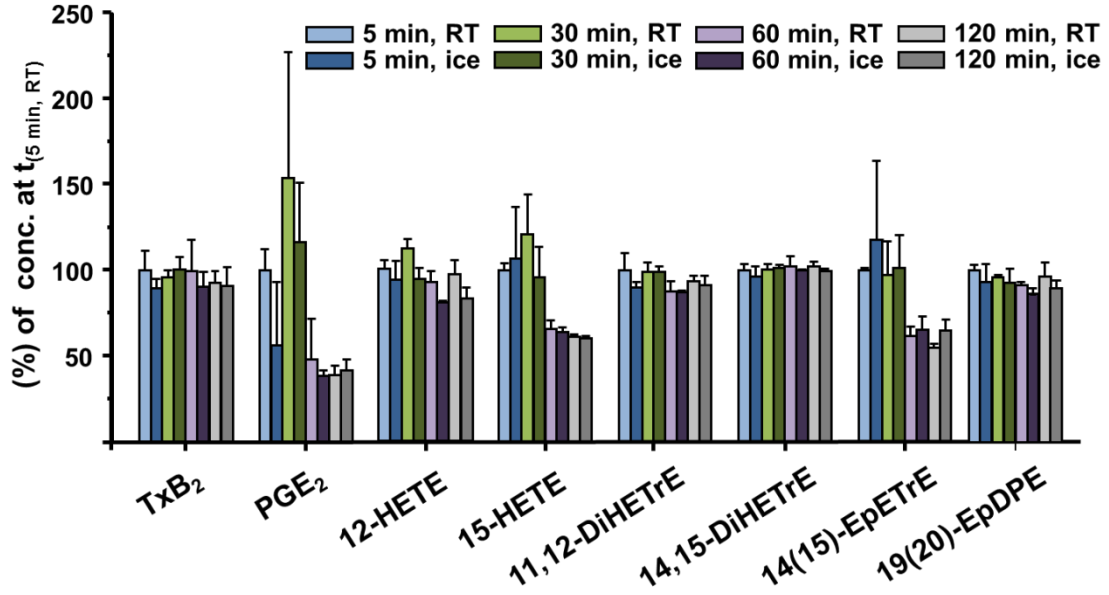

Fig. 4.3: *Ex-vivo* degradation/formation of oxylipins in human whole blood after blood withdrawel. Blood of a healthy human volunteer was collected in EDTA tubes, pooled and left for 5 min, 30 min, 60 min or 120 min either at room temperature (RT) or on ice. After centrifugation (1200 g, 15 min, 4 °C), the plasma was immediately frozen (-80 °C) and the oxylipin concentration was analyzed within 5 days (Oasis SPE [4, 11, 12]). The resulting concentrations after different periods of time in sample preparation are compared to those with direct sample preparation (t(5min, RT)). The results clearly show, that after 60 min storage of whole blood the levels of several oxylipins are massively reduced (e.g. 15-HETE and 14(15)-EpETrE) while other analytes are formed *ex-vivo* (e.g. PGE_2). Shown are mean ± SD (n=4). More results about the effect of storage during sample preparation of human blood can be found in appendix (Fig. 11.1, Fig. 11.2, Fig. 11.3).

Prolonged storage in the freezer can also lead to degradation and loss of the analytes as revealed for several DHA and EPA derived resolvins and prostanoides [5]. In a few studies COX and sEH inhibitors as well as protease and esterase inhibitors are added to the samples to prevent enzymatic formation and/or degradation [26]. More frequently antioxidants, for example radical scavenging butylated hydroxytoluene (BHT) and chelating ethylenediaminetetraacetic acid (EDTA), are used to prevent oxylipin degradation or formation (e.g. 11-HETE, 9-HETE, isoprostanes) by autoxidation during sample preparation [4, 10, 11, 26]. However, the benefit of these procedures has not yet been systematically evaluated for a comprehensive set of oxylipins. Overall, artificial (*ex-vivo*) formation and/or degradation of the lipid

mediators is one of the major challenges in the analysis of biological samples which can only be addressed by strict standard operating procedures (SOPs) including rapid sample processing and optimized storage conditions (-80 °C, short time). For few oxylipins, *ex-vivo* formation and/or degradation can be excluded and/or measured by additional determination of their endogenously formed metabolites, e.g. 11-dehydro-TxB_2 [27] together with TxB_2 or bicycloprostaglandin E_2 as stable degradation product of PGE_2 [28].

4.3.2 Plasma or serum?

Both, plasma and serum should be regarded as appropriate matrices for quantitative oxylipin analysis of circulating oxylipins [5, 16]. For plasma, the anticoagulant should be chosen carefully: EDTA seems to be the best choice because for example heparin is known to cause artifacts [29]. For serum it has to be kept in mind that coagulation is in part mediated by the AA cascade and causes massive (*ex-vivo*) formation of several oxylipins including TxB_2 and 12-HETE (Fig. 1.2). Moreover, detectability of low concentrated mediators, for example resolvins is improved [5]. Regarding variability, it remains to be evaluated whether plasma or serum enables the determination of oxylipin concentrations in blood with a higher precision.

4.3.3 Accuracy and inter-lab comparability

In addition to high intersample variations, huge differences between the mean concentrations of the lipid mediators were found in different studies, e.g. for human plasma or serum (summarized in [15]). This indicates that the accuracy of current methods is a further problem. Because of the above summarized difficulties of oxylipin analysis and their nature as endogenously formed lipid mediators (biomarkers), validation procedures as suggested for drugs, e.g. by European Medicines Agency (EMA), are not or only in part applicable. With respect to accuracy, current methods have been used to determine, for example, the recovery in spiked plasma [10] or in (matrix free) saline phosphate

buffer [4]. Interestingly, others failed to recover oxylipins from buffer, probably because of low solubility of oxylipins in the aqueous solution [10]. Regardless of how rigid recovery rates in (spiked) quality control samples are determined, the quantification relies on the availability and purity of reference standards. In most cases these compounds have to be synthetized or are obtained commercially (currently from a single company). For the latter, the affordable quantities are so low that purity cannot be checked by standard chemical methods. Thus, a mistake in the concentration provided by the manufacturer leads directly to systemic errors. Matching LC-MS response from batch to batch and comparing peak areas of regioisomers in selected ion monitoring mode under isocratic LC conditions are the only possible ways to verify manufacturer information. To improve quality of the results in the future it will be important to agree on criteria which have to be fulfilled for a fit-for-purpose-validation in oxylipin analysis. With an exchange of samples, standards between groups and inter-laboratory tests this would help improve comparability.

4.4 Analytical challenges

4.4.1 The free, the bound, and the total… – or the analytical challenge in detecting esterified oxylipins

Although a significant portion of oxylipins is incorporated in lipids, it is believed that their paracrine and autocrine action is mainly mediated by their free, i.e. non-esterified form [16]. The esterified (bound) oxylipins can readily be liberated, e.g. by phospholipases [30]. In plasma, the concentrations of esterified epoxy-FAs and hydroxy-FAs exceed the concentrations of the free ones by approximately 50 to 350-fold and 10 to 40-fold, respectively [13, 16]. Esterified oxylipins are commonly quantified after saponification (base hydrolysis) [13, 16, 31-33]. For this purpose, the samples are incubated with sodium hydroxide (1.00-3.75 M) either overnight at 4 °C [31] or at 60 °C for 20-30 min [13, 16]. Other methods incubate the extracted lipids with 0.1 M

sodium carbonate at 4 °C overnight [33] or perform transesterification of lipids to methyl esters (0.35 M sodium methoxide solution for 60 min at 60 °C) with subsequent hydrolysis by the addition of water (60 min) [32]. The performance of the different cleavage-procedures has not been systematically compared. However, alkaline treatment degrades a large number of oxylipins, particularly PGs, e.g. β-hydroxy-keto prostanoids, e. g. PGE_2, PGD_2, or thromboxanes [31, 32] and thus information on their concentration is lost. Harsh alkaline treatment could even lead to the formation of conjugated FAs from PUFAs [34] and thus is prone to produce artifacts of the polyunsaturated analytes. In contrast, a moderate saponification could lead to incomplete liberation of esterified oxylipins. All current cleavage techniques yield a combined sum of free and esterified oxylipins and provide no information on how the analytes are bound in the samples. Yet, it is highly relevant to know whether a mediator is bound to the sn2-position of a phospholipid of the cell membrane, and thus rapidly releasable by phospholipases upon inflammatory stimuli or if it is bound in a triacylglyceride (fat) with unknown biological fate. One way of addressing this problem would be to separate the different lipid classes of a lipid extract before hydrolysis, as commonly performed for fatty acid analysis [35]. Another possibility is the direct detection of the esterified oxylipins, as recently successfully performed, e.g. for C16:0/12-HETE-phosphatidylethanolamine [36]. Combining all oxylipins and possible lipids results in a fairly large number of analytes. Thus, the integration of targeted oxylipin metabolomics in lipidomics is one of the biggest challenges for analytical chemistry of oxylipins. However, the low (total) concentration of the lipid mediators makes it doubtful whether the sensitivity of today´s instruments is sufficient for their detection if they are distributed in several individually detected lipids.

4.4.2 Detection of stereoisomers

A major task for instrumental analytical methods, and one which is important to address, is the differentiation between stereochemical configurations. *Cis-trans* isomers of epoxides (Fig. 1.2) can be well resolved by RP chromatography.

The enzymatically formed *cis*-isomers elute first, followed by the *trans*-epoxides formed by (aut)oxidation [37] (same SRM transition as the *cis*-isomer, eluting 1-3 min later). Although quite large peaks of *trans*-epoxides are found in biological samples, particularly after conjugate cleavage, these metabolites are not included in most current methods. Thus, the concentrations of *trans*-epoxides are not evaluated, which makes it impossible to assess their effect as lipid mediators. In particular, the important question of whether and to what extend *trans*-epoxy-FAs contribute to the biological effects attributted to *cis*-epoxy-FAs cannot be evaluated.

The robust and efficient RP chromatography fails to separate formed enantiomers. Thus, for example the lipid mediator referred to as 14(15)-EpETrE (or 14(15)-EET), is in fact 4 compounds, which are generated via CYP conversion and (aut)oxidation processes and can be hydrolyzed by sEH at isomer specific rates [37] (Fig. 1.2). With the exception of the epoxides, almost all oxylipins are chiral, and have different biological activity.

Whereas enzymatic routes form products at a distinct enantiomer ratio, aut(oxidation) processes result in the formation of racemats. Therefore, chiral separation can be very helpful to differentiate between the routes of formation. Moreover, in several cases, different enzymatic routes of formation can be distinguished on the basis of the enantiomer ratio, e.g. (±)15-HETE (Fig. 1.2). Whereas the formation of 15-(*S*)-H(p)ETE is catalyzed by 15-LOX, 15(*R*)-H(p)ETE is formed by aspirin acetylated COX-2 [2]. As revealed for this example, chiral separation would greatly assist in distinguishing the route of formation of the lipid mediators which is poorly understood for several oxylipins, e.g. for the dominantly formed and bioactive 18-HEPE (Fig. 1.2). Several chiral chromatographic separation methods have been developed as recently summarized by Mesaros and Blair [19]. However, because chiral-LC cannot achieve the robustness and (overall) separation power of RP chromatography, it is comparatively rarely used. Thus, targeted oxylipin metabolomics would greatly benefit from progress in chiral LC-MS approaches [38]. A promising

further tool for enantiomer separation might be ion mobility spectrometry using a chiral modifier [39] at the front end of the MS or (chiral) supercritical fluid chromatography. Of all challenges for instrumental analytical chemistry mentioned in this article, the integration of chiral separation in the routinely used targeted metabolomics techniques would have the largest effect on our understanding of the biology of oxylipins. With the data resulting from these methods, one could not only monitor the activity of distinct enzymatic and (aut)oxidative pathways *in vivo*, but also identify the biologically most active isomers.

4.5 Conclusions

Highly sensitive LC-MS methods have been developed which enable an impressive understanding of the biological importance of the lipid mediators formed in the AA cascade. However, numerous questions remain to be answered, e.g. determining the mechanisms of the effects of dietary n3-PUFA intake on human health. Comprehensive investigation of hydroxy-n3-PUFAs, resolvins and n3-epoxides by methods summarized in this article, could enable researchers to address this question.

With today´s “ultra-high-performance” liquid chromatography and high end QqQ-MS the instrumentation for highly sensitive and specific detection of oxylipins is available. Moreover, new HRMS instruments entering the field may bring about much progress in targeted lipid mediator analysis. With these instruments it is easy to generate peaks, areas and numbers. However, it will still be a challenge to obtain meaningful results, i.e. accurate concentrations in biological samples. In particular, the optimization of sample collection, stabilization and preparation seems to be required. With respect to instrumental analysis the greatest challenges are the differential detection of stereoisomers and analysis of esterified oxylipins. To achieve this progress in targeted oxylipin metabolomics, it is crucial that analytical chemistry is regarded as an integral part of medical and biological research. Thoroughly developed methods and

their continuous improvement require time and (grant) money. Although, not all method developments may address fundamental scientific questions (such as the detection of esterified oxylipins), in particular improvements to sample preparation, a fit-for-purpose validation and interlab comparison seem to be of particularly high importance for the field.

4.6 References

[1] Buczynski M. W., Dumlao D. S., Dennis E. A. *J Lipid Res* (2009) 50, 1015-1038

[2] Mesaros C., Blair I. A. *Metabolites* (2012) 2, 337-365

[3] Ostermann A. I., Willenberg I., Weylandt K. H., Schebb N. H. *Chromatographia* (2015) 78, 415-428

[4] Yang J., Schmelzer K., Georgi K., Hammock B. D. *Anal Chem* (2009) 81, 8085-8093

[5] Colas R. A., Shinohara M., Dalli J., Chiang N., Serhan C. N. *Am J Physiol Cell Physiol* (2014),

[6] Serhan C. N., Dalli J., Colas R. A., Winkler J. W., Chiang N. *Biochim Biophys Acta* (2014),

[7] Zhang G., Kodani S., Hammock B. D. *Prog Lipid Res* (2014) 53, 108-123

[8] Yang J., Dong H., Hammock B. D. *Curr Opin Lipidol* (2011) 22, 197-203

[9] Dumlao D. S., Buczynski M. W., Norris P. C., Harkewicz R., Dennis E. A. *Biochim Biophys Acta* (2011) 1811, 724-736

[10] Strassburg K., Huijbrechts A. M., Kortekaas K. A., Lindeman J. H., Pedersen T. L., Dane A., Berger R., Brenkman A., Hankemeier T., van Duynhoven J., Kalkhoven E., Newman J. W., Vreeken R. J. *Anal Bioanal Chem* (2012) 404, 1413-1426

[11] Inceoglu B., Wagner K. M., Yang J., Bettaieb A., Schebb N. H., Hwang S. H., Morisseau C., Haj F. G., Hammock B. D. *Proc Natl Acad Sci U S A* (2012) 109, 11390-11395

[12] Ostermann A. I., Willenberg I., Schebb N. H. *Anal Bioanal Chem* (2015) 407, 1403-1414

[13] Fischer R., Konkel A., Mehling H., Blossey K., Gapelyuk A., Wessel N., von Schacky C., Dechend R., Muller D. N., Rothe M., Luft F. C., Weylandt K., Schunck W. H. *J Lipid Res* (2014) 55, 1150-1164

[14] Yang R., Chiang N., Oh S. F., Serhan C. N. *Curr Protoc Immunol* (2011) Chapter 14, Unit 14 26

[15] Schuchardt J. P., Schmidt S., Kressel G., Dong H., Willenberg I., Hammock B. D., Hahn A., Schebb N. H. *Prostag Leukotr Ess* (2013) 89, 19-29

[16] Schebb N. H., Ostermann A. I., Yang J., Hammock B. D., Hahn A., Schuchardt J. P. *Prostag Oth Lipid M* (2014),

[17] Harkewicz R., Fahy E., Andreyev A., Dennis E. A. *J Biol Chem* (2007) 282, 2899-2910

[18] Masoodi M., Eiden M., Koulman A., Spaner D., Volmer D. A. *Anal Chem* (2010) 82, 8176-8185

[19] Bollinger J. G., Thompson W., Lai Y., Oslund R. C., Hallstrand T. S., Sadilek M., Turecek F., Gelb M. H. *Anal Chem* (2010) 82, 6790-6796

[20] Seiwert B., Karst U. *Anal Bioanal Chem* (2008) 390, 181-200

[21] Gilbert-Lopez B., Geltenpoth H., Meyer C., Michels A., Hayen H., Molina-Diaz A., Garcia-Reyes J. F., Franzke J. *Rapid Commun Mass Spectrom* (2013) 27, 419-429

[22] Fromel T., Jungblut B., Hu J., Trouvain C., Barbosa-Sicard E., Popp R., Liebner S., Dimmeler S., Hammock B. D., Fleming I. *Proc Natl Acad Sci U S A* (2012) 109, 9995-10000

[23] Nording M. L., Yang J., Georgi K., Hegedus Karbowski C., German J. B., Weiss R. H., Hogg R. J., Trygg J., Hammock B. D., Zivkovic A. M. *Plos One* (2013) 8, e76575

[24] Giordano R. M., Newman J. W., Pedersen T. L., Ramos M. I., Stebbins C. L. *Int J Sport Nutr Exerc Metab* (2011) 21, 471-479

[25] Schuchardt J. P., Schneider I., Willenberg I., Yang J., Hammock B. D., Hahn A., Schebb N. H. *Prostaglandins Other Lipid Mediat* (2014) 109-111, 23-31

[26] Balvers M. G. J., Verhoeckx K. C. M., Bijlsma S., Rubingh C. M., Meijerink J., Wortelboer H. M., Witkamp R. F. *Metabolomics* (2012) 8, 1130-1147

[27] Tsikas D., Zoerner A. A. *J Chromatogr B* (2014) 964, 79-88

[28] Granstrom E., Hamberg M., Hansson G., Kindahl H. *Prostaglandins* (1980) 19, 933-957

[29] Goodfriend T. L., Pedersen T. L., Grekin R. J., Hammock B. D., Ball D. L., Vollmer A. *Prostaglandins Leukot Essent Fatty Acids* (2007) 77, 363-366

[30] Shearer G. C., Newman J. W. *Curr Atheroscler Rep* (2009) 11, 403-410

[31] Shearer G. C., Harris W. S., Pedersen T. L., Newman J. W. *J Lipid Res* (2010) 51, 2074-2081

[32] Gladine C., Newman J. W., Durand T., Pedersen T. L., Galano J. M., Demougeot C., Berdeaux O., Pujos-Guillot E., Mazur A., Comte B. *Plos One* (2014) 9, e89393

[33] Morisseau C., Inceoglu B., Schmelzer K., Tsai H. J., Jinks S. L., Hegedus C. M., Hammock B. D. *J Lipid Res* (2010) 51, 3481-3490

[34] Holman R. T., Burr G. O. *Arch of Biochem* (1948) 19, 474-482

[35] Kaluzny M. A., Duncan L. A., Merritt M. V., Epps D. E. *J Lipid Res* (1985) 26, 135-140

[36] Morgan A. H., Hammond V. J., Morgan L., Thomas C. P., Tallman K. A., Garcia-Diaz Y. R., McGuigan C., Serpi M., Porter N. A., Murphy R. C., O'Donnell V. B. *Nat Protoc* (2010) 5, 1919-1931

[37] Jiang H. L., McGiff J. C., Quilley J., Sacerdoti D., Reddy L. M., Falck J. R., Zhang F., Lerea K. M., Wong P. Y. K. *Journal of Biological Chemistry* (2004) 279, 36412-36418

[38] Ward T. J., Ward K. D. *Anal Chem* (2010) 82, 4712-4722

[39] Kanu A. B., Dwivedi P., Tam M., Matz L., Hill H. H., Jr. *J Mass Spectrom* (2008) 43, 1-22

Chapter 5

Effect of Acute and Chronic DSS Induced Colitis on Plasma Eicosanoid and Oxylipin Levels in the Rat *

Eicosanoids and oxylipins are potent lipid mediators involved in the regulation of inflammation. In order to evaluate their role and suitability as biomarkers in colitis, we analyzed their systemic levels in the acute and chronic phase of dextran sulfate sodium (DSS) induced colitis. Male Fischer 344 rats were treated in three cycles with 4% DSS in the drinking water (4 days followed by 10 days recovery) and blood was drawn three days prior to the first DSS treatment and on day 4, 11, 32 and 39. Histopathological evaluation of the colon tissue after 42 days showed that the animals developed a mild to severe chronic colitis. Consistently, prostaglandin levels were massively (2-fold) elevated in the colonic tissue. LC-MS based targeted metabolomics was used to determine plasma oxylipin levels at the different time points. In the acute phase of inflammation directly after DSS treatment, epoxy-fatty acid (FA), dihydroxy-FA and hydroxy- FA plasma concentrations were uniformly elevated. With each treatment cycle the increase in these oxylipin levels was more pronounced. Our data suggest that in the acute phase of colitis release of polyunsaturated FAs from membranes in the inflamed tissue is reflected by an uniform increase of oylipins formed in different branches of the arachidonic acid cascade. However, during the recovery phases the systemic oxylipin pattern is not or only moderately altered and does not allow to evaluate the onset of chronic inflammation in the colon.

* Reprinted from *Prostaglandins & Other Lipid Mediators*, Willenberg I., Ostermann A.I., von Keutz A., Steinberg P., Schebb N.H., Effect of Acute and Chronic DSS Induced Colitis on Plasma Eicosanoid and Oxylipin Levels in the Rat, doi:10.1016/j.prostaglandins.2015.04.002, Copyright (2015), with permission from Elsevier.

Author contributions: IW: Designed research, performed experiments and wrote manuscript. AIO: Designed research, performed experiments; AvK: Performed experiments; PS: Designed research and wrote the manuscript; NHS: Designed research and wrote the manuscript.

5.1 Introduction

Ulcerative colitis (UC) is a chronic, tissue-destructive disease with unknown etiology and high prevalence in Europe with up to 500 affected persons per 100 000 [1]. Recent research indicates that UC derives from excessive inflammation [2, 3]. The arachidonic acid (AA) cascade is a central pathway in the paracrine and autocrine regulation of inflammation [4, 5]. The conversion of AA (20:4n6) by cyclooxygenases (COXs) and lipoxygenases (LOXs) leads to highly potent lipid mediators such as prostaglandins (PG) and leuktorienes (LT). Recent years have shown that products derived from other polyunsaturated fatty acids (PUFA), particularly docosahexaenoic acid (22:6n3, DHA) and eicosapentaenoic acid (20:5n3, EPA) – generally named oxylipins – also play key roles in the regulation of inflammation [6]. Another class of lipid mediators, the anti-inflammatory epoxy-FAs, are formed by cytochrome P450 monooxygenases (CYP). They are inactivated by hydrolysis to dihydroxy-FAs by soluble epoxide hydrolase (sEH) [7]. A large number of currently sold anti-inflammatory drugs target PG formation by COX inhibition. The first line treatment of mild and moderate UC is 5-aminosalicylic acid (5-ASA, Mesalazine) [8]. One mode of action of 5-ASA is a competitive inhibition of COXs [9]. However, the use of other COX inhibitors, i.e. non-steroidal anti-inflammatory drugs (NSAID), is controversial because of the central role of PGs in epithelia protection and homeostasis [10-12]. New studies in rodents suggest that inhibiting sEH and stabilizing epoxy-FAs in the CYP branch of the AA cascade could be a promising treatment of UC [13, 14]. Moreover, studies in animals and humans suffering from UC demonstrate that n3-PUFAs, which are believed to act mainly based on a modulation of the endogenous oxylipin pattern, act in a preventive/curative way on colitis [15-17]. However, only few data regarding the changes in oxylipin pattern occurring during UC are available. Particularly, information on the effect of colonic inflammation on systemic markers, i.e. oxylipins circulating in plasma, is scarce. Therefore, the aim of the present study was to characterize the effects of dextran sulfate

sodium (DSS) induced colitis on oxylipin plasma levels in acute inflammation, healing/regeneration and onset of chronic colitis.

5.2 Experimental

5.2.1 Chemicals

DSS (36-50 kDa) was purchased from MP Biomedicals (Heidelberg, Germany). LC-MS grade acetonitrile (ACN), acetic acid (HAc) and methanol (MeOH) were from Fisher Scientific (Nidderau, Germany). Oxylipin standards and internal standards were obtained from Cayman Chemicals (local distributor: Biomol, Hamburg, Germany). Further standards such as EpODEs and DiHODEs were a kind gift from the laboratory of Bruce Hammock (UC Davis, California, USA). 1-(1-(Ethyl-sulfonyl)piperidin-4-yl)-3-(4-(trifluoromethoxy)phenyl)urea synthesized as described [18] was used as internal standard 2 (IS 2). All other chemicals were from Sigma Aldrich (Schnelldorf, Germany).

5.2.2 DSS induced colitis model

Male Fischer 344 rats (95-115 g, 6 weeks) were obtained from Charles River Laboratories International Inc. (Sulzfeld, Germany) and kept in type IV polycarbonate cages (EHRET, Emmendingen, Germany). The bedding consisted of poplar granules (Lignocel select, Rosenberg, Germany), which were changed once a week. Before starting the DSS treatment the animals were allowed to acclimatize in our laboratory for two weeks. The animals had access to standard chow (#1324 Altromin, Lage, Germany) and water ad libitum and were kept at a 12 hour light/dark cycle.

Colitis was induced by three cycles of a four-day treatment with DSS in drinking water (4% *w*/*v*) followed by 10 days of recovery (Fig. 5.1) as described [19].

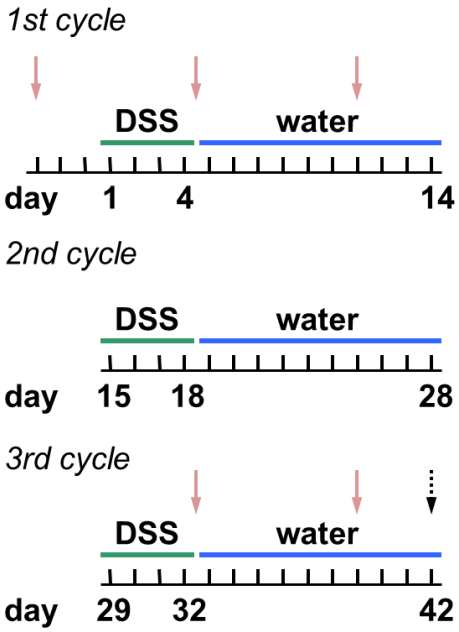

Fig. 5.1 DSS treatment regime of rats to induce acute and chronic colitis. Animals received 4% DSS in the drinking water for four days followed by a recovery phase with tap water for ten days. This cycle was repeated thrice. Animals of the control group received tap water over the whole period of time. Red arrows indicate blood sampling time points. At day 42 animals were sacrificed and colon tissue was sampled.

Five hundred microliters EDTA-blood were collected from the retrobulbar venous plexus three days prior first DSS treatment as well as on days 4, 11, 32 and 39. The obtained blood was centrifuged (1 500 x g, 10 min, 4°C) and the plasma was stored at -80°C until it was analysed. On day 42 the animals were killed by cardiac puncture after anesthesia with xylazine/ketamine (66/5 mg/kg bw). The gut was transferred to ice cold phosphate buffer saline and after measuring the colon length, the proximal colon, distal colon and rectum sections [20] were sampled. The intestine was opened longitudinally, cleaned with ice-cold buffered and cut into pieces. One piece of the distal colon (50-100 mg) was immediately frozen at -80°C for oxylipin analysis. The other piece and a sample of the proximal colon and rectum were fixed in 4% formalin at room temperature for the histopathological examination. Samples were prepared and scored as described [21] regarding the severity of inflammation (0 = none, 1 = minimal, 2 = mild, 3 = moderate, 4 = severe inflammation) and

the extent of inflammation (0 = none, 1 = mucosal, 2 = mucosal and submucosal, 3 = mucosal, submucosal and muscular, 4 = mucosal, submucosal, muscular and serosal layers involved). The health status of the animals was daily inspected, and the disease activity index (DAI) was determined based on body weight loss, faeces consistency and macroscopically visible blood in faeces [17, 22]. The study was approved by the animal welfare service of the state of Lower Saxony (Oldenburg, Germany).

5.2.3 LC-MS analysis of oxylipins

Quantification of oxylipins in plasma and colon tissue was carried out by LC-MS as described [23]. In brief, following addition of internal standards, 250 µL plasma were extracted utilizing Oasis HLB solid phase cartridges (Waters, Eschborn, Germany). Colon tissue (75 ± 25 mg) was homogenized in 500 µL MeOH/water 50/50 (*v*/*v*) with a ball mill (Retsch, Haan, Germany) for 10 min at 30 Hz. After centrifugation the supernatant was transferred to a preconditioned SPE column; the column was filled with wash solution and further processed like plasma samples. The residue of the evaporated solid phase extract was dissolved in 50 µL methanolic solution of IS2 and 5 µL were separated on an Agilent Zorbax Eclipse Plus C-18 reversed phase column (2.1 x 150 mm, particle size 1.8 µm) with a gradient of 0.1% aqueous HAc as solvent A and ACN/MeOH/HAc (800/150/1, *v/v/v*) as solvent B. Mass spectrometric detection was carried out on an AB Sciex 6500 QTRAP instrument (AB Sciex, Darmstadt, Germany) in scheduled selected reaction monitoring mode following negative electrospray ionization (ESI). Instrument controlling was performed with Analyst 1.6.2 and data analysis was carried out with Multiquant 2.1.1 (AB Sciex). A list of all oxylipins covered by the method can be found in the appendix (Tab. 11.1).

5.3 Results

5.3.1 Disease activity index (DAI) and histopathological examination

The time course of the DAI (weight loss, stool consistency and blood in feaces) during the DSS treatment and the results of the histopathological analysis of the colon are shown in Fig. 5.2.

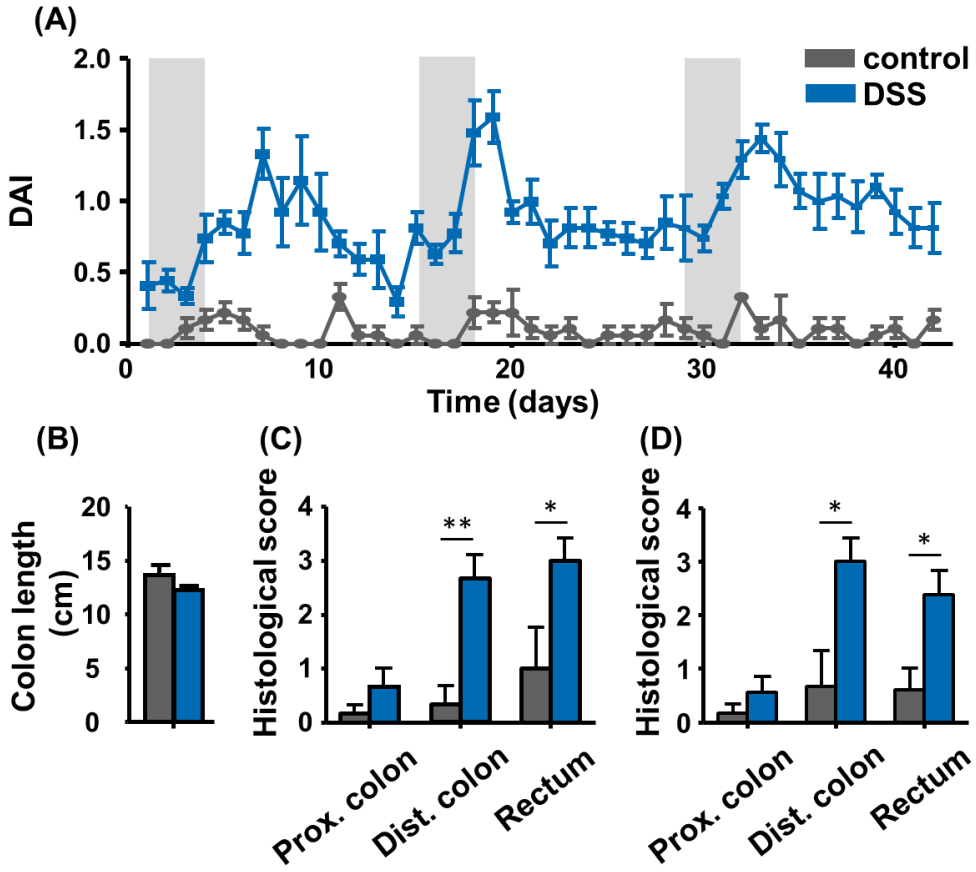

Fig. 5.2 Characterization of the acute and chronic phase of DSS induced colitis. (**A**) Disease activity index (DAI) of the DSS treated animals (blue line) in comparison to the control group (gray line). (**B**) Colon length of the DSS-treated and control group at day 42. Histopathological scoring of severity (**C**) and extent of inflammation (**D**) in different colon sections. Blue bars represent the DSS-treated group, gray bars the control group. Data is shown as mean ± SEM. (B-C) Statistically significant differences between the DSS-treated and the control group are indicated by asterisks; * $p < 0.05$, ** $p < 0.01$ calculated by the Mann-Whitney U test.

In treated rats, the DAI increased after the first 4-day treatment period with DSS, reaching a maximum at day 7 during the recovery phase. Following the second DSS treatment cycle (day 15-18) the DAI raised more rapidly to a maximum of 1.5 at day 18 and 19. Thereafter, during the second recovery phase the DAI decreased and reached a plateau at 0.7-0.8. Following the third treatment cycle the DAI remained at an even higher level (0.8-1.0), an indication of chronic inflammation. The DAI of the control animals was always below 0.35 (Fig. 5.2 A). At the end of the experiment (day 42) the colon length was not significantly different between the groups (DSS treated group: 12.2 ± 0.4 cm, control group: 13.7 ± 1.0 cm, Fig. 5.2 B). The histopathological examination of the colon at day 42 clearly showed that the DSS treatment caused a medium to severe chronic inflammation with a predominant lymphoplasmacytic infiltration, particularly in the distal colon and rectum. The scores of severity and extent of inflammation are shown in Fig. 5.2 C-D. The inflammation was much more pronounced in the distal colon and rectum compared to the proximal colon.

5.3.2 Prostaglandin (PG) levels in colonic tissue

Concentrations of PGs in the distal colon tissue are shown in Fig. 5.3. The most abundant PGs in the distal colon were found to be PGE_2, PGD_2 and 6 keto-$PGF_{1\alpha}$. Tissue levels of all detected PGs were dramatically elevated in the DSS-treated group undergoing a chronic colitis. For example, the PGE_2 level was significantly higher in the DSS-treated group (6.5 ± 0.5 pmol/mg) when compared to the control group (2.8 ± 0.6 pmol/mg; $p<0.01$). The same trend was observed for PGD_2 and 6-keto-$PGF_{1\alpha}$. The tissue levels of COX products of other PUFA were also elevated by chronic colitis (Fig. 5.3). Interestingly, the PGD metabolites were formed to a greater extent if compared to the corresponding PGE metabolites. However, both groups of PGs were increased about two-fold following the DSS treatment. For example, the PGE_3 tissue level was significantly higher in the DSS group than in the control group (27 ± 3 fmol/mg vs. 12 ± 2 fmol/mg; $p<0.01$) and this was also the case for PGD_3 (53 ± 8.4 fmol/mg vs. 25 ± 5.9 fmol/mg; $p<0.05$). The colonic tissue levels

of TxB_2 were 915 ± 132 fmol/mg in the DSS group and 805 ± 196 fmol/mg in the control group, and, thus, were unaffected by the treatment with DSS.

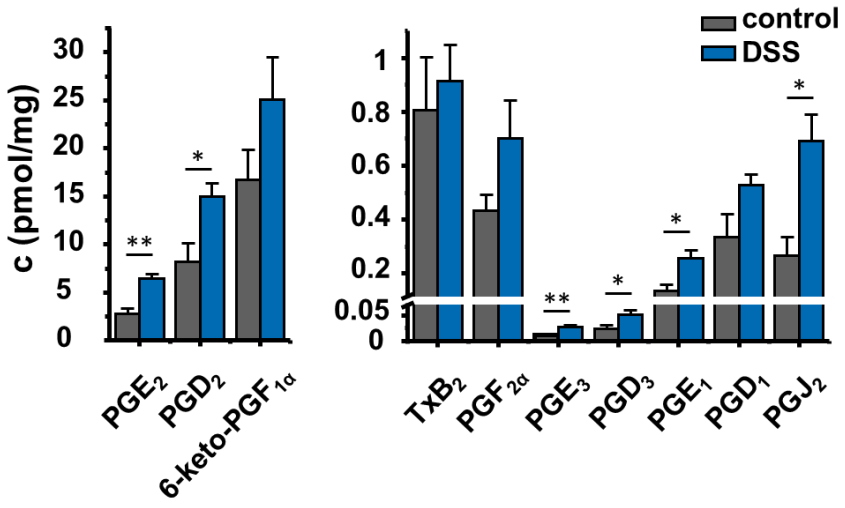

Fig. 5.3: Prostaglandin concentration in the distal colon tissue of the DSS treated animals at day 42 (blue bars, n=5) in comparison to the control group (gray bars, n=4). Statistically significant differences between the DSS-treated and the control group are indicated by asterisks; * $p < 0.05$, ** $p < 0.01$. Statistical differences were analyzed by t-test, only 6-keto-$PGF_{1\alpha}$ showed skew distribution and was analyzed by the Mann-Whitney U test.

5.3.3 Systemic oxylipin levels

The concentrations of oxylipins detected in plasma during the repeated treatment with DSS (Fig. 5.1) are shown in Tab. 5.1 and time courses of selected metabolites are presented in Fig. 5.4. For the plasma PGE_2 concentration only slight to moderate changes (not statistically significant) were observed during the onset of the chronic colitis (Fig. 5.4 F).

Epoxy-FAs of most PUFAs were slightly but not statistically significantly increased after the first DSS treatment cycle at day 4. During the recovery phase (day 11) the concentrations of epoxy-FAs decreased and were similar or even slightly lower than those of the control group.

Tab. 5.1: Plasma concentration of oxylipins at different time points during DSS induced colitis. Statistically significant differences between the DSS-treated (n=5) and the control (ctrl.) group (n=4) were calculated by two-way Anova with Bonferroni post-test.

Analyt (nM)		day 0		day 4		day 11		day 32		day 39	
		Ctrl.	DSS	Ctrl.	DSS	Ctrl.	DSS	Ctrl.	DSS	Ctrl.	DSS
PGE_2[a]	Mean	0.63	0.52	0.93	0.21	0.088	0.59	0.071	0.32	0.56	0.26
	SEM	0.49	0.23	0.76	0.076	0.021	0.36	0.018	0.093	0.22	0.13
	p	p > 0.05		p > 0.05		p > 0.05		p > 0.05		p > 0.05	
PGD_2[a]	Mean	0.62	0.52	0.80	0.27	0.21	0.63	0.23	0.37	0.49	0.31
	SEM	0.36	0.17	0.52	0.039	0.0058	0.30	0.017	0.095	0.15	0.10
	p	p > 0.05		p > 0.05		p > 0.05		p > 0.05		p > 0.05	
5-HETE[b]	Mean	3.0	3.1	2.8	4.4	3.7	3.9	3.8	5.9	3.7	4.7
	SEM	0.23	0.25	0.31	0.44	0.29	0.78	0.30	0.43	0.46	0.63
	p	p > 0.05		p > 0.05		p > 0.05		**p < 0.05**		p > 0.05	
15-HETE[c]	Mean	2.7	2.4	3.1	2.4	2.2	2.6	1.9	3.4	2.7	3.4
	SEM	0.99	0.56	1.3	0.24	0.13	1.0	0.12	0.07	0.45	0.55
	p	p > 0.05		p > 0.05		p > 0.05		p > 0.05		p > 0.05	
20-HETE[d]	Mean	0.85	0.78	0.62	1.0	0.86	0.75	0.79	1.01	0.76	0.77
	SEM	0.10	0.078	0.053	0.10	0.12	0.087	0.11	0.029	0.060	0.070
	p	p > 0.05		**p < 0.01**		p > 0.05		p > 0.05		p > 0.05	
11-HETE[e]	Mean	2.5	2.0	3.5	1.3	0.89	2.3	0.85	1.8	2.2	1.5
	SEM	1.5	0.67	2.3	0.11	0.079	1.1	0.038	0.12	0.62	0.28
	p	p > 0.05		p > 0.05		p > 0.05		p > 0.05		p > 0.05	
5(6)-EpETrE[f]	Mean	31	28	20	36	35	18	25	45	23	37
	SEM	2.9	8.1	3.0	9.3	3.3	7.9	3.9	10	5.9	11
	p	p > 0.05		p > 0.05		p > 0.05		p > 0.05		p > 0.05	

Tab. 5.1 continued

Analyt (nM)		day 0		day 4		day 11		day 32		day 39	
		Ctrl.	**DSS**	**Ctrl.**	**DSS**	**Ctrl.**	**DSS**	**Ctrl.**	**DSS**	**Ctrl.**	**DSS**
8(9)-EpETrE[f]	Mean	4.8	4.1	3.6	4.9	4.5	2.5	4.0	5.9	4.5	5.1
	SEM	0.36	1.1	0.27	0.97	0.63	0.94	0.28	1.1	0.97	1.2
	p	p > 0.05		p > 0.05		p > 0.05		p > 0.05		p > 0.05	
11(12)-EpETrE[f]	Mean	6.1	5.3	4.6	6.4	6.1	3.1	5.0	7.7	5.5	6.7
	SEM	0.49	1.5	0.4	1.5	1.0	1.3	0.49	1.7	1.2	1.6
	p	p > 0.05		p > 0.05		p > 0.05		p > 0.05		p > 0.05	
14(15)-EpETrE[f]	Mean	3.5	3.4	2.7	4.2	3.4	2.4	3.0	5.3	3.3	4.3
	SEM	0.26	0.80	0.20	0.76	0.50	0.78	0.28	0.83	0.62	0.96
	p	p > 0.05		p > 0.05		p > 0.05		p > 0.05		p > 0.05	
5,6-DiHETrE[g]	Mean	0.21	0.24	0.21	0.37	0.25	0.30	0.29	0.50	0.31	0.32
	SEM	0.026	0.014	0.032	0.031	0.015	0.024	0.036	0.051	0.041	0.024
	p	p > 0.05		**p < 0.01**		p > 0.05		**p < 0.001**		p > 0.05	
8,9-DiHETrE[g]	Mean	0.18	0.18	0.15	0.25	0.18	0.20	0.18	0.29	0.19	0.19
	SEM	0.024	0.0083	0.0086	0.010	0.010	0.029	0.012	0.020	0.023	0.020
	p	p > 0.05		**p < 0.01**		p > 0.05		**p < 0.01**		p > 0.05	
11,12-DiHETrE[g]	Mean	0.45	0.45	0.36	0.50	0.37	0.40	0.34	0.54	0.36	0.40
	SEM	0.085	0.019	0.020	0.019	0.017	0.071	0.039	0.035	0.049	0.047
	p	p > 0.05		p > 0.05		p > 0.05		**p < 0.05**		p > 0.05	
14,15-DiHETrE[g]	Mean	0.65	0.71	0.41	0.80	0.61	0.67	0.69	0.96	0.62	0.70
	SEM	0.096	0.020	0.129	0.026	0.034	0.087	0.039	0.077	0.048	0.055
	p	p > 0.05		**p < 0.05**		p > 0.05		**p < 0.05**		p > 0.05	

[a] formed via the COX pathway; [b] formed via the 5-LOX; [c] formed via the 15-LOX; [d] formed via CYP pathway (e.g. CYP4A and CYP4F family); [e] non-enzymatically formed autoxidation product; [f] formed via CYP pathway (e.g. CYP2C and CYP2J family), [g] sEH hydrolysis product of epoxy-FAs.

Following the third DSS treatment (day 32) the epoxide levels were massively increased reaching statistical significance for 9(10)-EpODE, 12(13)-EpODE, 15(16) EpODE, 9(10)-EpOME, 12(13)-EpOME and 19(20)-EpDPE when compared to the control group. During the recovery phase (day 39) the levels dropped again and were similar to those of the control group (Fig. 5.4 A-B).

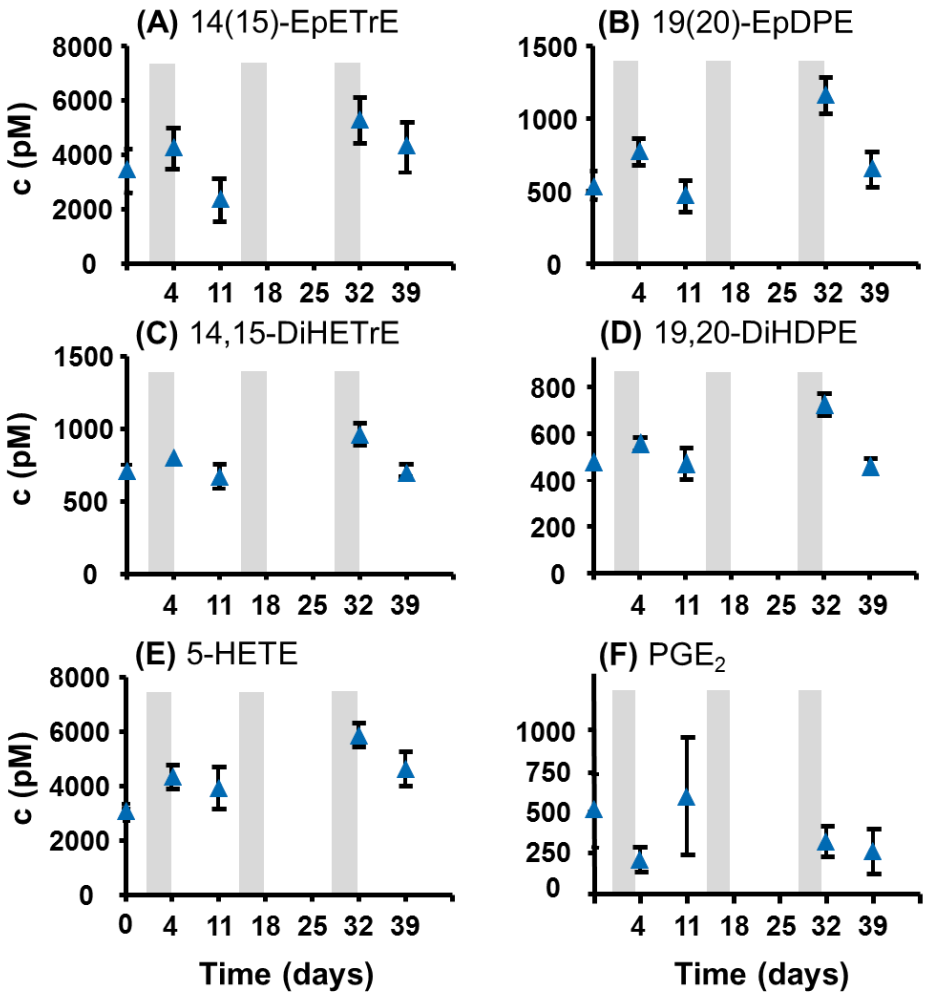

Fig. 5.4: Time course of plasma concentration of selected oxylipins during repeated DSS treatment: (**A**) 14(15)-EpETrE, (**B**) 19(20)-EpDPE, (**C**) 14,15-DiHETrE, (**D**) 19,20-DiHDPE, (**E**) 5-HETE and (**F**) PGE_2. The gray background indicates the periods of DSS treatment (4% in drinking water). The concentration of oxylipins detected in plasma can be found in Tab. 5.1.

A consistent time course was observed for the dihydroxy-FAs. After the first DSS treatment (day 4) all dihydroxy-FA levels, except for 17,18-DiHETrE, were

elevated (significantly in the case of 12,13-DiHODE, 12,13-DiHOME, 19,20-DiHDPE, 5,6-DiHETrE, 8,9-DiHETrE and 14,15-DiHETrE). During the recovery phase the concentrations decreased again and were similar to those of the control group. Directly after the third treatment with DSS (day 32), the levels of all detected dihydroxy-FAs, except for 17,18-DiHETE, were massively elevated and went back to baseline during the recovery phase (day 39) (Fig. 5.4 C-D). The effects of the DSS treatment on plasma hydroxy-FA concentrations were similar. After the first treatment with DSS (day 4) the levels of most hydroxy-FAs were increased, e. g. 20-HETE and 5-HEPE. However, 15-HETE, 11-HETE, 8-HETE and 12-HETE were detected at lower concentrations in the DSS-treated group than in the control group. During the first recovery (day 11) concentrations of most hydroxy-FAs in the DSS-treated group were found to be similar to those in the control group. After the third acute phase (day 32) the levels of all hydroxy-FAs of the treatment group were elevated, the increase reached statistical significance in the case of 9-HOTrE, 13-HOTrE, 9-HODE, 13-HODE, 8-HETE and 5-HETE. As already described for the epoxy- and dihydroxy-FAs, all hydroxy-FA levels decreased to a similar concentration range as the ones from the control group at day 39 during the third recovery phase (Fig. 5.4 E).

5.4 Discussion

In the present study a commonly used rodent model of colitis with similarities to human UC [24] was applied to investigate the effect of acute and chronic colitis on systemic oxylipin levels. Colonic inflammation was elicited by repeated treatment with DSS in the drinking water (Fig. 5.1). In line with earlier studies in the rat model [19], the observed DAI shows that repetitive DSS treatment is effective to induce cycles of acute colitis, leading to a chronic inflammation after 42 days (Fig. 5.2). This conclusion is based on the histopathological findings, showing an intense inflammation particularly in the distal colon sections. However, the effect of chronic inflammation in Fischer 344 rats seems to have a

minor effect on colon length when compared to the results in mice [15] and Sprague Dawley rats [25]. The oxyilipin levels in the distal colon tissue display the expected increase in PGs in response to chronic inflammation with a pronounced increase of the levels of PGE_2, PGD_2 and other PUFA analogs (Fig. 5.3). Playing a dominant role in the regulation of coagulation rather than in inflammation, the TXA_2 degradation product TXB_2 was not elevated in response to inflammation. The elevation of the tissue PG levels is comparable to earlier studies in mice and rats, in which an increased PGE_2 formation in response to colitis was reported [11, 26].

Acting predominantly as paracrine and autocrine lipid mediators [4, 5], the effect of colitis on the systemic non-esterified oxylipins in plasma was less pronounced. Among the PGs, only PGE_2 and PGD_2 as well as TxB_2 exceeded the limit of quantification. Thus, PGs formed in the intestine tissue do not reach the blood in considerable concentrations (<0.2 nmol/L; 70 pg/mL) or they are rapidly degraded and excreted. The determined concentration of the PGs varied massively in both groups, thereby making a biologically meaningful interpretation of the determined levels difficult. This variation is most probably caused by formation/degradation of PGs, especially PGE_2, during blood collection and sample preparation as discussed elsewhere [4].

For the epoxy-, dihydroxy-, and hydroxy-FAs overall, the same trend in the plasma levels was observed. In response to each cycle of acute colonic inflammation, their plasma concentrations were elevated, reaching a maximum 1-2 days after the DSS induced tissue damage. This indicated that these oxylipins are released from damaged/inflamed colon tissue into the blood in considerable concentrations. The uniform increase of the different oxylipins suggests that the acute colitis generally increases the formation of products of the AA cascade, rather than having a distinct effect on the pathways, such as CYP, LOX enzymes and autoxidation. This is consistent with earlier reports showing that the release of PUFA, e.g. by phospholipase A_2, is a rate limiting step in the generation of LOX and COX products in intestine tissue in DSS

induced colitis [12]. In addition to a release of epoxy-, dihydroxy-, and hydroxy-FAs from the inflamed colon tissue, it also has to be taken into account that acute colitis could lead to an elevated release of PUFAs and subsequent formation of the oxylipins in the blood or another tissue. However, the latter route of formation seems to be unlikely, since free fatty acids circulate in blood under physiological conditions transporting energy from the fat tissue e.g. to the muscles [27].

During recovery and healing of acute colitis, the plasma concentration of the oxylipins rapidly declines, and the oxylipin plasma concentration does not allow to gain information regarding (the onset of) chronic inflammation. However, the increase of epoxy-, dihydroxy-, and epoxy- FA becomes more pronounced with the DSS treatment cycles (Fig. 5.1, Fig. 5.4, Tab. 5.1). This can be explained in two ways: (i) the acute phase during repeated inflammation becomes more and more severe and/or (ii) in each inflammation phase oxylipins are formed from released PUFAs and a significant portion of them is re-esterified. In the following acute phase these oxylipins are directly released by phospholipases.

5.5 Conclusions

Overall the changes in the plasma oxylipin pattern support the relevance of the release of PUFAs from phospholipids during the acute phase of DSS induced colitis [12], as the plasma concentrations of several epoxy-, dihydroxy- and hydroxy-FAs are massively elevated during acute colitis. Taking into account that several of these oxylipins are potent lipid mediators, e.g. epoxy-FAs [7], our data suggest that oxylipins formed from AA and other unsaturated FAs play a key role in the biology of colitis. However, the rather unspecific increase of oxylipins derived from different enzymatically pathways make it difficult to pinpoint one branch of the AA cascade as potential target for pharmacological therapies. Finally, it has to be concluded that the plasma oxylipin concentration seems not to be a suitable biomarker to analyze the chronic phase of colitis.

5.6 References

[1] Molodecky N. A., Soon I. S., Rabi D. M., Ghali W. A., Ferris M., Chernoff G., Benchimol E. I., Panaccione R., Ghosh S., Barkema H. W., Kaplan G. G. *Gastroenterology* (2012) 142, 46-54

[2] Sartor R. B. *Nat Clin Pract Gastroenterol Hepatol* (2006) 3, 390-407

[3] Strober W., Fuss I., Mannon P. *J Clin Invest* (2007) 117, 514-521

[4] Willenberg I., Ostermann A. I., Schebb N. H. *Anal Bioanal Chem* (2014) 407, 2675-2683

[5] Buczynski M. W., Dumlao D. S., Dennis E. A. *J Lipid Res* (2009) 50, 1015-1038

[6] Weylandt K. H., Chiu C. Y., Gomolka B., Waechter S. F., Wiedenmann B. *Prostag Oth Lipid M* (2012) 97, 73-82

[7] Zhang G., Kodani S., Hammock B. D. *Prog Lipid Res* (2014) 53, 108-123

[8] Baumgart D. C., Sandborn W. J. *Lancet* (2007) 369, 1641-1657

[9] Reinacher-Schick A., Schoeneck A., Graeven U., Schwarte-Waldhoff I., Schmiegel W. *Carcinogenesis* (2003) 24, 443-451

[10] Köhnke T., Gomolka B., Bilal S., Zhou X. Z., Sun Y. P., Rothe M., Baumgart D. C., Weylandt K. H. *Biomed Research International* (2013) Art ID 748160

[11] Okayama M., Hayashi S., Aoi Y., Nishio H., Kato S., Takeuchi K. *Dig Dis Sci* (2007) 52, 2095-2103

[12] Montrose D. C., Nakanishi M., Murphy R. C., Zarini S., McAleer J. P., Vella A. T., Rosenberg D. W. *Prostaglandins Other Lipid Mediat* (2014) 116-117C, 26-36

[13] Zhang W., Liao J., Li H., Dong H., Bai H., Yang A., Hammock B. D., Yang G. Y. *Mol Carcinog* (2013), 52(9):726-738

[14] Zhang W., Yang A. L., Liao J., Li H., Dong H., Chung Y. T., Bai H., Matkowskyj K. A., Hammock B. D., Yang G. Y. *Dig Dis Sci* (2012) 57, 2580-2591

[15] Hudert C. A., Weylandt K. H., Lu Y., Wang J., Hong S., Dignass A., Serhan C. N., Kang J. X. *Proc Natl Acad Sci U S A* (2006) 103, 11276-11281

[16] Camuesco D., Galvez J., Nieto A., Comalada M., Rodriguez-Cabezas M. E., Concha A., Xaus J., Zarzuelo A. *J Nutr* (2005) 135, 687-694

[17] Camuesco D., Comalada M., Concha A., Nieto A., Sierra S., Xaus J., Zarzuelo A., Galvez J. *Clin Nutr* (2006) 25, 466-476

[18] Schebb N. H., Inceoglu B., Rose T., Wagner K., Hammock B. D. *Anal Methods* (2011) 3, 420-428

[19] Kullmann F., Messmann H., Alt M., Gross V., Bocker T., Scholmerich J., Ruschoff J. *Int J Colorectal Dis* (2001) 16, 238-246

[20] Nicken P., Hamscher G., Breves G., Steinberg P. *Toxicol Lett* (2010) 196, 60-66

[21] Rachmilewitz D., Karmeli F., Takabayashi K., Hayashi T., Leider-Trejo L., Lee J., Leoni L. M., Raz E. *Gastroenterology* (2002) 122, 1428-1441

[22] Cooper H. S., Murthy S. N., Shah R. S., Sedergran D. J. *Lab Invest* (1993) 69, 238-249

[23] Ostermann A. I., Willenberg I., Schebb N. H. *Anal Bioanal Chem* (2015) 407, 1403-1414

[24] Solomon L., S M., Mallon P., Donnelly E., Hoper M., Loughrey M., Kirk S., Gardiner K. *Comp Clin Pathol* (2010) 19, 235-239

[25] Gaudio E., Taddei G., Vetuschi A., Sferra R., Frieri G., Ricciardi G., Caprilli R. *Dig Dis Sci* (1999) 44, 1458-1475

[26] Melgar S., Drmotova M., Rehnstrom E., Jansson L., Michaelsson E. *Cytokine* (2006) 35, 275-283

[27] Frayn K. N., Summers L. K. M., Fielding B. A. *Proceedings of the Nutrition Society* (1997) 56, 713-721

Chapter 6

Characterization of Changes in Plasma and Tissue Oxylipin Levels in LPS and CLP Induced Murine Sepsis *

Objective: ***The present study aimed to comprehensively investigate the changes in lipid mediators during murine sepsis induced by lipopolysaccharide (LPS) or cecal ligation and puncture (CLP).***

Methods: ***24 h after induction of sepsis in male C57BL/6 mice by LPS or CLP, plasma and liver, lung, kidney and heart tissues were sampled. Lipid mediator levels in plasma and tissue were quantified by means of LC-MS. Moreover, aspartate transaminase (AST), alanine transaminase (ALT), lactate dehydrogenase (LDH) and urea and creatinine levels were determined in plasma.***

Results: ***Elevation of liver function plasma parameters within 24 h revealed that both models were successful in the induction of sepsis. LPS-induced sepsis resulted in dramatic increase of plasma PGE_2 (2100% change in comparison to control) and other cyclooxygenase metabolites, whereas this effect was less pronounced in CLP induced sepsis (97% increase of PGE_2). Plasma epoxy-fatty acids (FAs) and dihydroxy-FAs and most of the hydroxy-FAs were elevated in both models of sepsis. Changes of tissue oxylipin concentrations were organ dependent. Whereas only few changes were detected in the lung and liver tissue, epoxy-FAs were elevated in the kidney. In the heart tissue a trend towards lower levels of hydroxy-FAs and epoxy-FAs was observed.***

Conclusion: ***Both murine models of sepsis are characterized by changes of oxylipins formed in all branches of the arachidonic acid (AA) cascade. The more pronounced effects in the LPS model make this model more suitable for the investigation of the AA cascade and its pharmacological modulation in sepsis.***

* Willenberg I., Song R., Shushakova N., Gueler F., Schebb N. H. (2015) *Submitted for publication.*

Author contributions: IW: Designed research, performed experiments and wrote manuscript; SR: Performed experiments; NS: Performed experiments; FG: Designed research, helped writing the manuscript. NHS: Designed research and wrote the manuscript.

6.1 Introduction

Sepsis is a severe medical condition with high incidence and mortality [1-3]. Sepsis arises when a host is not able to contain an infection and is characterized through a complex deregulation of inflammation resulting in multiple organ failure [4]. Aside from cytokines the pro-inflammatory prostaglandins (PGs), especially PGE_2, play a role in sepsis [5]. Plasma PG levels are increased in several animal models of sepsis [6-9] and patients [10, 11]. PGs modulate a variety of biological functions and are enzymatically formed from arachidonic acid (AA) or other polyunsaturated fatty acids (PUFAs) by cyclooxygenases (COXs) and several PG-synthases [12]. For example, PGE_2 plays a role in the regulation of immune response, blood pressure, inflammation and pain [13]. PGI_2 is a potent vasodilator and inhibitor of platelet aggregation and therefore important for cardiovascular homeostasis [13]. 6-keto-$PGF_{1\alpha}$ is its inactive, non-enzymatically formed hydrolysis product and used as marker for the *in vivo* production of PGI_2 [13]. 13,14-dihydro-15-keto-$PGF_{2\alpha}$ is a plasma metabolite of $PGF_{2\alpha}$, which is involved in several physiological processes, such as luteolysis, oviarian function, parturition as well as in acute and chronic inflammation and cardiovascular diseases [14, 15]. Apart from the COX branch, PUFAs are converted in the AA cascade enzymatically by lipoxygenases (LOXs) and cytochrome P450 monooxygenases (CYPs) or non-enzymatically via autoxidation. Conversion by enzymes of the CYP2C or CYP2J families results in the formation of epoxy-FAs with vasodilatory, anti-inflammatory, and analgetic properties. They are subsequently hydrolyzed by soluble epoxide hydrolase (sEH) to the less biologically active dihydroxy-FAs [16, 17]. ω-hydroxylation of AA by members of the CYP4A or CYP4F families form 20-HETE, acting as a vasoconstrictor [18]. The primary products of LOXs are hydroperoxy-FAs, which can be subsequently reduced to the corresponding hydroxy-FAs, such as 5-, 12- or 15-HETE or the eicosapentaenoic acid (EPA) derived 5-, 12- or 15-HEPE [19]. These hydroxy-FAs can be used as markers for 5-, 12- or 15-LOX activity. Under physiological conditions, 5-HpETE can be further processed by 5-LOX to

LTA_4 which serves as precursor for several highly biological active lipid mediators, such as the chemoattractant LTB_4 or the anti-inflammatory LXA_4 [19]. Moreover, resolvins and related compounds, which are believed to be involved in the resolution of inflammation, are formed by the action of COX and LOX and primary products such as 18-HEPE and 17-HDHA are used as marker for this pathway [20]. Oxygenated FAs can be formed via autoxidation. Whereas enzymatic oxidation is stereoselective, autoxidation results in the formation of racemic mixtures. Primary autoxidation products are hydroperoxides, which can be reduced to hydroxy-FAs, such as 9- or 11-HETE [21]. Further reaction of the initially formed hydroperoxides results in the formation of F_2-isoprostanoids, such as 5-i$PF_{2\alpha}$-IV, which are used as markers of oxidative stress *in vivo* [22].

Previous studies investigating the role of lipid mediators, generally referred to as oxylipins, in sepsis focused only on single or few compounds [7-9, 23]. Although there is a crosstalk between different pathways [24, 25], comprehensive information about sepsis related changes in all pathways is scarce. Particularly, no data on differences in oxylipin pattern induced by different animal models of sepsis is available. Initiation of sepsis in animal models can be achieved via three strategies: (i) administration of exogenous toxins (such as lipopolysaccharide (LPS)), (ii) administration of viable pathogens or (iii) by an alteration of the intestinal barrier [4, 26]. LPS-induced sepsis and polymicrobial sepsis induced by cecal ligation and puncture (CLP) are the most commonly used animal models. LPS-induced sepsis can be simply and robustly achieved by i.p. injection and is characterized by a rapid and massive elevation of systemic cytokines, such as TNF-α, IL-1β and IL-6 and PG levels [8, 26]. Notably, in clinical sepsis the increase of systemic cytokine levels is more prolonged and the concentrations are lower. Thus, LPS-induced sepsis gives insights in septic processes albeit there are limitations regarding the complex physiological response in septic patients [4, 26]. The CLP model is considered to be the gold standard in sepsis models [4]. In CLP surgery the intestinal barrier is damaged, allowing bacterial translocation which leads to peritonitis and eventually multiorgan failure. The cytokine release after CLP

surgery is prolonged and resembles the cytokine profile observed in septic patients [4, 26, 27].

This study aims to comprehensively investigate and compare the role of lipid mediators in these two models of sepsis. For this purpose, both oxylipin plasma as well as tissue levels were analyzed using a targeted metabolomics approach and correlated with clinical chemistry parameters indicating multiorgan failure due to acute sepsis.

6.2 Experimental

6.2.1 Chemicals

LPS from *E.coli* O111:B4 was purchased from Sigma (Schnelldorf, Germany, L 2630 Lot#043M4104V). Oxylipin standards and internal standards were purchased from Cayman Chemicals (local distributor: Biomol, Hamburg). Epoxy octadecadienoic acids (EpODEs) and dihydroxy octadecadienoic acids (DiHODEs), 1-(1-methanesulfonyl-piperidin-4-yl)-3-(4-trifluoromethoxy-phenyl)-urea (TUPS) were a kind gift from the laboratory of Bruce Hammock (UC Davis, California, USA). LC-MS grade acetonitrile (ACN), acetic acid (HAc) and methanol (MeOH) were obtained from Fisher Scientific (Nidderau, Germany). *n*-hexane (HPLC grade) was from Carl Roth (Karlsruhe, Germany). All other chemicals were from Sigma (Schnelldorf, Germany).

6.2.2 In vivo studies

C57BL/6 male mice ($H2^b$, 11-13 weeks of age) were obtained from Charles River (Sulzfeld, Germany). Animals were cared for in accordance with the institution's guidelines for experimental animals and with the guidelines of the American Physiological Society. The animal protection committee of the local authorities (Lower Saxony state department for food safety and animal welfare

LAVES) approved all experiments (approval: 33.9-42502-04-12/0846). Mice were housed under conventional conditions in individually ventilated cages produced by Techniplast Inc. (Italy) with a 12h light/dark cycle and had free access to food (Altromin 1324 standard mouse diet) and domestic quality drinking water ad libitum.

LPS model

C57BL/6 mice were i. p. challenged with 10 mg/kg bw LPS (n=6) or vehicle (n=6). After 24 h mice were anesthetized with isofluorane for blood sampling and organ retrieval. After perfusion with cold PBS lung, liver, kidney and heart tissue was collected. Tissue was immediately shock frozen in liquid nitrogen for later analysis and stored at -80°C till analysis.

Cecal ligation puncture (CLP)

CLP surgery was performed under isofluran anesthesia as described previously [28]. Briefly, after incision of the left upper quadrant of the peritoneal cavity the cecum was exposed and a tight ligature was placed around the cecum distal to the insertion of the small bowel. One puncture wound was made with a 24-gauge needle into the cecum and small amounts of cecal contents were expressed through the wound, and 500 µL sterile normal saline solution was flushed into the abdomen. The cecum was placed back into the peritoneal cavity and the laparotomy site was closed in two layers. Finally, animals were returned to their cages with free access to food and water.

6.2.3 Blood sampling and clinical chemistry

Several days prior to sepsis induction and 24 h after blood was drawn from the retro orbital venus plexus using an EDTA coated capillary. After 10 min centrifugation at 4.000 g plasma was obtained and stored at -20°C to be used for clinical chemistry. Plasma urea, creatinine, aspartate transaminase (AST), alanine transaminase (ALT) and lactate dehydrogenase (LDH) levels were determined by using the fully automated Olympus AU 400 analyzer (Beckman

Coulter Inc.). Statistical differences between groups were determined by two-way ANOVA followed by Bonferroni post-test.

6.2.4 Oxylipin analysis

Oxylipin analysis in plasma and tissue was carried out by solid phase extraction (SPE) followed by LC-MS as described with slight changes [29]. In brief, internal standards and 10 µL of an antioxidant/inhibitor solution (0.2 mg/mL EDTA, 0.2 mg/mL buthylated hydroxytoluene, 100 µM indomethacin, 100 µM TUPS in MeOH/water (50/50 *v/v*)), 480 µL H_2O (pH 6) and 120 µL MeOH were added to 200 µL of plasma. Tissue samples were homogenized in 250 µL methyl formate in 1.5 mL tubes with a 3 mm metal bead using a ball mill (5 min, 25 Hz, Retsch, Haan, Germany) following addition of internal standards and antioxidant/inhibitor solution. After centrifugation, the supernatant was diluted with H_2O (pH 6) to a total volume of 6 mL. Extraction was carried out on Chromabond C 18 ec cartridges (500 mg, Machery-Nagel, Düren, Germany) preconditioned with 2 column volumes of methyl formate, 1 column volume of MeOH and 3 column volumes of H_2O (pH 6). Directly before plasma and tissue samples were loaded onto the SPE cartridge, samples were acidified with 80 µL HAc resulting in a pH of 3. After loading the sample, the cartridge was washed with 10 mL H_2O (pH 6) and 6 mL *n*-hexane. The cartiged was dried for 20 min at -200 mbar. The analytes were then eluted with 8 mL methyl formate in glass tubes containing 6 µL of 30% glycerol in MeOH. Utilizing a Speedvac (Christ, Oserode, Germany), the extract was evaporated to dryness until only the glycerol plug was left. The residue was dissolved in 50 µL methanol. After centrifugation, 5 µL of the supernatant was injected to the LC-MS system. Mass spectrometric detection after electrospray ionization using an AB Sciex 6500 QTRAP instrument (AB Sciex, Darmstadt, Germany) was performed as described [29, Chapter 5]. A list of all oxylipins covered by the method can be found in the appendix (Tab. 11.1). Multiquant (Sciex) was used for peak integration and determination of oxylipin concentration.

6.2.5 Data analysis

Data analysis was performed using GraphPad Prism 5.0 (GraphPad Software, San Diego, USA). For the clinical chemistry parameters statistical differences between groups and both time points were determined by two-way ANOVA followed by Bonferroni post-test. Regarding oxylipin concentrations statistical differences between groups were determined by one-way ANOVA followed by Tukey post-test.

6.3 Results

6.3.1 Clinical chemistry

The clinical chemistry parameters revealed that in both models sepsis with impairment of kidney and liver function was successfully induced. In comparison to the vehicle group with a bodyweight of 23.2 ± 0.5 g, the LPS group had a significantly reduced bodyweight of 21.8 ± 0.2 g 24 h after LPS treatment ($p < 0.05$). 24 hours after CLP the weight was also lower, however the difference between sham (24.1 ± 0.5 g) and the CLP (22.8 ± 0.5 g) group did not reach statistical significance. Plasma creatinine, urea, AST, ALT, urea and LDH levels at baseline and 24 h after treatment/surgery are shown in Fig. 6.1.

Plasma creatinine levels of the LPS group significantly increased from 29 ± 1.3 µmol/L to 54 ± 7.1 µmol/L 24 h after LPS treatment ($p < 0.001$). Additionally, an about five-fold increase of plasma urea concentration was observed ($p < 0.001$). Plasma activity of AST was significantly increased from 60 ± 7.2 U/L to 220 ± 20 U/L ($p < 0.05$), while ALT activity showed no statistically significant changes 24 h after LPS treatment. Plasma LDH levels almost doubled in the LPS treated animals indicating substantial cell damage ($p < 0.05$). CLP resulted in increased plasma urea levels (baseline: 8.1 ± 0.36 mmol/L, 24 h: 17 ± 5.2 mmol/L, $p < 0.05$) but the effect was less pronounced as after LPS treatment (Fig. 6.1).

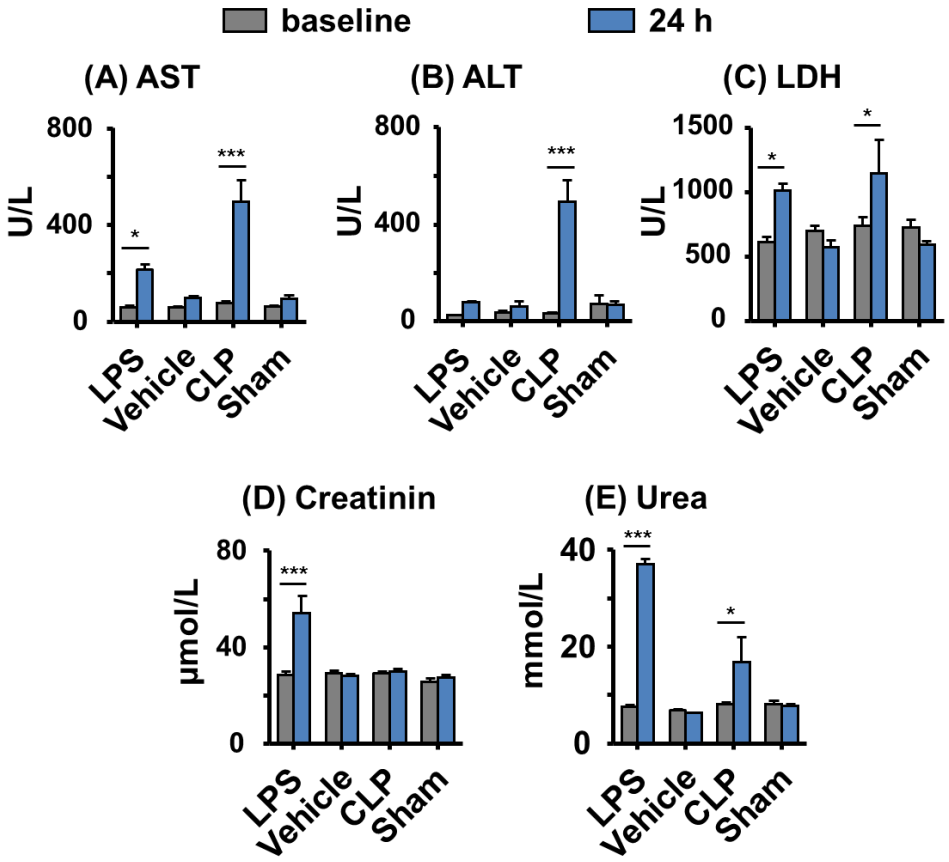

Fig. 6.1: Clinical chemistry of liver and renal function parameters prior to the experiment (baseline, gray bars) and 24 h after induction of sepsis by LPS or CLP (24 h, blue bars). Statistical differences were determined by two-way ANOVA followed by Bonferroni post-test test (*p<0.05, **p<0.01, ***p<0.001).

Plasma creatinine levels were not affected by CLP. AST and ALT activities were elevated 24 h after CLP surgery: ALT activity was increased more than ten-fold ($p < 0.001$), whereas AST activity changed from 77 ± 6.5 U/L to 490 ± 89 U/L ($p < 0.001$, Fig. 6.1). As observed in a similar manner for LPS treatment, plasma LDH level raised from 740 ± 60 U/L to 1150 ± 260 U/L 24 h after CLP surgery ($p < 0.05$).

6.3.2 Prostaglandins

Plasma concentrations of all detected oxylipins (concentration > LOQ) are shown in Tab. 11.2. In the LPS treated group PGE_2 and its analog derived from dihomo-γ-linoleic acid (DGLA 20:3, n-6), PGD_2 and its analog from EPA, the

PGI_2 metabolite 6-keto-$PGF_{2\alpha}$, $PGF_{2\alpha}$ and its analog from DGLA as well as its metabolite 13,14-dihydro-$PGF_{2\alpha}$, the adrenic acid (22:4 n-6) derived 1a,1b-dihomo$PGF_{2\alpha}$ and 5-$iPF_{2\alpha}$ were elevated in comparison to the vehicle. The increase was statistically significant ($p< 0.05$) for PGE_2, PGE_1, 6-keto-$PGF_{1\alpha}$, 5-$iPF_{2\alpha}$, dihomo-$PGF_{2\alpha}$, 13,14-dihydro-15-keto-$PGF_{2\alpha}$, $PGF_{1\alpha}$ and 13,14-dihydro-15-keto-PGE_1 (Fig. 6.2, Tab. 11.2).

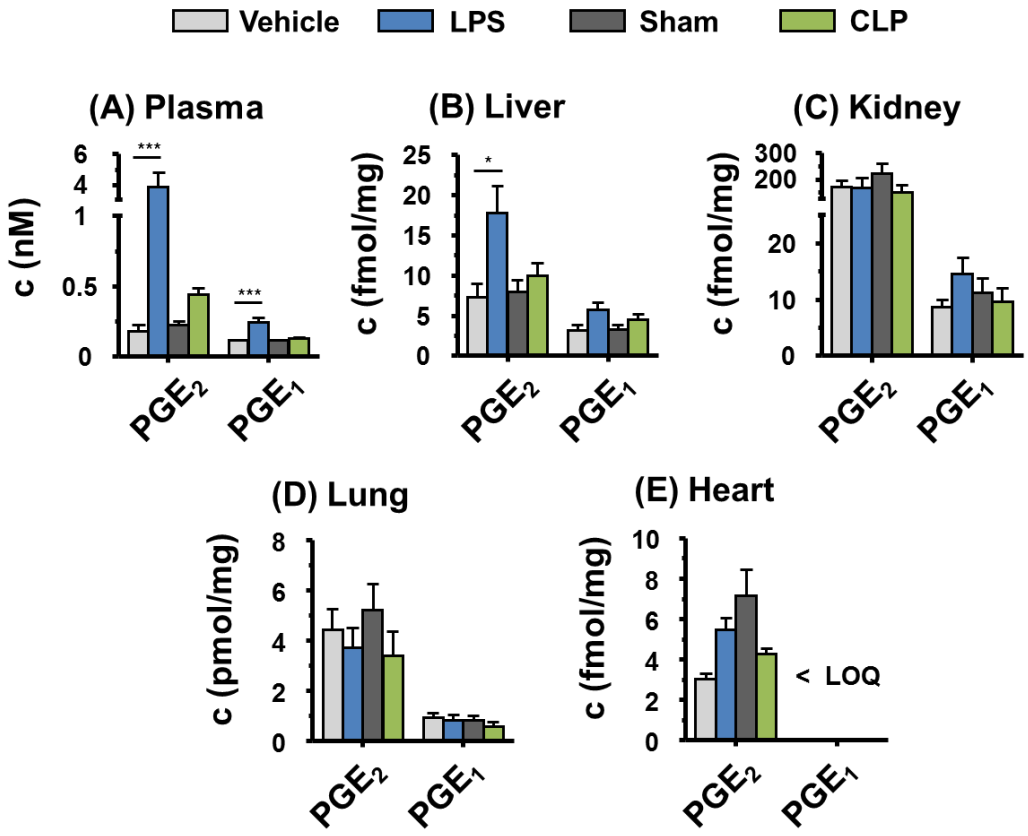

Fig. 6.2: PGE_2 and PGE_1 levels in plasma and different tissues 24 h after induction of sepsis by LPS i. p. injection or CLP surgery. Statistical differences were evaluated by one-way ANOVA followed by Tukeys post-test and shown for LPS vs. vehicle and CLP vs. sham (*p<0.05, **p<0.01, ***p<0.001).

For example, the PGE_2 plasma level was found to be 3.9 ± 0.92 nM in the LPS group in comparison to 0.18 ± 0.048 nM in the vehicle group ($p< 0.001$), corresponding to an increase of 2100%. The effect of LPS treatment on PG tissue levels was less pronounced. In the liver most of the PG concentrations were unchanged between the LPS and vehicle group, only PGE_2 and 5-$iPF_{2\alpha}$

were detected at statistically significant difference concentrations (Fig. 6.2, Tab. 11.3). In the kidney increased levels of PGD_1, dihomo-$PGF_{2\alpha}$ and PGF_{1a} were observed in the LPS group (Tab. 11.4), while the concentrations of the other detected PGs were unchanged. 6-keto $PGF_{1\alpha}$, 13,14-dihdydro-15-keto-PGE_1 ($p< 0.001$) and 13,14-dihydro-15-keto-$PGF_{2\alpha}$ ($p< 0,05$) were found to be elevated in the heart (Tab. 11.5). In lung tissue no changes in the detected PGs were observed (Tab. 11.6).

24 h after inducing sepsis by CLP slightly elevated levels of PGE_2 (CLP: 0.44 ± 0.04 nM; sham: 0.22 ± 0.02 nM), 6-keto $PGF_{1\alpha}$ (CLP: 3.1 ± 1.2 nM; sham: 0.81 ± 0.02 nM) and 13,14-dihydro-15-keto-PGE_1 (CLP: 0.28 ± 0.066 nM; sham: < LOQ (0.036 nM)) were observed in the treatment group (Tab. 11.2). Except for PGD_2, the concentrations of the other detected PGs were not different between CLP and sham control. Interestingly, PGD_2 levels were decreased in the CLP group (0.75 ± 0.11 nM, $p< 0.01$) compared to the sham group (4.2 ± 1.1 nM). PGD_2 levels in the heart tissue showed the same trend: In the CLP group lower PGD_2 concentrations (8.5 ± 1.0 fmol/mg) were detected compared to the sham group (20 ± 4.7 fmol/mg, $p< 0.05$, Tab. 11.5). For all other PGs no obvious changes in the tissue levels were observed (Tab. 11.3, Tab. 11.4, Tab. 11.5, Tab. 11.6).

6.3.3 Hydroxy-FAs

LPS treatment showed different effects on the hydroxy-FAs. Plasma levels of 8-, 12- and 20-HETE, 15-HETrE and 10-, 14- and 17-HDHA were increased 24 h after LPS treatment in comparison to the vehicle group ($p< 0.05$, Tab. 11.2). A consistent trend towards higher concentrations in the LPS treated group were found for 8-HEPE, 12-HETE and 15-HEPE and 13-HDHA (Tab. 11.2, Fig. 6.3 A,B). 5-HEPE and 9-HOTrE were detected at slightly lower levels after treatment, whereas the other detected hydroxy-FAs, such as 5- and 9-HETE, 18-HEPE and 4-, 7-, 8- and 11-HDHA were found to be unaffected (Tab. 11.2). In the liver tissue the levels of 20-HETE, 10- and 20-HDHA were increased by

53-230% in the LPS group ($p < 0.05$, Tab. 11.3). 12-HETE, 12-HEPE and 14-HDHA showed also trends towards higher levels in the LPS group. Interestingly the concentrations of 5- and 15-HEPE were decreased by about 50% in the LPS treated animals ($p < 0.05$, Tab. 11.3). The concentrations of other hydroxy-FAs, such as 9- and 13-HOTrE, 5-, 8-, 9-, 11- and 15-HETE, 18- and 20-HEPE and 4-, 7-, 8- and 11-HDHA were unchanged (Tab. 11.3). Similar observations were found in the kidney: 5-HEPE concentration was about 20% lower in the LPS group ($p < 0.001$), whereas concentrations of other hydroxy-FAs, e.g. 20-HETE, 9- and 13-HODE and 7-, 10- and 11-HDHA were elevated ($p < 0.05$, Tab. 11.4). 12-HETE, 12-HEPE and 14-HDHA were found at 140-310% higher concentrations in the LPS group (Tab. 11.4), most other hydroxy-FAs, such as 9- and 13-HOTrE, 5-, 8-, 9-, 11- and 15-HETE, 18- and 20-HEPE and 4- and 8-HDHA, were unaffected. Only a minor modulation of the hydroxy-FAs concentrations in the lung tissue was observed in the sepsis models. Following LPS treatment, only 5-HEPE, 20-HETE and 7-HDHA were elevated in the LPS group ($p < 0.05$, Tab. 11.6) and for 5-HETE a trend towards higher levels was observed.

Interestingly, the change in the hydroxy-FAs pattern in the heart revealed a different picture (Tab. 11.5): Most of the hydroxy-FAs, e. g. 13-HODE, 5-HETE and 4- and 11-HDHA showed a trend towards about 30% lower levels in the LPS group, reaching statistical significance ($p < 0.05$) for 5- and 12-HEPE, 12-HETE and 10-, 14- and 17-HDHA.

Similar to LPS treatment, CLP induced sepsis resulted in different changes in plasma hydroxy-FA concentrations. 9-HOTrE and 8-, 12- and 20-HETE were significantly elevated (83-300 %, $p < 0.05$). A similar trend of increased levels was observed for 8- and 12-HETE, 8-, 12- and 15-HEPE, 15-HETrE and 10-, 13-, 14- and 17-HDHA (200-1200, Tab. 11.2, Fig. 6.3 A,B). The concentration of 9-HOTrE was decreased by 71% in the CLP group ($p < 0.01$). Levels of 5-, 9- and 11-HETE, 18-HEPE and 9- and 13-HODE were not affected by CLP induced sepsis (Tab. 11.2).

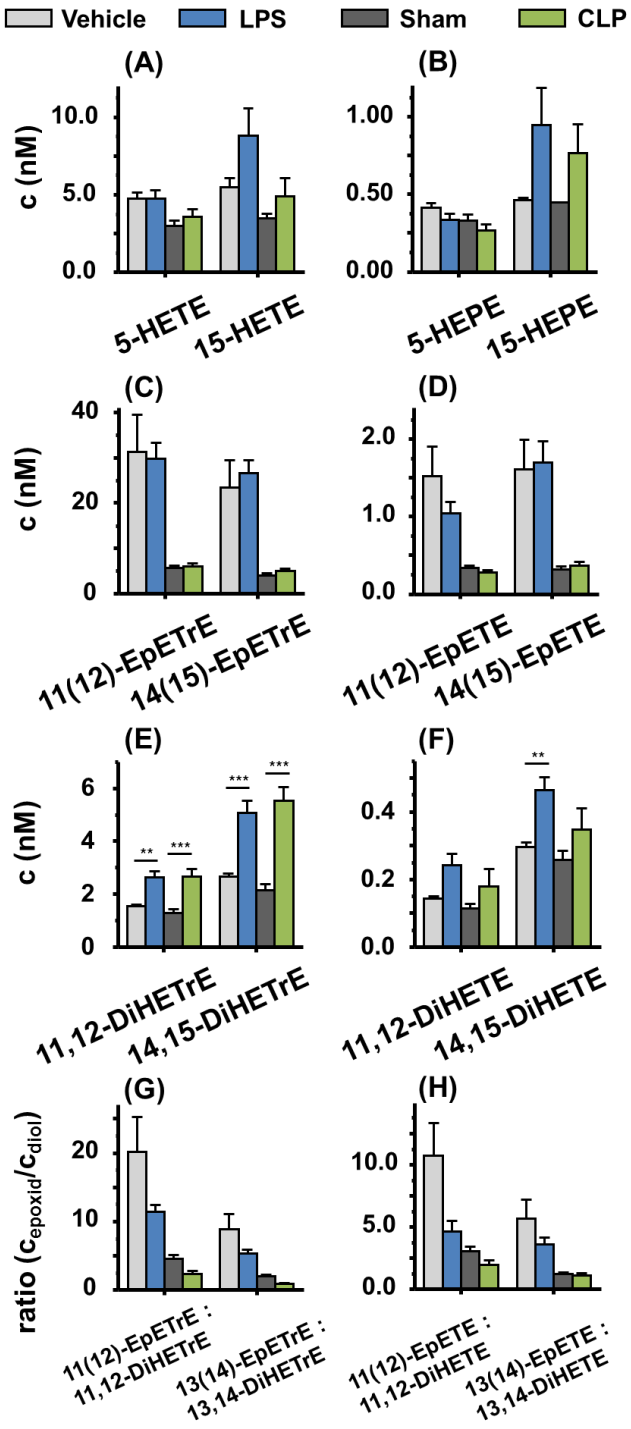

Fig. 6.3: Plasma concentrations of selected metabolites of the LOX and CYP branch of the AA cascade 24 h after induction of sepsis by i. p. LPS injection or CLP surgery. Statistical differences were determined by one-way ANOVA followed by Tukeys post-test and shown for LPS vs. vehicle and CLP vs. sham (*p<0.05, **p<0.01, ***p<0.001).

Consistent with the LPS model the concentration of 5-HEPE was decreased ($p < 0.01$) in the liver tissues of the CLP treated animals. Additionally, 9-HOTrE was also found at 47% lower levels while concentrations of 12-HETE, 12-HEPE and 10- and 12-HDHA were elevated by 99-580% during CLP induced sepsis ($p < 0.05$). The concentrations of the other hydroxy-FAs detected in the liver, e.g. 9- and 13-HODE, 5-, 8-, 9-, 11-, 15-HETE, 8-, 18- and 20-HEPE and 4-, 7-, and 8-HDHA were unchanged (Tab. 11.3). Similar to liver tissue, kidney 5-HEPE level is decreased in CLP induced sepsis (18%, $p < 0.01$). Except for 16-HDHA (increase by 48%, $p < 0.05$) and 14-HDHA (increase by 200%) which concentrations were elevated, other hydroxy-FAs detected were unaffected, e. g. 8-, 9-, 11-, 12-, 15-HETE and 4-, 7-, 8- and 11-HDHA (Tab. 11.4). In accordance to the LPS model, a trend towards lower hydroxy-FA levels in the heart was observed in CLP induced sepsis. The decrease was significant for 9- and 13-HOTrE, 9- and 13-HODE, 5-HEPE, 5-, and 9-HETE and 11-HDHA ($p < 0.05$, Tab. 11.5). CLP surgery had no effect on the hydroxy-FA concentrations in the lung (Tab. 11.6).

6.3.4 Epoxy-FAs

The plasma epoxy-FA levels during LPS induced sepsis were either increased or unchanged. 9(10)- and 12(13)-EpODE, 9(10)- and 12(13)-EpOME and 19(20)-EpDPE were found at 62-170% higher concentrations 24 h after LPS treatment ($p < 0.05$ Tab. 11.2). The levels of other detected epoxy-FAs, such as 15(16)-EpODE, 5(6)-, 8(9)-, 11(12) and, 14(15)-EpETrE, 8(9)-, 14(15)-EpETE were unchanged (Fig. 6.3 C,D). In the kidney the effect of LPS on epoxy-FA levels was more pronounced: 14 out of 18 detected epoxy-FA concentrations were changed after LPS treatment ($p < 0.5$). Interestingly, the AA-derived epoxides 8(9)-, 11(12)- and 14(15) EpETrE were decreased by 13-25%, whereas most epoxy-FAs, e.g. 9(10)-, 12(13)- and 15(16)-EpODE, 9(10)- and 12(13)-EpOME, 10(11)-EpDPE or 11(12)- and 14(15)-EpETE were found at 11-87% higher concentrations ($p < 0.05$, Tab. 11.4). Only 17(18)-EpETE, 5(6)-EpETrE, 8(9)-EpETE and 9(10)-epoxystearic acid kidney levels were not

affected by LPS treatment. Heart tissue epoxy-FA concentrations after LPS treatment were decreased by about 35% for the DHA derived epoxides 10(11)-, 13(14)- and 16(17)-EpDPE ($p < 0.05$). The effects of LPS treatment on lung epoxy-FA levels were marginal, only 5(6)-EpETrE was found in an about two-fold higher concentration ($p < 0.05$). In the liver no changes of epoxy-FA concentrations were detected.

The CLP surgery showed only effects on a single plasma epoxy-FA level (Fig. 6.3 C, D): Only 16(17)-EpDPE was increased in the treatment group (55%, $p < 0.001$). The other epoxy-FAs were unchanged and no obvious trend could be observed (Tab. 11.2). Similar to LPS induced sepsis, there was a trend towards decreased epoxy-FA levels in the heart 24 h after CLP. These differences were found to be statistically significant for the ALA derived epoxy metabolites 9(10), 12(13)- and 15(16)-EpODE (decrease about 60%, $p < 0.05$, Tab. 11.5). Regarding the epoxy-FA concentrations in liver, lung and kidney no changes by the CLP surgery were detected (Tab. 11.3, Tab. 11.4, Tab. 11.6).

6.3.5 Dihydroxy-FAs

LPS treatment resulted in increased plasma dihydroxy-FA levels. Out of 20 detected dihydroxy-FAs 12 were significantly elevated by 57-170% ($p < 0.05$), e. g. 8(9)-, 11(12)- and 14,15-DiHETrE, 10,11-; 13,14- and 16,17-DiHDPE or 14,15- and 17,18-DiHETE (Fig. 6.3 E,F, Tab. 11.2). In kidney all dihydroxy metabolites derived from LA and DHA were monitored at 49-101% higher concentrations in the LPS treated group ($p < 0.05$, Tab. 11.4). Dihydroxy-FAs derived from AA, ALA and DHA showed no significant change with a slight trend towards higher levels in LPS induced sepsis. Dihydroxy-FA levels in the lung were elevated in the LPS group, reaching statistically significance for 9,10- and 12,13-DiHODE, 9,10-DiHOME, 4,5-; 7,8- and 10,11-DiHDPE and 5,6 and 8,9-DiHETrE (Tab. 11.6). In contrast to the other oxylipins (see above) detected in the heart tissue, dihydroxy-FA levels of 4,5-, 10,11-, 13,14- and 19,20-DiHDPE and 8,9- and 14,15-DiHETrE were increased by 22-78% in the

LPS treated group ($p < 0.05$, Tab. 11.5). The dihydroxy-FA metabolites in the liver were not affected by LPS treatment (Tab. 11.3).

Dihydroxy-FA levels in plasma showed a trend towards higher concentrations in CLP induced sepsis. 8 out of 20 detected plasma dihydroxy-FA levels were significantly elevated by 72-170% after CLP surgery (9,10- and 12, 13-DiHOME, 11,12- and 14,15-DiHETrE, 10,11-; 13,14-; 16,17- and 19,20-DiHDPE, $p < 0.05$, Fig. 6.3 E, F, Tab. 11.2). In the kidney 14,15-DiHETE, 9,10-DiHOME and 4,5-; 10,11-; 13,14-; 16,17- and 19,20 DiHDPE were increased by 43-71% after CLP surgery ($p < 0.05$, Tab. 11.4). Interestingly, for 15,16-DiHODE a 46% lower concentration after CLP was observed ($p < 0.05$). The other dihydroxy-FA levels in kidney, such as 9,10-DiHODE, 12,13-DiHOME, 8,9-; 11,12- and 14,15-DiHETrE and 7,8-DiHDPE were unaffected. In the heart tissue inconsistent effects of LPS induced sepsis on dihydroxy-FA levels were observed: 15,16-DiHODE and 9,10-dihydroxystearic acid concentration were decreased by 69 and 32%, respectively ($p < 0.01$). Levels of 17,18-DiHETE, 10,11- and 19,20-DiHDPE and 14,15-DiHETrE were elevated by 27-75% ($p < 0.05$, Tab. 11.5). In the liver 12,13- and 15,16-DiHODE, 17,18-DiHETE and 12,13-DiHOME were significantly decreased by 30-62% after CLP surgery ($p < 0.05$). Except for the 15-LOX metabolite 8,15-DiHETE, which was decreased by 56% ($p < 0.05$) in the treatment group, no changes were observed for the CYP/sEHi formed dihydroxy-FAs detected in the lung tissue.

6.4 Discussion

Sepsis is a severe medical condition characterized by the release of pro-inflammatory mediators resulting in centralization and multi organ failure. Aside from interleukins, induction of COX-2 leads to an increase of PGE_2 in sepsis [5]. This study aims to comprehensively investigate if and how other lipid mediators derived from AA or other n-3 FAs and PGs are involved in the inflammatory processes of sepsis by comparing two commonly used sepsis models, the LPS and CLP model.

Both models successfully induced sepsis as characterized by clinical chemistry. The increased plasma creatinine and urea levels in the LPS group indicate an acute kidney injury (AKI), a common condition in human sepsis [30]. Liver injury was moderate in the LPS group, with only a slight increase in AST levels. CLP surgery resulted in a dramatic increase of AST and ALT, indicating a more pronounced liver damage. No change in plasma creatinine and only ~50% increase in serum urea compared to the LPS model was observed in the CLP induced sepsis model. Elevation of urea without s-creatinine elevation points towards increased catabolism [31] but subclinical AKI cannot be excluded. Comparing both models the LPS induced sepsis resulted in AKI, whereas after CLP surgery the liver failure was more pronounced.

The induction of sepsis is characterized by increased COX-2 expression, e. g. in activated macrophages, and as a consequence by increased levels of PGs [5]. Utilizing targeted metabolomics we simultaneously monitored the increase of a large number of PGs, such as PGE_2, the prostacyclin metabolite 6-keto-$PGF_{1\alpha}$ and the $PGF_{2\alpha}$ metabolite 13,14-dihydro-15-keto-$PGF_{2\alpha}$. Moreover, metabolites derived from other FAs, e. g. 13,14-dihydro-15-keto-PGE_1 were observed for the first time in LPS-induced sepsis. The massive increase of PGE_2 and 6-keto-$PGF_{1\alpha}$ after LPS treatment is consistent the results of previous studies [8]. CLP surgery led to a comparable moderate increase in PG levels, indicating a significant difference between both models. Similar observations have been made regarding cytokine production, which were about 100-fold higher in the LPS model in comparison to the CLP model [4, 32]. Moreover, it has been reported that LPS injection is followed by fast and transient increase of systemic cytokine levels, whereas after CLP surgery the increase is more continuous and sustained [4, 26]. Since both models were only analyzed after 24 hours it can only be assumed that the increase of PGs may follow a similar kinetics. In other studies a rapid increased of PGE_2 levels in serum or peritoneal lavage fluid was observed after 5 h, 12 h or 18 h after surgery [9, 33, 34]. Overall, it is difficult to compare different CLP studies because different

numbers of cecal punctures and needle puncture size influence the release of intestinal bacteria which affects the onset and progression of sepsis [4].

Regarding lipid mediators formed in the LOX and CYP pathway of the AA cascade a large number of oxylipins is elevated in the LPS and CLP induced sepsis. Only a slight to moderate increase of the non-enzymatically formed autoxidation markers 9- and 11-HETE was observed indicating a specific effect rather than an unspecific formation in response to elevated activity of PLA_2 or other lipases, as observed in inflammatory *in vivo* models [35, C*hapter 5*]. Remarkably, there is a trend towards increased 12-LOX products (12-HETE, 12-HEPE) in plasma, liver and kidney, indicating an elevated 12-LOX and 12-lipoxygenating ALOX-15 activity during sepsis. The massive plasma increase of the neutrophil chemoattractant 12-HETE [36, 37] suggests an involvement of this lipid mediator in the development of sepsis. A pharmacological decrease of this pro-inflammatory mediator may help to reduce neutrophil recruitment, as already shown in mouse models of acute lung injury [38], and therefore might allow attenuating multi organ failure during sepsis. However, it has to be considered that a reduced neutrophil recruitment is controversial in early stage of sepsis [39]. Interestingly, plasma, liver, kidney and lung levels of the vasoconstrictor 20-HETE [40] are increased after LPS treatment or CLP surgery, although one would expect based on the reduced blood pressure during acute septic shock a low level of this oxylipin.

It is remarkable that sepsis leads to a general elevation of dihydroxy-FA plasma levels, which is consistent with earlier studies [8, 23, 41]. The CLP model elicits the same effect, albeit less pronounced. Regarding epoxy-FAs as precursors of dihydroxy FAs, only few were elevated during sepsis. This suggests that sepsis increases CYP formation of highly biological active epoxy FAs [42] which are rapidly hydrolyzed to less active dihydroxy-FA by soluble epoxide hydrolase (sEH). This assumption is substantiated by the observation that the most abundant epoxides, e. g. 9(10)- and 12(13)-EpOME, are increased in sepsis.

These might be formed at such high concentrations that the capacity of sEH is too low to abolish the massive increase in epoxy-FAs completely.

Although clinical chemistry revealed a severe kidney injury in the LPS group, no effect on AA derived PGs was observed. Only levels of PGD_1 and $PGF_{1\alpha}$ derived from DGLA and dihomo $PGF_{2\alpha}$ derived from adrenic acid - known to be produced in renal medulla - were elevated [43]. Interestingly, most of the changes in oxylipin levels in the kidney were detected in the CYP branch, especially for the epoxy-FAs resulting in increased epoxy to dihydroxy ratios of LA and ALA. The vasodilatory properties of the epoxides [42] may contribute to the development of hypotension during sepsis. However, the best investigated EpETrEs derived from AA were found at decreased concentrations.

Consistent with clinical chemistry which revealed no acute kidney injury in the CLP group, no effect on kidney PGs, hydroxy- and epoxy-FA levels was found, showing again differences in LPS and CLP induced sepsis. The liver injury in the CLP group was not accompanied by increased PG levels and only a small number of hydroxy-FAs were elevated. Because LPS treatment resulted in changes of few oxylipins as well, it is concluded that oxylipins are not a suitable marker for liver damage in LPS and CLP sepsis models.

6.5 Conclusions

Overall, the present study shows that both *in vivo* models of sepsis are characterized by massive changes in plasma oxylipin derived from all enzymatic branches of the AA cascade. Comparing both models 24 h after induction of sepsis the LPS model caused a more pronounced increase in oxylipins. Thus, this model seems to be better suited to investigate effects on the AA cascade than CLP.

6.6 References

[1] Angus D. C., van der Poll T. *N Engl J Med* (2013) 369, 840-851

[2] Annane D., Aegerter P., Jars-Guincestre M. C., Guidet B. *Am J Respir Crit Care Med* (2003) 168, 165-172

[3] Martin G. S. *Exp Rev Anti Infect Ther* (2012) 10, 701-706

[4] Buras J. A., Holzmann B., Sitkovsky M. *Nat Rev Drug Discov* (2005) 4, 854-865

[5] Cohen J. *Nature* (2002) 420, 885-891

[6] Ertel W., Morrison M. H., Wang P., Ba Z. F., Ayala A., Chaudry I. H. *Ann Surg* (1991) 214, 141-148

[7] Liu J.-Y., Tsai H.-J., Hwang S. H., Jones P. D., Morisseau C., Hammock B. D. *Br J Pharmacol* (2009) 156, 284-296

[8] Schmelzer K. R., Kubala L., Newman J. W., Kim I.-H., Eiserich J. P., Hammock B. D. *Proc Natl Acad Sci* (2005) 102, 9772-9777

[9] Uozumi N., Kita Y., Shimizu T. *J Immunol* (2008) 181, 3558-3566

[10] Halushka P. V., Reines H. D., Barrow S. E., Blair I. A., Dollery C. T., Rambo W., Cook J. A., Wise W. C. *Crit Care Med* (1985) 13, 451-453

[11] Reines H. D., Cook J. A., Halushka P. V., Wise W. C., Rambo W. *Lancet* (1982) 320, 174-175

[12] Smyth E. M., Grosser T., Wang M., Yu Y., FitzGerald G. A. *J Lipid Res* (2009) 50, S423-S428

[13] Ricciotti E., Fitzgerald G. A. *Arterioscler Thromb Casc Biol* (2011) 31, 986-1000

[14] Basu S. *Med Res Rev* (2007) 27, 435-468

[15] Samuelsson B., Goldyne M., Granstrom E., Hamberg M., Hammarstrom S., Malmsten C. *Annu Rev Biochem* (1978) 47, 997-1029

[16] Imig J. D. *Physiol Rev* (2012) 92, 101-130

[17] Morisseau C., Inceoglu B., Schmelzer K., Tsai H.-J., Jinks S. L., Hegedus C. M., Hammock B. D. *J Lipid Res* (2010) 51, 3481-3490

[18] Kroetz D. L., Xu F. *Annu Rev Pharmacol Toxicol* (2004) 45, 413-438

[19] Haeggström J. Z., Funk C. D. *Chem Rev* (2011) 111, 5866-5898

[20] Serhan C. N., Petasis N. A. *Chem Rev* (2011) 111, 5922-5943

[21] Yin H., Brooks J. D., Gao L., Porter N. A., Morrow J. D. *J Biol Chem* (2007) 282, 29890-29901

[22] Milne G. L., Musiek E. S., Morrow J. D. *Biomarkers* (2005) 10, 10-23

[23] Liu J.-Y., Lin Y.-P., Qiu H., Morisseau C., Rose T. E., Hwang S. H., Chiamvimonvat N., Hammock B. D. *Eur J Pharm Sci* (2013) 48, 619-627

[24] Meirer K., Steinhilber D., Proschak E. *Basic Clin Pharmacol Toxicol* (2013) 114, 83-91

[25] Peri K. G., Varma D. R., Chemtob S. *FEBS Letters* (1997) 416, 269-272

[26] Dejager L., Pinheiro I., Dejonckheere E., Libert C. *Trends Microbiol* (2011) 19, 198-208

[27] Schabbauer G. *Drug Discov Today* (2012) 9, e17-e21

[28] Kümpers P., Gueler F., David S., Van Slyke P., Dumont D., Park J.-K., Bockmeyer C., Parikh S., Pavenstadt H., Haller H., Shushakova N. *Crit Care* (2011) 15, R261

[29] Ostermann A. I., Willenberg I., Schebb N. H. *Anal Bioanal Chem* (2015) 407, 1403-1414

[30] Zarjou A., Agarwal A. *J Am Soc Nephrol* (2011) 22, 999-1006

[31] Hosten A. O. BUN and Creatinine. In: Clinical Methods: The History, Physical, and Laboratory Examinations, Walker H. K., Hall W. D., Hurst J. W. (eds) (1990)

[32] Deitch E. A. *Shock* (1998) 9, 1-11

[33] Bitto A., Minutoli L., David A., Irrera N., Rinaldi M., Venuti F., Squadrito F., Altavilla D. *Crit Care* (2012) 16, R32

[34] Spite M., Norling L. V., Summers L., Yang R., Cooper D., Petasis N. A., Flower R. J., Perretti M., Serhan C. N. *Nature* (2009) 461, 1287-1291

[35] Hamaguchi K., Kuwata H., Yoshihara K., Masuda S., Shimbara S., Oh-ishi S., Murakami M., Kudo I. *Biochim Biophys Acta* (2003) 1635, 37-47

[36] Cunningham F. M., Wollard P. M. *Prostaglandins* (1987) 34, 71-78

[37] Wiggings R. E., Jafri M. S., Proia A. D. *Prostaglandins* (1990) 40, 131-141

[38] Rossaint J., Nadler J., Ley K., Zarbock A. *Crit Care* (2012) 16, 1-15

[39] Craciun F. L., Schuller E. R., Remick D. G. *J Immunol* (2010) 185, 6930-6938

[40] Zou A. P., Fleming J. T., Falck J. R., Jacobs E. R., Gebremedhin D., Harder D. R., Roman R. J. *Am J Physiol* (1996) 270, R228-R237

[41] Kubala L., Schmelzer K. R., Klinke A., Kolarova H., Baldus S., Hammock B. D., Eiserich J. P. *Free Radic Biol Med* (2010) 48, 1311-1320

[42] Morisseau C., Hammock B. D. *Annu Rev Pharmacol Toxicol* (2013) 53, 37-58

[43] Sprecher H., VanRollins M., Sun F., Wyche A., Needleman P. *J Biol Chem* (1982) 257, 3912-3918

Chapter 7

Determining COX-2 Activity in Three Different Test Systems Utilizing online-SPE-LC-MS for Parallel Quantification of Prostaglandin E_2, D_2 and Thromboxane B_2 *

Cyclooxygenase-2 (COX-2) catalyzes the formation of PGH_2 from arachidonic acid. PGH_2 is further converted to different prostaglandins (PG), such as PGE_2, PGD_2 and TxB_2. In this study a rapid online-SPE-LC-MS method for the simultaneous quantification of PGE_2, PGD_2 and TxB_2 streamlined for COX-2 enzyme assays is presented. Baseline separation of all analytes was achieved in only 7.1 min per sample, including sample preparation by online SPE. The method showed high sensitivity (LODs of 0.65-1.25 fmol on column) and accuracy (89-113%) in protein containing media. Because of online-SPE, no manual sample preparation was required, except for addition of IS solution, allowing to use the approach as rapid read-out in COX-2 activity assays. This was demonstrated by applying the method on three in vitro test systems: a cell-free enzyme assay, an assay using HCA-7 cells constitutively expressing COX-2 and primary human monocytes. In these assays, the potency of three popular drugs celecoxib, indomethacin and dexamethasone was successfully characterized with the new online-SPE-LC-MS method. The comparison of the results showed that the inhibitory effects of PG formation strongly depend on the test system. Thus we suggest that the modulation of COX-2 activity of a test compound should be at least characterized in two assay systems. With the online-SPE-LC-MS method described in here we present a versatile tool as read-out for these types of assays.

* Reprinted from *Journal of Chromatography A*, vol. 1391, Willenberg I., Meschede A. K., Schebb N. H., Determining COX-2 Activity in Three Different Test Systems Utilizing online-SPE-LC-MS for Parallel Quantification of Prostaglandin E_2, D_2 and Thromboxane B_2, pp. 40-48, Copyright (2015), with permission from Elsevier.

Author contributions: IW: Designed research, performed experiments, and wrote manuscript; AKM: Performed Western Blots as part of her master thesis under the supervision of IW; NHS: Designed research and wrote the manuscript.

7.1 Introduction

Cyclooxygenases (COX) are enzymes of the arachidonic acid (AA) cascade catalyzing the conversion of AA to prostaglandin (PG) H_2 (Fig. 7.1) [1]. This reaction comprises two steps: In the first step PGG_2 is formed by addition of two molecules of oxygen to the fatty acid. In the second step the peroxidase activity of COX reduces the hydroperoxide leading to PGH_2 which is further metabolized via various downstream enzymes (Fig. 7.1) [1].

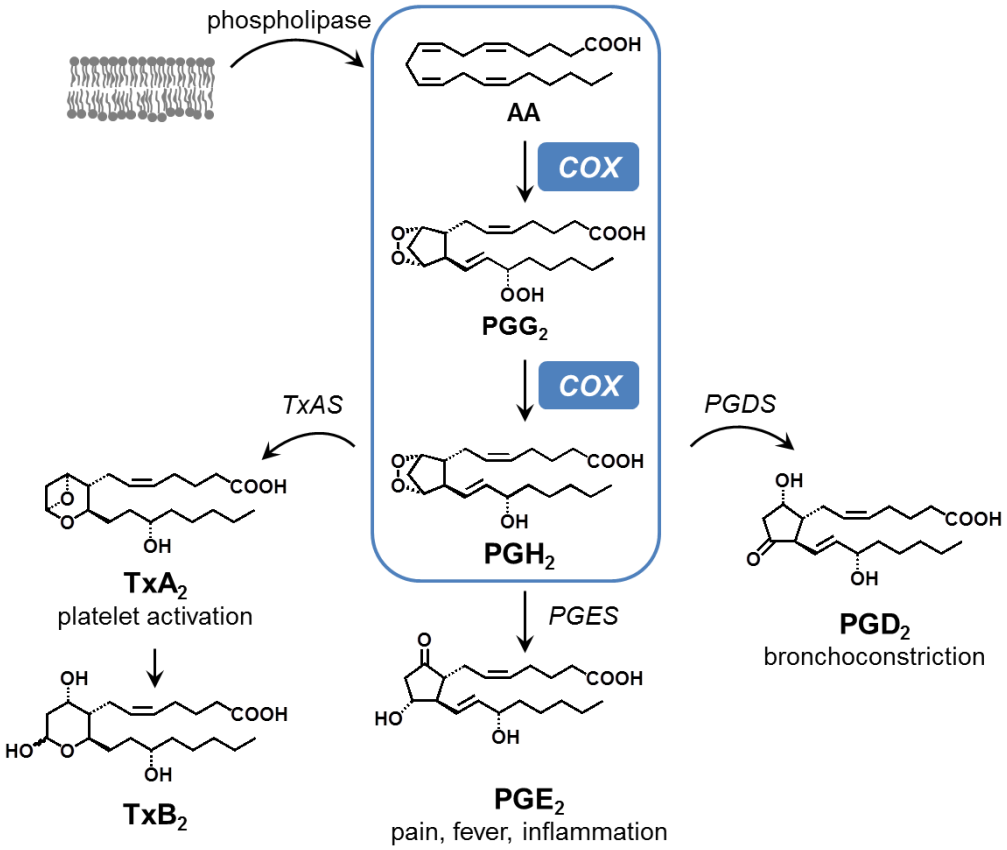

Fig. 7.1: Prostaglandin formation: Arachidonic acid is released from membrane phospholipids by phospholipases. Cyclooxygenases (COX) convert AA via PGG_2 to the endoperoxid PGH_2. Subsequent formation of PGE_2 and PGD_2 is catalysed by prostaglandin-E/D-synthase (PGE/DS). TxA_2 is formed by thromboxane-A-synthase (TxAS) and under aqueous conditions rapidly hydrolysed to the biologically inactive TXB_2 [1].

COXs exist in different isoforms [2]. Simplified, COX-1 is constitutively expressed regulating homeostasis, e. g. stomach acidity or renal function [1]. By

contrast, COX-2 is induced by several growth factors such as cytokines and mechanical stress e. g. during inflammatory processes [3]. Moreover a third isoform, COX-3, of unclear biological relevance has been described. Downstream processing of PGH_2 leads to several potent lipid mediators such as TxA_2 which is formed by thromboxane-A-synthase. TxA_2 is under aqueous conditions unstable and rapidly hydrolyzed to the biologically inactive TxB_2 [1]. Prostaglandin-E-synthase yields PGE_2 which mediates pain, fever and inflammation among several other biological functions [4]. Prostaglandin-D-synthase catalyzes the conversion from PGH_2 to PGD_2 [1], a bronchoconstrictory lipid mediator [5] (Fig. 7.1). Which metabolite is formed depends on the specific cell or tissue where the precursor PGH_2 is formed: thromoboxane-A-synthase is for example located in platelets, while prostaglandin-D-synthase is expressed in mast cells and in the brain [4]. Prostaglandin-E-synthase can be found in most cells and tissues [4, 6].

The biological role of PGE_2 in regulation of pain, fever and inflammation makes COX, especially COX-2, a prominent drug target. Non-steroidal anti-inflammatory drugs (NSAIDs), which are one of the most used classes of pharmaceuticals, act by inhibiting COX resulting in reduced prostaglandin levels [7]. In order to overcome side effects of NSAIDs caused by inhibition of both COX isoforms, many efforts were made to develop COX-2 selective inhibitors (e. g. celecoxib, valdecoxib) [8, 9]. To characterize compounds for their ability to inhibit COX, *in vitro* screening assays are performed. For this purpose several assays have been developed, for example cell-free enzyme inhibition assays with recombinant COX-1 or COX-2 in the presence of cofactors and the endogenous substrate AA [10]. Other approaches use cell lines which constitutively express COX-2 [11] or which express COX-2 upon inflammatory stimulus [12, 13]. All test systems have in common that they determine enzyme activity and inhibition based on substrate consumption or product formation. One possible read-out is to measure the oxygen (substrate) consumption [8] or to apply spectrophotometric assays with a dye which is oxidized during the reduction of PGG_2 to PGH_2 [14]. However, methods which directly quantify the

formed PGs are more reliable [15]. Analysis of the direct COX products PGG_2 and PGH_2 is not suitable because of their short half-lifes in aqueous solution [16]. If no further downstream processing enzyme is present, the amount of PGE_2 can be monitored because PGH_2 spontaneously reacts to PGE_2, PGD_2 and $PGF_{2\alpha}$ in aqueous solution with PGE_2 as main product [16]. Thus, most commonly formation of PGE_2 is used for the determination of COX activity and inhibitory potency (expressed as IC_{50} value) of test compounds. However, the fate of initially formed PGH_2 depends on the test system, and the TxB_2 concentration is also commonly used as read-out. Quantification of PGs and TxB_2 can be achieved either by applying ELISA [17], the use of radiolabeled AA followed by a separation technique and scintillation counting [18] or liquid chromatography (LC) coupled to mass spectrometry [10, 19]. The disadvantage of ELISAs is the potential risk of insufficient selectivity due to cross-reactivities of the antibodies. For the radioisotope assay the labeled substrate has to be available and it requires permissions, specialized handling and disposal of waste. Therefore LC-MS analysis seems - if instrumentation is available - to be the most straightforward read-out. Several comprehensive LC-MS methods for the quantification of PGs and other oxidative metabolites of AA and other polyunsaturated fatty acids have been developed [20]. Additionally, methods covering only some metabolites of the COX branch of the AA cascade, are described [10, 16, 21-23] and used in COX inhibition assays. However, all of these methods require a time consuming and laborious sample preparation by liquid/liquid extraction or solid phase extraction (SPE) impeding sample throughput. COX activity assays, e.g. for the characterization of the inhibitory potency of drugs, result in a large number of samples. The present study describes the development of a rapid online-SPE-LC-MS method streamlined for these kinds of analyses. PGE_2, PGD_2 and TxB_2 are simultaneously quantified in biological samples with minimal manual sample preparation. The applicability of the approach is demonstrated for three COX-2 inhibitory *in vitro* test systems: (I) a cell-free system utilizing recombinant COX-2, (II) the human colon carcinoma cell line HCA-7 constitutively expressing COX-2 and (III)

primary human monocytes which express COX-2 upon lipopolysaccharide (LPS) stimulus.

7.2 Experimental

7.2.1 Chemicals and biological materials

Oxylipin standards and internal standards (IS), human recombinant COX-2 and arachidonic acid were from Cayman Chemicals (local distributor: Biomol, Hamburg, Germany). Methanol (MeOH), LC-MS grade acetonitrile (ACN) and acetic acid were purchased from Fisher Scientific (Schwerte, Germany). TRIS and DMSO were obtained from Roth (Karlsruhe, Germany) and hydrochloric acid from Merck (Darmstadt, Germany). LPS from *Escherichia coli* 0111:B4 and other chemicals were purchased from Sigma-Aldrich (Schnelldorf, Germany). Dulbecco's modified Eagle's medium (DMEM), RPMI 1640 buffered with 20 mM HEPES, fetal calf serum (FCS) and all other cell culture reagents, except DME/High modified (Sigma-Aldrich Cat. No. 56436C) were purchased from Biochrom (Berlin, Germany). HCA-7 cells were obtained from the European Collection of Cell Cultures (ECACC, Salisbury, United Kingdom).

7.2.2 Online-SPE-LC-MS method

Quantification of TxB_2, PGE_2 and PGD_2 was carried out by LC-MS with online-SPE in backflush mode (Fig. 7.2) [24]. Samples were kept at 4 °C in a xt-PAL autosampler (CTC Analytics, Zwingen, Switzerland) equipped with a 100 µL syringe. Wash solution 1 was 0.1% acetic acid in water and wash solution 2 was ACN. The LC system consisted of an Agilent 1290 column oven (Agilent, Waldbronn, Germany) operated at 40 °C with a high pressure two-way six port valve (valve 1, Fig. 7.2) and two Agilent 1290 binary pumps (Agilent). An Agilent Inline Filter (Part No. 50674638) was connected to the outlet of the autosampler. Detection was carried out on a QTRAP 6500 triple quadrupol

mass spectrometer (ABSciex, Darmstadt, Germany) equipped with a high pressure two-way six port valve (valve 2, Fig. 7.2).

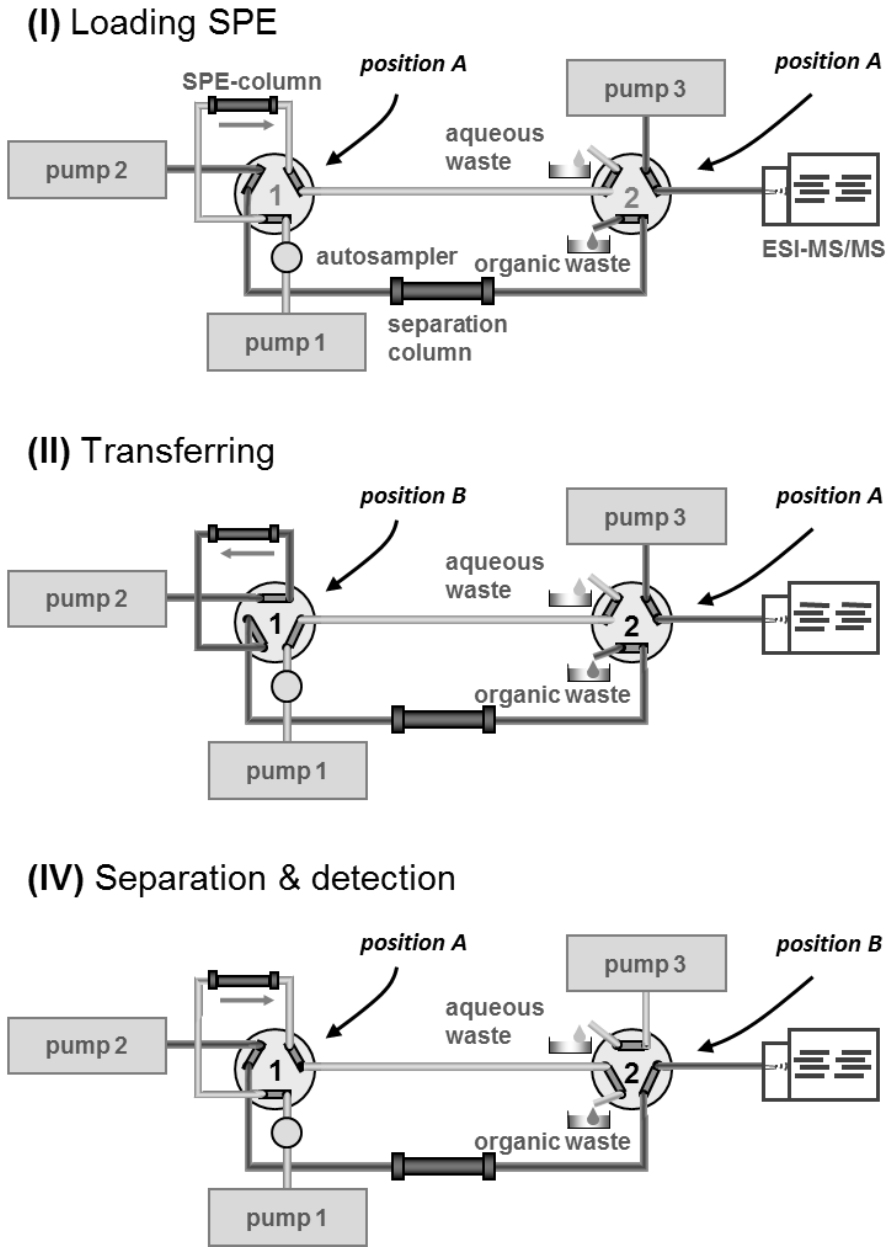

Fig. 7.2: Setup of the online-SPE-LC-ESI-MS/MS system [24]. The samples are loaded on the SPE column by the flow of pump 1 (**I**). After 0.5 min the six port valve 1 (V1) is switched and the analytes are backflushed toward the separation column by the flow of pump 2 (**II**). After 2.5 min V1 is switched back to position A and the eicosanoids are separated by the gradient delivered by pump 2. Meanwhile the SPE column is cleaned and re-equlibrated (**IV**). The second six port valve (V2) reduces contamination of the ESI source by directing polar matrix compounds eluting close to the void volume to waste. Moreover, it enables separation of aqueous and organic waste and therefore reduces environmental impact.

The samples were injected into the loading flow delivered by pump 1((eluent A: 0.1% acetic acid; eluent B: 95/5 (*v/v*) ACN/water acidified with 0.1% acetic acid). During this step of analysis the analytes were retained by the SPE material while proteins and salts were washed to waste. After switching valve 1 to position B (Fig. 7.2) the analytes were backflushed toward the separation column by the flow of pump 2 (eluent A: 95/5 (*v/v*) water/eluent B, acidified with 0.1% acetic acid, eluent B: 800/150/1 (*v/v/v*) ACN/MeOH/acetic acid). After analyte transfer from the SPE column to the analytical column, valve 1 was switched back to position A. Polar matrix compounds eluting close to the void volume of the analytical column were directed to waste. Thereafter valve 2 was switched directing the eluent of the separation column to the MS and enabling detection of the analytes. During chromatographic separation, the SPE column was cleaned with solvent B. Shortly after elution of all analytes valve 2 was switched back to position A and the SPE column was equilibrated for the next run while the separation column was washed and reconditioned. The final switching times of both valves are shown in Tab. 7.1.

Tab. 7.1: Valve positions during the different steps of analysis (Fig. 7.2).

Step	Time (min)	V1	V2	SPE column	Separation column
I	0-0.5	A	A	loading	equilibrating
II	0-2.5	B	A	eluting	loading
III	2.5-3.2	A	A	-	eluting
IV	3.2-5.8	A	B	cleaning	eluting
V	5.8-7.1	A	A	equilibrating	cleaning

Three SPE columns were tested for their performance extracting PGE_2, PGD_2 and TxB_2: (I) Waters HLB direct connect HP (2.1 × 30 mm, 20 µm particle; Waters, Eschborn, Germany), (II) Cyclone (0.5 × 50 mm, 50 µm particle; Thermo Fisher Scientific, Schwerte, Germany) and (III) a Kinetex C-18 pre-column (2 × 4 mm, 1-5 µm particle; Phenomenex, Aschaffenburg, Germany).

The chromatographic separation was optimized on a Kinetex C-18 column (50 × 2.1 mm, 1.3 µm fused core particles, pore size 100 Å) (Phenomenex) equipped with a KrudKatcher inlet filter (Phenomenex). The optimized solvent gradients and flow rates are shown in Fig. 7.3.

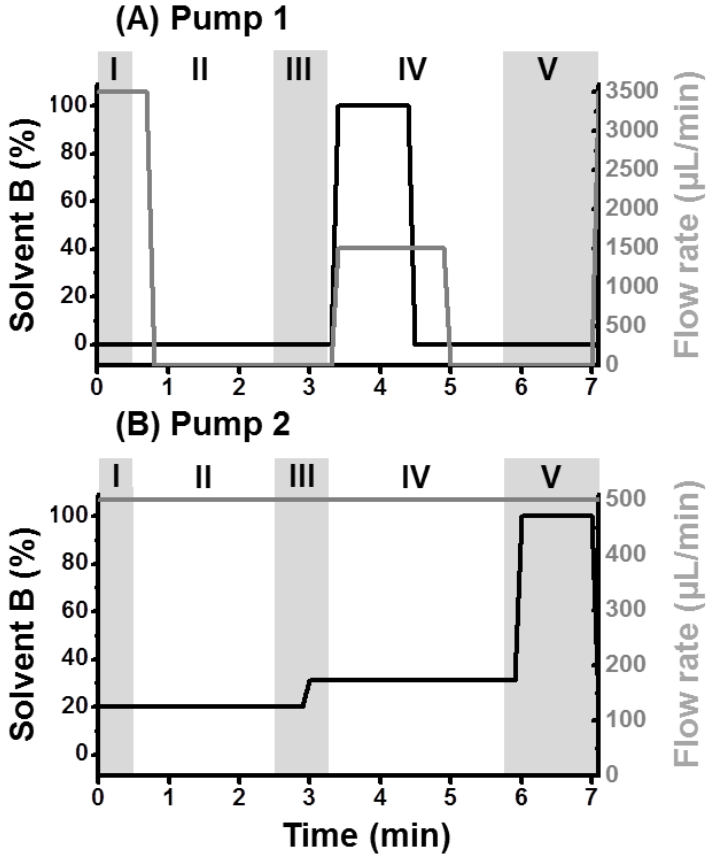

Fig. 7.3: Solvent gradients (black line) and the flow rate (gray line) of (**A**) pump 1 and (**B**) punp 2. The background color (gray and white) indicates the switching of the valve positions.

Mass spectrometric detection following electrospray ionization (ESI) in the negative mode was carried out in selected reaction monitoring (SRM) mode using the following parameters optimized for PGE_2 detection: ion spray voltage -4.5 kV, entrance potential -10 V, curtain gas 35 psi, gas 1 and gas 2 both 60 psi, temperature 450°C, collision-activated dissociation (CAD) gas was set to high value (12 psi). For the transition of each analyte declustering potential (DP), collision energy (CE) and collision cell exit potential (CXP) were optimized

(Tab. 7.3). Nitrogen was used as nebulizer, desolvation and collision gas. The instrument was operated in scheduled SRM mode with a detection window of ± 22.5 s around the expected retention time. Quantification was performed by an external calibration and $^{2}H_4$-PGE_2, $^{2}H_4$-PGD_2 and $^{2}H_4$-TxB_2 (20 nM) as IS. For calibration, the analyte to IS area ratios were linearly fitted reciprocally weighted by concentration. Instrument controlling was performed with Analyst 1.6.1 and data analysis was carried out with Multiquant 2.2 (AB Sciex).

In order to test the extraction efficacy of the different SPE columns the eluent of the SPE column was connected to the MS (split 1:10).

Accuracy and precision of the method was tested in spiked cell culture medium (RPMI 1640, 20 mM HEPES, 10% FBS, 2 mM glutamine, penicillin (100 U/mL) and streptomycin (10 µg/mL)). For this purpose 990 µL medium was mixed with 10 µL standard solution in MeOH yielding concentrations of 10, 100 and 250 nM PGE_2, PGD_2 and TxB_2, respectively. The spiked solutions were prepared in triplicate in order to determine intersample variation. The intrasample variation was determined by non-consecutively injecting the same spiked sample three times. Accuracy was calculated as recovery rate by dividing the measured concentration to the spiked amount. For calculation of the interday variation a QS sample standard (20 nM) was analyzed seven times over a period of 6 weeks.

7.2.3 Sample preparation

The only sample preparation carried out was mixing the sample with IS solution prior to the injection of 5 µL supernatant into the online-SPE-LC-MS system. 50 µL cell culture supernatant derived from incubations of HCA-7 cells was spiked with 10 µL IS solution in MeOH. For the monocyte and cell-free assays volumes of supernatant (30 µL) or buffer (75 µL) were mixed with equal volumes of IS in MeOH. Samples from cell based assays were centrifuged (20 000 x *g*, 5 min, 4°C) prior to injection.

7.2.4 Cell-free COX-2 activity assay

The cell-free COX-2 assay was performed as described [10] and adapted to a 96-well plate format. In brief, different concentrations of the test compound (final DMSO concentration 0.8%) were incubated in 100 mM TRIS buffer (pH 8) containing 50 ng COX-2 protein/mL (0.5 U/mL), 1 µM hematin and 2 mM L-epinephrin. After 10 min preincubation at 37°C the reaction was started by the addition of AA (final 5 µM). After 10 min HCl (final 0.2 N) was added to terminate the enzyme reaction.

7.2.5 HCA-7 cell based assay

HCA-7 cells were cultured in DMEM with 10% FCS, 2 mM glutamine, penicillin (100 U/mL) and streptomycin (10 µg/mL) in a humidified 37°C incubator with 5% carbon dioxide. Stock cultures were split at a confluence of 70-80% by using trypsin/EDTA and seeded at a density of 270.000 cells/cm^2. For the COX-2 inhibition assay the cells were seeded at a density of 750.000 cells/well in 6 plate dishes. After 24 h the about 70-80% confluent cells were washed with PBS and treated with the test compound solved in assay medium (DME/High modified without FCS and phenol red adjusted to pH 7.4 with 50 mM TRIS and supplemented with 5 µg/mL AA, 0.1% DMSO). Celecoxib and dexamethasone were tested in a concentration range between 1 nM and 10 µM, the concentrations used for indomethacin ranged between 1 nM and 25 µM. After 24 h of incubation with the test compound the cell culture supernatant was collected and stored at -20 °C until online-SPE-LC-MS analysis. The cells were detached with trypsin/EDTA. After washing the pellet with PBS, it was stored at -80°C till Western Blot analysis. The cytotoxicity of the test compounds in HCA-7 cells was evaluated by a lactate dehydrogenase leakage test (Cyto-Tox-ONE, Promega Mannheim, Germany). Indomethacin showed no cytotoxicity up to a concentration of 25 µM, celecoxib and dexamethasone showed no cytotoxicity up to 10 µM within 24 h of incubation (data not shown).

7.2.6 Primary monocyte based assay

Freshly collected whole EDTA-blood from healthy human subjects was layered over the same volume of Polymorphprep (Axis-Shield, Oslo, Norway) in a 50 mL centrifugation tube. The tubes were centrifuged for 30 min at 555 x *g* at 22 °C in a swing-out rotor without brake. After centrifugation, the upper band containing the mononuclear cells was collected utilizing a pasteur pipette. After centrifugation for 5 min at 500 x *g* the pellet of the mononuclear cells was washed two times with PBS-EDTA buffer (0.5% BSA in PBS with 2 mM EDTA). Finally, the pellet was resuspended in RPMI 1640, buffered with 20 mM HEPES and supplemented with 10% FCS, 2 mM glutamine, penicillin (100 U/mL) and streptomycin (10 µg/mL). The cells were seeded at a density of 6-8 x 10^6 cells per well in 6-well plates in 2 mL medium. After 3 h, non-adherent cells were removed by washing the cells two times with PBS. Test compound dissolved in DMSO was added to freshly prepared medium containing LPS (10 µg/mL). This medium (final DMSO 0.1%) was added to the cells. Indomethacin and celecoxib were tested in a concentration range from 0.1 nM to 10 µM and dexamethasone from 0.01 nM to 1 µM. After 24 h of incubation cell culture supernatant was collected for LC-MS analysis and the cells were harvested for Western Blot (see above). Cell viability was determined by counting the cells in the supernatant and the pellet after mixing with trypan blue solution (0.5%, Biochrom, Berlin, Germany) in a Neubauer chamber. No effects of the compounds in the tested concentrations were observed (data not shown).

7.2.7 COX-2 specific Western Blot

Cells were lysed in ice cold RIPA-buffer (50 mM TRIS, 150 mM NaCl, 1 mM EDTA, 1% (*v/v*) Triton X-100, 1% (*w/v*) sodium desoxycholat, 0.1 % (*w/v*) SDS, pH 7.4, protease inhibitors (Complete Mini Protease-Inhibitor Cocktail tablet, Hoffmann-La Roche Ltd, Switzerland). After centrifugation (16000 x *g*, 5 min, 4 °C) protein concentration was determined with the bicinchoninic acid (BCA) method (BCA assay kid, Sigma, Schnelldorf, Germany) and BSA as standard

for quantification. Aliquots (20 µg protein) and a prestained protein marker (Thermo Scientific, Schwerte, Germany) were separated by SDS-PAGE under reducing conditions on a 10% polyacrylamide gel with a 4% stacking gel and then blotted onto a nitrocellulose membrane (GE, Amersham, UK). Membranes were blocked for 1 h at room temperature with 5% (*w/v*) non-fat dry milk powder (Fluka, Switzerland, Buchs) in TRIS-buffered saline with tween (TBST: 3.5 mM TRIS, 16.5 mM TRIS hydrochloride, 150 mM NaCl, 0.1% (*v/v*) Tween 20, pH 7.5). After cutting the membrane at the 55 kDa marker, the upper part of the membrane containing the COX-2 protein was incubated overnight at 4 °C with mouse monoclonal anti-COX-2 antibody (Cayman, product no. 160112) diluted 1:1000 in TBST. The lower part of the membrane was incubated the same way with a mouse monoclonal anti-β-actin antibody (Biovision, local distributor BioCat, Heidelberg, Germany) diluted 1:4000 in TBST. After three times washing for 10 min in TBST, the membranes were incubated with a horseradish peroxidase labeled goat anti-mouse IgG antibody (Santa Cruz Biotechnology, Heidelberg, Germany) diluted 1:4000 in TBST for 1 h at room temperature. COX-2 and β-actin were detected by enhanced chemiluminescence (Super Signal West Pico Chemiluminescent Substrate, Thermo) by a Chemocam Imager (INTAS, Göttingen, Germany).

7.2.8 Data processing

Inhibitory effects were calculated based on the PGE_2 formation. GraphPad Prism 5.0 (GraphPad Software, San Diego, USA) was used for the fitting of the resulting dose response curve and calculation of the IC_{50} values.

7.3 Results and discussion

7.3.1 Online SPE-LC-MS method development

Central aim of this study was the development of a LC-MS method for the quantification of TxB_2, PGE_2 and PGD_2 as rapid read-out for determining COX-2 activity in different *in vitro* test systems. The most promising strategy to reduce manual sample preparation in LC-MS methods to a minimum is the use of online-SPE as already successfully demonstrated in the field of oxylipin analysis for the quantification of hydroxy-FAs [25] or epoxy-FAs and dihydroxy-FAs [26]. Using an online-SPE setup with two valves enables also the separation of organic and aqueous waste and thus reduces environmental impact and contamination of the MS source (Fig. 7.2) [24].

For the development of the online-SPE, the choice of an appropriate SPE column is crucial: On the one hand the column has to ensure complete extraction of the analytes from the matrix in the loading flow and on the other hand a rapid transfer from the SPE column to the separation column. In order to identify a suitable SPE column both criteria were evaluated for three different SPE columns. At an injection volume of 20 µL (10 nM solution in 50/50 (*v*/*v*) MeOH/water) the Thermo Fisher cyclone column showed a significant breakthrough for TxB_2 (13%), PGE_2 (6%) and PGD_2 (5%). Utilizing the Waters HLB direct connect column and the Kinetex RP-18-pre-column, the breakthrough was for all analytes <1%. Based on the breakthrough of all analytes, the Thermo Fisher cyclone does not seem to be suitable as online-SPE column for extraction of TxB_2, PGE_2 and PGD_2. This may be explained by the properties of the polymeric styrol-divinylbenzene phase of the Thermo Fisher cyclone allowing only non-polar and π-π interactions. In contrast, the HLB column consists of a mixed mode phase which enables both hydrophilic and lipophilic interactions and therefore may better retain the moderate polar TxB_2 and PGs. The (non-polar) C-18 material (Phenomenex C-18 pre-column) led with higher injection volumes (25, 50 and 90 µL) to breakthrough (Tab. 7.2).

Tab. 7.2: Comparison of the breakthrough test of the Waters Oasis direct connect HP (2.1 x 30 mm, 20 µm particle) and a phenomenex RP-18 pre-column (2 x 4 mm, particle 1-5 µm). Different volumes (25, 50 and 90 µL) of a 10 nM multi-standard solution (50/50 water/ACN) were injected in the loading flow (3500 µL min^{-1}, 0.1% acetic acid). The eluent of the SPE was monitored by MS/MS (split 1:10). After 1.5 minutes the eluent was changed to 100 % B (95/5 ACN/water, 0.1% acetic acid) in order to elute the loaded analytes. The breakthrough (%) of each analyte was calculated by the peak areas at a mobile phase composition of 100% aquaous acetic acid in comparison to that of 100% B

	Breakthrough (%)					
Injection volume	**Waters direct connect**			**Phenomenex RP-18 pre-column**		
	TxB_2	**PGE_2**	**PGD_2**	**TxB_2**	**PGE_2**	**PGD_2**
25 µL	0.1	0.2	0.1	3.3	0.3	0.3
50 µL	0.1	0.1	0.1	60	43	44
90 µL	0.1	0.1	0.1	100	100	100

While the most polar analyte TxB_2 already showed a slight breakthrough (3%) at an injection volume of 25 µL, an injection of 50 µL let to a breakthrough of all analytes (43-60%). The injection of 50 µL of the same amount of multi-standard solution solved in 10/90 (*v/v*) ACN/water resulted for all analytes in a breakthrough of below 0.1% indicating sufficient extraction capacity of the material to retain the injected 0.5 pmol of analytes. However, the elution power for 50/50 (*v/v*) ACN/water causes a poor extraction efficacy on this material already at 50 µL injection volume despite high flow rate of 3.5 mL/min water. By contrast, no (<0.2%) breakthrough was observed for the Waters HLB direct connect column up to an injection volume of 90 µL in 50/50 ACN/water (v/v), thus showing clearly the best extraction efficacy and was selected for further analysis.

As a next step the elution profile - in backflush mode - of the analytes from Waters SPE column was investigated with different concentrations of solvent B (15, 20 and 30%). 15% B resulted in a broad signal, and transfer was

completed in 3.0 min while elution at 20 and 30% B yielded only moderately tailing peaks of the analytes and a transfer time of 1.5 min (Fig. 7.4).

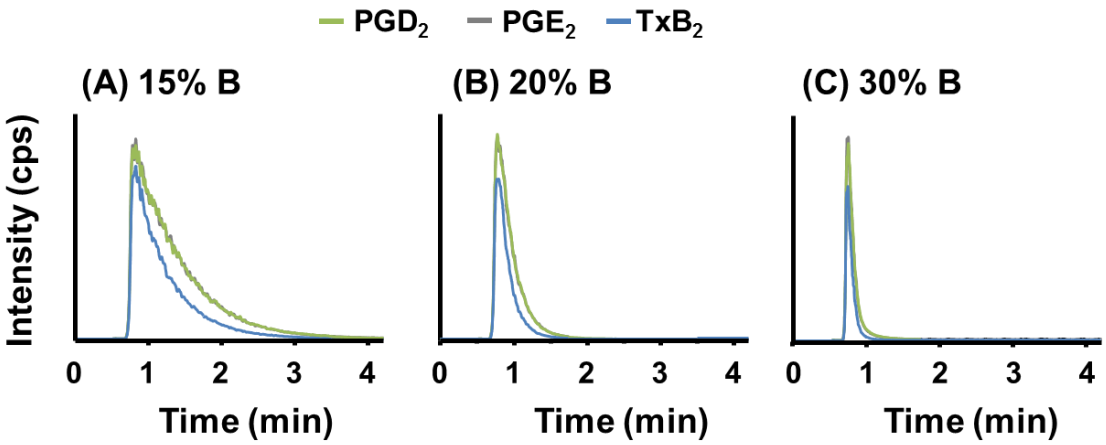

Fig. 7.4: Elution profile from Waters Oasis direct connect HP (2.1 x 30 mm, 20 µm particle). The separation column was removed from the online-SPE-LC-MS setup and the eluent of the SPE at (**A**) 15%, (**B**) 20% and (**C**) 30 % eluent B was directly monitored by ESI-MS/MS. The SRM signals of the analytes of an injection (5 µL) of a 10 nM multi-standard solution are shown.

In order to ensure rapid analysis and sharp chromatographic peaks, elution from the SPE column towards the separation column has therefore to be carried out with at least 20% B. The injection volume also influenced the elution profile probably causing a deeper penetration of the analytes into the SPE column requiring a longer elution. For the injection of 20 µL (50/50 (*v*/*v*) ACN/water) and elution with 20% B the transfer time of was 2.5 min. Higher injection volumes (25 µL and more) in this solvent led to massive tailing. Based on these results SPE of TxB_2, PGE_2 and PGD_2 was carried out on the Waters HLB direct connect with a maximal injection volume of 20 µL (50/50 (*v*/*v*) water/ACN), elution at 20% B and a minimum switching time of valve 1 back to position A of 2.5 min (Fig. 7.2, Tab. 7.1).

The chromatographic separation was carried out on a Kinetex C-18 column (50 × 2.1 mm, 1.3 µm) in standard LC mode. This represents the latest development in RP high performance liquid chromatography combining the advantages of sub-2-µm particles with the improved mass transfer of solid

(fused) core particles. Baseline separation of the analytes was achieved with an isocratic flow of 31% B in less than 3 min. Retention times: TxB_2 (1.4 min), PGE_2 (2.3 min), PGD_2 (2.7 min). Due to similar MS spectra of both PGs the same SRM transitions were used for the regioisomers PGE_2 and PGD_2.The use of a more selective transition for PGD_2 (*m/z* 351/233) dramatically decreased sensitivity, while not being fully selective for this isomer [27]. Therefore the chromatographically separation is crucial to quantify both PGs independently from each other with high sensitivity.

When combining the online-SPE setup with the analytical column using 31% B for both, the transfer and the separation, broad peaks and insufficient separation of PGE_2 and PGD_2 resulted (Fig. 7.5).

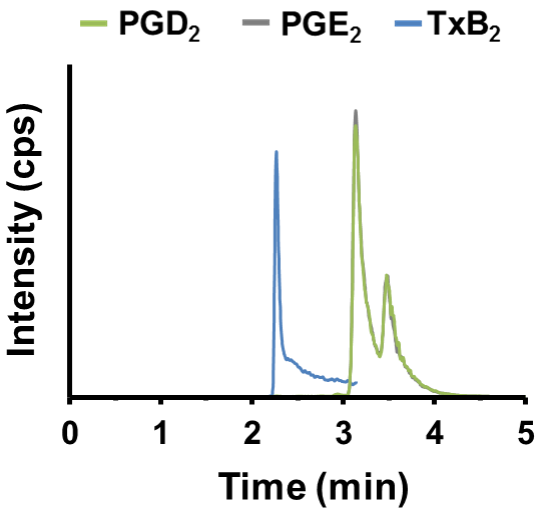

Fig. 7.5: Insufficient separation of PGE_2 and PGD_2 utilizing the online-SPE-LC-MS setup with an isocratic flow of 30% B of pump 2. Shown are the SRM transitions of the injection of 20 µL of a 40 nM standard solution.

By including a focusing step of the analytes on the analytical column at organic solvent concentration <30% the separation improved dramatically. Transfer from SPE to analytical column with 20% B followed by isocratic elution at 31% B led to baseline separation of TxB_2, PGE_2 and PGD_2 (Fig. 7.6).

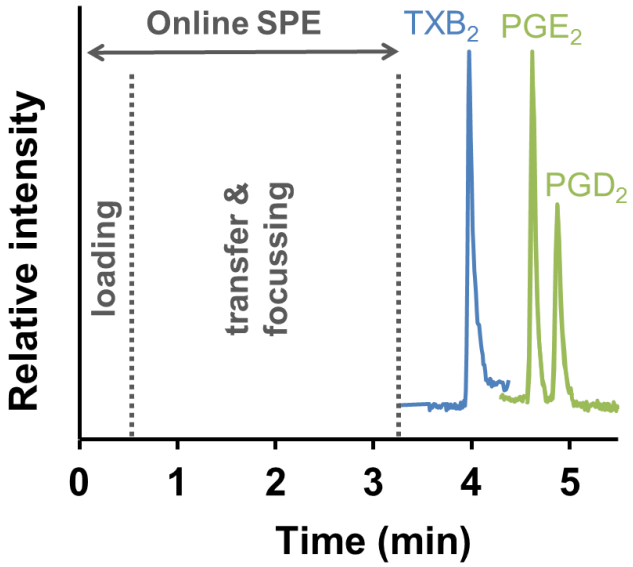

Fig. 7.6: SRM chromatogram (*m/z* 369 → 169: blue; *m/z* 351 → 271: green) of the online-SPE-LC-MS system utilizing a Waters Oasis direct connect HP (2.1 × 30 mm, 20 µm particle) and a Phenomenex Kinetex C_{18} separation column (2.1 × 50 mm, 1.3 µm). Shown is the chromatogram of an injection of 5 µL standard solution (4 nM).

The total analysis time of 7.1 min per sample is much longer than those of other online-SPE-LC-MS methods for oxylipins [26]. However, separation of the PGs by RP chromatography is challenging, and even the use of a state of the art 1.3 µm solid core particle filled column does not allow a shorter analysis time. Nevertheless, in comparison to other online-SPE methods including PGs the presented method is faster. For example, the online-SPE-LC-MS method for quantification of PGs described by Rinne et al. required an analysis time of 14 min [19], other online-SPE methods had total runtimes of 13 min [28] and 27 min [29]. An earlier described online-SPE-LC-UV method for PGE_2 had a run time of 28 min per sample [30]. Moreover, it is not clear if the latter one is able to distinguish between PGE_2 and PGD_2 which is mandatory for precise measurement of COX activity because both PGs are formed in the cell-free and cell based test systems.

With the online-SPE-LC-MS method a limit of detection (LOD; *signal to noise ratio* ≥ *3*) of 0.13 nM (0.65 fmol on column) was determined for TxB_2, both PGs showed a LOD of 0.25 nM (1.25 fmol on column) (Tab. 7.3).

Tab. 7.3: Method characteristics of the online-SPE-LC-MS/MS method. Shown are MS parameters, retention time (t_R), LOD, dynamic range (dyn. range) of the linear regression. The coefficient of determination (r^2) was < 0.999 for all analytes.

Analyte	Parent ion *m/z*	Frag. ion *m/z*	DP (V)	CE (V)	CXP (V)	t_R[a] (min)	LOD[b] (nM)	LOD[b] on column (fmol)	Dyn. range[c] (nM)
TxB_2	369	169	-50	-28	-20	4.02 ± 0.03	0.13	0.65	0.25 - 500
PGE_2	351	271	-50	-28	-10	4.69 ± 0.04	0.25	1.25	0.5 - 500
PGD_2	352	271	-40	-30	-15	4.96 ± 0.04	0.25	1.25	0.5 - 500
$^2H_4$-TxB_2	373	173	-50	-28	-20	4.02 ± 0.02	-	-	-
$^2H_4$-PGD_2	355	275	-50	-28	-10	4.67 ± 0.03	-	-	-
$^2H_4$-PGD_2	355	275	-40	-30	-15	4.93 ± 0.04	-	-	-

[a] Shown is the mean over a period of 6 month (n=6)
[b] Limit of detection (LOD) is defined as *s/n = 3*
[c] Lower limit of dynamic range match with the limit of quantification (LOQ, definded as *s/n = 9*); 500 nM is highest concentration tested, upper limit of dynamic range might be higher as 500 nM; accuracy ± 15%
[d] Coefficient of determination

This high sensitivity was due to the narrow peaks and the high ion transmission efficacy of the used MS instrument. In comparison with the sensitivity of other methods applied for the measurement of COX metabolites in cell culture samples the developed method shows a comparable sensitivity. Cao et al. reported LODs for PGs of 0.55 fmol on column [10, 31], other studies described LODs of 23 fmol (PGE_2) and 28 fmol on column (PGD_2) [22], or a lower limit of quantification (LLOQ) at 2.8 fmol on column [21] and at 28 fmol on column [23]. All earlier reported online-SPE-LC-MS methods for PGs found higher LODs of 28 fmol (PGE_2) and 51 fmol (PGD_2) on column [19] or 116 fmol (PGE_2) and 159 fmol (PGD_2) on column [29] and 28 fmol on column for PGE_2 and PGD_2 and 27 fmol on column for TxB_2 [28]. Even the sensitivity (LOD 1-5 fmol on column) of state-of-the-art targeted metabolomics approaches which simultaneously monitor a large number of 80 oxidative metabolites of AA and other LC-PUFA after offline SPE [32-34] are comparable to the developed method.

The linear range covers for all analytes at least four orders of magnitude. The LLOQ (*signal to noise ratio* ≥ *9* and accuracy of <±15%) was 0.25 nM for TxB_2 and 0.5 nM for PGE_2 and PGD_2. The upper limit of quantification (ULOQ) was set to the highest injected standard (500 nM). The calibration fulfills common validation criteria e.g. EMA Guideline on Bioanalytical Method Validation [35] with respect to accuracy of each calibration standards below ±15% and the LLOQ is at least five times the signal of a blank. Moreover, calibration was stable for at least six weeks resulting in consistent concentrations (± 5%). Thus, it is not necessary to analyze a new calibration curve each working day. These results clearly demonstrate that the analytical performance is not adversely affected using online-SPE.

Accuracy and precision of the method were determined in DMEM supplemented with 10% FBS for three concentration levels (Tab. 7.4).

Tab. 7.4: Accuracy and precision of quantification in spiked cell culture media (DMEM) with 10% FBS. Shown are the recovery rates, intersample variation of independent prepared samples (n=3) and intrasample variation based on non-consecutive repeated injection of the same samples (n=3). Interday variation was below 6% (n=7, analysed in a period of 1.5 month).

Analyte	Spiked concentration (nM)	Recovery (%)	Intersample variation (%)	Intrasample variation (%)
TxB_2	10	105	8.9	3.7
	100	95.5	8.2	1.3
	250	104	3.3	0.8
PGE_2	10	104	7.1	1.3
	100	88.6	8.5	1.0
	250	100	4.2	1.1
PGD_2	10	112	8.4	0.9
	100	101	7.0	0.4
	250	113	3.5	0.4

For TxB_2 the accuracy expressed as recovery rate was 95.5 - 105%. The accuracy for PGE_2 was found to be 88.6 to 104% and 101 to 113% for PGD_2.

Precision was high, with an intrasample variation of <1.4% except for TxB_2 (10 nM) at 3.7%. For all analytes interday and intersample variation were below 9%. Performing the spiking experiments with other media used in the assays resulted in similar recoveries. The good accuracy and precision fulfill common validation criteria [35] and demonstrate that the developed method is suited for the quantification of TxB_2, PGE_2 and PGD_2 in protein containing biological matrices. The most striking advantage of the presented method in comparison to other methods quantifying PGs is the minimized sample preparation and the analysis time of 7.1 min per sample including the online SPE. The only step to be carried out before the injection to the online-SPE-LC-MS system is the addition of IS. Most other methods for the quantification of PGs in biological matrices such as cell culture supernatant require a laborious and time-consuming sample preparation either via liquid/liquid extraction or offline SPE [10, 16, 21-23, 31]. Even in comparison to earlier attempts to apply online-SPE-LC-MS for the quantification of PGs the analysis time of the presented method is reduced and additionally more sensitive [19, 29]. Therefore the developed method is a fast and powerful tool for enzyme activity studies, requiring specific and sensitive detection of PGE_2, PGD_2 and TXB_2 in large sets of samples.

7.3.2 Application of the online-SPE-LC-MS method on three different COX-2 inhibition assays

The applicability of the presented online-SPE-LC-MS method was tested by analyzing the PGE_2 formation in different COX-2 inhibitory assays. Three different *in vitro* test systems were compared regarding observed effects of the major drugs celecoxib, indomethacin and dexamethasone on the modulation of COX-2 activity. In the cell-free system AA was incubated with recombinant COX-2 and the inhibitory effects of the pharmaceuticals on COX-2 were evaluated by monitoring the PGE_2 formation at different inhibitor concentrations. Fig. 7.7 A shows the formation of PGE_2 when incubating the system with vehicle (DMSO) only.

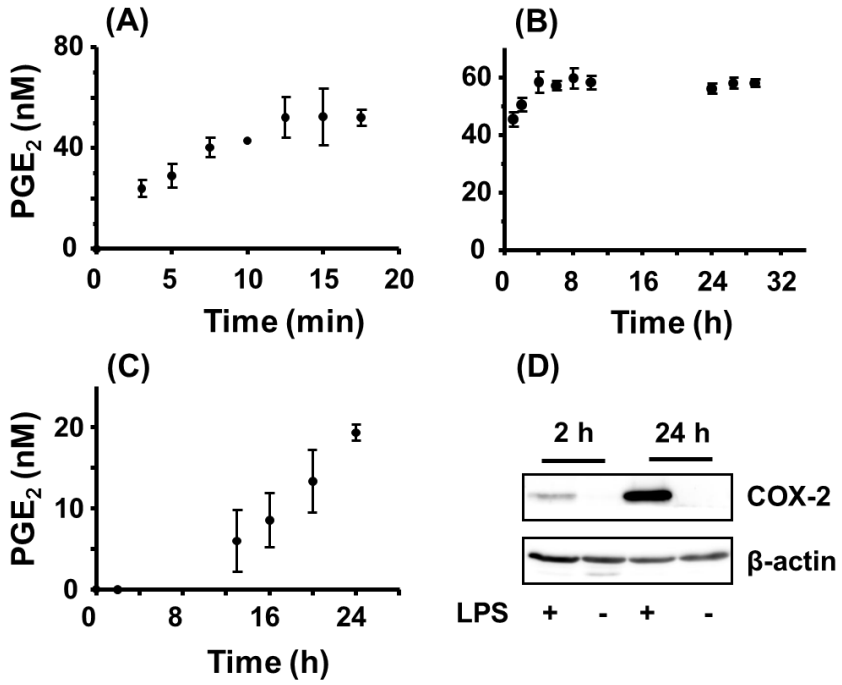

Fig. 7.7: PGE_2 formation in different *in vitro* test systems. (**A**) PGE_2 formation in the cell free assay utilizing recombinant human COX-2 (0.05 µg/mL). (**B**) HCA-7 cells were incubated with 10 µM AA and PGE_2 formation in cell culture media was measured at different time points. (**C**) Time dependant PGE_2 formation in LPS (10 µg/mL) treated primary monocytes. (**D**) COX-2 specific Western Blot in primary monocytes after 2 h and 24 h incubation either with or without LPS.

Under the applied conditions the PGE_2 formation is linear up to 12.5 min. Therefore, an incubation time of 10 min was used for the determination of the inhibitory potential. As expected the glucocorticoid dexamethasone, which acts by reducing COX-2 expression [3, 36] showed no COX-2 inhibitory effect in this assay. The COX-2 selective inhibitor celecoxib inhibited the enzyme with a potency of an IC_{50} of 242 nM (Fig. 7.8 A) and for the non-selective COX inhibitor indomethacin an IC_{50} of 362 nM was calculated (Tab. 7.5). Cao et al. reported IC_{50} values of 50 nM and 2590 nM for celecoxib and indomethacin respectively using a similar *in vitro* assay with recombinant COX-2 and quantification of PGE_2 by LC-MS [10]. Further studies using other cell-free *in vitro* assays, e.g. enzyme immune assays (EIA), spectrophotometric assays or scintillation analysis after LC, reported IC_{50} values between 40 nM and 440 nM for celecoxib [8, 37, 38] and IC_{50} values of 340-1000 nM for indomethacin [8, 17, 18, 38, 39].

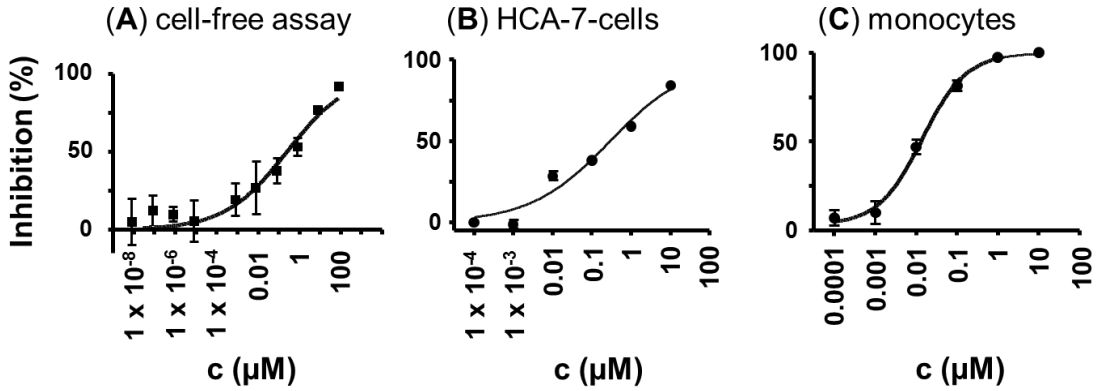

Fig. 7.8: Exemplary dose-response curves of celecoxib in the different assay systems: (**A**) cell-free assay, (**B**) HCA-7 and (**C**) primary human monocytes COX-2 inhibition (mean ± SD, n=3) is calculated based on the PGE_2 formation.

These data suggest that even for cell-free assays the IC_{50} value strongly depends on the assay conditions and the applied read-out. Studies which aim to investigate the COX-2 inhibitory potential of new compounds should therefore include a suitable reference compound in order to classify the effects on COX-2 in comparison to already known pharmaceuticals.

Tab. 7.5: Effects of celecoxib, indomethacin and dexamethasone on COX-2 activity in different test systems. IC50 values are calculated based on PGE2 formation determined by online-SPE-LC-MS. Results are presented as mean with the 95% confidence interval (CI) of the fitting of the dose response curve (n=3). In addition the effects of the compounds on COX-2 expression in the cell assays is described half quantitatively based on the results from western blot analysis.

	cell-free	**HCA-7**		**primary monocytes**	
	IC_{50} (nM) (95% CI)	**IC_{50} (nM) (95% CI)**	**COX-2 expression**	**IC_{50} (nM) (95% CI)**	**COX-2 expression**
Celecoxib	242 (102-578)	292 (179-477)	no effect (up to 10 µM)	14 (8.0-24)	no effect (up to 1 µM)
Indo-methacin	362 (195-671)	583 (254-1360)	no effect (up to 25 µM)	10 (6.7-16)	no effect (up to 100 µM)
Dexa-methasone	no effect (up to 100 µM)	no effect (up to 10 µM)	no effect (up to 100 µM)	1.6 (1.4-1.9)	1 µM - 3 nM: COX-2 ↓

The second system in which the newly developed online-SPE-LC-MS method was applied was a cell based assay with the human colon carcinoma derived cell line HCA-7 which constitutively expresses COX-2 [40]. Incubation of the cells with vehicle (DMSO) resulted in a time-dependent increase of PGE_2 levels in the cell culture supernatant for the first 4 h of incubation. After 4 h the PGE_2 concentration in the media remained constant up to an incubation time of 32 h (Fig. 7.7 B). Based on these results and to enable analysis of COX-2 expression, cells were incubated for 24 h with the test compounds. Here, IC_{50} values of 292 nM and 583 nM resulted for celecoxib (Fig. 7.8 B) and indomethacin, respectively. Both competitive active side inhibitors [41, 42] showed no effects on COX-2 expression in HCA-7 (Fig. 7.9 A, B).

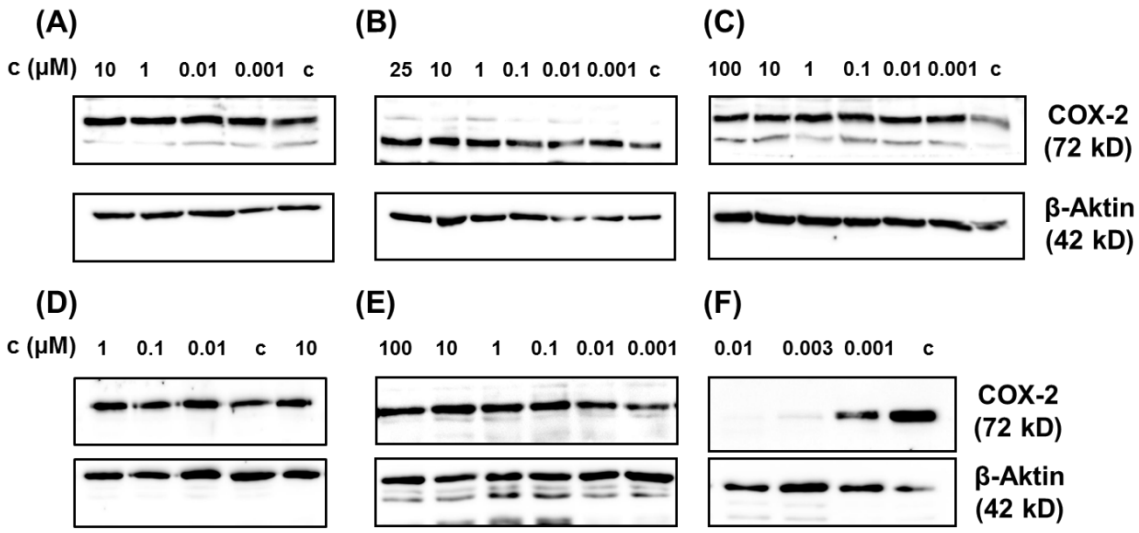

Fig. 7.9: Western Blot analysis of (**A-C**) HCA-7 cells and monocytes (**D-E**) after 24 h incubation with different concentrations of celecoxib (**A, D**), indomethacine (**B, E**) and dexamethasone (**C, F**). Shown are the signals for COX-2 and the loading control β-Actin.

Interestingly, dexamethasone showed no effect on PGE_2 formation (Tab. 7.5) and COX-2 expression in HCA-7 cells (Fig. 7.9 C). This may indicate that COX-2 overexpression in tumor cells cannot be modulated by glucocorticoids.

The third assay utilizes primary monocytes in which the expression of COX-2 was elicited by LPS [43] (Fig. 7.7 D). Following LPS treatment, PGE_2 formation in these cells increased in a time-dependent manner (Fig. 7.7 C). In order to

test the ability of the drugs to modulate COX-2 expression and activity in primary monocytes the cells were incubated with LPS and the test substance for 24 h. All three pharmaceuticals significantly reduced LPS elicited PGE_2 formation resulting in IC_{50} values of 14 nM, 10 nM and 1.6 nM for celecoxib (Fig. 7.8), indomethacin and dexamethasone (Tab. 7.5). Regarding the effects on COX-2 expression Western Blot analysis showed that incubation with 3 nM to 1000 nM dexamethasone resulted in a decreased COX-2 expression while the expression was not affected by celecoxib and indomethacin (Fig. 7.9 D-F). In comparison to the cell-free assay and HCA-7 cell assay the effects on COX-2 activity were for all compounds more pronounced in LPS triggered monocytes.

One explanation could be a higher uptake of the inhibitors in the monocytes compared to the HCA-7 cells. The large deviation in IC_{50} values obtained with different test systems clearly demonstrates that the selection of an appropriate *in vitro* test system is crucial to get meaningful results for biological questions regarding COX-2 inhibition. For a comprehensive analysis of the potency of COX inhibitors, the compound should be at least tested in two different assay systems and results should be compared with common compounds. The presented online-SPE-LC-MS method with its sensitivity and short analysis time per sample is ideally suited as read-out for these types of COX-2 inhibitory studies resulting in large sets of samples.

7.4 Conclusions

In the present study an online-SPE-LC-MS method for the quantification of PGE_2, PGD_2 and TxB_2 in biological matrices was developed. Regarding the sensitivity the method is comparable or even better than other LC-MS methods. The accuracy and precision for direct analysis of protein containing cell culture media was high (102 ± 7.60%, variation < 9%).

Sample preparation only includes mixing the sample with IS and if necessary centrifugation. Time consuming manual sample preparation such as laborious

offline SPE or liquid/liquid extraction can be omitted. With an analysis time of 7.1 min it can compete with the fasted LC-MS method for the simultaneous analysis of TXB_2, PGE_2 and PGD_2, while including online sample preparation. Therefore the new method is ideally suited as read-out for enzyme activity and inhibition assays with large sample sets.

As demonstrated for the drugs celecoxib, indomethacin and dexamethasone the method can be applied to both pure enzyme as well as cell assays. Interestingly, our results show that the observed potencies strongly depend on the test system. For example celecoxib and indomethacin showed similar inhibitory effects in the cell-free assay and in the HCA-7 cells. However, comparing the cell based assays both drugs showed more potent COX-2 inhibitory effects in primary monocytes compared to the colon carcinoma derived cell line HCA-7. Thus, it is crucial to choose an appropriate *in vitro* test system to study effects on COX-2 to answer biological questions. The online-SPE-LC-MS method described here is a versatile tool for all different *in vitro* assays.

7.5 References

[1] Buczynski M. W., Dumlao D. S., Dennis E. A. *J Lipid Res* (2009) 50, 1015-1038

[2] Chandrasekharan N. V., Dai H., Roos K. L. T., Evanson N. K., Tomsik J., Elton T. S., Simmons D. L. *Proc Natl Acad Sci* (2002) 99, 13926-13931

[3] Morita I. *Prostag Oth Lipid M* (2002) 68-69, 165-175

[4] Funk C. D. *Science* (2001) 294, 1871-1875

[5] Hardy C. C., Robinson C., Tattersfield A. E., Holgate S. T. *N Engl J Med* (1984) 311, 209-213

[6] Samuelsson B., Morgenstern R., Jakobsson P.-J. *Pharmacol Rev* (2007) 59, 207-224

[7] Simmons D. L., Botting R. M., Hla T. *Pharmacol Rev* (2004) 56, 387-437

[8] Gierse J. K., Zhang Y., Hood W. F., Walker M. C., Trigg J. S., Maziasz T. J., Koboldt C. M., Muhammad J. L., Zweifel B. S., Masferrer J. L., Isakson P. C., Seibert K. *J Pharmacol Exp Ther* (2005) 312, 1206-1212

[9] Penning T. D., Talley J. J., Bertenshaw S. R., Carter J. S., Collins P. W., Docter S., Graneto M. J., Lee L. F., Malecha J. W., Miyashiro J. M., Rogers R. S., Rogier D. J., Yu S. S., Anderson G. D., Burton E. G., Cogburn J. N., Gregory S. A., Koboldt C. M., Perkins W. E., Seibert K., Veenhuizen A. W., Zhang Y. Y., Isakson P. C. *J Med Chem* (1997) 40, 1347-1365

[10] Cao H., Yu R., Tao Y., Nikolic D., van Breemen R. B. *J Pharmaceut Biomed* (2011) 54, 230-235

[11] Al-Fayez M., Cai H., Tunstall R., Steward W., Gescher A. *Cancer Chemoth Pharm* (2006) 58, 816-825

[12] Guo Y., Sakulnarmrat K., Konczak I. *Toxicology Reports* (2014) 1, 385-390

[13] Park H. Y., G-Y K., H. C. Y. *Int J Mol Med* (2012) 30, 204-210

[14] Reddy C. M., Bhat V. B., Kiranmai G., Reddy M. N., Reddanna P., Madyastha K. M. *Biochim Biophys Acta* (2000) 277, 599-603

[15] Cuendet M., Mesecar A. D., DeWitt D. L., Pezzuto J. M. *Nat. Protocols* (2006) 1, 1915-1921

[16] Yu R., Xiao L., Zhao G., Christman J. W., van Breemen R. B. *J Pharm Exp Ther* (2011) 339, 716-725

[17] Landa P., Kokoska L., Pribylova M., Vanek T., Marsik P. *Archives of Pharm Res* (2009) 32, 75-78

[18] Cruz-López O., Díaz-Mochón J. J., Campos J. M., Entrena A., Núñez M. T., Labeaga L., Orjales A., Gallo M. A., Espinosa A. *ChemMedChem* (2007) 2, 88-100

[19] Rinne S., Ramstad Kleiveland, C., Kassem, M., Lea, T., Lundanes, E. and Greibrokk, T. *J Sep Science* (2007) 30, 1860-1869

[20] Willenberg I., Ostermann A.I., Schebb N.H. *Anal Bioanal Chem* (2015) 407, 2675-2683

[21] Furugen A., Yamaguchi H., Tanaka N., Ito H., Miyamori K., Fujikawa A., Takahashi N., Ogura J., Kobayashi M., Yamada T., Mano N., Iseki K. *J Chromatogra B* (2011) 879, 3378-3385

[22] Martins C. A. F., Weffort-Santos A. M., Gasparetto J. C., Trindade A. C. L. B., Otuki M. F., Pontarolo R. *Biomed Chromatogr* (2014) 28, 986-993

[23] Takabatake M., Hishinuma T., Suzuki N., Chiba S., Tsukamoto H., Nakamura H., Saga T., Tomioka Y., Kurose A., Sawai T., Mizugaki M. *Prostag Leukotr Ess* (2002) 67, 51-56

[24] Willenberg I., von Elsner L., Steinberg P., Schebb N. H. *Food Chem* (2015) 166, 537-543

[25] Ostermann A. I., Willenberg I., Weylandt K. H., Schebb N. H. *Chromatographia* (2015), 78, 415-428

[26] Schebb N. H., Huby M., Morisseau C., Hwang S. H., Hammock B. D. *Anal Bioanal Chem* (2011) 400, 1359-1366

[27] Harkewicz R., Fahy E., Andreyev A., Dennis E. A. *J Biol Chem* (2007) 282, 2899-2910

[28] Kortz L., Dorow J., Becker S., Thiery J., Ceglarek U. *J Chromatogr B* (2013) 927, 209-213

[29] Ferreiro-Vera C., Mata-Granados J. M., Priego-Capote F., Luque de Castro M. D. *J Chromatogra A* (2011) 1218, 2848-2855

[30] Fabian J. r. *J Chromatogra B* (2008) 875, 557-561

[31] Cao H., Xiao L., Park G., Wang X., Azim A. C., Christman J. W., van Breemen R. B. *Anal Biochem* (2008) 372, 41-51

[32] Dumlao D. S., Buczynski M. W., Norris P. C., Harkewicz R., Dennis E. A. *Biochim Biophys Acta* (2011) 1811, 724-736

[33] Ostermann A. I., Willenberg I., Schebb N. H. *Anal Bioanal Chem* (2015) 407, 1403-1414

[34] Strassburg K., Huijbrechts A. L., Kortekaas K., Lindeman J., Pedersen T., Dane A., Berger R., Brenkman A., Hankemeier T., van Duynhoven J.,

Kalkhoven E., Newman J., Vreeken R. *Anal Bioanal Chem* (2012) 404, 1413-1426

[35] European Medicine Agency, Guideline on bioanalytical method validation. (2011)

[36] Lasa M., Brook M., Saklatvala J., Clark A. R. *Mol Cell Biol* (2001) 21, 771-780

[37] Chen Q.-H., Praveen Rao P. N., Knaus E. E. *Bioorgan Med Chem* (2005) 13, 6425-6434

[38] Tsai W.-J., Shiao Y.-J., Lin S.-J., Chiou W.-F., Lin L.-C., Yang T.-H., Teng C.-M., Wu T.-S., Yang L.-M. *Bioorg Med Chem Lett* (2006) 16, 4440-4443

[39] Marsik P., Kokoska L., Landa P., Nepovim A., Soudek P., Vanek T. *Planta Med* (2005) 71, 739-742

[40] Shao J., Sheng H., Inoue H., Morrow J. D., DuBois R. N. *J of Biol Chem* (2000) 275, 33951-33956

[41] Hawkey C. J. *Lancet* (1999) 353, 307-314

[42] Ricciotti E., Fitzgerald G. A. *Arterioscler Thromb Casc Biol* (2011) 31, 986-1000

[43] Fu J. Y., Masferrer J. L., Seibert K., Raz A., Needleman P. *J Biol Chem* (1990) 265, 16737-16740

Chapter 8

Food Polyphenols Fail to Cause a Biologically Relevant Reduction of COX-2 Activity *

Epidemiologic studies show a correlation between the dietary intake of food polyphenols and beneficial health effects. Several in vitro studies indicate that the anti-inflammatory potential of polyphenols is, at least in part, mediated by a modulation of the enzymes of the arachidonic acid cascade, such as the prostaglandin forming cyclooxygenases (COX). Evidence that this mode of action can be transferred to the situation in vivo is scarce. This study characterized the effects of a small library of polyphenols on COX-2 expression and activity in vitro and compared the potency with known drugs. In the next step, the in vivo relevance of the observed in vitro effects was tested. Enzyme assays and incubations of polyphenols with the cancer cell line HCA-7 and lipopolysaccharide (LPS) stimulated primary monocytes support the hypothesis that polyphenols can affect COX-2 expression and activity in vitro. The effects were most pronounced in the monocyte assay for wogonin, apigenin, resveratrol and genistein with IC_{50} values of 1.5 µM, 2.6 µM, 2.8 µM and 7.4 µM. However, these values are 100 to 1000-fold higher in comparison to those of the known pharmaceuticals celecoxib, indomethacin and dexamethasone. In an animal model of LPS induced sepsis, pretreatment with polyphenols (i. p. 100 mg/kg bw) did not result in decreased plasma or tissue prostaglandin levels, whereas the positive control celecoxib effectively attenuated LPS induced prostaglandin formation. These data suggest that despite the moderate potency in vitro, an effect of polyphenols on COX-2 during acute inflammation is unlikely, even if a high dose of polyphenols is ingested.

* Willenberg I., Meschede A. K., Gueler F., Jang M. S., Shushakova N., Schebb N. H. (2015) *in preparation*

Author contributions: IW: Designed research, performed experiments and wrote manuscript; AKM: Performed Western Blots as part of her master thesis under the supervision of IW, MSJ: Performed PCR experiments, NS: Performed *in vivo* experiment; FG: Designed research, helped writing the manuscript. NHS: Designed research and wrote the manuscript.

8.1 Introduction

The dietary intake of fruits and vegetables is correlated with a longer healthier life. Health promoting effects are discussed for secondary plant metabolites in particular for polyphenols: Epidemiological studies suggest beneficial effects of polyphenols on cardiovascular diseases and the risk for the development of cancer [1, 2]. Chronic inflammation plays an important role in the development of these diseases and a large number of studies report anti-inflammatory effects for polyphenols [3, 4]. Aside from their antioxidative and radical scavenging properties, a modulation of pro-inflammatory mediators formed in the arachidonic acid (AA) cascade, such as cyclooxygenase-2 (COX-2) products, are suggested as modes of action underlying the anti-inflammatory effects [3]. COX-2 is expressed during inflammatory processes, giving rise to a large number of biologically active prostaglandins (PGs), for example the pain, fever and inflammation mediating PGE_2 [5]. Based on this central role COX-2 is a major target of selective COX-2 inhibitors (COX-2i) and non-steroidal anti-inflammatory drugs (NSAIDs), which also inhibit the constitutively expressed COX-1. Effects of polyphenols on COX-2 activity have been demonstrated in a vast number of *in vitro* studies [6-11]. However, different test systems were used and the lack of a correlation with the efficacy of known COX-2i or NSAIDs makes it impossible to compare and evaluate the potency of polyphenols. Moreover, a highly potent inhibition of COX-2 *in vitro* does not directly translate into an anti-inflammatory potential *in vivo*. The aim of the present study was to evaluate if food polyphenols could elicit a pharmacological relevant inhibition of COX-2. Therefore, polyphenols, which are known to inhibit COX-2 *in vitro*, i.e. nobiletin [9, 12], naringenin [7, 13], apigenin [6, 10, 13], wogonin [8, 14], genistein [10], epigallocatechingallate (EGCG) [10, 15] and resveratrol [11, 16, 17], as well as the resveratrol oligomers ε-viniferin and hopeaphenol, were comprehensively analyzed regarding their effects on COX-2. In a tiered approach the effect on COX-2 was tested in a cell-free enzyme assay, in a cancer cell line and in lipopolysaccharide (LPS) stimulated primary human

monocytes. Finally, the most potent COX-2 inhibitors were tested for their ability to modulate COX-2 activity during acute inflammation in the LPS induced sepsis model with multi organ failure. In this model a modulation of all branches of the AA cascade by polyphenols was analyzed by means of targeted metabolomics in plasma and different organs.

8.2 Experimental

8.2.1 Chemicals

Trans-resveratrol (≥ 99%), apigenin (≥ 97%), genistein (≥ 98%), naringenin (≥ 95%), EGCG (≥ 95%) and wogonin (≥ 98%) were purchased from Sigma (Schnelldorf, Germany). Hopeaphenol (≥ 90%) and ε-viniferin (≥ 90%) were obtained from Actichem (Montauban, France). Celecoxib was purchased from Santa Cruz Biotechnology (Dallas, USA).

8.2.2 In vitro assays

The *in vitro* assays were performed as described [6, 16, 18] and COX metabolites were quantified by LC-MS [18].

In the cell-free assay polyphenols were incubated with ovine recombinant COX-1 (70 ng/mL, Cayman Chemicals/ Biomol, Hamburg, Germany) or human recombinant COX-2 (50 ng/mL, Cayman Chemicals).

HCA-7 cells were incubated with sub-cytotoxic concentrations of the polyphenols dissolved in TRIS-buffered DMEM medium. Cytotoxicity of the polyphenols was evaluated by the lactate dehydrogenase leakage test (Cyto-Tox-ONE, Promega Mannheim, Germany). After 24 h the supernatant was collected for LC-MS analysis and the cells were harvested to analyze the COX-2 expression by Western Blotting.

Freshly isolated primary human monocytes were incubated with media containing 10 µg/mL LPS from *Escherichia coli* 0111:B4 (Sigma, Schnelldorf, Germany, L2630) and sub-cytotoxic concentrations of the polyphenols. After 24 h, the supernatant was sampled for LC-MS and cells were collected for the COX-2 expression analysis by Western Blotting. In all assays, the concentrations of the polyphenols were stable (recovery > 80%) for up to 24 h, as determined by LC. Inhibitory effects were calculated based on the PGE_2 formation determined by LC-MS.

8.2.3 Animals

Twelve week old male C57BL/6N mice (Charles River, Sulzfeld, Germany) were used for all experiments. C57BL/6 male mice ($H2^b$, 11-13 weeks of age) were obtained from Charles River (Sulzfeld, Germany). Animals were cared for in accordance with the institution's guidelines for experimental animals and with the guidelines of the American Physiological Society. The animal protection committee of the local authorities (Lower Saxony state department for food safety and animal welfare LAVES) approved all experiments (approval: 33.9-42502-04-12/0846). Mice were housed under conventional conditions in individually ventilated cages produced by Techniplast Inc. (Italy) with a 12 h light/dark cycle and had free access to food (Altromin 1324 standard mouse diet) and domestic quality drinking water ad libitum. Mice were monitored closely and if they appeared compromised (i.e. inactivity, no intake of food or water) after compound or LPS injection the experiment was terminated.

8.2.4 In vivo model

C57BL/6N mice were pretreated with the polyphenols (i. p., 100 mg/kg bw) or vehicle (80/20 (*v/v*) PEG 400/DMSO, 5µL/g bw). After 2 h mice were i. p. challenged with 10 mg/kg bw LPS (from *E.coli* 0111:B4, Sigma, L2630) or vehicle (10 µL/g bw). The control group, received COXi vehicle and LPS vehicle (n=8), the LPS control group received the COXi vehicle and LPS (n=7). 24 h

after LPS treatment animals were sacrificed in general isofluran anesthesia by whole body perfusion with ice cold PBS. Thereafter, organ retrieval of liver, kidney samples was done and tissues were shock frozen and fixed in RNA later. Samples were stored at -80°C till further analysis. Blood drawing form the retro orbital venus plexus with an EDTA coated capillary was done at baseline (i.e. 4 days prior to study start) and 24 h thereafter. Plasma was generated by centrifugation at 4000 g at 4°C and stored at -80°C till further analysis.

8.2.5 Oxylipin analysis

Oxylipin levels were analyzed in plasma and tissues by LC-MS following SPE extraction of 200 µL plasma or tissue homogenate (50 mg) on Chromabond C_{18} ec cartridges (Machery-Nagel, Düren, Germany) [19, *Chapter 6*]. A list of the covered analytes can be found in the appendix (Tab. 11.1).

8.2.6 Clinical chemistry

Clinical chemistry parameters (urea, creatinine, aspartate transaminase (AST), alanine transaminase (ALT), lactate dehydrogenase (LDH)) in plasma were analyzed at baseline (4 days prior the experiment) and 24 h after LPS injection. Parameters were determined by using the fully automated Olympus AU 400 analyzer (Beckman Coulter Inc.). Only healthy mice (AST below 80 U/mL and a LDH below 1000 U/mL) were included in the experiment.

8.2.7 RNA extraction and real time quantitative PCR

Tissue sections were stored in RNA-later immediately after organ retrieval. Total RNA was extracted using the RNeasy mini kit system (Qiagen, Hilden, Germany) and transcribed using Superscript II Reverse transcriptase (Invitrogen). Quantitative (q) PCR was performed on Lightcycler 420 II (Roche Diagnostics, Penzberg, Germany) using FastStart Sybr-Green chemistry. Gene-specific primers for IL-6 (Quantitec QT00098875, Qiagen) and MCP-1

(Quantitec QT00167832, Qiagen) were used for the gene of interest and HPRT served as house keeping gene for normalization (Quantitec QT00166768, Qigaen). Quantification was carried out using qgene software.

8.2.8 Data analysis

GraphPad Prism 5.0 (GraphPad Software, San Diego, USA) was used for data analysis, the fitting of dose response curves and calculation of the IC_{50} values. Statistical differences were determined by Dunnetts test (LPS vs. other groups).

8.3 Results

8.3.1 Enzyme assay

In the cell-free enzyme assay nobiletin, naringenin, wogonin and genistein showed no effect on COX-1 or COX-2 dependent PGE_2 formation (Tab. 8.1). Incubation of COX-1 with 100 µM apigenin resulted in a 31% decreased PGE_2 formation in comparison to the control, while the COX-2 activity remained unaffected. EGCG, resveratrol, ε-viniferin and hopeaphenol dose-dependently decreased the product formation of both isoforms (Tab. 8.1, Fig. 8.1). Resveratrol was the most potent compound tested and the IC_{50} values of 0.49 µM (COX-1) and 0.43 µM (COX-2) were comparable for both isoforms. For EGCG, ε-viniferin and hopeaphenol the IC_{50} values to inhibit the COX-2 isoform were higher in comparison to those required to inhibit COX-1, e.g. 1.6 µM (COX-1) and 11 µM (COX-2) for ε-viniferin (Tab. 8.1).

8.3.2 Modulation of COX-2 activity in cells

Incubation of HCA-7 cells with non-cytotoxic concentrations of the polyphenols nobiletin, EGCG, wogonin, ε-viniferin and hopeaphenol resulted in no or only slight (inhibition < 50%) changes of PGE_2 formation (Tab. 8.1).

Tab. 8.1: Effect of polyphenols on COX activity in the different *in vitro* test systems.

	cell-free COX-1	cell-free COX-2	HCA-7		primary monocytes	
	IC_{50} (nM) (95% CI)	**IC_{50} (nM) (95% CI)**	**IC_{50} (nM) (95% CI)**	**COX-2 expression**	**IC_{50} (nM) (95% CI)**	**COX-2 expression**
Nobiletin	no effect (up to 100 µM)	no effect (up to 100 µM)	inhibition < 50% (up to 100 µM)	100 µM: COX-2 ↓	**24** (18-34)	no effect (up to 100 µM)
Naringenin	no effect (up to 100 µM)	no effect (up to 100 µM)	100 µM: 53% inhibition	100 µM: COX-2 ↓	**29** (27-30)	100, 30 µM: COX-2 ↓
Genistein	no effect (up to 30 µM)	no effect (up to 30 µM)	100 µM: 54% inhibition	100 µM: COX-2 ↓	**7.4** (4.4-13)	n.d.
Apigenin	inhibition <50% (up to 100 µM)	no effect (up to 100 µM)	10 µM: 59% inhibition	no effect (up to 10 µM)	**2.6** (2.4-3.0)	10, 3 µM: COX-2 ↓
EGCG	**17** (2.6-108)	**32** (16-64)	no effect (up to 10 µM)	no effect (up to 10 µM)	no effect (up to 10 µM)	10 µM: COX-2 ↓
Wogonin	no effect (up to 100 µM)	no effect (up to 100 µM)	inhibition < 50% (up to 10 µM)	no effect (up to 10 µM)	**1.5** (0.89-2.5)	n.d.
Resveratrol	**0.49** (0.34-0.71)	**0.43** (0.27-0.67)	**4.7** (2.9-7.7)	no effect (up to 50 µM)	**2.8** (2.2-3.5)	50, 10 µM: COX-2 ↓
ε-viniferin	**1.6** (0.97-2.6)	**11** (2.5-44)	no effect (up to 1 µM)	no effect (up to 1 µM)	inhibition < 50% (up to 1 µM)	no effect (up to 1 µM)
Hopeaphenol	**4.0** (2.4-6.7)	**22** (6.9-68)	no effect (up to 1 µM)	no effect (up to 1 µM)	inhibition < 50% (up to 1 µM)	1 µM: COX-2 ↓

[a] IC_{50} values were calculated based on the PGE_2 formation (n=3).
[b] COX-2 protein levels were analyzed by COX-2 specific Western Blot; decreased COX-2 protein in comparison to the control is indicated by ↓.
n. d. no data
For comparison to pharmaceuticals refer to Tab. 7.5; IC_{50} values in in the cell free COX-1 assay: celecoxib: 21500 nM, indomethacin 17 nM, dexamethasone no effect (up to 100 µM).

Naringenin (100 µM), genistein (100 µM) and apigenin (10 µM) inhibited the formation of PGE_2, and the IC_{50} values were estimated to be about 100 µM. In contrast, resveratrol potently reduced PGE_2 formation in HCA-7 cells at an IC_{50} of 4.7 µM (Tab. 8.1, Fig. 8.1).

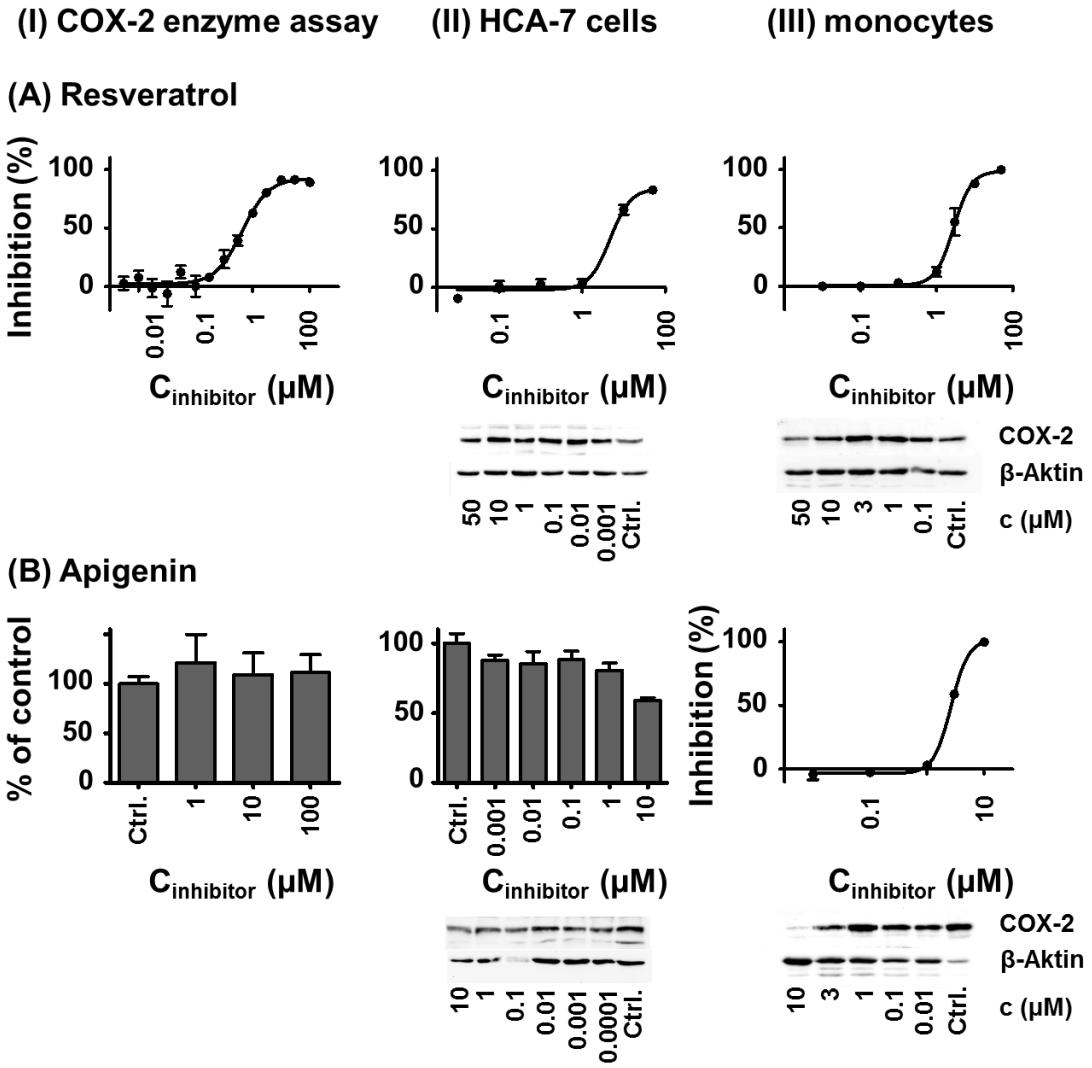

Fig. 8.1: Effects of resveratrol (**A**) and apigenin (**B**) on PGE_2 formation and COX-2 expression in the COX-2 enzyme assay (I), in HCA-7 cells (ii) and in LPS-stimulated primary human monocytes (III). The inhibition (% of control) was calculated based on the PGE_2 formation.

A COX-2-specific Western Blot analysis of the cells treated with the polyphenols indicated for nobiletin, naringenin and genistein a decreased COX-2 expression, while all other compounds did not affect the COX-2 protein levels (Tab. 8.1).

COX-2 activity in LPS stimulated primary human monocytes was slightly reduced by ε-viniferin and hopeaphenol (inhibition < 50%, Tab. 8.1). The other active polyphenols inhibited PGE_2 formation with IC_{50} values between 1.5 and 29 µM (Tab. 8.1). The most potent polyphenols tested were wogonin (1.5 µM), apigenin (2.6 µM), resveratrol (2.8 µM) and genistein (7.4 µM). Decreased COX-2 protein levels were found in incubations with naringenin, apigenin, EGCG, resveratrol and hopeaphenol (Tab. 8.1, Fig. 8.1).

8.3.3 In vivo model

In acute systemic inflammation caused by LPS (i. p. 10 mg/kg, no COX-i) plasma PG levels were massively elevated compared to the control (Fig. 8.2).

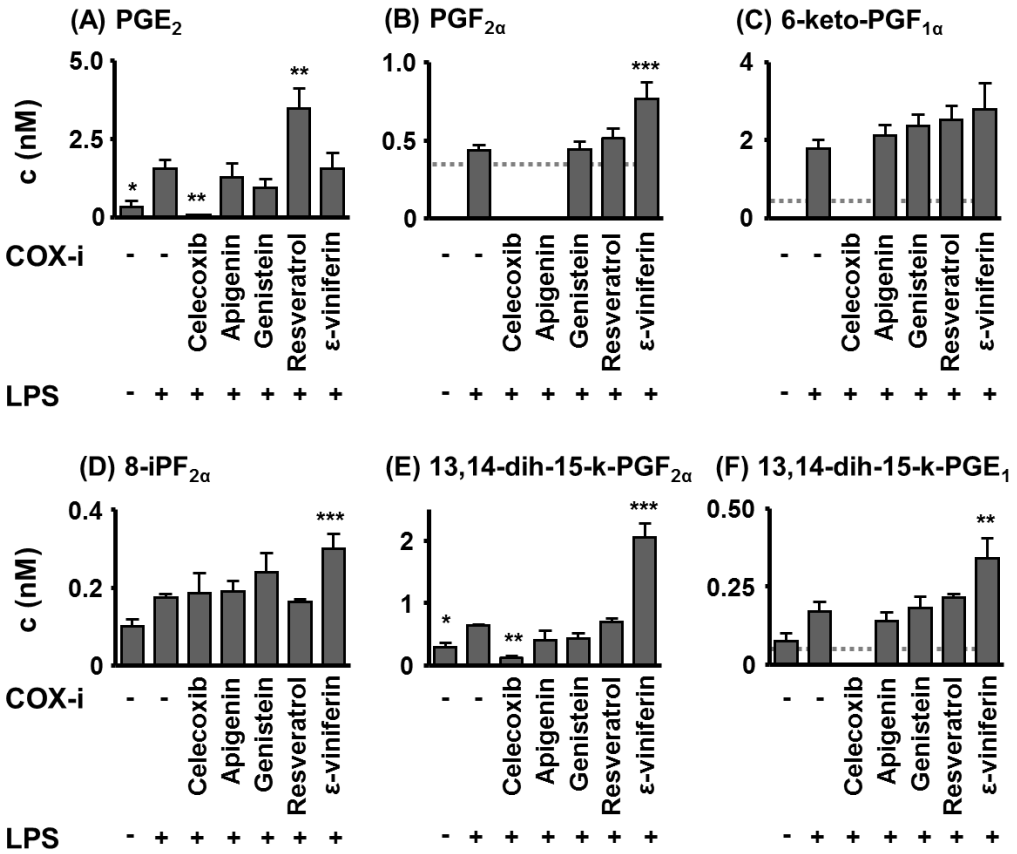

Fig. 8.2: Plasma PG levels in acute (24 h) LPS induced sepsis in mice. The test compounds were administered 2 h prior to the induction of sepsis by LPS (100 mg/kg bw, i. p.). PG concentration is below the limit of quantification (LOQ, dotted line) if no bar is displayed. Shown are mean ± SE. (n= 4-8, ANOVA followed by Dunnett's test *p<0.05, **p<0.01, ***p<0.001).

The plasma concentration of the non-enzymatically formed 8-iPF$_{2\alpha}$ was not significantly elevated by LPS induced sepsis. Treatment with a high dose of the selective COX-2i celecoxib – serving as positive control – attenuated LPS induced PG increase: 6-keto-PGF$_{1\alpha}$, PGF$_{2\alpha}$ and 13,14-dihydro-15-keto-PGE$_1$ were below the limit of quantification (LOQ). PGE$_2$ ($p< 0.01$) and 13,14-dihydro-15-keto-PGF$_{2\alpha}$ ($p< 0.01$) were massively decreased in comparison to the LPS group (Fig. 8.2). Treatment with the polyphenols (i. p. 100 mg/kg) did not result in decreased PG levels in comparison to the LPS group (Fig. 8.2). The PGE$_2$ levels were even elevated ($p< 0.01$) following resveratrol administration. For the polyphenol ε-viniferin, high levels of PGF$_{2\alpha}$ ($p< 0.001$), 13,14-dihydro-15-keto-PGF$_{2\alpha}$ ($p< 0.001$), 13,14-dihydro-15-keto-PGE$_1$ ($p< 0.01$) and the non-enzymatically formed autoxidation marker 8-iPF$_{2\alpha}$ ($p< 0.001$) were detected.

It is noteworthy, that the COX blockade by the celecoxib group did not shunt oxylipin formation towards the CYP- or LOX pathway of the AA cascade (Fig. 8.3, Tab. 11.7) as described in earlier studies [20]. The epoxy- and dihydroxy-fatty acid (FA) metabolites were even decreased in the CYP pathway (Fig. 8.3, Tab. 11.7). A similar decrease was observed for the sum of linoleic acid (LA) derived epoxy-metabolites in the apigenin ($p< 0.05$) and the resveratrol ($p <0.01$) group and the sum of DiHETrEs in the case of apigenin ($p< 0.05$), as exemplary shown in Fig. 8.3 for the metabolites of LA and AA.

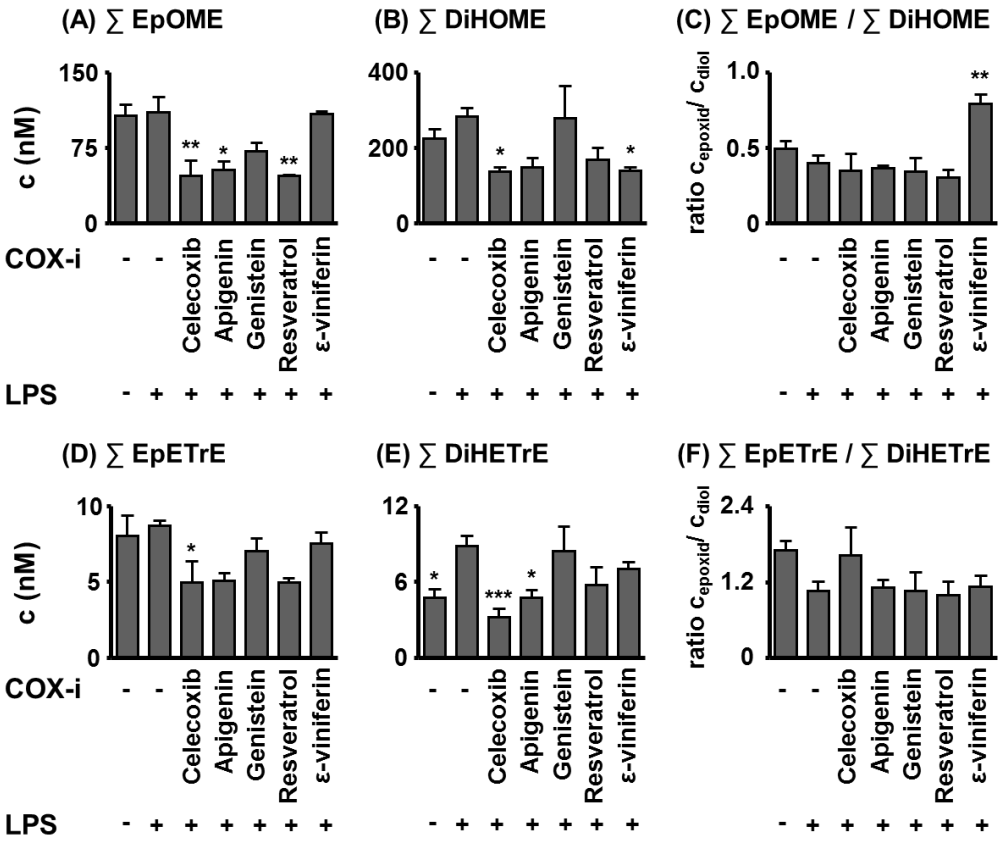

Fig. 8.3: Sum of LA and AA plasma epoxy fatty acid and dihydroxy fatty acid levels in acute (24 h) LPS-induced sepsis in mice. The test compounds were administered 2 h prior induction of sepsis by LPS (100 mg/kg bw, i. p.). Shown are mean ± SE. (n= 4-8, ANOVA followed by Dunnett's test *p<0.05, **p<0.01, ***p<0.001).

The kidney PG levels 24 h after LPS injection showed a similar trend as in plasma. Slightly increased PG levels were observed in the LPS group (Fig. 8.4, Tab. 11.8). The selective COX-2 inhibitor celecoxib lowered PG concentrations in comparison to the LPS group ($PGE_{2\alpha}$ metabolite 13,14-dihydro-15-keto-$PGE_{2\alpha}$ ($p< 0.01$), PGE_1 metabolite 13,14-dihydro-15-keto-PGE_1 <LOQ.). Kidney levels of PGE_2 ($p< 0.001$), $PGF_{2\alpha}$ ($p< 0.001$), 6-keto-$PGF_{1\alpha}$ ($p< 0.05$), 13,14-dihydro-15-keto-PGE_1 ($p< 0.001$) and 8-iso-$PF_{2\alpha}$ ($p< 0.001$) in the resveratrol group were increased in comparison to the animals only receiving LPS. 6-keto-$PGF_{1\alpha}$ ($p< 0.001$), 13,14-dihydro-15-keto-PGE_1 ($p< 0.001$) and 8-iso-$PF_{2\alpha}$ ($p< 0.01$) kidney levels were elevated in the ε-viniferin treated mice (Fig. 8.4).

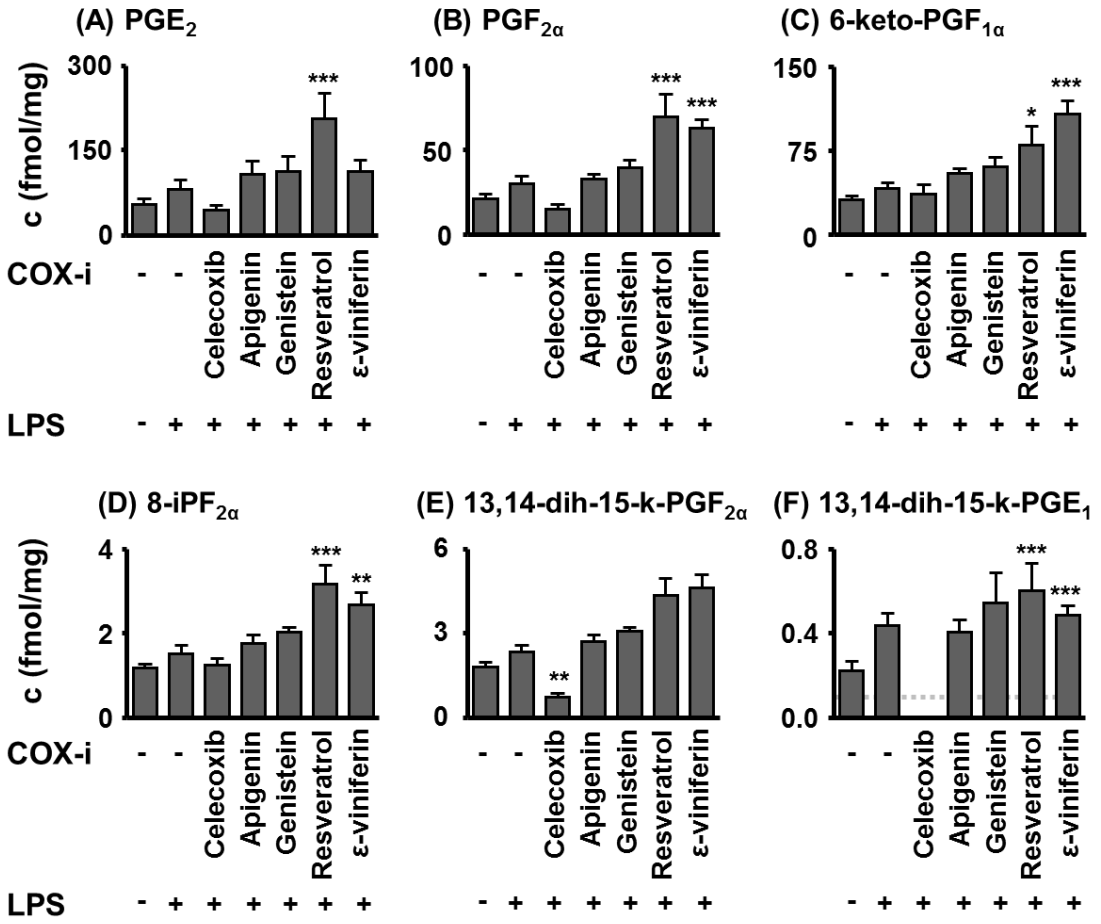

Fig. 8.4: Kidney PG levels in acute (24 h) LPS induced sepsis in mice. The test compounds were administered 2 h prior to the induction of sepsis by LPS (100 mg/kg bw, i. p.). Shown are mean ± SE. (n= 4-8, ANOVA followed by Dunnett's test *p<0.05, **p<0.01, ***p<0.001).

Clinical chemistry markers of kidney function (plasma creatinine and urea levels) were moderately increased in the LPS group, while treatment with celecoxib and ε-viniferin caused an elevation of both parameters (Fig. 8.5) indicating worsening of renal function. The chemoattractant and pro-inflammatory molecule MCP-1 was measured by qPCR in renal tissue and revealed elevated mRNA levels in the LPS group (p< 0.05 LPS versus vehicle group). Combined treatment with LPS and celecoxib or polyphenols did not affect MCP-1 levels in comparison to the LPS group (Fig. 8.6). The pro-inflammatory IL-6 mRNA expression in the kidney was about 10-fold increased

due to LPS injection in comparison to vehicle control (p> 0.05). Treatment with apigenin, resveratrol and genistein resulted in similar IL-6 mRNA elevation as in the LPS group, whereas celecoxib und ε-viniferin caused further increase of IL-6 mRNA expression compared to the LPS group (celecoxib 9-fold, ε-viniferin 28 fold in comparison to LPS group, Fig. 8.6).

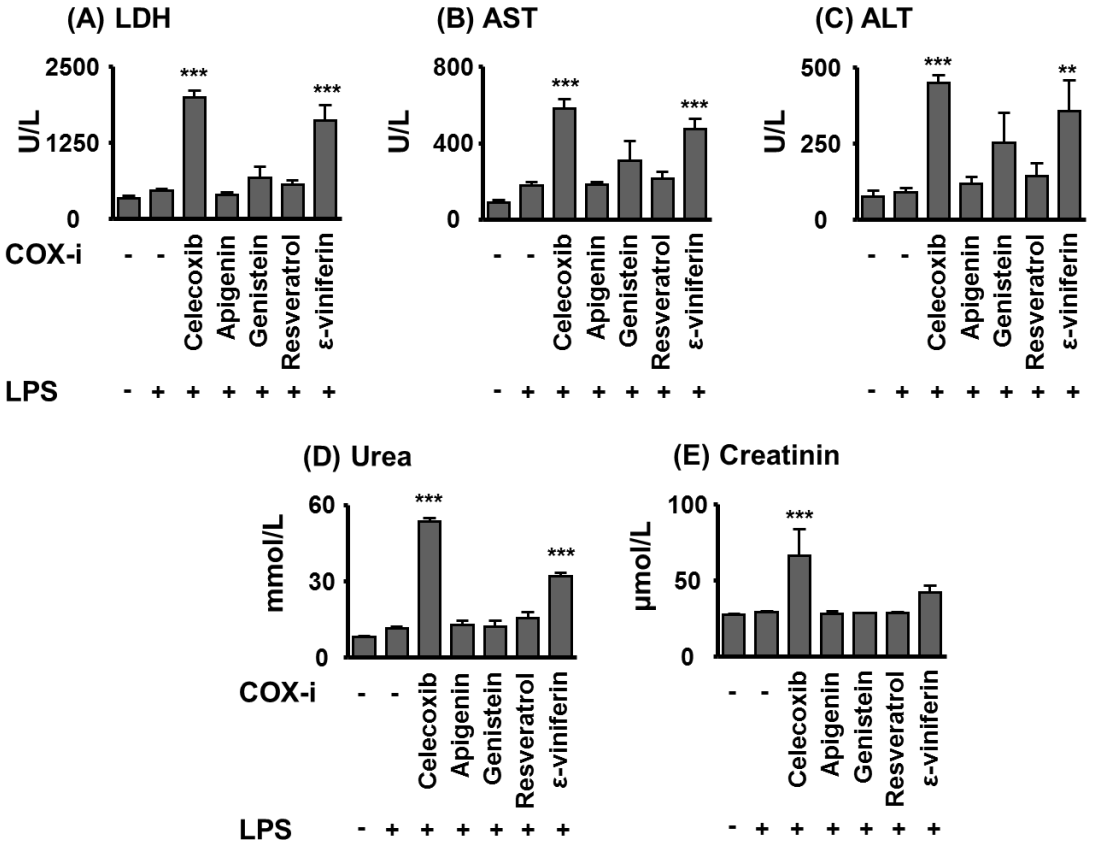

Fig. 8.5: Plasma urea and creatinine levels as well as plasma AST, ALT and LDH activites in acute (24 h) LPS-induced sepsis in mice. The test compounds were administered 2 h prior to the induction of sepsis LPS (100 mg/kg bw, i. p.). Shown are mean ± SE. (n= 4-8, ANOVA followed by Dunnett's test *p<0.05, **p<0.01, ***p<0.001).

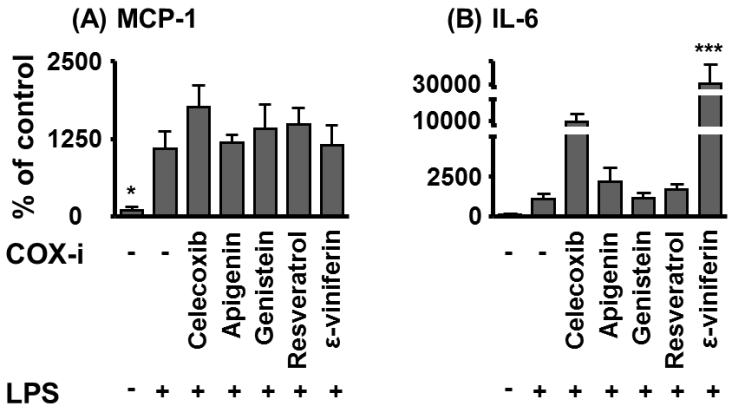

Fig. 8.6: Kidney MCP-1 and IL-6 mRNA levels in acute (24 h) LPS induced sepsis in mice. The test compounds were administered 2 h prior to the induction of sepsis by LPS (100 mg/kg bw, i. p.). Shown are mean ± SE. (n= 3-5, ANOVA followed by Dunnett's test *p<0.05, **p<0.01, ***p<0.001).

In the liver tissue no change in PG levels was observed between the LPS and the control group (Fig. 8.7, Tab. 11.9). Consistently, only a slight increase in plasma ALT activity and a moderate increase in AST activity were observed (Fig. 8.5). The mice treated with celecoxib, ε-viniferin and genistein showed elevated AST and ALT activities in plasma, thereby indicating aggravated liver injury of the high dose (Fig. 8.5).

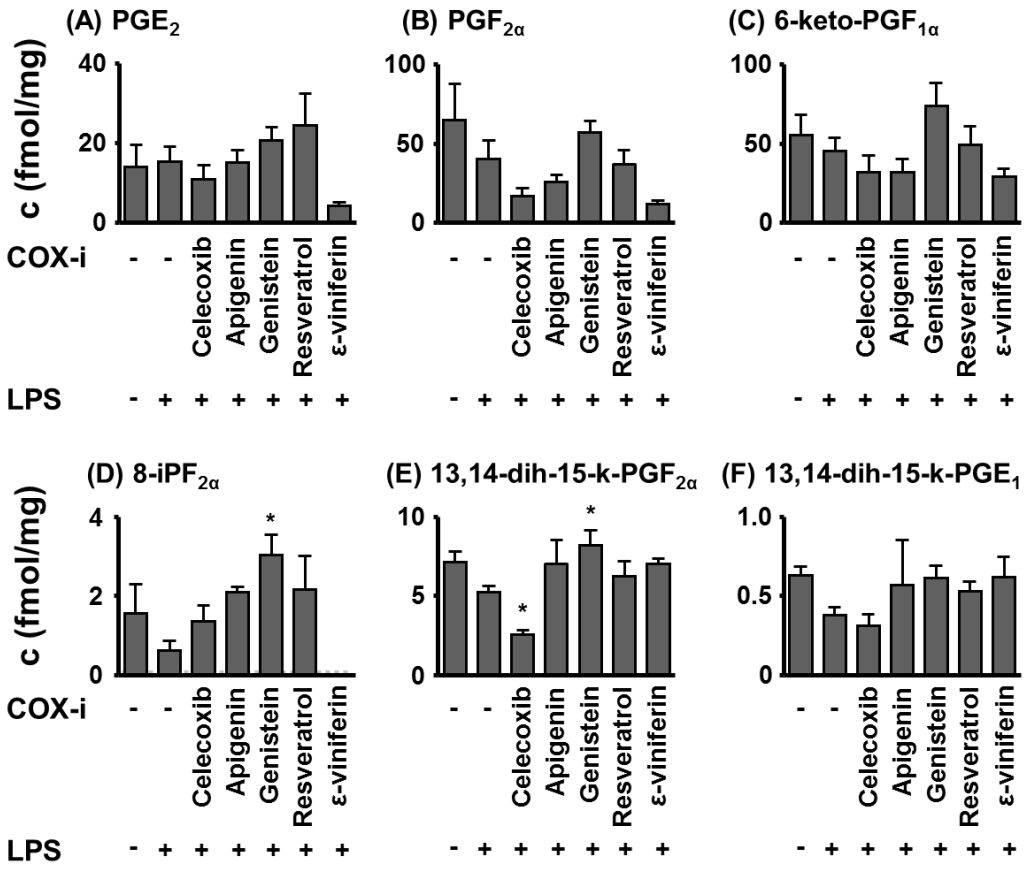

Fig. 8.7: Liver PG levels 24 h in acute (24 h) LPS induced sepsis in mice. The test compounds were administered 2 h prior to the induction of sepsis by LPS (100 mg/kg bw, i. p.). Shown are mean ± SE. (n= 4-8, ANOVA followed by Dunnett's test *p<0.05, **p<0.01, ***p<0.001).

8.4 Discussion

The current concept is that several food ingredients elicit effects on human health by a modulation of the activity of enzymes of the AA cascade [21]. Particularly for food polyphenols a large number of studies report a potentially beneficial reduction of COX-2 activity [3]. The aim of the present work was to reevaluate these findings, analyzing the effects of a library of polyphenols on COX-2 in three *in vitro* test systems and in a robust *in vivo* inflammation model.

EGCG, resveratrol, ε-viniferin and hopeaphenol inhibited COX-1 and COX-2 in the cell free assay (Tab. 8.1). The most potent polyphenol tested was resveratrol with an IC_{50} of 0.49 µM (COX-1) and 0.43 µM (COX-2) (Tab. 8.1). The potency is consistent with previous studies reporting IC_{50} values for resveratrol ranging from 0.5 to 0.9 µM in the case of COX-1 and from 1.0 to 3.1 in the case of COX-2 [16, 22, 23]. Thus, our data support the hypothesis that polyphenols could indeed act as COXi. It is remarkable that the polyphenols inhibited COX-2 at potency levels comparable to those of the NSAID indomethacin (0.36 µM) and the selective COX-2i celecoxib (0.24 µM) in this test system (Tab. 7.5). Both compounds are frequently used in the clinic for analgetic treatment of patients [24]. Taking the tyrosyl radical involved in the enzyme catalysis and the radical scavenging properties of polyphenols into account the inhibition of COX by polyphenols is discussed as being a rather unspecific mechanism [25, 26]. However, the polyphenols naringenin, genistein and apigenin with a strong antioxidative capacity [27, 28] showed no effect on COX. Hence, the inhibition by EGCG, resveratrol, ε-viniferin and hopeaphenol seems not to be based on a fully unspecific mechanism.

In order to evaluate the biological relevance of enzyme inhibitors, cell assays are more predictive because the enzyme acts in its intact cellular compartment (ER) and changes at the expression level can be monitored. Moreover, the uptake of the inhibitor into the cell is taken into account. When studying biological questions in cellular systems, it is crucial to choose an adequate cell line. COX-2 expression is increased in many types of cancer, e. g. colon, breast or lung cancer, and, thus, some cell lines derived thereof, such as the colon adenocarcinoma derived cell line HCA-7, abundantly express COX-2 [29]. Therefore, these HCA-7 cells were selected as a cell culture model for the *in vitro* studies of the effects of polyphenols on COX-2 activity.

In HCA-7 cells, only naringenin, nobiletin, genistein, apigenin and resveratrol affected COX-2 dependent PGE_2 formation (Tab. 8.1). In the case of resveratrol, the unchanged COX-2 protein levels after 24 hours suggest that

resveratrol acts by inhibiting COX-2 activity, which is consistent with earlier findings [17]. However, at longer incubation times (48 h and 96 h) resveratrol has been reported to decrease COX-2 expression [17]. The slight change in PGE_2 formation and the unchanged COX-2 protein levels after incubation with apigenin are comparable to a previous study [6]. Interestingly, the effects of genistein, nobiletin and naringenin can be in part explained by a decreased COX-2 expression (Tab. 8.1). This mode of action is supported by the lack of effect on the COX-2 activity in the cell-free enzyme assay. However, the effects only occurred at high concentrations of the compounds. Among the compounds tested only resveratrol effectively decreased the PGE_2 formation in HCA-7 cells. However, with its IC_{50} of 4.7 µM resveratrol was more than 10-fold lower than that of celecoxib (IC_{50} 0.29 µM) and indomethacin (IC_{50} 0.58 µM) (Tab. 7.5), which may be explained by a low metabolic stability of resveratrol [30]. Based on these data, it seems unlikely that polyphenols could affect COX-2 expression and PGE_2 formation of cancer cells *in vivo*.

An up-regulated expression of COX-2 in monocytes, macrophages and other cells plays a key role in acute inflammation [31]. This makes COX-2 to one of the main drug targets in inflammation. Although cell line models, e. g. the murine macrophage cell line RAW 264.7, are often used to study effects on COX-2 during inflammatory processes *in vitro* [7, 8, 12, 14], LPS stimulated primary human monocytes better reflect the *in vivo* situation in patients. In stimulated primary human monocytes, all tested polyphenols potently inhibited LPS induced PGE_2 production except for EGCG, ε-viniferin and hopeaphenol. Resveratrol, apigenin, genistein and wogonin were the most potent polyphenols with IC_{50} values below 10 µM. Although comparison of different cellular systems has its limitations, these results are consistent with earlier studies in RAW 264.7 cells reporting an IC_{50} value of 8 µM and reduced COX-2 levels for apigenin, reduced PGE_2 formation and COX-2 levels for genistein as well as a lack of effect of EGCG on PGE_2 levels with even a slight increase in COX-2 protein levels [10]. Incubation of LPS stimulated murine macrophages with wogonin resulted in a suppression of COX-2 protein expression and an IC_{50} of 0.3 µM

[8], whereas for naringenin and nobiletin decreased COX-2 protein levels were found in LPS stimulated RAW 264.7 cells [7, 9]. The decreased COX-2 protein levels for naringenin and apigenin in combination with the absence of inhibitory effects in the enzyme assay suggest that these polyphenols reduce PGE_2 production in primary monocytes by down-regulation of COX-2 expression. As described earlier [11], resveratrol acts by two different mechanisms, the down-regulation of COX-2 protein and the inhibition of the COX-2 activity (Tab. 8.1, Fig. 8.1). In comparison with pharmaceutically used COX inhibitors, the polyphenols are about 100 to 1000-fold less potent, the celecoxib, indomethacin and dexamethasone IC_{50} values being 14, 10 and 1.6 nM, respectively (Tab. 7.5). Nevertheless, plasma concentrations close to their IC_{50} value in the µM range seem to be realistic following the intake of a high dose of polyphenols [32]. In order to evaluate potential health effects of polyphenols on COX-2 a robust *in vivo* model with a highly induced expression of COX-2 and elevated PGE_2 levels was selected. The LPS induced sepsis model is a reliable and often used animal model to study the effects of compounds on the AA cascade and in this context in particular on the COX-2 mediated branch [33, 34, *Chapter 6*]. However, this does not intend to utilize polyphenols to treat sepsis. Compounds were administered i. p. to prevent low intestinal absorption and tested in a high dose to ensure that even low to moderate inhibitory effects can be detected. Similar high doses have been used in previous studies investigating the effect of apigenin and resveratrol or celecoxib on LPS induced sepsis [20, 35, 36]. It should be noted that celecoxib and ε-viniferin caused moderate elevation of liver function parameters AST, ALT, and LDH indicating liver function impairment (Fig. 8.5). As previously described, celecoxib reduced plasma and kidney PG levels significantly [20], thus demonstrating as a positive control that the chosen experimental model allows to detect the modulation of COX-2 *in vivo*. None of the polyphenols tested attenuated the PG levels. Taking the high dose administered into account, this observation suggests that their potential to affect COX-2 *in vivo* is negligible. Resveratrol, as well as its dimer increased the PGE_2 plasma concentration, which might indicate that the

stilbene might even aggravate at high concentrations the inflammatory process (Fig. 8.2).

The targeted metabolomics approach enables the parallel detection of a large number of products being part of the COX pathway. This allowed us to characterize the COX-2 inhibition in more detail. In animals treated with celecoxib not only PGE_2, but also the plasma metabolites of PGI_2 (6-keto-$PGF_{1\alpha}$), PGE_1 (13,14-dihydro-15-keto-PGE_1) and $PGF_{2\alpha}$ (13,14-dihydro-15-keto-$PGF_{2\alpha}$) were decreased, thereby additionally supporting an inhibition of COX-2 by celecoxib. However, all these metabolites were not lowered by treatment with polyphenols (Fig. 8.2), thus substantiating the fact that the polyphenols cannot modulate COX-2 *in vivo*.

The targeted metabolomics approach led to an interesting additional finding: Both apigenin and resveratrol reduced the levels of the CYP derived epoxy-FAs and their hydrolysis products (dihydroxy-FAs, Fig. 8.3). This indicates that CYPs are inhibited by these compounds, a mode of action of polyphenols that is well known for drug metabolizing CYPs [37]. This unexpected activity of the compounds should be addressed in further studies.

The treatment with polyphenols did not attenuate tissue inflammation of the kidney or systemic liver function and renal function impairment as measured by clinical chemistry in the LPS sepsis model (Fig. 8.5, Fig. 8.6). Thus, it has to be concluded that the food ingredients do not alleviate the inflammation and organ damage caused by acute sepsis under the conditions of our study. The outcome of earlier studies analyzing the effects of polyphenols on LPS induced sepsis were inconsistent: Nicholas et al. [36] reported a reduced LPS-induced mortality following administration of apigenin. Larossa et al. [35] observed no effect on the levels of a number of inflammatory biomarkers after resveratrol treatment, which is consistent with the findings in our study.

8.5 Conclusions

Overall our data support earlier findings that food polyphenols inhibit COX-2 *in vitro*. However, if more biological relevant systems are used, the efficacies of these natural products compared to drugs are lower (factor 10 in cancer cells, factor 100-1000 in primary monocytes). *In vivo*, even a high dose of polyphenols had no effect on COX-2 activity during acute inflammation in the LPS sepsis model. Taking the poor bioavailability of polyphenols [38] into account, it seems highly unlikely that the highest dose, that can possibly be ingested would modulate acute inflammation. However, direct effects in the gastrointestinal tract might take place, as reduced COX-2 expression and PGE_2 production have been observed for resveratrol in different murine colitis models [39, 40].

8.6 References

[1] Arts I. C. W., Hollman P. C. H. *Am J Clin Nutr* (2005) 81, 317S-325S

[2] Riboli E., Norat T. *Am J Clin Nutr* (2003) 78, 559S-569S

[3] Garcia-Lafuente A., Guillamon E., Villares A., Rostagno M. A., Martinez J. A. *Inflamm Res* (2009) 58, 537-552

[4] Murakami A., Ohigashi H. *Int J Cancer* (2007) 121, 2357-2363

[5] Buczynski M. W., Dumlao D. S., Dennis E. A. *J Lipid Res* (2009) 50, 1015-1038

[6] Al-Fayez M., Cai H., Tunstall R., Steward W., Gescher A. *Cancer Chemoth Pharm* (2006) 58, 816-825

[7] Chao C.-L., Weng C.-S., Chang N.-C., Lin J.-S., Kao S.-T., Ho F.-M. *Nutr Res* (2010) 30, 858-864

[8] Chi Y. S., Jong H. G., Son K. H., Chang H. W., Kang S. S., Kim H. P. *Biochem Pharmacol* (2001) 62, 1185-1191

[9] Choi S.-Y., Hwang J.-H., Ko H.-C., Park J.-G., Kim S.-J. *J Ethnopharmacol* (2007) 113, 149-155

[10] Liang Y.-C., Huang Y.-T., Tsai S.-H., Lin-Shiau S.-Y., Chen C.-F., Lin J.-K. *Carcinogenesis* (1999) 20, 1945-1952

[11] Subbaramaiah K., Chung W. J., Michaluart P., Telang N., Tanabe T., Inoue H., Jang M., Pezzuto J. M., Dannenberg A. J. *J Biol Chem* (1998) 273, 21875-21882

[12] Murakami A., Nakamura Y., Torikai K., Tanaka T., Koshiba T., Koshimizu K., Kuwahara S., Takahashi Y., Ogawa K., Yano M., Tokuda H., Nishino

H., Mimaki Y., Sashida Y., Kitanaka S., Ohigashi H. *Cancer Res* (2000) 60, 5059-5066

[13] Raso G. M., Meli R., Di Carlo G., Pacilio M., Di Carlo R. *Life Sci* (2001) 68, 921-931

[14] Wakabayashi I., Yasui K. *Eur J Pharmacol* (2000) 406, 477-481

[15] Peng G., Dixon D. A., Muga S. J., Smith T. J., Wargovich M. J. *Mol Carcinog* (2006) 45, 309-319

[16] Cao H., Yu R., Tao Y., Nikolic D., van Breemen R. B. *J Pharmaceut Biomed* (2011) 54, 230-235

[17] Sale S., Tunstall R. G., Ruparelia K. C., Potter G. A., Steward W. P., Gescher A. J. *Int J Cancer* (2005) 115, 194-201

[18] Willenberg I., Meschede A. K., Schebb N. H. *J Chromatogr A* (2015) 1391, 40-48

[19] Ostermann A. I., Willenberg I., Schebb N. H. *Anal Bioanal Chem* (2015) 407, 1403-1414

[20] Schmelzer K. R., Inceoglu B., Kubala L., Kim I.-H., Jinks S. L., Eiserich J. P., Hammock B. D. *Proc Natl Acad Sci* (2006) 103, 13646-13651

[21] Mitjavila M. T., Moreno J. J. *Biochem Pharmacol* (2012) 84, 1113-1122

[22] Kang S. S., Cuendet M., Endringer D. C., Croy V. L., Pezzuto J. M., Lipton M. A. *Bioorg Med Chem* (2009) 17, 1044-1054

[23] Murias M., Handler N., Erker T., Pleban K., Ecker G., Saiko P., Szekeres T., Jäger W. *Bioorg Med Chem* (2004) 12, 5571-5578

[24] Ungprasert P., Cheungpasitporn W., Crowson C. S., Matteson E. L. *Eur J Intern Med* (2015),

[25] Simmons D. L., Botting R. M., Hla T. *Pharmacol Rev* (2004) 56, 387-437

[26] Gryglewski R. J., Krobut R., Robak J., Swies J. *Biochem Pharmacol* (1987) 36, 317-322

[27] Rice-Evans C. A., Miller N. J., Bolwell P. G., Bramley P. M., Pridham J. B. *Free Rad Res* (1995) 22, 375-383

[28] Soobrattee M. A., Neergheen V. S., Luximon-Ramma A., Aruoma O. I., Bahorun T. *Mut Res* (2005) 579, 200-213

[29] Sharma R. A., Gescher A., Plastaras J. P., Leuratti C., Singh R., Gallacher-Horley B., Offord E., Marnett L. J., Steward W. P., Plummer S. M. *Carcinogenesis* (2001) 22, 1557-1560

[30] Willenberg I., Brauer W., Empl M. T., Schebb N. H. *J Agr Food Chem* (2012) 60, 7844-7850

[31] Ricciotti E., Fitzgerald G. A. *Arterioscler Thromb Casc Biol* (2011) 31, 986-1000

[32] Manach C., Scalbert A., Morand C., Remesy C., Jimenez L. *Am J Clin Nutr* (2004) 79, 727-747

[33] Reddy R. C., Chen G. H., Tateda K., Tsai W. C., Phare S. M., Mancuso P., Peters-Golden M., Standiford T. J. *Am J Physiol Lung Cell Mol Physiol* (2001) 281, L537-L543

[34] Schmelzer K. R., Kubala L., Newman J. W., Kim I.-H., Eiserich J. P., Hammock B. D. *Proc Natl Acad Sci* (2005) 102, 9772-9777

[35] Larrosa M., Azorin-Ortuno M., Yanez-Gascon M. J., Garcia-Conesa M. T., Tomas-Barberan F., Espin J. C. *Eur J Nutr* (2011) 50, 673-680

[36] Nicholas C., Batra S., Vargo M. A., Voss O. H., Gavrilin M. A., Wewers M. D., Guttridge D. C., Grotewold E., Doseff A. I. *J Immunol* (2007) 179, 7121-7127

[37] Detampel P., Beck M., Krähenbül S., Huwyler J. *Drug Metab Rev* (2012) 44, 253-265

[38] Manach C., Williamson G., Morand C., Scalbert A., Rémésy C. *Am J Clin Nutr* (2005) 81, 230S-242S

[39] Martín A. R., Villegas I., Sánchez-Hidalgo M., De La Lastra C. A. *Br J Pharmacol* (2006) 147, 873-885

[40] Singh U. P., Singh N. P., Singh B., Hofseth L. J., Price R. L., Nagarkatti M., Nagarkatti P. S. *The Journal of Pharmacology and Experimental Therapeutics* (2009) 332, 829-839

Chapter 9

Concluding Remarks and Future Perspectives

Within this thesis, the potential anti-inflammatory effects of polyphenols by inhibition of cyclooxygenase-2 (COX-2) were investigated. The bioavailability of dietary ingredients is an important factor regarding the effectiveness to elicit biological actions. The first part of this thesis deals therefore with the metabolism and intestinal absorption of the resveratrol oligomers hopeaphenol and ε-viniferin. Hopeaphenol showed a unique metabolic stability regarding glucuronidation by human and rat liver microsomes (*Chapter 2*). Therefore, the tetramer seems to be no substrate for glucuronosyltransferases. Although conjugation with glucuronic acid is a major metabolic pathway for polyphenols, further studies are needed to elucidate its fate in other metabolic pathways such as conversion by cytochrome P 450 monooxygenases or sulfotransferases. The intestinal absorption of the resveratrol oligomers was studied in a Caco-2 cellular transwell model (*Chapter 3*). Although a minor portion of both oligomers was detected in the cellular fraction, neither ε-viniferin nor hopeaphenol were able to pass the Caco-2 cell monolayer. This observation suggests low oral bioavailability for both compounds. However, to investigate the bioavailability in more detail, further experiments, preferably supplementation studies in humans are necessary. In these studies the quantification of compound and metabolites in plasma or tissues is a major challenge, due to lack of standards and isotopically labeled internal standards.

In the second part of this thesis effects of polyphenols on the COX branch of the arachidonic acid (AA) cascade were investigated. Different animal models of inflammation were characterized for changes in oxylipin levels to identify a

suitable *in vivo* model for studying the effects of polyphenols on COX-2 (*Chapter 5 and 6*). In the selected models a general increase of lipid mediators during acute inflammation was observed. The extent, however, differed considerably between the models. Even the two sepsis models showed different effects of the acute inflammation on systemic oxylipin levels. The increase in plasma prostaglandin (PG) and other lipid mediator concentrations was more pronounced in the LPS-induced murine sepsis in comparison to sepsis induced by cecal ligation and puncture (CLP). It would be of high scientific value to investigate if the changes in oxylipin pattern observed during experimental sepsis resemble the situation in septic patients. In particular, it is of high interest to answer the question which model is the most predictive one for oxylipin levels in septic patients. This would allow developing new treatment strategies which target the AA cascade in sepsis.

The investigation of a small library of polyphenols in different *in vitro* test systems supported earlier findings that polyphenols are able to modulate COX-2 activity *in vitro* (*Chapter 8*). However, pretreatment with a high dose of polyphenols in an animal model of acute inflammation revealed that they did not affect COX-2 activity. The positive control celecoxib resulted in decreased PG levels, demonstrating that effects on COX-2 can be detected within the chosen model. Thus, a modulation of the activity of this branch of the AA cascade by polyphenols does not seem to be a relevant *in vivo* mechanism during acute inflammation. Dosage and route of administration are critical parameters for the investigation of effects of compounds in animal models. In this study the compounds were administered i. p. at a high dose. This approach was chosen to bypass low intestinal absorption. Based on the assumption that this strategy allows to detect even moderate effects of compounds with a low bioavailability, the study clearly demonstrates that a single dose of polyphenols has no beneficial effects on acute inflammation. It remains to be elucidated if polyphenols can elicit beneficial effects on diseases characterized by chronic or less severe inflammation. Moreover, repeated administration of polyphenols may enhance the potential effects of these compounds.

Overall this thesis demonstrates that it is not possible to transfer the *in vitro* modulation of COX-2 by polyphenols to an efficacy *in vivo*. Nevertheless, the compounds may act on other targets involved in the development of inflammation.

Although epidemiological data suggest that the protective effects of fruits and vegetables are mediated by polyphenols, up to now evidence is missing that a single compound or a class of substances is responsible for the effects. Further research is needed to elucidate if the beneficial health effects of fruits and vegetables can be explained by single ingredients. Another possible explanation for the protective effects would be that they are mediated by the complex natural mixture of the different ingredients present in fruits and vegetables. Studies in animals and patients, which investigate the effects of the dietary intake of whole fruits and vegetables on chronic inflammation, would address this aspect.

Summary

The dietary intake of fruits and vegetables is associated with beneficial effects on human health. Polyphenols are discussed to play a key role in this process. Several *in vitro* studies propose an anti-inflammatory potential of polyphenols mediated by a modulation of the cyclooxygenase-2 (COX-2) activity. The bioavailability of polyphenols is a key factor for their potential effects *in vivo*. The compounds can only elicit biological effects if the substance reaches the target cell or tissue in a sufficient concentration.

This thesis aims to investigate the effects of polyphenols mediated by a modulation of COX-2 activity. For this purpose a tiered approach was applied:

1. Investigation of bioavailability and chemical stability. (*Chapter 2-3*)
2. Development of an analytical methodology for the investigation of COX-2 inhibition in *in vitro*. (*Chapter 7*)
3. Determination of COX-2 inhibitory potential of polyphenols *in vitro*. (*Chapter 8*)
4. Identification of an *in vivo* model and analytical technique for studying effects on COX-2 *in vivo*. (*Chapter 4-6*)
5. Investigation of the most potent polyphenols in the *in vivo* model. (*Chapter 8*)

Investigation of the metabolic and chemical stability of resveratrol and its oligomers revealed a unique stability for the tetramer hopeaphenol. Microsomal incubation of hopeaphenol and ε-viniferin showed that hopeaphenol, in contrast to resveratrol and ε-viniferin, is no substrate for glucuronosyltransferases. This metabolic stability towards glucuronidation may result in an increased

bioavailability of this polyphenol. However, neither hopeaphenol nor ε-viniferin showed a flux through the Caco-2-cell monolayer, a commonly used cell-line model for intestinal absorption. Because significant amounts of hopeaphenol and ε-viniferin were detected in the cellular fraction, these compounds may act on the intestine. Overall the data suggest that it is unlikely that the oligomers pass the human intestinal barrier in biologically relevant amounts.

In order to study effects of polyphenols on COX-2, a reliable and preferably fast read-out for COX activity assays is necessary. For this purpose, a fast online-solid phase extraction-LC-MS method for the quantification of TxB_2, PGE_2, and PGD_2 was developed. This method allows the quantification of COX products in 7.1 min per sample, including online sample preparation. Regarding sensitivity and accuracy in biological matrices, the presented method is comparable or even better than described approaches.

In the next step the method was applied as read-out to characterize the effects of selected polyphenols on COX-2 in three *in vitro* test systems: (i) an enzyme assay, (ii) a cancer cell line and (iii) primary human monocytes stimulated with lipopolysaccharide (LPS). These studies supported that polyphenols are indeed able to modulate COX-2 activity *in vitro*. Apigenin, wogonin, resveratrol and genistein were found to be the most potent polyphenols tested in the primary monocytes. However, their inhibitory potencies were 100 to 1000-fold lower in comparison to pharmaceuticals.

Apart from TxB_2, PGE_2 and PGD_2 several other metabolites are formed in the COX branch *in vivo*. Therefore, targeted metabolomics is an ideal tool to investigate if the observed effects of polyphenols on COX-2 are of *in vivo* relevance. Additionally, this approach enables to detect effects of polyphenols on the other branches of the AA cascade. Applying this technique, different inflammation models were characterized regarding their oxylipin pattern to identify an *in vivo* model which allows investigating COX-2 activity modulation of polyphenols *in vivo*. In an animal model for inflammatory bowel disease a general increase of plasma oxylipins derived from the lipoxygenase and

cytochrome P450 branch of the AA cascade was observed during the acute phase of inflammation. However, no increased plasma COX metabolites could be detected. In the chronic phase of colitis neither COX metabolites nor lipid mediators derived from other pathways were elevated. Thus, systemic oxylipin levels are no suitable markers for chronic inflammation within this model. In two commonly used animal models of sepsis, the LPS induced murine sepsis model and the cecal ligation and puncture (CLP) model, changes in COX metabolites were more pronounced. Plasma prostaglandin (PG) levels were dramatically elevated. In the LPS model PGE_2 concentration was found at 2100% of the control. PG increase was lower after CLP induced sepsis (97% increase in PGE_2). Additionally to the PG levels, plasma epoxy-fatty acid (FA), dihydroxy-FA and most of the hydroxy-FA levels were elevated in both models of sepsis. The pronounced changes in the COX branch during LPS induced sepsis demonstrate that this model is suitable for the investigation of effects of polyphenols on COX-2 activity *in vivo*.

The most potent polyphenols *in vitro*, resveratrol, apigenin, genistein and ε viniferin, were tested for their ability to act on COX-2 *in vivo* in the LPS induced sepsis model. Pretreatment with polyphenols (100 mg/kg bw i. p.) failed to decrease plasma and tissue PG levels, whereas the positive control celecoxib significantly reduced LPS induced PG formation. Thus, despite the moderate *in vitro* activity, polyphenols were not able to inhibit COX-2 activity *in vivo*. These data suggest that an effect of polyphenols on COX-2 during acute inflammation seems rather unlikely, even if a high dose is ingested.

Appendix

Chapter 4

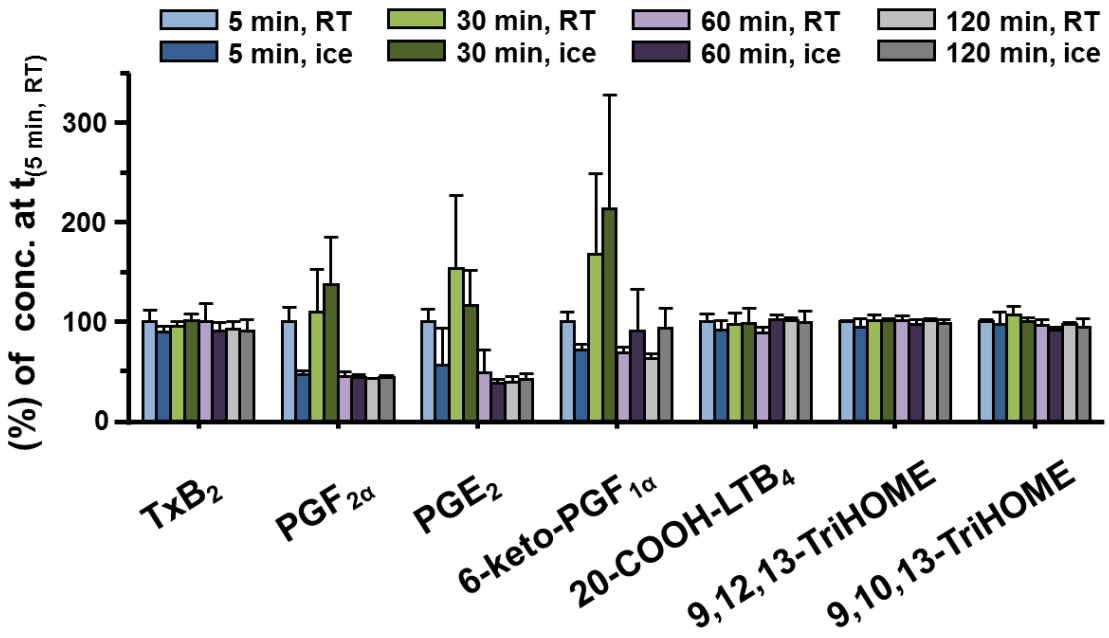

Fig. 11.1: *Ex-vivo* degradation/formation of TxB_2, prostaglandins (PGs) and trihomes in human whole blood after blood withdrawal. Blood of a healthy human volunteer was collected in EDTA tubes, pooled and left for 5 min, 30 min, 60 min or 120 min either at room temperature (RT) or on ice. After centrifugation (1200 x g, 15 min, 4 °C), the plasma was immediately frozen (-80 °C) and the oxylipin concentration was analyzed within 5 days (Oasis SPE). The resulting concentrations after different periods of time in sample preparation are compared to those with direct sample preparation ($t_{(5\ min,\ RT)}$). In comparison to 5 min storage at RT the concentration of the PGs was significantly decreased already 5 min after storage on ice. After 30 min (ice and RT) the PG levels were increased before they finally decreased again after 60 min. The concentrations of TxB_2, 20-COOH-LTB_4 and trihomes were stable up to 120 min either on ice or at RT. Shown are mean ± SD (n=4).

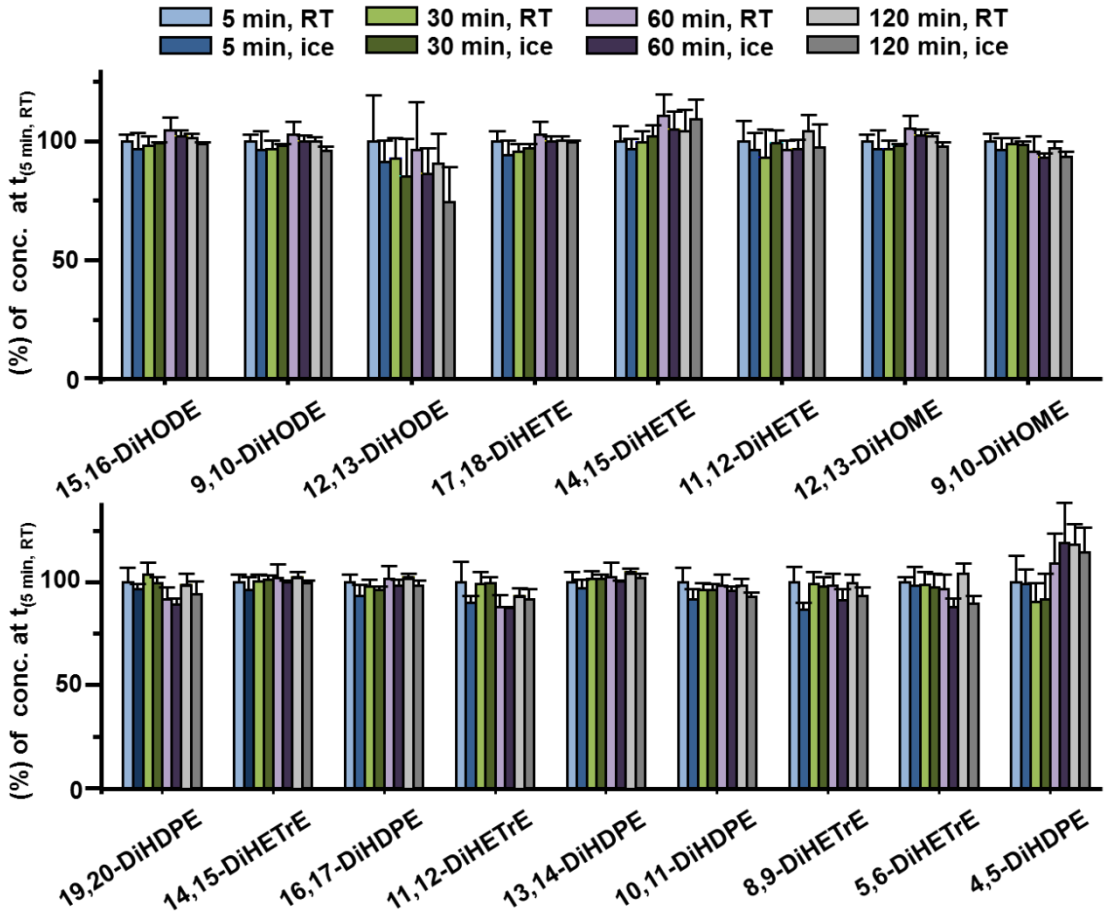

Fig. 11.2: *Ex-vivo* degradation/ formation of diols in human whole blood after blood withdrawal. Blood of a healthy human volunteer was collected in EDTA tubes, pooled and left for 5 min, 30 min, 60 min or 120 min either at room temperature (RT) or on ice. After centrifugation (1200 x g, 15 min, 4 °C), the plasma was immediately frozen (-80 °C) and the oxylipin concentration was analyzed within 5 days (Oasis SPE)The resulting concentrations after different periods of time in sample preparation are compared to those with direct sample preparation ($t_{(5\ min,\ RT)}$). Shown are mean ± SD (n=4).

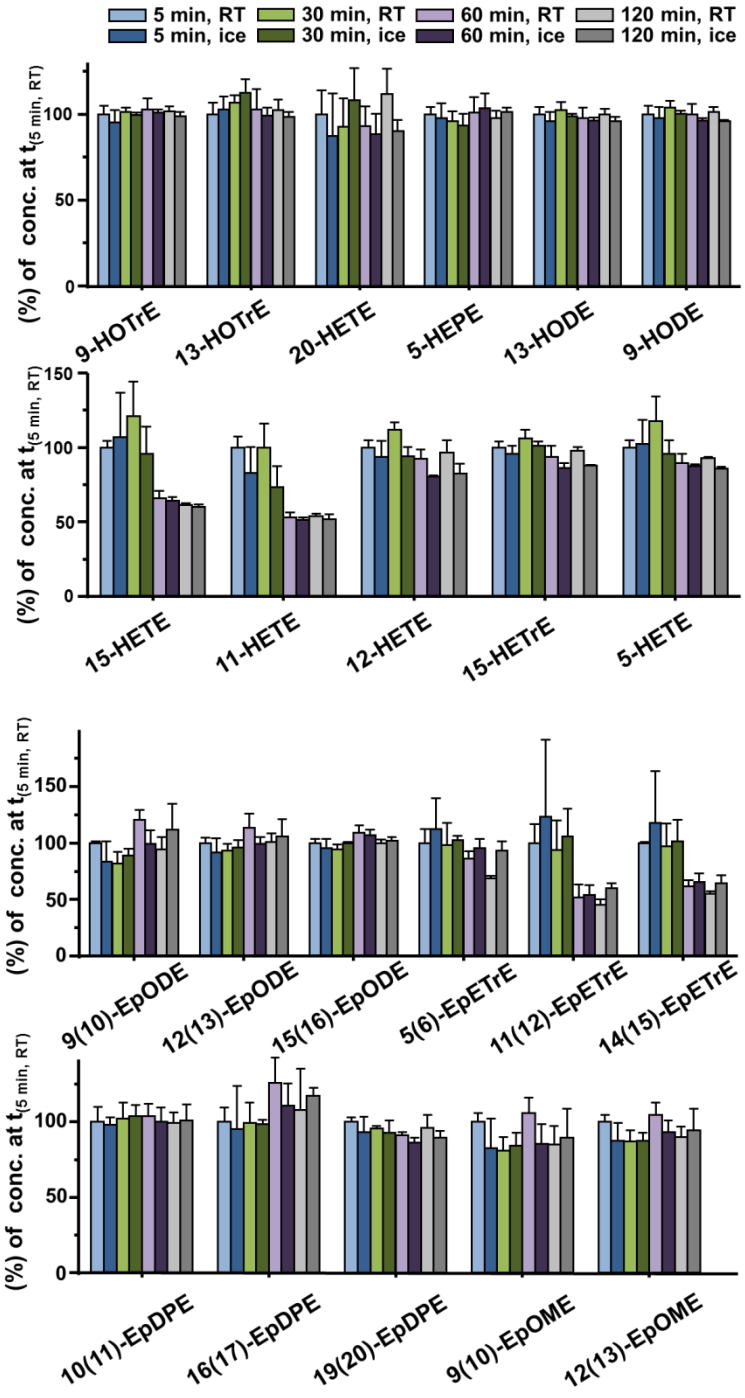

Fig. 11.3: *Ex-vivo* degradation/ formation of alcohols and epoxy fatty acids in human whole blood after blood withdrawal. Blood of a healthy human volunteer was collected in EDTA tubes, pooled and left for 5 min, 30 min, 60 min or 120 min either at room temperature (RT) or on ice. After centrifugation (1200 x g, 15 min, 4 °C), the plasma was immediately frozen (-80 °C) and the oxylipin concentration was analyzed within 5 days (Oasis SPE). The resulting concentrations after different periods of time in sample preparation are compared to those with direct sample preparation ($t_{(5\ min,\ RT)}$). While concentrations of 11- and 15-HETE halved after 60 min on ice or at RT, the levels of further alcohols were stable up to 120 min. The concentrations of 11(12)- and 14(15)-EpETrE were halved after 60 min of storage either on ice or at RT. The other epoxides were not affected up to 120 min of storage. Shown are mean ± SD (n=4).

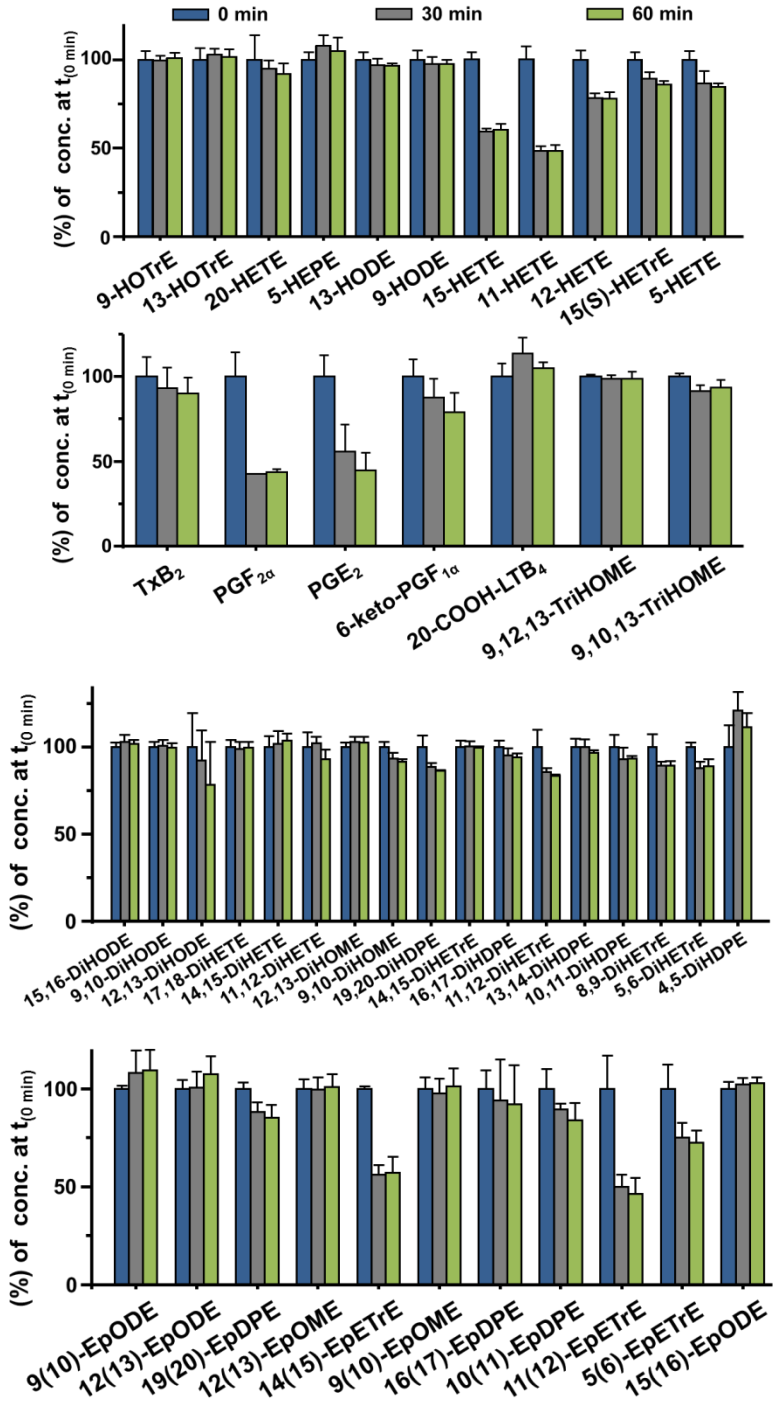

Fig. 11.4: *Ex-vivo* degradation/ formation of oxylipins in freshly centrifuged human plasma. Blood of a healthy human volunteer was collected in EDTA tubes, pooled and centrifuged (1200 x g, 15 min, 4 °C) after 5 min at room temperature (RT). The resulting plasma was left with the cell pellet for 0 min, 30 min or 60 min on ice before freezing at -80 °C till analysis. Oxylipin concentrations were analyzed within 5 days (Oasis SPE). The resulting concentrations after different periods of time in sample preparation are compared to those with direct sample preparation ($t_{(0\ min)}$). While the concentrations of 11- and 15-HETE halved in the first 30 min after centrifugation, most other alcohols showed no losses. The levels of PGE_2 and $PGF_{2\alpha}$ significantly decreased in the first 30 min of storage while TxB_2, 20-COOH-LTB_4, 6-keto-$PGF_{1\alpha}$ and the trihomes showed no changes up to 60 min. The detected diols and most of the epoxides showed no or only minor losses during this storage. However, the concentrations of all EpETrEs decreased within the first 30 min. Shown are mean ± SD (n=4).

Chapter 5, 6, 8

Tab. 11.1: Parameters of the LC-MS method used for the quantification of oxylipins in chapter 5, 6 and 8. Shown are the analytes with their mass transitions for quantification in the scheduled SRM mode, electronic MS parameters (declustering potential (DP), collision energy (CE), collision exit potential (CXP)), retention time (t_R) and the calibration range (lower limit of quantification (LLOQ), upper limit of quantification (ULOQ)).

Analyte	Mass transition m/z (Q1)	Mass transition m/z (Q2)	MS parameter DP (V)	MS parameter CE (V)	MS parameter CXP (V)	Internal standard	t_R (min)	LLOQ [1] (nM)	ULOQ [2] (nM)	Ch. 5 [3]	Ch. 6 [4]	Ch. 8 [5]
20-COOH-LTB$_4$	365.2	347.2	-80	-25	-8	^{2}H$_4$-TxB$_2$	3.21	1.00	200	x	x	x
6-keto-PGF$_{1\alpha}$	369.3	163.2	-70	-36	-6	^{2}H$_4$-6-keto-PGF$_{1a}$	3.23	0.90	361	x	x	x
Resolvin E$_1$	349.3	195.0	-65	-22	-10	^{2}H$_4$-TxB$_2$	3.24	1.20	480	x	x	x
20-OH-LTB$_4$	351.2	195.2	-80	-25	-8	^{2}H$_4$-TxB$_2$	3.36	0.25	200	x	x	x
TxB$_3$	367.3	169.3	-70	-34	-8	^{2}H$_4$-TxB$_2$	3.39	0.50	500		x	x
TxB$_1$	371.3	171.2	-70	-34	-10	^{2}H$_4$-TxB$_2$	3.76	0.50	500		x	x
8-iPF$_{2\alpha}$	353.3	193.3	-100	-32	-4	^{2}H$_4$-PGE$_2$	3.92	0.10	500			x
TXB$_2$	369.2	169.1	-60	-25	-7	^{2}H$_4$-TxB$_2$	3.95	0.63	500	x	x	x
PGE$_3$	349.3	269.2	-60	-22	-6	^{2}H$_4$-PGE$_2$	4.01	0.30	120	x	x	x
11β-PGF$_{2\alpha}$	353.3	193.1	-30	-36	-12	^{2}H$_4$-PGE$_2$	4.04	1.00	500			x
5-iPF$_{2\alpha}$	353.3	115.1	-60	-38	-11	^{2}H$_4$-PGE$_2$	4.14	1.00	500		x	x
PGD$_3$	349.3	269.2	-60	-22	-6	^{2}H$_4$-PGE$_2$	4.22	1.00	200	x	x	x
9,12,13-TriHOME	329.2	211.1	-80	-32	-10	^{2}H$_4$-PGE$_2$	4.29	1.25	1000	x	x	x
PGF$_{1\alpha}$	355.4	293.2	-90	-36	-6	^{2}H$_4$-PGE$_2$	4.36	0.10	500		x	x
9,10,13-TriHOME	329.2	171.1	-80	-32	-8	^{2}H$_4$-PGE$_2$	4.37	0.50	400	x	x	x
PGF$_{2\alpha}$	353.2	309.2	-80	-26	-7	^{2}H$_4$-PGE$_2$	4.38	0.70	281	x	x	x
PGE$_2$	351.2	271.3	-60	-24	-6	^{2}H$_4$-PGE$_2$	4.57	0.10	200	x	x	x
PGE$_1$	353.3	317.2	-60	-20	-6	^{2}H$_4$-PGE$_2$	4.70	0.33	260	x	x	x
PGD$_1$	353.3	317.2	-60	-20	-6	^{2}H$_4$-PGD$_2$	4.81	0.50	200	x	x	x
PGD$_2$	351.2	271.3	-60	-24	-6	^{2}H$_4$-PGD$_2$	4.84	1.00	200	x	x	x
15-keto-PGF$_{1\alpha}$	353.3	193.1	-40	-38	-6	^{2}H$_4$-PGE$_2$	4.87	0.25	500		x	x
11,12-,15-TriHETrE	353.2	167.1	-80	-28	-10	^{2}H$_4$-PGE$_2$	5.23	1.00	100	x	x	x
LXA$_4$	351.2	115.2	-60	-21	-8	^{2}H$_4$-PGE$_2$	5.25	0.18	70	x	x	x
RvD$_1$	375.3	141	-50	-20	-8	^{2}H$_4$-PGE$_2$	5.25	0.10	100			x

Tab. 11.1 continued

Analyte	Mass transition m/z (Q1)	m/z (Q2)	MS parameter DP (V)	CE (V)	CXP (V)	Internal standard	t_R (min)	LLOQ [1] (nM)	ULOQ [2] (nM)	Ch. 5 [3]	Ch. 6 [4]	Ch. 8 [5]
13,14-dihydro-15-keto-$PGF_{2\alpha}$	353.3	183.3	-80	-36	-10	$^2H_4$-PGE_2	5.44	0.10	500		x	x
dihomo-$PGF_{2\alpha}$	381.4	221.1	-60	-38	-10	$^2H_4$-PGE_2	5.74	0.25	500		x	x
13,14-dihydro-15-keto-PGE_1	353.3	221.2	-40	-30	-6	$^2H_4$-PGE_2	5.79	0.10	500		x	x
RvE_2	333.2	253.3	-60	-20	-9	$^2H_4$-PGE_2	6.04	1.00	100			x
PGJ_2	333.3	189.2	-60	-25	-8	$^2H_4$-PGE_2	6.57	1.60	160	x	x	x
LTB_5	333.3	195.2	-65	-22	-8	$^2H_4$-LTB_4	6.60	0.25	200	x	x	x
PGB_2	333.3	175.1	-60	-28	-8	$^2H_4$-PGE_2	6.69	0.40	800	x	x	x
THF diol	353.2	127.1	-80	-32	-8	$^2H_4$-LTB_4	6.78	0.25	100	x	x	x
18(S)-RvE_3	333.2	201.3	-60	-20	-9	$^2H_4$-PGE_2	7.11	0.50	100			x
12-OH-17(18)-EpETE	333.1	179.3	-65	-20	-6	$^2H_4$-9,10-DiHOME	7.19	0.25	100			x
bicyclo PGE_2	333.3	113.2	-90	-36	-4	$^2H_4$-PGE_2	7.28	1.00	500		x	x
15,16-DiHODE	311.2	223.2	-80	-29	-10	$^2H_4$-9,10-DiHOME	7.37	0.50	400	x	x	x
9,10-DiHODE	311.2	201.2	-65	-27	-10	$^2H_4$-9,10-DiHOME	7.41	0.20	400	x	x	x
8,15-DiHETE	335.2	235.2	-65	-22	-4	$^2H_{11}$-14,15-DiHETrE	7.43	0.80	80	x	x	x
12,13-DiHODE	311.2	183.1	-80	-30	-8	$^2H_4$-9,10-DiHOME	7.48	2.00	400	x	x	x
18(R)-RvE_3	333.2	201.3	-60	-20	-9	$^2H_4$-PGE_2	7.66	1.00	100			x
6-trans-LTB4	335.2	195.1	-65	-23	-9	$^2H_4$-LTB_4	7.78	0.50	200	x	x	x
5,15-DiHETE	335.3	173.2	-60	-21	-8	$^2H_{11}$-14,15-DiHETrE	7.79	0.25	100	x	x	x
17,18-DiHETE	335.3	247.2	-65	-24	-8	$^2H_{11}$-14,15-DiHETrE	7.92	0.25	100	x	x	x

Tab. 11.1 continued

Analyte	Mass transition m/z (Q1)	m/z (Q2)	MS parameter DP (V)	CE (V)	CXP (V)	Internal standard	t_R (min)	LLOQ [1] (nM)	ULOQ [2] (nM)	Ch. 5 [3]	Ch. 6 [4]	Ch. 8 [5]
LTB4	335.2	195.1	-65	-23	-9	$^2H_4$-LTB4	8.20	0.50	200	x	x	x
14,15-DiHETE	335.3	207.2	-65	-25	-10	$^2H_{11}$-14,15-DiHETrE	8.44	0.25	100	x	x	x
11,12-DiHETE	335.2	167.1	-65	-26	-5	$^2H_{11}$-14,15-DiHETrE	8.64	0.25	100	x	x	x
12,13-DiHOME	313.2	183.2	-80	-30	-8	$^2H_4$-9,10-DiHOME	8.83	1.25	1000	x	x	x
8,9-DiHETE	335.2	127.1	-65	-26	-5	$^2H_4$-9,10-DiHOME	9.00	0.50	100	x	x	x
9,10-DiHOME	313.2	201.2	-80	-29	-8	$^2H_4$-9,10-DiHOME	9.26	0.50	1000	x	x	x
14,15-DiHETrE	337.2	207.1	-65	-25	-10	$^2H_{11}$-14,15-DiHETrE	9.88	0.25	200	x	x	x
19,20-DiHDPE	361.2	273.2	-65	-24	-6	$^2H_{11}$-14,15-DiHETrE	9.90	1.00	100	x	x	x
LTB_3	337.2	195.2	-65	-22	-8	$^2H_4$-LTB4	10.14	0.50	200	x	x	x
9,10-Dihydroxystearic acid	315.0	170.8	-60	-36	-9	$^2H_4$-9,10-DiHOME	10.41	2.00	500		x	x
16,17-DiHDPE	361.2	233.2	-65	-24	-6	$^2H_{11}$-14,15-DiHETrE	10.48	0.50	100	x	x	x
11,12-DiHETrE	337.2	167.1	-65	-26	-8	$^2H_{11}$-14,15-DiHETrE	10.64	0.25	200	x	x	x
13,14-DiHDPE	361.2	193.2	-65	-24	-6	$^2H_{11}$-14,15-DiHETrE	10.73	0.25	100	x	x	x
20-HEPE	317.2	287.3	-50	-20	-8	$^2H_8$-12-HETE	10.83	0.50	100		x	x
9-HOTrE	293.2	171.2	-65	-22	-8	$_2H^4$-9-HODE	11.01	0.50	100	x	x	x
10,11-DiHDPE	361.2	153.2	-65	-24	-6	$^2H_{11}$-14,15-DiHETrE	11.11	0.50	100	x	x	x
8,9-DiHETrE	337.2	127.1	-70	-30	-8	$^2H_{11}$-14,15-DiHETrE	11.26	0.50	200	x	x	x

Tab. 11.1 continued

Analyte	Mass transition m/z (Q1)	m/z (Q2)	MS parameter DP (V)	CE (V)	CXP (V)	Internal standard	t_R (min)	LLOQ [1] (nM)	ULOQ [2] (nM)	Ch. 5 [3]	Ch. 6 [4]	Ch. 8 [5]
EKODE	309.2	291.1	-65	-20	-6	$^2H_4$-9-HODE	11.33	0.50	100	x	x	x
13-HOTrE	293.2	195.1	-70	-24	-8	$^2H_4$-9-HODE	11.34	0.60	60	x	x	x
18-HEPE	317.2	259.2	-55	-17	-7	$^2H_4$-9-HODE	11.40	0.10	100		x	x
5,6-DiHETE	335.2	115.2	-60	-21	-8	$^2H_{11}$-14,15-DiHETrE	11.79	0.25	100	x	x	x
15-deoxy-PGJ_2	315.2	271.2	-65	-20	-6	$^2H_{11}$-14,15-DiHETrE	11.84	1.00	400	x	x	x
7,8-DiHDPE	361.2	113.1	-65	-24	-6	$^2H_{11}$-14,15-DiHETrE	11.91	1.00	100	x	x	x
15-HEPE	317.2	219.2	-60	-20	-10	$^2H_8$-12-HETE	12.08	1.25	500	x	x	x
20-HETE	319.2	275.1	-80	-23	-6	$^2H_6$-20-HETE	12.10	2.60	260	x	x	x
5,6-DiHETrE	337.2	145.1	-70	-26	-10	$^2H_{11}$-14,15-DiHETrE	12.17	0.50	200	x	x	x
8-HEPE	317.2	155.2	-60	-20	-8	$^2H_8$-12-HETE	12.42	0.63	500	x	x	x
12-HEPE	317.2	179.2	-65	-20	-8	$^2H_8$-12-HETE	12.59	0.63	500	x	x	x
5-HEPE	317.2	115.1	-60	-20	-6	$^2H_8$-12-HETE	13.12	0.50	400	x	x	x
4,5-DiHDPE	361.2	229.3	-65	-24	-6	$^2H_{11}$-14,15-DiHETrE	13.13	2.00	100	x	x	x
13-HODE	295.2	195.2	-80	-26	-9	$^2H_4$-9-HODE	13.33	1.00	2000	x	x	x
9-HODE	295.2	171.1	-80	-26	-7	$^2H_4$-9-HODE	13.44	1.00	2000	x	x	x
20-HDHA	343.2	241.1	-55	-19	-7	$^2H_8$-12-HETE	13.72	0.25	20		x	x
15(16)-EpODE	293.3	235.2	-65	-20	-4	$^2H_4$-9(10)-EpOME	13.96	0.25	100	x	x	x
15-HETE	319.2	219.2	-60	-20	-8	$^2H_8$-12-HETE	14.02	1.25	1000	x	x	x
9(10)-EpODE	293.3	171.2	-65	-20	-8	$^2H_4$-9(10)-EpOME	14.11	0.20	80	x	x	x
17(18)-EpETE	317.2	215.2	-65	-20	-6	$^2H_{11}$-14(15)-EpETrE	14.15	0.50	100	x	x	x

Tab. 11.1 continued

Analyte	Mass transition m/z (Q1)	m/z (Q2)	MS parameter DP (V)	CE (V)	CXP (V)	Internal standard	t_R (min)	LLOQ [1] (nM)	ULOQ [2] (nM)	Ch. 5 [3]	Ch. 6 [4]	Ch. 8 [5]
16-HDHA	343.2	233.2	-55	-19	-7	$^2H_8$-12-HETE	14.21	0.10	20		x	x
17-HDHA	343.2	201.2	-60	-20	-6	$^2H_8$-12-HETE	14.33	0.50	100		x	x
13-HDHA	343.2	193.1	-55	-19	-7	$^2H_8$-12-HETE	14.47	0.10	20		x	x
12(13)-EpODE	293.2	183.1	-65	-24	-8	$^2H_4$-9(10)-EpOME	14.50	0.25	100	x	x	x
13-oxo-ODE	293.2	195.1	-75	-20	-8	$^2H_4$-9-HODE	14.50	1.00	100	x	x	x
11-HETE	319.2	167.2	-60	-23	-7	$^2H_8$-12-HETE	14.52	0.50	1000	x	x	x
10-HDHA	343.2	153.2	-45	-21	-7	$^2H_8$-12-HETE	14.68	0.10	20		x	x
14-HDHA	343.2	205.2	-50	-19	-7	$^2H_8$-12-HETE	14.68	0.25	500		x	x
15-oxo-ETE	317.2	113.1	-65	-25	-8	$^2H_8$-5-HETE	14.70	0.50	100	x	x	x
9-oxo-ODE	293.2	185.1	-90	-28	-8	$^2H_4$-9-HODE	14.73	1.00	100	x	x	x
14(15)-EpETE	317.2	207.2	-65	-20	-6	$^2H_{11}$-14(15)-EpETrE	14.78	0.25	100	x	x	x
8-HETE	319.2	155.2	-60	-22	-6	$^2H_8$-12-HETE	14.86	2.50	1000	x	x	x
12-HETE	319.2	179.2	-60	-20	-8	$^2H_8$-12-HETE	14.88	0.50	1000	x	x	x
11(12)-EpETE	317.2	167.2	-65	-20	-6	$^2H_{11}$-14(15)-EpETrE	14.91	0.50	100	x	x	x
11-HDHA	343.2	121.1	-45	-20	-7	$^2H_8$-5-HETE	14.93	0.10	20		x	x
7-HDHA	343.2	141.2	-55	-19	-7	$^2H_8$-5-HETE	15.06	0.25	500		x	x
8(9)-EpETE	317.2	127.2	-65	-20	-6	$^2H_{11}$-14(15)-EpETrE	15.07	1.00	100	x	x	x
9-HETE	319.2	167.2	-60	-23	-7	$^2H_8$-5-HETE	15.16	2.50	1000	x	x	x
15(S)-HETrE	321.2	221.2	-70	-23	-10	$^2H_8$-5-HETE	15.19	0.50	200	x	x	x
8-HDHA	343.2	189.2	-50	-19	-7	$^2H_8$-5-HETE	15.22	0.10	20		x	x

Tab. 11.1 continued

Analyte	Mass transition m/z (Q1)	m/z (Q2)	MS parameter DP (V)	CE (V)	CXP (V)	Internal standard	t_R (min)	LLOQ [1] (nM)	ULOQ [2] (nM)	Ch. 5 [3]	Ch. 6 [4]	Ch. 8 [5]
5-HETE	319.2	115.2	-60	-21	-7	$^2H_8$-5-HETE	15.38	1.25	1000	x	x	x
4-HDHA	343.2	101.1	-55	-19	-7	$^2H_8$-5-HETE	15.78	0.10	500		x	x
19(20)-EpDPE	343.2	241.2	-65	-20	-7	$^2H_{11}$-14(15)-EpETrE	15.83	0.25	100	x	x	x
12(13)-EpOME	295.3	195.2	-80	-23	-8	$^2H_4$-9(10)-EpOME	15.91	0.25	200	x	x	x
14(15)-EpETrE	319.2	219.3	-65	-20	-4	2H11-14(15)-EpETrE	16.03	0.50	100	x	x	x
9(10)-EpOME	295.3	171.1	-80	-23	-8	$^2H_4$-9(10)-EpOME	16.08	0.25	200	x	x	x
16(17)-EpDPE	343.2	233.2	-65	-20	-7	$^2H_{11}$-14(15)-EpETrE	16.20	0.25	100	x	x	x
13(14)-EpDPE	343.2	193.2	-65	-20	-7	$^2H_{11}$-14(15)-EpETrE	16.28	0.50	100	x	x	x
5-oxo-ETE	317.2	273.2	-65	-22	-6	$^2H_4$-9(10)-EpOME	16.36	2.00	100	x	x	x
10(11)-EpDPE	343.2	153.2	-65	-20	-7	$^2H_{11}$-14(15)-EpETrE	16.36	0.25	100	x	x	x
11(12)-EpETrE	319.3	167.2	-60	-20	-7	$^2H_{11}$-14(15)-EpETrE	16.48	0.50	200	x	x	x
8(9)-EpETrE	319.2	155.2	-65	-20	-6	$^2H_{11}$-14(15)-EpETrE	16.63	2.00	100	x	x	x
5(6)-EpETrE	319.2	191.1	-60	-20	-7	$^2H_{11}$-14(15)-EpETrE	16.78	1.00	100	x	x	x
9(10)-Epoxystearic acid	297.0	170.8	-100	-28	-11	$^2H_4$-9(10)-EpOME	17.25	1.00	100		x	x

[1] LLOQ was set to the lowest calibration standard injected yielding a signal to noise ratio ≥ 9 and an accuracy within ± 20%.
[2] ULOQ does not reflect the end of the linear range but the concentration of the highest calibrator.
[3] Analytes included in the targeted metabolomics LC-MS method of chapter 5 are marked as “x”.
[4] Analytes included in the targeted metabolomics LC-MS method of chapter 6 are marked as “x”.
[5] Analytes included in the targeted metabolomics LC-MS method of chapter 8 are marked as “x”.

Chapter 6

Tab. 11.2: Plasma concentration of oxylipins (>LOQ) 24 h after induction of sepsis by i. p. LPS injection or CLP survery. Statistical differences were determined by one-way ANOVA followed by Tukeys post-test test (*p<0.05, **p<0.01, ***p<0.001).

	LPS		**Vehicle**		**Δ (%)[a]**	**p LPS vs. vehicle**	**CLP**		**Sham**		**Δ (%)[a]**	**p CLP vs. Sham**	**p LPS vs. CLP[b]**
	Mean	**SE**	**Mean**	**SE**			**Mean**	**SE**	**Mean**	**SE**			
							c (nM)						
TXB_2	6.5	2.0	9.7	2.8	-33	> 0.05	5.7	1.7	11	2.0	-50	> 0.05	
$PGF_{2\alpha}$	1.5	0.32	0.88	0.16	75	> 0.05	0.93	0.20	1.24	0.30	-25	> 0.05	
PGE_2	3.9	0.92	0.18	0.048	2100	**< 0.001**	0.44	0.044	0.22	0.023	97	> 0.05	
6-keto-$PGF_{1\alpha}$	4.1	0.87	0.74	0.16	450	**< 0.05**	3.1	1.2	0.81	0.060	280	> 0.05	
PGD_3	0.58	0.054	0.45	0.027	29	> 0.05	0.49	0.038	0.40	0.035	23	> 0.05	
PGE_1	0.24	0.036	0.12[#]	-	100	**< 0.001**	0.12	0.0082	0.12[#]	-	3.5	> 0.05	
6-trans-LTB_4	0.32	0.073	0.18[#]	-	76	> 0.05	0.27	0.067	0.18[#]	-	48	> 0.05	
PGD_2	1.7	0.25	0.36[#]	-	380	> 0.05	0.75	0.11	4.2	1.1	-82	**< 0.01**	
5-iPF$_{2\alpha}$-VI	0.77	0.11	0.36[#]	-	110	**< 0.01**	0.64	0.12	0.36[#]	-	77	> 0.05	
1a,1b-dihomo-$PGF_{2\alpha}$	0.22	0.054	0.089[#]	-	-40	**< 0.01**	0.089[#]	-	0.089[#]	-		> 0.05	
13,14-dihydro-15-keto-$PGF_{2\alpha}$	3.5	0.82	0.45	0.11	670	**< 0.001**	1.0	0.15	0.57	0.056	80	> 0.05	
$PGF_{1\alpha}$	0.36	0.058	0.14	0.013	160	**< 0.01**	0.17	0.054	0.10	0.010	77	> 0.05	
13,14-dihydro-15-keto-PGE_1	0.59	0.12	0.036[#]	-	1500	**< 0.001**	0.28	0.066	0.036[#]	-	690	> 0.05	
9-HOTrE	5.1	0.73	7.8	0.58	-35	> 0.05	2.2	0.49	7.6	1.7	-71	**< 0.01**	
13-HOTrE	13	3.2	9.4	0.98	38	> 0.05	7.2	2.8	10	2.4	-29	> 0.05	
20-HETE	2.9	0.35	0.93[#]	-	210	**< 0.001**	1.7	0.13	0.93[#]	-	83	**< 0.05**	**< 0.01**
15-HEPE	0.95	0.24	0.46	0.017	100	> 0.05	0.76	0.19	0.45[#]	-	70	> 0.05	
8-HEPE	0.77	0.22	0.32	0.043	140	> 0.05	0.66	0.19	0.22	0.000052	200	> 0.05	
12-HEPE	139	42	23	7.0	500	> 0.05	120	43	9.3	1.7	1200	> 0.05	
5-HEPE	0.33	0.04	0.4	0.032	-19	> 0.05	0.27	0.037	0.33	0.039	-18	> 0.05	

Tab. 11.2 continued

	LPS		Vehicle		Δ (%)[a]	p LPS vs. vehicle	CLP		Sham		Δ (%)[a]	p CLP vs. Sham	p LPS vs. CLP[b]
	Mean	SE	Mean	SE			Mean	SE	Mean	SE			
	c (nM)												
13-HODE	270	50	240	22	12	> 0.05	190	51	190	38	-1.5	> 0.05	
9-HODE	140	18	134	10	4.2	> 0.05	98	23	104	18	-5.8	> 0.05	
15-HETE	8.8	1.7	5.5	0.59	61	> 0.05	4.9	1.2	3.5	0.30	42	> 0.05	
11-HETE	5.3	0.81	3.3	0.36	62	> 0.05	2.8	0.59	2.4	0.21	14	> 0.05	
8-HETE	10	1.9	4.6	0.56	120	**< 0.05**	8.4	1.8	2.8	0.23	200	**< 0.05**	> 0.05
12-HETE	1200	240	360	71	220	**< 0.05**	961	250	240	28	300	**< 0.05**	> 0.05
9-HETE	1.6	0.22	1.3	0.18	26	> 0.05	1.0	0.10	0.91	0.017	13	> 0.05	
15-HETrE	4.8	1.3	1.4	0.15	240	**< 0.05**	2.7	0.82	0.89	0.089	210	> 0.05	
5-HETE	4.7	0.54	4.7	0.41	-0.56	> 0.05	3.6	0.48	3.0	0.31	20	> 0.05	
18-HEPE	0.75	0.12	0.66	0.083	14	> 0.05	0.45	0.10	0.34	0.046	31	> 0.05	
20-HEPE	3.2	0.39	1.7	0.087	88	**< 0.01**	1.3	0.23	1.4	0.15	-6.1	> 0.05	
20-HDHA	4.3	0.66	2.9	0.50	45	> 0.05	2.3	0.38	1.3	0.094	81	> 0.05	
16-HDHA	2.8	0.38	2.0	0.36	39	> 0.05	1.5	0.22	0.79	0.06	90	> 0.05	
13-HDHA	3.7	0.76	1.8	0.33	100	> 0.05	2.1	0.54	0.67	0.054	210	> 0.05	
17-HDHA	24	6.63	7.0	1.2	250	**< 0.05**	16	5.3	2.7	0.28	510	> 0.05	
10-HDHA	17	4.70	3.3	0.64	400	**< 0.05**	13	4.2	1.4	0.18	810	> 0.05	
14-HDHA	440	130	60	17	630	**< 0.05**	360	120	28	4.5	1200	> 0.05	
11-HDHA	1.6	0.24	1.5	0.31	6.9	> 0.05	0.82	0.14	0.54	0.047	52	> 0.05	
7-HDHA	1.3	0.18	1.1	0.18	15	> 0.05	0.70	0.07	0.56	0.046	25	> 0.05	
8-HDHA	5.5	0.68	4.1	0.45	36	> 0.05	3.6	0.41	2.5	0.18	41	> 0.05	

Tab. 11.2 continued

	LPS		Vehicle		Δ (%)[a]	p LPS vs. vehicle	CLP		Sham		Δ (%)[a]	p CLP vs. Sham	p LPS vs. CLP[b]
	Mean	SE	Mean	SE			Mean	SE	Mean	SE			
							c (nM)						
4-HDHA	3.6	0.50	2.8	0.44	30	> 0.05	1.6	0.19	1.1	0.089	43	> 0.05	
9,12,13-TriHOME	18	3.15	11	1.3	68	> 0.05	12	2.7	14	3.1	-17	> 0.05	
9,10,13-TriHOME	3.5	0.68	2.4	0.32	47	> 0.05	2.3	0.47	2.5	0.41	-6.1	> 0.05	
13-oxo-ODE	21	3.5	12	2.4	72	**< 0.05**	2.9	0.55	4.2	0.58	-30	> 0.05	
15-oxo-ETE	0.87	0.15	1.1	0.25	-19	> 0.05	0.37	0.047	0.36	0.026	2.7	> 0.05	
9-oxo-ODE	27	3.5	19	2.7	45	> 0.05	12	1.7	13	1.5	-2.7	> 0.05	
5-oxo-ETE	1.0	0.14	1.03	0.18	-0.81	> 0.05	0.71[#]	-	0.71[#]	-		> 0.05	
EKODE	17	2.8	12	2.0	42	> 0.05	7.0	1.0	5.4	0.46	29	> 0.05	
15,16-DiHODE	38	6.5	23	3.7	65	> 0.05	22	4.4	25	4.6	-14	> 0.05	
9,10-DiHODE	4.8	0.34	3.3	0.30	44	> 0.05	4.3	0.53	3.7	0.74	17	> 0.05	
12,13-DiHODE	3.9	0.47	3.5	0.44	11	> 0.05	3.2	0.36	4.9	1.1	-35	> 0.05	
17,18-DiHETE	2.8	0.26	1.5	0.10	86	**< 0.01**	1.9	0.27	1.3	0.10	48	> 0.05	
14,15-DiHETE	0.47	0.037	0.30	0.015	57	**< 0.01**	0.35	0.062	0.26	0.03	35	> 0.05	
11,12-DiHETE	0.24	0.033	0.14	0.0064	69	> 0.05	0.18	0.052	0.11	0.01	57	> 0.05	
12,13-DiHOME	200	19	116	11	71	**< 0.01**	220	17	103	13	110	**< 0.001**	> 0.05
8,9-DiHETE	0.29	0.03	0.18[#]	-	61	> 0.05	0.26	0.05	180[#]	-	44	> 0.05	
9,10-DiHOME	66	2.2	55	6.4	21	> 0.05	95	7.9	35	5.3	170	**< 0.001**	
19,20-DiHDPE	25	3.6	9.1	0.55	170	**< 0.001**	17	1.9	7.8	0.86	120	**< 0.05**	> 0.05
14,15-DiHETrE	5.1	0.46	2.7	0.13	91	**< 0.001**	5.5	0.51	2.1	0.24	160	**< 0.001**	> 0.05
16,17-DiHDPE	2.7	0.17	1.5	0.089	75	**< 0.001**	2.3	0.24	1.4	0.14	72	**< 0.01**	> 0.05

Tab. 11.2 continued

	LPS		Vehicle		Δ (%)[a]	$p_{LPS\ vs.\ vehicle}$	CLP		Sham		Δ (%)[a]	$p_{CLP\ vs.\ Sham}$	$p_{LPS\ vs.\ CLP}$[b]
	Mean	SE	Mean	SE			Mean	SE	Mean	SE			
	c (nM)												
11,12-DiHETrE	2.6	0.25	1.6	0.064	69	**< 0.01**	2.7	0.28	1.3	0.15	110	**< 0.001**	> 0.05
13,14-DiHDPE	1.1	0.08	0.63	0.037	68	**< 0.01**	1.1	0.10	0.59	0.060	80	**< 0.01**	> 0.05
10,11-DiHDPE	1.1	0.11	0.61	0.044	89	**< 0.01**	1.2	0.12	0.55	0.055	120	**< 0.001**	> 0.05
8,9-DiHETrE	3.7	0.51	2.3	0.19	63	**< 0.05**	3.3	0.39	2.0	0.24	67	> 0.05	
7,8-DiHDPE	1.7	0.21	1.0	0.065	62	**< 0.05**	1.4	0.16	0.96	0.11	40	> 0.05	
5,6-DiHETrE	1.5	0.23	1.2	0.10	27	> 0.05	0.96	0.14	1.0	0.13	-3.2	> 0.05	
4,5-DiHDPE	17	1.7	7.7	0.84	120	**< 0.001**	9.4	1.5	5.4	0.59	74	> 0.05	
9,10-Dihydroxy-stearic acid	7.5	2.1	7.9	1.1	-5.0	> 0.05	9.9	2.6	7.2	1.5	38	> 0.05	
9(10)-EpODE	32	4.8	17	3.9	87	**< 0.05**	3.9	0.83	4.1	0.58	-5.9	> 0.05	
17(18)-EpETE	2.3	0.27	1.7	0.34	32	> 0.05	0.84	0.083	0.52	0.059	62	> 0.05	
12(13)-EpODE	17	2.5	9.6	1.9	80	**< 0.05**	2.1	0.41	3.3	0.46	-38	> 0.05	
14(15)-EpETE	1.7	0.27	1.6	0.39	5.8	> 0.05	0.37	0.050	0.32	0.031	14	> 0.05	
11(12)-EpETE	1.0	0.14	1.5	0.38	-32	> 0.05	0.28	0.030	0.33	0.031	-16	> 0.05	
8(9)-EpETE	1.4	0.23	1.4	0.34	-1.1	> 0.05	0.40	0.029	0.37	0.0078	8.0	> 0.05	
19(20)-EpDPE	35	3.7	20	3.6	76	**< 0.01**	13	1.1	6.5	0.80	95	> 0.05	
12(13)-EpOME	250	30	149	28	67	**< 0.05**	52	6.7	52	4.5	0.41	> 0.05	
14(15)-EpETrE	27	2.9	24	6.0	13	> 0.05	5.0	0.64	4.2	0.46	20	> 0.05	
9(10)-EpOME	280	33	160	32	77	**< 0.01**	57	8.4	42	4.2	35	> 0.05	
16(17)-EpDPE	21	3.0	15	3.9	37	> 0.05	4.1	0.60	2.7	0.28	55	**< 0.001**	
13(14)-EpDPE	21	3.3	15	4.0	37	> 0.05	4.0	0.60	2.7	0.27	52	> 0.05	

Tab. 11.2 continued

	LPS		Vehicle		Δ (%)[a]	p LPS vs. vehicle	CLP		Sham		Δ (%)[a]	p CLP vs. Sham	p LPS vs. CLP[b]
	Mean	SE	Mean	SE			Mean	SE	Mean	SE			
	c (nM)												
10(11)-EpDPE	30	4.5	21	5.2	40	> 0.05	5.7	0.85	4.0	0.38	45	> 0.05	
11(12)-EpETrE	30	3.5	31	8.1	-4.8	> 0.05	6.0	0.77	5.7	0.52	5.5	> 0.05	
8(9)-EpETrE	16	2.1	15	3.8	9.4	> 0.05	3.6	0.47	3.1	0.27	16	> 0.05	
5(6)-EpETrE	74	12	70	17	7.0	> 0.05	14	1.8	14	1.2	0.5	> 0.05	
15(16)-EpODE	67	4.0	60	5.8	12	> 0.05	25	3.9	46	7.4	-45	> 0.05	
9(10)-Epoxy-stearic acid	190	19	170	33	13	> 0.05	60	7.7	46	3.1	31	> 0.05	

[#] Limit of quantification (LOQ).
[a] The relative change (% Δ) of treatment in comparison to the control is calculated as % Δ = 100 × ($c_{treatment}$-$c_{control}$)/$c_{control}$.
[b] p value for LPS vs. CLP is only shown, if both treatment groups significantly differ from each control.

Tab. 11.3: Liver tissue concentration of oxylipins (>LOQ) 24 h after induction of sepsis by i. p. LPS injection or CLP survery. Statistical differences were determined by one-way ANOVA followed by Tukeys post-test test (*p<0.05, **p<0.01, ***p<0.001).

	LPS		Vehicle		Δ (%)[a]	p LPS vs. vehicle	CLP		Sham		Δ (%)[a]	p CLP vs. Sham	p LPS vs.[b] CLP
	Mean	SE	Mean	SE			Mean	SE	Mean	SE			
	c (fmol/mg)												
6-keto-$PGF_{1\alpha}$	63	9.6	56	6.4	12	> 0.05	79	15	69	16	15	> 0.05	
TXB_2	23	3.5	23	5.1	0.20	> 0.05	25	7.1	69	5.8	-63	> 0.05	
PGD_3	1.7	0.17	1.3	0.13	29	> 0.05	1.4	0.09	1.1[#]	-	29	> 0.05	
$PGF_{2\alpha}$	80	12.0	110	35.1	-28	> 0.05	66	12	110	18	-40	> 0.05	
PGE_2	18	3.4	7.3	1.7	140	**< 0.05**	9.9	1.6	7.9	1.5	25	> 0.05	
PGE_1	5.7	0.88	3.2	0.65	79	> 0.05	4.6	0.61	3.3	0.56	39	> 0.05	
PGD_1	2.8	0.41	2.0	0.39	43	> 0.05	2.7	0.41	1.8	0.37	53	> 0.05	
PGD_2	42	6.2	43	8.0	-1.4	> 0.05	33	6.1	33	6.2	-2.3	> 0.05	
5-$iPF_{2\alpha}$	3.1	0.54	1.2	0.067	160	**< 0.01**	1.9	0.28	1.3	0.076	46	> 0.05	
1a,1b-dihomo-$PGF_{2\alpha}$	8.7	1.6	5.6	1.5	56	> 0.05	5.7	0.43	4.9	0.69	16	> 0.05	
13,14-dihydro-15-keto-$PGF_{2\alpha}$	8.7	0.88	6.1	0.77	43	> 0.05	8.2	1.4	6.2	0.72	32	> 0.05	
TxB_3	1.1	0.15	1.2	0.16	-4.4	> 0.05	1.1	0.25	1.1	0.19	-1.9	> 0.05	
TxB_1	0.74	0.074	0.66	0.052	12	> 0.05	0.83	0.14	0.50[#]	-	67	> 0.05	
$PGF_{1\alpha}$	14	2.1	16	3.7	-15	> 0.05	13	1.4	16	2.1	-18	> 0.05	
13,14-dihydro-15-keto-PGE_1	0.92	0.15	0.39	0.055	140	> 0.05	0.74	0.21	0.36	0.059	100	> 0.05	
9-HOTrE	4.5	0.57	6.4	0.69	-30	> 0.05	3.3	0.37	6.2	0.69	-47	**< 0.05**	
13-HOTrE	12	1.5	24	7.9	-52	> 0.05	8.6	1.7	5.2	0.63	64	> 0.05	
20-HETE	12	2.9	3.6	0.36	230	**< 0.05**	8.8	1.4	3.2	0.21	170	> 0.05	
15-HEPE	2.4	0.14	4.6	1.0	-48	**< 0.05**	2.1	0.22	1.9	0.18	8.0	> 0.05	
8-HEPE	0.87	0.083	0.72	0.050	22	> 0.05	0.84	0.070	0.71	0.016	18	> 0.05	

Tab. 11.3 continued

	LPS		Vehicle		Δ (%)[a]	p LPS vs. vehicle	CLP		Sham		Δ (%)[a]	p CLP vs. Sham	p LPS vs. CLP[b]
	Mean	SE	Mean	SE			Mean	SE	Mean	SE			
	c (fmol/mg)												
12-HEPE	200	50	36	9.2	470	> 0.05	250	68	36	12	580	**< 0.05**	
5-HEPE	1.8	0.23	3.3	0.13	-43	**< 0.001**	2.3	0.18	3.4	0.19	-32	**< 0.01**	> 0.05
13-HODE	530	60	600	80	-11	> 0.05	500	74	430	64	16	> 0.05	
9-HODE	590	64	530	71	10	> 0.05	530	75	480	67	11	> 0.05	
15-HETE	33	2.6	32	4.0	3.5	> 0.05	29	3.6	30	3.7	-5.0	> 0.05	
11-HETE	29	2.7	25	4.2	15	> 0.05	26	4.2	25	4.1	3.6	> 0.05	
8-HETE	12	1.5	8.6	0.72	44	> 0.05	12	1.6	9.2	1.2	26	> 0.05	
12-HETE	780	19	200	52	290	> 0.05	840	230	200	88	310	**< 0.05**	
9-HETE	5.3	0.73	4.1	0.27	27	> 0.05	4.7	0.45	4.7	0.36	0.71	> 0.05	
15-HETrE	18	1.2	17	1.6	5.8	> 0.05	15	1.6	13	0.90	17	> 0.05	
5-HETE	15	1.6	19	0.63	-19	> 0.05	19	1.7	19	0.84	4.0	> 0.05	
18-HEPE	3.0	0.20	3.0	0.18	0.93	> 0.05	3.0	0.25	3.4	0.21	-9.2	> 0.05	
20-HEPE	16	2.2	13	0.94	19	> 0.05	10	1.4	13	1.5	-21	> 0.05	
20-HDHA	14	1.3	9.3	0.63	53	**< 0.01**	13	1.0	12	0.93	14	> 0.05	
16-HDHA	4.1	0.29	3.3	0.22	24	> 0.05	4.0	0.34	4.4	0.37	-8.4	> 0.05	
13-HDHA	11	1.0	8.3	1.2	36	> 0.05	11	1.5	9.2	1.2	16	> 0.05	
17-HDHA	13	0.84	23	4.9	-43	> 0.05	13	1.6	8.9	1.2	46	> 0.05	
10-HDHA	7.1	0.93	3.6	0.29	99	**< 0.05**	8.1	1.4	4.0	0.51	99	**< 0.05**	> 0.05
14-HDHA	190	44	80	19	130	> 0.05	230	56	56	21	310	**< 0.05**	
11-HDHA	3.7	0.46	2.6	0.19	38	> 0.05	4.1	0.48	3.1	0.22	31	> 0.05	

Tab. 11.3 continued

	LPS		Vehicle		Δ (%)[a]	p LPS vs. vehicle	CLP		Sham		Δ (%)[a]	p CLP vs. Sham	p LPS vs. CLP[b]
	Mean	SE	Mean	SE			Mean	SE	Mean	SE			
	c (fmol/mg)												
7-HDHA	3.6	0.39	2.8	0.13	28	> 0.05	3.6	0.32	3.6	0.22	0.39	> 0.05	
8-HDHA	17	2.0	13	0.50	32	> 0.05	15	1.3	15	1.3	-0.86	> 0.05	
4-HDHA	7.2	0.79	5.8	0.34	24	> 0.05	6.4	0.39	6.8	0.31	-5.8	> 0.05	
9,12,13-TriHOME	34	6.5	98	43	-65	> 0.05	23	1.9	50	18	-53	> 0.05	
9,10,13-TriHOME	5.0	0.67	8.0	1.1	-37	> 0.05	4.3	0.38	7.7	2.7	-45	> 0.05	
13-oxo-ODE	7.5	1.1	7.0	1.2	8.1	> 0.05	5.8	1.1	6.1	0.41	-4.8	> 0.05	
15-oxo-ETE	3.5	0.36	4.3	0.53	-19	> 0.05	3.0	0.39	4.8	0.34	-39	**< 0.05**	
9-oxo-ODE	45	9.7	42	8.5	6.7	> 0.05	35	9.8	33	3.3	6.7	> 0.05	
5-oxo-ETE	4.0	0.40	4.8	0.60	-17	> 0.05	3.3	0.40	5.3	0.34	-39	**< 0.05**	
EKODE	28	4.2	30	3.5	-7.2	> 0.05	23	3.0	31	2.1	-27	> 0.05	
15,16-DiHODE	50	7.2	56	4.8	-11	> 0.05	26	1.3	70	9.8	-62	**< 0.001**	
9,10-DiHODE	9.0	2.1	5.9	1.0	53	> 0.05	4.4	0.67	6.6	0.82	-34	> 0.05	
12,13-DiHODE	5.1	1.0	4.8	0.6	7.2	> 0.05	2.5	0.13	9.2	2.7	-73	**< 0.05**	
17,18-DiHETE	25	1.8	26	1.1	-3.7	> 0.05	20	1.3	31	2.5	-34	**<0.01**	
14,15-DiHETE	13	2.0	12	1.5	7.2	> 0.05	13	0.89	14	1.3	-10	> 0.05	
11,12-DiHETE	4.0	0.55	4.0	0.62	-1.7	> 0.05	4.2	0.38	4.3	0.39	-4.0	> 0.05	
12,13-DiHOME	210	16	190	13	15	> 0.05	170	10	240	21	-30	**< 0.05**	
8,9-DiHETE	4.3	0.80	3.8	0.89	14	> 0.05	3.6	0.45	4.0	0.37	-9.3	> 0.05	
9,10-DiHOME	100	17	72	8.1	49	> 0.05	82	8.0	73	5.5	12	> 0.05	
19,20-DiHDPE	160	15	130	7.5	17	> 0.05	150	14	180	8.5	-18	> 0.05	

Tab. 11.3 continued

	LPS		Vehicle		Δ (%)[a]	p LPS vs. vehicle	CLP		Sham		Δ (%)[a]	p CLP vs. Sham	p LPS vs. CLP[b]
	Mean	SE	Mean	SE			Mean	SE	Mean	SE			
							c (fmol/mg)						
14,15-DiHETrE	110	8.8	89	3.6	26	> 0.05	130	6.0	130	8.8	-0.8	> 0.05	
16,17-DiHDPE	42	3.3	35	2.2	21	> 0.05	47	2.6	47	2.8	-0.013	> 0.05	
11,12-DiHETrE	41	4.7	37	2.1	13	> 0.05	45	2.4	51	3.3	-11	> 0.05	
13,14-DiHDPE	17	1.9	12	1.1	41	> 0.05	21	1.7	18	0.92	14	> 0.05	
10,11-DiHDPE	14	3.5	9.2	1.1	54	> 0.05	15	1.8	13	0.9	18	> 0.05	
8,9-DiHETrE	26	5.6	20	2.7	30	> 0.05	19	2.2	24	2.8	-24	> 0.05	
7,8-DiHDPE	9.8	2.3	6.1	0.76	60	> 0.05	8.1	1.1	8.4	0.88	-4.0	> 0.05	
5,6-DiHETrE	11	2.9	8.1	1.2	31	> 0.05	7.6	1.1	9.8	1.1	-23	> 0.05	
4,5-DiHDPE	85	17	52	8.3	64	> 0.05	70	10	55	8.1	27	> 0.05	
9,10-Dihydroxy-stearic acid	74	9.3	77	8.5	-3.9	> 0.05	70	8.5	57	12	23	> 0.05	
9(10)-EpODE	6.5	0.64	5.7	0.75	14	> 0.05	5.3	0.58	5.9	0.47	-10	> 0.05	
17(18)-EpETE	3.2	0.32	3.3	0.47	-2.1	> 0.05	3.7	0.49	4.0	0.21	-6.3	> 0.05	
12(13)-EpODE	3.7	0.41	3.3	0.45	11	> 0.05	3.1	0.38	3.6	0.28	-15	> 0.05	
14(15)-EpETE	2.7	0.28	2.9	0.42	-6.6	> 0.05	3.3	0.43	3.7	0.19	-10	> 0.05	
11(12)-EpETE	2.3	0.23	2.4	0.35	-4.4	> 0.05	2.7	0.33	2.8	0.15	-5.2	> 0.05	
8(9)-EpETE	1.7	0.14	1.7	0.16	-1.6	> 0.05	2.0	0.17	2.0	0.09	0.33	> 0.05	
19(20)-EpDPE	20	1.9	21	2.0	-3.6	> 0.05	24	2.6	27	1.9	-11	> 0.05	
12(13)-EpOME	85	7.1	84	9.9	0.45	> 0.05	100	10	97	7.4	4.6	> 0.05	
14(15)-EpETrE	41	4.9	47	5.3	-13	> 0.05	47	7.0	64	5.0	-27	> 0.05	
9(10)-EpOME	94	8.2	90	10	4.3	> 0.05	110	11	100	7.9	5.3	> 0.05	

Tab. 11.3 continued

	LPS		Vehicle		Δ (%)[a]	p LPS vs. vehicle	CLP		Sham		Δ (%)[a]	p CLP vs. Sham	p LPS vs. CLP[b]
	Mean	SE	Mean	SE			Mean	SE	Mean	SE			
	c (fmol/mg)												
16(17)-EpDPE	13	1.2	13	1.2	1.3	> 0.05	16	1.7	18	1.4	-10	> 0.05	
13(14)-EpDPE	14	1.2	13	1.4	5.7	> 0.05	18	2.0	19	1.4	-5.3	> 0.05	
10(11)-EpDPE	18	1.3	17	1.6	3.7	> 0.05	22	2.0	23	1.6	-6.3	> 0.05	
11(12)-EpETrE	46	4.3	50	5.5	-8.5	> 0.05	50	5.8	62	4.7	-20	> 0.05	
8(9)-EpETrE	17	1.7	17	1.8	-2.5	> 0.05	17	1.8	22	1.5	-24	> 0.05	
5(6)-EpETrE	59	5.3	57	5.6	4.5	> 0.05	56	4.1	63	4.0	-12	> 0.05	
15(16)-EpODE	12	1.3	12	1.5	2.3	> 0.05	10	1.3	12	0.91	-16	> 0.05	
9(10)-Epoxy-stearic acid	140	30	110	13	26	> 0.05	110	11	94	3.2	21	> 0.05	

[#] Limit of quantification (LOQ).
[a] The relative change (% Δ) of treatment in comparison to the control is calculated as $\% \Delta = 100 \times (c_{treatment}-c_{control})/c_{control}$.
[b] p value for LPS vs. CLP is only shown, if both treatment groups significantly differ from each control.

Tab. 11.4: Kidney tissue concentration of oxylipins (>LOQ) 24 h after induction of sepsis by i. p. LPS injection or CLP survery. Statistical differences were determined by one-way ANOVA followed by Tukeys post-test test (*p<0.05, **p<0.01, ***p<0.001).

	LPS		Vehicle		Δ (%)[a]	p LPS vs. vehicle	CLP		Sham		Δ (%)[a]	p CLP vs. Sham	p LPS vs.[b] CLP
	Mean	SE	Mean	SE			Mean	SE	Mean	SE			
	c (fmol/mg)												
6-keto-$PGF_{1\alpha}$	140	17	72	8.7	89	> 0.05	93	33	71	16	32	> 0.05	
TXB_2	6.5	0.77	4.4	0.34	48	> 0.05	5.0	2.3	5.2	1.2	-3.5	> 0.05	
PGE_3	1.8	0.32	0.92	0.089	93	> 0.05	1.6	0.57	1.3	0.17	26	> 0.05	
$PGF_{2\alpha}$	100	8.1	73	6.1	38	> 0.05	59	16	83	14	-29	> 0.05	
PGE_2	170	37	170	25	-0.55	> 0.05	150	29	220	38	-33	> 0.05	
PGE_1	15	2.9	8.7	1.3	67	> 0.05	9.6	2.3	11	2.6	-15	> 0.05	
PGD_1	1.8	0.31	0.59	0.054	210	**< 0.01**	0.85	0.32	0.61	0.06	39	> 0.05	
PGD_2	27	5.0	14	2.9	92	> 0.05	15	3.9	20	5.3	-26	> 0.05	
1a,1b-dihomo-$PGF_{2\alpha}$	5.2	0.57	2.2	0.23	140	**< 0.01**	2.4	0.57	2.6	0.51	-7.5	> 0.05	
13,14-dihydro-15-keto-PGF_{2a}	4.9	0.32	4.3	0.21	13	> 0.05	4.0	1.5	4.4	0.56	-10	> 0.05	
$PGF_{1\alpha}$	12	1.0	5.7	0.53	100	**< 0.05**	5.8	1.8	6.5	0.93	-11	> 0.05	
13,14-dihydro-15-keto-PGE_1	0.47	0.061	0.31	0.070	52	> 0.05	0.55	0.14	0.67	0.07	-17	> 0.05	
9-HOTrE	3.0	0.25	2.3	0.21	27	> 0.05	1.7	0.31	2.8	0.40	-39	> 0.05	
13-HOTrE	3.9	0.44	4.1	1.0	-5.6	> 0.05	2.3	0.43	3.1	0.38	-27	> 0.05	
20-HETE	4.5	0.55	2.7[#]	-	68	**< 0.001**	2.7[#]	-	2.7[#]	-		> 0.05	
12-HEPE	9.7	2.9	2.4	0.42	310	> 0.05	5.8	4.2	1.5	0.25	290	> 0.05	
5-HEPE	0.76	0.03	1.0	0.031	-21	**< 0.001**	0.68	0.03	0.83	0.029	-18	**< 0.01**	> 0.05
13-HODE	380	34	170	16	120	**< 0.01**	210	70	180	13.4	15	> 0.05	
9-HODE	470	44	170	9.8	180	**< 0.01**	250	89	200	20.9	29	> 0.05	
15-HETE	31	2.8	30	1.6	3.5	> 0.05	31	8.0	38	4.5	-18	> 0.05	

Tab. 11.4 continued

	LPS		Vehicle		Δ (%)[a]	p LPS vs. vehicle	CLP		Sham		Δ (%)[a]	p CLP vs. Sham	p LPS vs. CLP[b]
	Mean	SE	Mean	SE			Mean	SE	Mean	SE			
	c (fmol/mg)												
11-HETE	33	3.7	28	2.5	15	> 0.05	31	12	34	5.3	-8.6	> 0.05	
8-HETE	3.3	0.29	3.2	0.2	3.5	> 0.05	2.8	0.19	2.7	0.08	2.3	> 0.05	
12-HETE	71	19	30	5.2	140	> 0.05	39	23	26	11	48	> 0.05	
9-HETE	2.8	0.13	2.7	0.12	2.1	> 0.05	2.9	0.21	3.0	0.10	-0.11	> 0.05	
15-HETrE	11	0.91	7.8	0.55	39	> 0.05	9.0	2.4	9.7	0.80	-6.9	> 0.05	
5-HETE	12	0.67	12	0.48	-2.0	> 0.05	10	1.0	12	0.37	-16	> 0.05	
18-HEPE	1.2	0.12	0.93	0.038	30	> 0.05	1.2	0.20	1.1	0.036	13	> 0.05	
20-HEPE	8.1	1.3	6.4	0.45	26	> 0.05	9.1	0.73	8.0	0.41	13	> 0.05	
20-HDHA	13	1.0	9.3	0.47	40	> 0.05	14	1.8	11	0.40	27	> 0.05	
16-HDHA	5.6	0.28	3.8	0.24	46	> 0.05	6.8	0.8	4.6	0.27	48	**< 0.05**	
13-HDHA	9.7	0.76	7.0	0.27	39	> 0.05	11	3.9	8.0	0.79	38	> 0.05	
17-HDHA	13	0.53	11	1.4	21	> 0.05	12	1.7	9.0	0.48	35	> 0.05	
10-HDHA	3.0	0.26	2.0	0.1	54	**< 0.05**	2.5	0.38	1.8	0.059	40	> 0.05	
14-HDHA	34	8.6	13	2.6	160	> 0.05	21	12	7.0	1.3	200	> 0.05	
11-HDHA	3.4	0.20	2.4	0.2	44	**< 0.05**	3.2	0.33	2.7	0.11	19	> 0.05	
7-HDHA	2.6	0.12	1.7	0.1	53	**< 0.01**	2.1	0.27	1.9	0.067	8.4	> 0.05	
8-HDHA	17	0.60	14	0.71	22	> 0.05	13	1.4	14	0.34	-2.2	> 0.05	
4-HDHA	15	1.1	12	0.58	22	> 0.05	14	1.8	12	0.49	18	> 0.05	
9,12,13-TriHOME	23	1.8	18	1.3	27	> 0.05	17	1.3	16	0.70	7.0	> 0.05	
9,10,13-TriHOME	4.1	0.30	3.2	0.18	27	> 0.05	2.9	0.30	3.0	0.11	-1.6	> 0.05	

Tab. 11.4 continued

	LPS		Vehicle		Δ (%)[a]	p LPS vs. vehicle	CLP		Sham		Δ (%)[a]	p CLP vs. Sham	p LPS vs. CLP[b]
	Mean	SE	Mean	SE			Mean	SE	Mean	SE			
							c (fmol/mg)						
13-oxo-ODE	5.4	0.40	2.6	0.17	10	**< 0.001**	1.8	0.16	1.6	0.07	13	> 0.05	
15-oxo-ETE	5.6	0.70	5.7	0.38	-3	> 0.05	4.0	0.54	4.4	0.31	-7.3	> 0.05	
9-oxo-ODE	40	3.8	21	0.51	88	**< 0.001**	21	3.7	15	0.57	43	> 0.05	
5-oxo-ETE	7.1	0.88	7.4	0.71	-4	> 0.05	4.0	0.43	5.1	0.36	-22	> 0.05	
EKODE	39	3.8	18	0.46	120	**< 0.001**	23	2.7	16	0.87	45	> 0.05	
15,16-DiHODE	20	2.0	18	2.1	8.9	> 0.05	11	2.2	20	2.8	-46	**< 0.05**	
9,10-DiHODE	1.6	0.15	1.0	0.089	59	> 0.05	0.9	0.16	1.2	0.19	-26	> 0.05	
17,18-DiHETE	4.7	0.42	3.4	0.14	39	**< 0.05**	4.2	0.33	3.5	0.14	20	> 0.05	
14,15-DiHETE	1.2	0.15	0.90	0.033	32	> 0.05	1.5	0.11	1.0	0.044	50	**< 0.05**	
12,13-DiHOME	60	3.9	38	3.6	60	**< 0.05**	51	6.6	40	4.0	29	> 0.05	
9,10-DiHOME	35	1.5	21	2.0	66	**< 0.001**	26	3.2	17	1.3	55	**< 0.05**	**< 0.05**
19,20-DiHDPE	110	8.1	84	3.5	29	> 0.05	150	12.1	100	8.0	49	**< 0.01**	
14,15-DiHETrE	10	0.86	8.2	0.25	26	> 0.05	11	0.92	9.8	0.69	15	> 0.05	
16,17-DiHDPE	14	1.6	15	0.50	-5.7	> 0.05	30	2.8	20	1.4	51	**< 0.01**	
11,12-DiHETrE	3.9	0.30	3.1	0.083	25	> 0.05	3.9	0.35	3.4	0.19	15	> 0.05	
13,14-DiHDPE	4.8	0.59	3.2	0.12	49	**< 0.05**	6.2	0.43	3.7	0.20	66	**< 0.01**	> 0.05
10,11-DiHDPE	3.0	0.14	1.7	0.0	71	**< 0.001**	2.6	0.20	1.8	0.08	43	**< 0.01**	> 0.05
8,9-DiHETrE	2.5	0.17	2.0	0.050	27	> 0.05	1.9	0.21	1.8	0.12	2.2	> 0.05	
7,8-DiHDPE	3.0	0.13	1.9	0.10	59	**< 0.001**	2.0	0.20	1.9	0.098	2.2	> 0.05	
5,6-DiHETrE	2.5	0.16	2.2	0.11	16	> 0.05	2.2	0.21	1.8	0.16	26	> 0.05	

Tab. 11.4 continued

	LPS		Vehicle		Δ (%)[a]	p LPS vs. vehicle	CLP		Sham		Δ (%)[a]	p CLP vs. Sham	p LPS vs. CLP[b]
	Mean	SE	Mean	SE			Mean	SE	Mean	SE			
	c (fmol/mg)												
4,5-DiHDPE	25	0.95	12	0.62	101	**< 0.001**	19	1.5	11	0.57	71	**< 0.001**	**< 0.01**
9,10-Dihydroxystearic acid	34	2.1	33	2.9	1.8	> 0.05	28	1.1	30	1.9	-5.8	> 0.05	
9(10)-EpODE	5.7	0.63	2.1	0.12	170	**< 0.001**	0.58	0.084	0.48	0.057	21	> 0.05	
17(18)-EpETE	2.2	0.18	1.8	0.060	18	> 0.05	0.52[#]	-	0.52[#]	-		> 0.05	
12(13)-EpODE	3.1	0.32	1.2	0.045	170	**< 0.001**	0.39	0.048	0.34	0.031	14	> 0.05	
14(15)-EpETE	1.9	0.15	1.6	0.038	19	**< 0.05**	0.28	0.010	0.28	0.011	-1.0	> 0.05	
11(12)-EpETE	1.7	0.13	1.4	0.030	22	**< 0.05**	0.52[#]	-	0.52[#]	-		> 0.05	
8(9)-EpETE	1.3	0.065	1.1	0.065	11	> 0.05	1.0[#]	-	1.0[#]	-		> 0.05	
19(20)-EpDPE	40	1.2	36	0.7	11	**< 0.05**	14	0.83	12	0.66	16	> 0.05	
12(13)-EpOME	85	6.4	39	1.8	120	**< 0.001**	11	0.84	9.2	0.84	18	> 0.05	
14(15)-EpETrE	45	3.1	60	3.5	-25	**< 0.01**	6.4	0.47	8.2	0.71	-22	> 0.05	
9(10)-EpOME	110	6.9	43	2.6	140	**< 0.001**	11	0.94	9.3	0.90	20	> 0.05	
16(17)-EpDPE	25	0.8	22	0.66	15	**< 0.01**	4.9	0.43	4.2	0.39	18	> 0.05	
13(14)-EpDPE	27	1.1	23	0.72	16	**< 0.01**	5.3	0.45	4.4	0.41	22	> 0.05	
10(11)-EpDPE	35	0.9	28	1.2	24	**< 0.001**	6.5	0.53	5.5	0.56	18	> 0.05	
11(12)-EpETrE	50	3.1	67	2.3	-26	**< 0.001**	9.0	0.73	12	0.93	-24	> 0.05	
8(9)-EpETrE	21	1.0	24	0.72	-13	**< 0.05**	3.8	0.32	4.9	0.45	-22	> 0.05	
5(6)-EpETrE	56	2.1	54	4.9	3.8	> 0.05	18	1.3	22	2.4	-18	> 0.05	
15(16)-EpODE	9.6	1.1	5.2	0.22	87	**< 0.001**	1.3	0.18	1.8	0.21	-27	> 0.05	
9(10)-Epoxystearic acid	63	4.2	54	1.7	17	> 0.05	21	2.0	25	2.1	-16	> 0.05	

[#] Limit of quantification (LOQ). [a] The relative change (% Δ) of treatment in comparison to the control is calculated as $\% \Delta = 100 \times (c_{treatment} - c_{control})/c_{control}$. [b] p value for LPS vs. CLP is only shown, if both treatment groups significantly differ from each control.

Tab. 11.5: Heart tissue concentration of oxylipins (>LOQ) 24 h after induction of sepsis by i. p. LPS injection or CLP survery. Statistical differences were determined by one-way ANOVA followed by Tukeys post-test test (*p<0.05, **p<0.01, ***p<0.001).

	LPS		Vehicle		Δ (%)[a]	p LPS vs. vehicle	CLP		Sham		Δ (%)[a]	p CLP vs. Sham	p LPS[b] vs. CLP
	Mean	SE	Mean	SE			Mean	SE	Mean	SE			
	c (fmol/mg)												
6-keto-$PGF_{1\alpha}$	130	14	73	5.5	79	**< 0.001**	130	7.1	180	37	-25	> 0.05	
TXB_2	1.9	0.25	2.1	0.19	-10	> 0.05	3.0	0.28	4.1	1.0	-26	> 0.05	
$PGF_{2\alpha}$	23	3.2	22	2.2	7.1	> 0.05	35	6.2	59	11	-40	> 0.05	
PGE_2	5.5	0.58	3.0	0.30	83	> 0.05	4.2	0.30	7.1	1.3	-41	> 0.05	
PGD_2	6.5	0.69	7.0	0.72	-7.8	> 0.05	8.5	1.0	20	4.7	-57	**< 0.05**	
1a,1b-dihomo-$PGF_{2\alpha}$	2.9	0.54	3.3	0.42	-12	> 0.05	4.7	0.51	3.6	0.57	30	> 0.05	
13,14-dihydro-15-keto-$PGF_{2\alpha}$	3.2	0.21	1.9	0.17	69	**< 0.05**	2.9	0.15	3.4	0.49	-17	> 0.05	
$PGF_{1\alpha}$	5.3	0.73	6.4	0.76	-17	> 0.05	7.5	0.82	8.3	1.3	-10	> 0.05	
13,14-dihydro-15-keto-PGE_1	0.43	0.044	0.10[#]	-	330	**< 0.001**	0.25	0.05	0.10[#]	-	150	> 0.05	
9-HOTrE	2.7	0.41	4.0	0.33	-32	> 0.05	2.2	0.25	9.6	2.9	-77	**< 0.01**	
13-HOTrE	6.0	1.4	8.3	0.73	-28	> 0.05	3.5	0.53	11	3.4	-69	**< 0.05**	
12-HEPE	3.1	0.36	10	1.3	-69	**< 0.001**	3.4	0.55	4.7	0.29	-28	> 0.05	
5-HEPE	0.50[#]	-	0.67	0.020	-26	**< 0.01**	0.50[#]	-	0.73	0.058	-31	**< 0.001**	> 0.05
13-HODE	210	17	300	17	-31	> 0.05	240	29	470	97	-49	**< 0.05**	
9-HODE	220	19	290	21	-22	> 0.05	280	33	520	110	-47	**< 0.05**	
15-HETE	13	1.2	13	0.74	5.5	> 0.05	17	0.83	22	3.3	-23	> 0.05	
11-HETE	15	1.2	10	0.66	52	> 0.05	16	0.93	20	3.5	-17	> 0.05	
8-HETE	2.9	0.30	3.1	0.16	-9.1	> 0.05	3.3	0.14	4.3	0.37	-22	> 0.05	
12-HETE	48	8.6	99	12	-52	**< 0.05**	57	7.6	86	13	-34	> 0.05	
9-HETE	2.5[#]	-	2.5[#]	-		> 0.05	2.8	0.11	3.6	0.3	-23	**< 0.05**	

Tab. 11.5 continued

	LPS		Vehicle		Δ (%)[a]	p LPS vs. vehicle	CLP		Sham		Δ (%)[a]	p CLP vs. Sham	p LPS vs. CLP[b]
	Mean	SE	Mean	SE			Mean	SE	Mean	SE			
	c (fmol/mg)												
15-HETrE	4.5	0.43	5.8	0.37	-22	> 0.05	5.3	0.48	5.7	0.64	-6.3	> 0.05	
5-HETE	6.2	0.45	8.3	0.38	-25	> 0.05	11	0.58	16	1.6	-32	**< 0.01**	
18-HEPE	0.45	0.034	0.57	0.021	-20	> 0.05	0.61	0.046	0.72	0.080	-15	> 0.05	
20-HEPE	1.4	0.067	1.0	0.055	37	**< 0.01**	0.92	0.086	0.64	0.061	44	**< 0.05**	**< 0.001**
20-HDHA	3.8	0.19	4.5	0.31	-15	> 0.05	5.3	0.16	6.4	0.55	-18	> 0.05	
16-HDHA	1.8	0.078	2.0	0.12	-11	> 0.05	2.3	0.10	2.7	0.27	-16	> 0.05	
13-HDHA	3.7	0.27	4.3	0.36	-14	> 0.05	4.5	0.19	5.3	0.52	-15	> 0.05	
17-HDHA	7.3	0.93	14	2.8	-49	**< 0.05**	8.5	0.77	9.3	0.79	-9.0	> 0.05	
10-HDHA	1.2	0.094	1.8	0.095	-34	**< 0.01**	1.7	0.056	2.1	0.14	-19	> 0.05	
14-HDHA	16	2.6	39	4.3	-59	**< 0.001**	16	2.3	23	2.4	-29	> 0.05	
11-HDHA	1.2	0.090	1.7	0.10	-28	> 0.05	1.7	0.074	2.3	0.21	-23	**< 0.05**	
7-HDHA	1.0	0.038	1.3	0.074	-24	> 0.05	1.5	0.065	1.9	0.20	-22	> 0.05	
8-HDHA	4.6	0.18	5.2	0.23	-11	> 0.05	6.1	0.19	7.3	0.70	-17	> 0.05	
4-HDHA	3.9	0.16	5.3	0.32	-27	> 0.05	6.2	0.39	7.7	0.71	-20	> 0.05	
9,12,13-TriHOME	20	2.3	19	1.2	8.2	> 0.05	16	1.3	25	3.0	-38	**< 0.05**	
9,10,13-TriHOME	3.7	0.38	3.2	0.09	17	> 0.05	3.0	0.13	4.7	0.48	-35	> 0.05	
13-oxo-ODE	2.5	0.078	2.4	0.14	5.6	> 0.05	2.0	0.25	3.5	0.72	-42	> 0.05	
15-oxo-ETE	2.4	0.28	3.1	0.14	-22	> 0.05	3.9	0.091	4.9	0.60	-21	> 0.05	
9-oxo-ODE	29	1.8	31	1.6	-6.0	> 0.05	27	3.0	48	8.0	-42	> 0.05	
5-oxo-ETE	2.6	0.21	3.3	0.29	-21	> 0.05	4.3	0.13	5.5	0.80	-22	> 0.05	

Tab. 11.5 continued

	LPS		Vehicle		Δ (%)[a]	p LPS vs. vehicle	CLP		Sham		Δ (%)[a]	p CLP vs. Sham	p LPS vs. CLP[b]
	Mean	SE	Mean	SE			Mean	SE	Mean	SE			
							c (fmol/mg)						
5-oxo-ETE	2.6	0.21	3.3	0.29	-21	> 0.05	4.3	0.13	5.5	0.80	-22	> 0.05	
EKODE	31	2.2	38	1.8	-20	> 0.05	32	3.8	48	3.1	-33	> 0.05	
15,16-DiHODE	50	3.5	66	6.5	-25	> 0.05	37	4.3	120	30	-69	**< 0.01**	
9,10-DiHODE	1.5	0.087	2.2	0.33	-30	> 0.05	1.5	0.27	4.1	1.3	-63	> 0.05	
17,18-DiHETE	2.4	0.10	1.6	0.11	46	**< 0.01**	3.1	0.16	1.8	0.16	75	**< 0.001**	**< 0.01**
12,13-DiHOME	39	2.9	47	6.2	-16	> 0.05	46	8.2	72	17	-35	> 0.05	
9,10-DiHOME	30	1.1	37	5.2	-18	> 0.05	42	6.5	45	8.0	-6.8	> 0.05	
19,20-DiHDPE	21	1.6	12	0.63	78	**< 0.001**	20	1.1	13	1.6	51	**< 0.01**	> 0.05
14,15-DiHETrE	2.0	0.094	1.7	0.080	20	> 0.05	2.3	0.13	1.7	0.13	32	**<0.05**	
16,17-DiHDPE	1.1	0.035	1.0	0.063	10	> 0.05	1.1	0.061	1.0	0.082	10	> 0.05	
11,12-DiHETrE	1.2	0.082	1.1	0.046	15	> 0.05	1.4	0.056	1.3	0.11	15	> 0.05	
13,14-DiHDPE	0.58	0.018	0.47	0.025	22	**< 0.01**	0.67	0.016	0.51	0.052	31	> 0.05	
10,11-DiHDPE	0.82	0.038	0.60	0.035	36	**< 0.05**	0.91	0.059	0.71	0.047	27	**<0.05**	
8,9-DiHETrE	2.5	0.22	1.6	0.039	57	**< 0.01**	2.7	0.15	2.0	0.22	33	> 0.05	
5,6-DiHETrE	1.7	0.18	1.4	0.067	19	> 0.05	2.1	0.23	1.7	0.21	21	> 0.05	
4,5-DiHDPE	9.7	1.1	5.7	0.25	70	**< 0.01**	6.4	0.39	5.0	0.67	29	> 0.05	
9,10-Dihydroxystearic acid	19	2.1	19	1.3	1.8	> 0.05	17	1.2	25	1.3	-32	**< 0.01**	
9(10)-EpODE	0.93	0.028	1.1	0.11	-14	> 0.05	0.69	0.13	1.5	0.32	-54	**< 0.05**	
12(13)-EpODE	0.49	0.023	0.63	0.080	-22	> 0.05	0.40	0.08	0.87	0.18	-54	**< 0.05**	
19(20)-EpDPE	7.2	0.44	8.3	0.44	-14	> 0.05	9.5	0.60	7.8	0.78	22	> 0.05	

Tab. 11.5 continued

	LPS		Vehicle		Δ (%)[a]	p LPS vs. vehicle	CLP		Sham		Δ (%)[a]	p CLP vs. Sham	p LPS vs. CLP[b]
	Mean	SE	Mean	SE			Mean	SE	Mean	SE			
	c (fmol/mg)												
12(13)-EpOME	32	2.7	32	3.9	0.78	> 0.05	24	3.2	35	5.4	-31	> 0.05	
14(15)-EpETrE	7.4	0.63	7.4	0.89	-0.35	> 0.05	8.0	0.56	11	1.6	-24	> 0.05	
9(10)-EpOME	34	2.4	34	3.7	2.1	> 0.05	26	3.1	39	6.5	-35	> 0.05	
15,16-DiHODE	2.0	0.13	3.2	0.24	-38	**< 0.05**	2.5	0.19	3.3	0.38	-25	> 0.05	
13(14)-EpDPE	2.2	0.13	3.4	0.24	-36	**< 0.05**	2.7	0.18	3.6	0.41	-24	> 0.05	
10(11)-EpDPE	2.7	0.13	4.1	0.28	-35	**< 0.05**	3.3	0.22	4.4	0.54	-25	> 0.05	
11(12)-EpETrE	9.3	0.62	10	1.0	-7.7	> 0.05	9.8	1.1	14	1.7	-30	> 0.05	
8(9)-EpETrE	4.2	0.28	4.4	0.36	-2.8	> 0.05	4.4	0.36	5.7	0.73	-22	> 0.05	
5(6)-EpETrE	22	1.6	22	1.8	-1.6	> 0.05	26	2.0	31	3.7	-17	> 0.05	
15(16)-EpODE	2.0	0.087	5.0	0.47	-60	> 0.05	1.9	0.26	6.0	1.6	-68	**< 0.05**	
9(10)-Epoxystearic acid	33	3.3	33	3.1	-0.34	> 0.05	26	3.2	24	1.5	11	> 0.05	

[#] Limit of quantification (LOQ).
[a] The relative change (% Δ) of treatment in comparison to the control is calculated as $\% \Delta = 100 \times (c_{treatment}-c_{control})/c_{control}$.
[b] p value for LPS vs. CLP is only shown, if both treatment groups significantly differ from each control.

Tab. 11.6 Lung tissue concentration of oxylipins (>LOQ) 24 h after induction of sepsis by i. p. LPS injection or CLP survery. Statistical differences were determined by one-way ANOVA followed by Tukeys post-test test (*p<0.05, **p<0.01, ***p<0.001).

	LPS		Vehicle		Δ (%)[a]	p LPS vs. vehicle	CLP		Sham		Δ (%)[a]	p CLP vs. Sham	p LPS vs. CLP[b]
	Mean	SE	Mean	SE			Mean	SE	Mean	SE			
	c (fmol/mg)												
6-keto-$PGF_{1\alpha}$	12000	1300	13000	1500	-8.3	> 0.05	15000	2600	18000	2400	-17	> 0.05	
TXB_2	450	80	600	79	-26	> 0.05	400	110	700	160	-43	> 0.05	
PGE_3	41	11	37	6.8	12	> 0.05	24	7.6	25	5.3	-4.0	> 0.05	
PGD_3	8.3	1.7	9.2	1.7	-10	> 0.05	6.0	1.8	5.4	0.93	10	> 0.05	
$PGF_{2\alpha}$	900	210	1700	330	-46	> 0.05	1300	420	2200	500	-39	> 0.05	
PGE_2	3700	800	4400	800	-17	> 0.05	3400	960	5200	1000	-35	> 0.05	
PGE_1	840	210	930	180	-9.3	> 0.05	580	190	810	200	-29	> 0.05	
PGD_1	130	30	150	29	-13	> 0.05	110	30	123	22	-11	> 0.05	
PGD_2	1100	250	1300	260	-17	> 0.05	1100	310	1400	270	-23	> 0.05	
5-$iPF_{2\alpha}$	1.1[#]	-	1.6	0.15	-30	> 0.05	2.3	0.72	2.1	0.50	12	> 0.05	
1a,1b-dihomo-$PGF_{2\alpha}$	250	66	310	62	-18	> 0.05	230	71	240	58	-1.7	> 0.05	
13,14-dihydro-15-keto-$PGF_{2\alpha}$	120	13	150	30	-19	> 0.05	150	25	210	50	-28	> 0.05	
TxB_3	8.1	1.3	7.7	1.0	4.4	> 0.05	5.2	1.3	5.1	0.82	1.0	> 0.05	
TxB_1	12	2.6	17	2.6	-31	> 0.05	9.2	2.3	14	3.2	-34	> 0.05	
$PGF_{1\alpha}$	120	32	200	38	-37	> 0.05	130	41	190	45	-32	> 0.05	
13,14-dihydro-15-keto-PGE_1	48	7.1	49	15	-1.4	> 0.05	53	15	83	30	-36	> 0.05	
9-HOTrE	20	3.4	16	2.8	26	> 0.05	8.0	1.6	13	2.8	-38	> 0.05	
13-HOTrE	63	14	88	23	-29	> 0.05	17	3.0	62	22	-73	> 0.05	
20-HETE	12	1.8	2.8[#]	-	330	**< 0.001**	4.4	0.56	2.8[#]	-	57	> 0.05	
15-HEPE	16	2.6	16	2.4	-3	> 0.05	10	2.0	14	2	-26	> 0.05	

Tab. 11.6 continued

	LPS		Vehicle		Δ (%)[a]	p LPS vs. vehicle	CLP		Sham		Δ (%)[a]	p CLP vs. Sham	p LPS vs. CLP[b]
	Mean	SE	Mean	SE			Mean	SE	Mean	SE			
	c (fmol/mg)												
12-HEPE	590	230	1300	260	-53	> 0.05	180	170	850	290	-56	> 0.05	
5-HEPE	3.8	0.77	1.9	0.33	100	**< 0.05**	1.3	0.31	1.7	0.27	-25	> 0.05	
13-HODE	7800	1400	6600	980	18	> 0.05	3700	688	5000	940	-26	> 0.05	
9-HODE	9100	1700	7400	1100	24	> 0.05	4500	849	5600	960	-20	> 0.05	
15-HETE	930	130	940	110	-0.96	> 0.05	1100	199	1200	140	-10	> 0.05	
11-HETE	1400	190	1500	180	-10	> 0.05	1500	280	1800	220	-16	> 0.05	
8-HETE	33	7.2	52	4.6	-36	> 0.05	29	8.4	63	15	-54	> 0.05	
12-HETE	5600	1400	9800	950	-43	> 0.05	4700	1669	11000	2800	-56	> 0.05	
9-HETE	12	1.3	12	1.0	2.3	> 0.05	13	1.3	18	2.4	-23	> 0.05	
15-HETrE	390	72	420	59	-7.8	> 0.05	320	72	370	63	-14	> 0.05	
5-HETE	100	21	49	10	110	> 0.05	51	11	81	15	-37	> 0.05	
18-HEPE	8.1	1.4	8.1	1.2	0.64	> 0.05	6.4	1.3	5.8	0.72	10	> 0.05	
20-HEPE	1.4	0.25	1.0	0.12	50	> 0.05	0.80	0.17	0.68	0.06	18	> 0.05	
20-HDHA	62	7.6	51	5.2	22	> 0.05	60	10	47	4.6	28	> 0.05	
16-HDHA	45	4.4	37	4.9	22	> 0.05	36	5.5	32	4.1	14	> 0.05	
13-HDHA	270	36	280	34	-4.4	> 0.05	240	39	190	22	23	> 0.05	
17-HDHA	110	22	160	30	-28	> 0.05	89	19	130	32	-31	> 0.05	
10-HDHA	39	14	84	16	-53	> 0.05	26	10	70	27	-63	> 0.05	
14-HDHA	1800	680	4200	780	-56	> 0.05	1200	507	3400	1300	-65	> 0.05	
11-HDHA	3.0	0.29	2.3	0.15	27	> 0.05	2.6	0.29	2.4	0.34	9.1	> 0.05	

Tab. 11.6 continued

	LPS		Vehicle		Δ (%)[a]	p LPS vs. vehicle	CLP		Sham		Δ (%)[a]	p CLP vs. Sham	p LPS vs. CLP[b]
	Mean	SE	Mean	SE			Mean	SE	Mean	SE			
							c (fmol/mg)						
7-HDHA	4.3	0.72	1.9	0.29	130	**< 0.05**	2.1	0.45	2.2	0.41	-5.0	> 0.05	
8-HDHA	8.1	1.0	6.9	0.75	19	> 0.05	8.6	1.0	6.9	0.65	24	> 0.05	
4-HDHA	6.9	0.80	4.7	0.36	47	> 0.05	7.3	0.72	4.9	0.58	48	> 0.05	
9,12,13-TriHOME	76	13	59	8.2	28	> 0.05	41	6.3	72	17	-44	> 0.05	
9,10,13-TriHOME	15	1.7	9.9	1.1	49	> 0.05	7.9	1.2	8.7	1.3	-9.2	> 0.05	
13-oxo-ODE	5.6	1.0	4.6	0.58	22	> 0.05	3.8	0.7	4.0	0.7	-6.1	> 0.05	
15-oxo-ETE	22	3.2	20	3.8	12	> 0.05	35	6.6	33	5.6	8.0	> 0.05	
9-oxo-ODE	200	40	150	24	36	> 0.05	84	14	94	20	-10	> 0.05	
5-oxo-ETE	6.1	1.2	4.4	0.47	37	> 0.05	10	1.4	7.0	1.3	42	> 0.05	
EKODE	40	12	24	2.8	64	> 0.05	40	8.9	27	5.3	51	> 0.05	
15,16-DiHODE	13	2.9	12	2.4	3.5	> 0.05	4.6	0.8	11.0	2.6	-58	> 0.05	
8,15-DiHETE	4.1	0.9	5.4	0.8	-25	> 0.05	3.8	0.5	8.6	1.8	-56	**< 0.05**	
9,10-DiHODE	5.7	1.2	1.9	0.34	210	**< 0.01**	1.6	0.25	1.8	0.34	-11	> 0.05	
5,15-DiHETE	4.7	1.0	2.4	0.47	94	> 0.05	2.4	0.44	4.7	0.95	-50	> 0.05	
17,18-DiHETE	1.6	0.29	1.4	0.19	20	> 0.05	1.2	0.25	1.3	0.21	-8.1	> 0.05	
12,13-DiHOME	100	20	49	10	120	**< 0.05**	46	7.4	36	6.1	25	> 0.05	
9,10-DiHOME	99	16	32	5.8	210	**< 0.001**	47	7.2	26	3.4	84	> 0.05	
19,20-DiHDPE	63	10	39	6.2	59	> 0.05	45	11.0	41	6.8	10	> 0.05	
14,15-DiHETrE	9.8	1.6	7.5	1.3	32	> 0.05	12	2.4	11	1.8	4.5	> 0.05	
16,17-DiHDPE	3.7	0.59	3.1	0.55	22	> 0.05	3.0	0.60	3.6	0.81	-15	> 0.05	

Tab. 11.6 continued

	LPS		Vehicle		Δ (%)[a]	p LPS vs. vehicle	CLP		Sham		Δ (%)[a]	p CLP vs. Sham	p LPS vs. CLP[b]
	Mean	SE	Mean	SE			Mean	SE	Mean	SE			
	c (fmol/mg)												
11,12-DiHETrE	8.7	1.2	6.7	1.1	29	> 0.05	9.9	1.9	10.8	2.0	-8.4	> 0.05	
13,14-DiHDPE	3.4	0.32	1.8	0.38	87	> 0.05	2.8	0.46	2.3	0.60	25	> 0.05	
10,11-DiHDPE	2.8	0.38	1.3	0.19	120	**< 0.05**	2.3	0.44	1.7	0.26	36	> 0.05	
8,9-DiHETrE	11	1.6	4.9	0.74	120	**< 0.05**	9.1	1.5	8.8	1.3	3.2	> 0.05	
5,6-DiHETE	0.91	0.22	0.50	0.12	84	> 0.05	0.39	0.06	0.8	0.22	-53	> 0.05	
7,8-DiHDPE	2.6	0.39	1.1	0.0080	140	**< 0.01**	1.6	0.27	1.3	0.093	24	> 0.05	
5,6-DiHETrE	1.8	0.18	0.78	0.079	130	**< 0.001**	1.2	0.12	1.1	0.12	8.1	> 0.05	
4,5-DiHDPE	14	2.2	5.1	0.58	170	**< 0.001**	5.0	0.65	3.2	0.28	56	> 0.05	
9,10-Dihydroxy-stearic acid	29	2.0	33	3.6	-13	> 0.05	35	5.8	41	3.9	-14	> 0.05	
9(10)-EpODE	1.3	0.36	1.0	0.15	27	> 0.05	0.76	0.13	1.0	0.13	-24	> 0.05	
17(18)-EpETE	0.93	0.19	0.59	0.016	56	> 0.05	0.77	0.15	0.6	0.044	25	> 0.05	
12(13)-EpODE	0.92	0.22	0.60	0.084	53	> 0.05	0.39	0.052	0.51	0.066	-25	> 0.05	
14(15)-EpETE	0.52	0.12	0.40	0.039	29	> 0.05	0.63	0.11	0.43	0.044	47	> 0.05	
19(20)-EpDPE	20	3.9	10	1.1	93	> 0.05	17	3.7	11.7	1.3	48	> 0.05	
12(13)-EpOME	45	10	33	3.8	39	> 0.05	32	5.7	34	3.4	-7.8	> 0.05	
14(15)-EpETrE	30	8.0	26	1.8	17	> 0.05	55	9.8	44	4.0	26	> 0.05	
9(10)-EpOME	38	9.6	30	3.5	29	> 0.05	30	5.6	32	3.1	-8.5	> 0.05	
16(17)-EpDPE	6.0	1.5	3.9	0.40	52	> 0.05	7.4	1.5	5.2	0.47	41	> 0.05	
13(14)-EpDPE	5.8	1.5	3.9	0.41	47	> 0.05	7.4	1.5	5.3	0.45	39	> 0.05	

Tab. 11.6 continued

	LPS		Vehicle		Δ (%)[a]	$p_{LPS\ vs.\ vehicle}$	CLP		Sham		Δ (%)[a]	$p_{CLP\ vs.\ Sham}$	$p_{LPS\ vs.\ CLP}$[b]
	Mean	SE	Mean	SE			Mean	SE	Mean	SE			
							c (fmol/mg)						
10(11)-EpDPE	8.4	2.0	5.4	0.58	56	> 0.05	9.5	1.9	7.2	0.65	33	> 0.05	
11(12)-EpETrE	37	8.6	31	2.2	18	> 0.05	62	10	53	4.3	17	> 0.05	
8(9)-EpETrE	21	6.6	22	3.0	-3.0	> 0.05	27	5.5	41	12	-33	> 0.05	
5(6)-EpETrE	62	9.5	30	2.8	100	**< 0.05**	68	11	55	3.8	24	> 0.05	
15(16)-EpODE	9.8	2.5	13	2.9	-23	> 0.05	3.7	0.62	10	2.6	-65	> 0.05	
9(10)-Epoxy-stearic acid	97	10	66	2.9	47	> 0.05	91	21	59	4.2	56	> 0.05	

[#] Limit of quantification (LOQ).

[a] The relative change (% Δ) of treatment in comparison to the control is calculated as $\% \Delta = 100 \times (c_{treatment}-c_{control})/c_{control}$.

[b] p value for LPS vs. CLP is only shown, if both treatment groups significantly differ from each control.

Chapter 8

Tab. 11.7: Oxylipin concentrations in plasma 24 h after LPS treatment.

COXi	-			-			Celecoxib			Apigenin			Genistein			Resveratrol			ε-viniferin	
LPS	-			+			+			+			+			+			+	
Analyte (nM)	**Mean**	**SE**		**Mean**	**SE**		**Mean**	**SE**		**Mean**	**SE**		**Mean**	**SE**		**Mean**	**SE**		**Mean**	**SE**
TXB_2	2.4	0.67		1.9	0.73		0.80	0.191		1.1	0.25		2.6	0.77		1.1	0.075		4.2	0.75
PGE_2	0.33*	0.19		1.6	0.23		0.079†	0.016		1.3	0.36		0.95	0.28		3.5†	0.52		1.6	0.50
6-keto-$PGF_{1\alpha}$	< 0.45	-		1.8	0.18		< 0.45	-		2.1	0.22		2.4	0.31		2.5	0.30		2.8	0.67
$PGF_{2\alpha}$	0.40	0.023		0.44	0.030		0.35	-		0.42	0.059		0.44	0.051		0.51	0.050		0.77‡	0.10
PGD_2	< 0.50	-		< 0.50	-		< 0.50	-		< 0.50	-		< 0.50	-		< 0.50	-		0.90	0.13
5-$iPF_{2\alpha}$	< 0.50	-		< 0.50	-		0.63	0.078		< 0.50	-		< 0.50	-		< 0.50	-		0.91‡	0.12
1a,1b-dihomo-$PGF_{2\alpha}$	0.20	0.020		0.22	0.013		0.28	0.043		0.27	0.018		0.33	0.054		0.21	0.021		0.42†	0.061
13,14dihydro-15-keto-$PGF_{2\alpha}$	0.30*	0.062		0.64	0.015		0.13†	0.033		0.41	0.12		0.43	0.091		0.70	0.046		2.1‡	0.23
$PGF_{1\alpha}$	0.11	0.015		0.10	0.017		0.073	0.013		0.10	0.025		0.13	0.032		0.088	0.011		0.25‡	0.029
13,14-dihydro-15-keto-PGE_1	< 0.05	-		0.17	0.025		< 0.050	-		0.14	0.022		0.18	0.037		0.22	0.0087		0.34†	0.066
8-$iPF_{2\alpha}$	0.10	0.015		0.17	0.0079		0.19	0.052		0.19	0.021		0.24	0.049		0.16	0.0053		0.30*	0.037
9-HOTrE	33	8.1		15	7.8		7.5	1.5		6.1	1.6		4.1	0.50		3.6	0.28		12	8.1
13-HOTrE	44	11		25	11		18	4.5		5.7	0.82		15	5.2		11	2.4		61	32
20-HETE	1.3	0.013		1.4	0.039		1.7	0.22		1.6	0.18		1.7	0.12		1.5	0.11		2.7‡	0.19
15-HEPE	< 0.63	-		0.68	0.028		0.88	0.14		0.63	-		0.96	0.21		0.63	-		1.5‡	0.30
8-HEPE	< 0.31	-		0.46	0.042		0.65	0.17		0.31	-		0.72	0.21		0.56	0.16		1.2†	0.22
12-HEPE	20	7.6		59	10		130	49		25	12		140	61		75	24		240†	50
5-HEPE	0.34	0.017		0.37	0.017		0.25	-		0.27	0.0091		0.33	0.021		0.29	0.014		0.25*	-
13-HODE	490	83		300	95		260	51		110*	15		240	66		150	24		540	180
9-HODE	290	52		170	61		109	15		83	13		96	16		73	3.0		210	85
15-HETE	2.6	0.45		4.0	0.32		3.9	0.90		2.5	0.27		5.1	1.3		3.4	0.39		7.9†	1.2
11-HETE	1.5*	0.24		2.6	0.16		1.5	0.30		1.8	0.12		2.7	0.39		2.8	0.20		3.8*	0.50
8-HETE	2.7	0.49		4.9	0.52		8.5	2.3		3.1	0.76		9.6	3.4		5.1	1.2		12*	1.5

Tab. 11.7 continued

COXi	-		-		Celecoxib		Apigenin		Genistein		Resveratrol		ε-viniferin	
LPS	-		+		+		+		+		+		+	
Analyte (nM)	**Mean**	**SE**	**Mean**	**SE**	**Mean**	**SE**	**Mean**	**SE**	**Mean**	**SE**	**Mean**	**SE**	**Mean**	**SE**
12-HETE	230	60	480	60	1100	350	260	100	1200	490	520	132	1700†	210
15-HETrE	0.84	0.16	1.6	0.18	2.2	0.61	0.94	0.17	2.7	0.85	1.7	0.31	5.7‡	1.14
5-HETE	2.4	0.24	3.1	0.15	2.4	0.30	2.4	0.30	3.1	0.17	2.8	0.10	2.8	0.16
20-HEPE	2.0*	0.22	3.6	0.24	1.8†	0.44	1.7*	0.22	2.8	0.27	2.7	0.48	5.7†	0.75
18-HEPE	0.41	0.043	0.52	0.035	0.32	0.061	0.26	0.024	0.45	0.026	0.44	0.049	0.81	0.35
20-HDHA	1.9	0.36	3.1	0.27	3.0	0.67	2.2	0.19	3.7	0.77	2.2	0.12	3.6	0.15
16-HDHA	0.78*	0.18	1.6	0.14	1.1	0.25	1.0	0.062	1.9	0.33	1.1	0.10	1.1	0.068
13-HDHA	0.72	0.18	1.7	0.17	2.3	0.68	0.98	0.13	2.8	1.0	1.7	0.32	3.9*	0.68
17-HDHA	4.2	1.24	10	1.4	21	7.2	5.2	1.2	21	11	12	3.8	39†	7.1
10-HDHA	2.3	0.74	6.8	1.1	16	5.5	3.0	1.1	16	7.8	9.7	3.2	27†	5.4
14-HDHA	56	20	170	28	470	170.0	71	30	450	240	270	94	800†	170
11-HDHA	0.53	0.10	0.92	0.084	1.0	0.23	0.67	0.046	1.2	0.36	0.61	0.051	0.91	0.089
7-HDHA	0.41	0.064	0.62	0.044	0.52	0.11	0.47	0.045	0.64	0.11	0.35	0.024	0.55	0.042
8-HDHA	2.4	0.28	3.6	0.21	3.8	0.62	3.0	0.17	4.0	0.63	2.9	0.13	3.8	0.19
4-HDHA	1.1	0.20	1.7	0.16	1.9	0.45	1.3	0.096	2.0	0.35	1.1	0.029	1.7	0.070
9,12,13-TriHOME	18	2.0	14	2.2	22	4.2	38	20	9.6	2.6	11	2.7	17	7.1
9,10,13-TriHOME	3.2	0.28	2.5	0.29	2.7	0.24	3.3	1.2	1.5	0.30	1.6	0.24	2.2	0.54
13-oxo-ODE	11	1.9	7.1	2.2	2.7	0.62	2.5	0.34	2.7	0.24	2.7	0.12	8.3	3.1
15-oxo-ETE	0.35	0.05	0.39	0.024	0.39	0.089	0.29	0.033	0.42	0.068	0.28	0.013	0.34	0.023
9-oxo-ODE	42	5.8	31	9.0	18	2.9	16	2.7	16	1.7	16	0.89	38	16
5-oxo-ETE	3.4	0.65	2.8	0.28	< 1.0	-	< 1.0	-	1.2	0.13	1.0	-	4.7	0.71
EKODE	9.3	1.4	11	1.0	12	2.1	7.0	0.73	9.9	1.1	11	1.6	16	3.4
9(10)-EpODE	4.3	0.73	5.5	0.41	2.6*	0.99	2.2*	0.31	3.5	0.50	2.2*	0.17	6.5	0.18

Tab. 11.7 continued

COXi	-		-		Celecoxib		Apigenin		Genistein		Resveratrol		ε-viniferin	
LPS	-		+		+		+		+		+		+	
Analyte (nM)	**Mean**	**SE**	**Mean**	**SE**	**Mean**	**SE**	**Mean**	**SE**	**Mean**	**SE**	**Mean**	**SE**	**Mean**	**SE**
17(18)-EpETE	0.70†	0.14	1.4	0.085	0.66†	0.076	0.68*	0.12	1.2	0.28	1.1	0.073	1.1	0.056
12(13)-EpODE	6.7	0.64	4.6	1.4	1.8	0.51	1.8	0.38	1.8	0.18	1.4	0.042	3.3	0.024
14(15)-EpETE	0.25	0.045	0.30	0.019	0.13	-	0.14†	0.0065	0.21	0.021	0.16*	0.0085	0.18*	0.015
19(20)-EpDPE	6.8†	1.5	14	1.0	10	0.96	9.4	1.1	14	1.8	13	1.1	13	0.90
12(13)-EpOME	70	4.1	60	10.13	24†	6.8	29*	5.3	34	3.3	23†	1.1	48	1.7
14(15)-EpETrE	2.6	0.36	2.8	0.11	1.2†	0.40	1.5*	0.12	2.0	0.19	1.5*	0.089	2.4	0.21
9(10)-EpOME	36	7.3	50	2.3	24*	8.1	24*	3.2	37	5.0	24*	1.1	61	1.7
16(17)-EpDPE	1.8	0.40	2.6	0.096	1.3	0.53	1.2	0.042	2.1	0.36	1.3	0.061	2.8	0.21
13(14)-EpDPE	1.7	0.39	2.4	0.099	1.3	0.53	1.2	0.036	2.0	0.34	1.3	0.071	2.9	0.23
10(11)-EpDPE	2.4	0.56	3.5	0.14	2.0	0.74	1.7	0.077	3.0	0.58	1.9	0.11	3.9	0.30
11(12)-EpETrE	3.6	0.51	3.4	0.14	1.7*	0.57	2.0	0.13	2.7	0.37	1.7	0.028	2.6	0.25
8(9)-EpETrE	1.9	0.31	2.4	0.15	2.0	0.55	1.5	0.21	2.3	0.31	1.7	0.19	2.5	0.27
5(6)-EpETrE	8.3	1.3	10	0.24	6.9	1.3	6.8	1.2	8.9	0.91	7.0	0.088	11	0.85
15(16)-EpODE	1.7	0.39	2.4	0.099	1.3	0.53	1.2	0.036	2.0	0.34	1.3	0.071	2.9	0.23
9(10)-Epoxy-stearic acid	26	3.7	29	1.2	23	6.1	18	1.8	31	4.9	17	0.93	37	1.1
15,16-DiHODE	44	3.8	39	4.1	43	5.8	24	4.9	40	8.4	26	1.8	53	5.8
9,10-DiHODE	7.2	0.94	6.5	1.1	3.9	0.38	4.0	0.84	4.8	1.1	3.4	0.43	4.5	0.34
12,13-DiHODE	9.7	1.3	7.5	1.4	4.1	0.53	4.5	1.1	4.7	1.5	3.6	0.78	2.8	0.20
17,18-DiHETE	1.2†	0.12	2.3	0.16	0.79‡	0.18	1.2*	0.11	2.3	0.39	1.8	0.31	1.8	0.37
14,15-DiHETE	0.26*	0.029	0.46	0.031	< 0.13	-	0.19†	0.020	0.41	0.11	0.32	0.079	0.36	0.026
11,12-DiHETE	< 0.13	-	0.22	0.016	< 0.13	-	< 0.13	-	0.19	0.030	0.17	0.022	0.38‡	0.062
12,13-DiHOME	180	18	230	16	110*	8.0	110	17	210	69	130	22	110*	7.3
9,10-DiHOME	46	5.0	56	3.8	33	2.9	34	4.3	63	17	36	3.4	30	1.7

Tab. 11.7 continued

COXi	-			+			+			+			+			+		
LPS	-			+			+			+			+			+		
Analyte (nM)	Mean	SE		Mean	SE		Mean	SE		Mean	SE		Mean	SE		Mean	SE	
19,20-DiHDPE	7.6†	1.4		17	1.4		6.1‡	1.2		11	0.87		19	2.8		14	2.0		14	1.8	
14,15-DiHETrE	2.2*	0.33		4.4	0.39		1.1‡	0.20		2.2	0.32		4.3	1.3		2.8	0.66		2.5	0.24	
16,17-DiHDPE	1.1†	0.17		2.4	0.20		0.76‡	0.12		1.2*	0.13		2.2	0.52		1.7	0.37		1.1†	0.078	
11,12-DiHETrE	1.0†	0.15		2.1	0.18		0.83†	0.21		1.1*	0.12		1.9	0.41		1.4	0.29		2.0	0.17	
13,14-DiHDPE	0.50†	0.073		1.0	0.076		0.39‡	0.072		0.58*	0.062		0.96	0.18		0.73	0.14		0.55*	0.048	
10,11-DiHDPE	0.49‡	0.065		1.0	0.080		0.40‡	0.064		0.58*	0.0671		0.90	0.16		0.66	0.11		0.62*	0.054	
8,9-DiHETrE	1.5*	0.17		2.3	0.15		1.3†	0.22		1.4	0.16		2.1	0.29		1.6	0.20		2.5	0.15	
7,8-DiHDPE	0.74	0.055		1.1	0.076		0.67*	0.12		0.64	0.042		1.1	0.16		0.71	0.091		1.1	0.11	
5,6-DiHETrE	0.59	0.047		0.71	0.039		0.61	0.082		0.62	0.10		0.72	0.063		0.65	0.021		1.3‡	0.12	
4,5-DiHDPE	3.9	0.59		7.5	0.60		12	1.4		7.8	1.1		10	1.3		8.6	0.58		23‡	3.9	
9,10-Dihydroxy-stearic acid	18	1.8		11	1.3		32†	5.4		47‡	7.4		15	2.3		20	4.4		10	1.2	

If analyte concentration is below the limit of quantification (LOQ), it is indicated as <. The given value represents the LOQ.

* p <0.05 Dunnetts test vs. LPS

† p <0.01 Dunnetts test vs. LPS

‡ p <0.001 Dunnetts test vs. LPS

Tab. 11.8: Oxylipin concentrations in kidney tissue 24 h after LPS treatment.

COXi	-		-		Celecoxib		Apigenin		Genistein		Resveratrol		ε-viniferin	
LPS	-		+		+		+		+		+		+	
Analyte (fmol/mg)	Mean	SE	Mean	SE	Mean	SE	Mean	SE	Mean	SE	Mean	SE	Mean	SE
TXB_2	1.5	0.24	1.5	0.19	1.3	0.22	2.0	0.12	3.2*	0.21	3.8†	0.56	4.9‡	0.66
$PGF_{2\alpha}$	21	2.7	30	3.3	15	2.8	33	2.4	40	4.1	70‡	11	63‡	5.2
PGE_2	55	8.5	81	13	45	8.7	110	19	110	23	210‡	36	110	20
6-keto-$PGF_{1\alpha}$	31	3.4	41	4.3	36	8.7	55	3.4	61	7.2	80*	14	108‡	12
$PGF_{2\alpha}$	21	2.7	30	3.3	15	2.8	33	2.4	40	4.1	70	11	63	5.2
PGE_1	2.0	0.33	5.0	0.73	2.5	0.42	4.7	0.49	6.3	1.4	11†	2.1	8.3	1.0
PGD_1	< 0.50	-	< 0.5	-	< 0.50	-	< 0.50	-	< 0.50	-	0.72	0.093	0.84†	0.12
PGD_2	8.4	1.2	9.0	1.4	7.4	1.0	13	1.6	9.6	1.4	20†	3.0	19†	3.4
5-i$PF_{2\alpha}$	< 1.0	-	< 1.0	-	< 1.0	-	< 1.0	-	< 1.0	-	< 1.0	-	1.5‡	0.18
1a,1b-dihomo-$PGF_{2\alpha}$	0.57*	0.11	1.7	0.29	0.54*	0.16	1.3	0.19	1.9	0.28	3.9‡	0.50	3.2†	0.39
13,14-dihydro-15-keto-$PGF_{2\alpha}$	1.8	0.17	2.3	0.19	0.72†	0.14	2.7	0.18	3.1	0.12	4.3‡	0.50	4.6‡	0.50
$PGF_{1\alpha}$	1.8*	0.21	3.4	0.48	1.4†	0.23	2.8	0.40	3.7	0.38	6.2†	0.65	7.7‡	0.44
13,14-dihydro-15-keto-PGE_1	0.22	0.038	0.44	0.049	< 0.1	-	0.41	0.046	0.5	0.13	0.6	0.10	0.49	0.042
8-iPF_{2a}	1.2	0.089	1.5	0.16	1.2	0.17	1.8	0.16	2.0	0.09	3.2‡	0.37	2.7†	0.31
9-HOTrE	6.6	1.3	4.1	0.44	4.3	0.40	3.2	0.49	5.0	0.75	3.9	0.46	5.8	0.22
13-HOTrE	8.4*	1.4	4.5	0.35	5.2	0.51	3.3	0.51	6.0	1.1	3.6	0.61	6.0	0.45
20-HETE	< 2.7	-	< 2.7	-	< 2.7	-	< 2.7	-	< 2.7	-	< 2.7	-	3.6*	0.48
12-HEPE	3.7	1.2	1.8	0.46	2.9	0.85	1.1	0.093	2.2	0.66	2.1	0.55	5.0	1.2
5-HEPE	0.87	0.038	0.92	0.082	1.5‡	0.13	1.0	0.11	1.3	0.088	1.1	0.12	1.1	0.036
13-HODE	170	27	170	23	140	14	120	18	230	35	270	43	310†	20
9-HODE	160	23	200	28	160	17	150	24	280	46	350*	52	380†	33
15-HETE	18	1.5	21	1.5	19	1.1	22	1.6	31*	2.5	38‡	2.9	30*	2.1
11-HETE	9.8	1.1	13	1.2	10	1.2	16	1.8	18	1.6	31‡	3.1	22†	3.1

Tab. 11.8 continued

COXi	-			+		Celecoxib		Apigenin		Genistein		Resveratrol		ε-viniferin	
LPS	-		+			+		+		+		+		+	
Analyte (fmol/mg)	Mean	SE	Mean	SE	Mean	SE	Mean	SE	Mean	SE	Mean	SE	Mean	SE	Mean	SE
8-HETE	3.8	0.21	3.6	0.22	4.6	0.27	3.4	0.33	4.9	0.63	4.2	0.46	4.4	0.10		
12-HETE	43	16	17	3.2	29	9.6	10	0.91	21	4.4	24	6.6	47	11		
9-HETE	3.0	0.16	3.1	0.20	4.0*	0.16	3.5	0.24	4.3†	0.37	3.1	0.20	3.6	0.19		
15-HETrE	3.7	0.24	4.7	0.40	4.0	0.22	4.6	0.34	6.4	0.38	7.4‡	0.74	8.0‡	0.36		
5-HETE	10	0.72	9.9	0.90	16‡	0.60	12	1.2	15†	0.71	12	1.0	13	0.48		
20-HEPE	7.0	0.40	7.1	0.54	5.3	1.7	5.2	0.75	5.9	0.45	5.3	0.76	11	2.1		
18-HEPE	1.0	0.10	1.4	0.16	1.3	0.052	1.5	0.14	2.0*	0.19	1.3	0.092	1.5	0.11		
20-HDHA	13	1.3	18	1.7	18	0.82	18	1.7	25*	2.0	19	1.7	17	0.90		
16-HDHA	4.6†	0.29	7.0	0.57	6.1	0.45	6.3	0.46	9.1	0.78	6.9	0.65	4.9*	0.32		
13-HDHA	4.3†	0.30	6.7	0.43	6.0	0.52	6.9	0.45	9.1*	0.70	11‡	0.58	7.7	0.53		
17-HDHA	12	1.2	16	1.3	18	1.4	17	1.6	22	2.2	17	1.6	15	0.67		
10-HDHA	2.5	0.28	3.2	0.28	4.3	0.32	3.6	0.31	4.3	0.46	3.5	0.38	3.6	0.22		
14-HDHA	20	7.1	11	1.5	17	4.8	8.6	0.72	14	1.9	12	1.8	20	3.5		
11-HDHA	3.2	0.31	4.5	0.48	6.6*	0.38	5.7	0.69	7.7†	0.56	4.9	0.54	5.4	0.27		
7-HDHA	1.9	0.19	2.4	0.29	4.8‡	0.40	3.5	0.47	4.0*	0.40	2.7	0.28	2.7	0.10		
8-HDHA	11	0.71	13	1.2	24‡	1.0	20†	1.1	23‡	1.0	16	1.3	18*	0.61		
4-HDHA	14	1.4	17	2.6	21	1.1	19	0.94	28†	1.4	16	1.3	22	1.7		
9,12,13-TriHOME	44	11	50	12	24	2.1	27	3.5	24	1.2	45	5.5	69‡	27		
9,10,13-TriHOME	6.5	1.3	8.2	2.2	4.1	0.26	4.8	0.51	4.3	0.088	7.4	0.86	10	3.7		
13-oxo-ODE	3.7	0.43	7.4	1.3	9.2	0.88	8.5	1.5	11	1.7	6.1	1.2	8.3	0.24		
15-oxo-ETE	7.2	0.80	7.1	1.0	8.4	0.68	8.2	1.4	12*	1.3	7.5	1.0	9.3	0.64		
9-oxo-ODE	25	3.7	53	12	51	3.3	46	9.4	65	11	43	5.5	73	3.23		
5-oxo-ETE	24	3.4	27	2.7	31	1.4	28	3.3	45	5.3	17	3.2	24	2.9		

Tab. 11.8 continued

COXi	-		-		Celecoxib		Apigenin		Genistein		Resveratrol		ε-viniferin	
LPS	-		+		+		+		+		+		+	
Analyte (fmol/mg)	Mean	SE	Mean	SE	Mean	SE	Mean	SE	Mean	SE	Mean	SE	Mean	SE
EKODE	23	2.2	41	8.6	41	4.6	40	7.7	58	6.8	45	7.6	92‡	9.8
9(10)-EpODE	3.5	0.45	9.1	1.5	15	1.9	13	2.5	14	4.5	8.2	3.0	9.9	1.1
17(18)-EpETE	1.7	0.14	3.0	0.39	4.7	0.63	6.2‡	0.66	5.7†	0.56	2.5	0.66	2.4	0.25
12(13)-EpODE	1.6	0.19	4.2	0.72	6.4	0.80	6.0	1.2	8.1*	0.84	3.4	1.1	4.3	0.37
14(15)-EpETE	1.1	0.11	2.3	0.38	4.2*	0.56	5.4‡	0.54	4.7†	0.44	1.7	0.55	1.7	0.20
11(12)-EpETE	1.1*	0.10	2.5	0.45	3.5*	0.46	4.4	0.51	4.0	0.46	1.5	0.41	1.4	0.10
8(9)-EpETE	< 1.0	-	1.5	0.14	2.4*	0.30	2.9†	0.18	2.8†	0.37	< 1.0	-	1.2	0.079
19(20)-EpDPE	31	2.5	51	6.5	78*	7.7	92‡	4.1	88†	6.2	43	7.8	36	2.3
12(13)-EpOME	30	3.5	66	11	120†	12	110	15	120*	11	59	19	80	8.0
14(15)-EpETrE	28	2.7	31	4.0	57†	5.8	60†	4.3	57*	5.9	28	8.4	29	3.6
9(10)-EpOME	37	4.0	91	15	160*	17	150	23	170*	12	81	26	110	11
16(17)-EpDPE	16	1.8	27	3.7	52‡	5.9	61‡	3.2	52†	3.6	23	6.0	21	1.8
13(14)-EpDPE	16	1.8	28	3.9	55†	6.5	65†	3.4	56†	4.0	24	6.4	22	1.8
10(11)-EpDPE	20	2.2	36	4.9	70‡	7.9	82‡	3.9	71†	4.5	30	8.1	27	1.9
11(12)-EpETrE	40	3.8	41	4.8	77†	7.9	80†	5.5	82†	7.1	35	9.4	35	2.2
8(9)-EpETrE	14	1.4	17	2.1	30†	2.7	32†	2.4	34‡	3.1	15	4.0	15	0.82
5(6)-EpETrE	60	5.6	78	11	130†	12	130*	8.4	140†	12	66	17	70	5.6
15(16)-EpODE	16	1.8	28	3.9	55	6.5	65	3.4	56†	4.0	24	6.4	22	1.8
9(10)-Epoxy-stearic acid	29	2.6	46	6.1	81†	7.1	77*	6.5	75*	5.3	40	10	64	8.4
15,16-DiHODE	29	3.2	26	2.4	21	2.1	13	1.8	26	5.3	20	1.9	22	2.3
9,10-DiHODE	1.7	0.25	1.7	0.14	1.3	0.13	1.1	0.18	1.6	0.35	1.3	0.20	2.0	0.15
12,13-DiHODE	2.6	0.25	< 2.0	-	< 2.0	-	< 2.0	-	< 2.0	-	< 2.0	-	< 2.0	-
17,18-DiHETE	2.7*	0.074	3.7	0.20	2.1‡	0.049	2.7	0.28	4.4	0.63	2.6*	0.47	1.8‡	0.15

Tab. 11.8 continued

COXi	-		-		Celecoxib		Apigenin		Genistein		Resveratrol		ε-viniferin	
LPS	-		+		+		+		+		+		+	
Analyte (fmol/mg)	Mean	SE	Mean	SE	Mean	SE	Mean	SE	Mean	SE	Mean	SE	Mean	SE
14,15-DiHETE	0.73	0.027	1.0	0.050	0.34‡	0.026	0.7	0.12	1.1	0.20	0.62	0.13	0.38‡	0.030
12,13-DiHOME	54	6.2	77	8.2	28†	2.2	32*	3.0	78	19	48	12	32†	0.62
9,10-DiHOME	18*	2.5	30	2.9	17*	1.7	15†	1.4	31	6.2	22	3.1	27	1.5
19,20-DiHDPE	55*	2.3	95	6.5	29‡	0.77	59	15	100	21	68	16	31‡	1.7
14,15-DiHETrE	5.3†	0.37	8.0	0.60	3.3‡	0.16	5.9	0.37	8.5	0.90	7.1	1.0	3.4‡	0.11
16,17-DiHDPE	9.9	0.55	14	1.0	2.8‡	0.16	8.2	2.6	15	3.6	8.5	2.4	2.7‡	0.18
11,12-DiHETrE	1.7*	0.061	2.7	0.32	1.7*	0.085	2.1	0.12	2.8	0.31	2.6	0.36	1.8‡	0.07
13,14-DiHDPE	2.6†	0.081	4.9	0.43	1.5‡	0.10	3.0	0.67	5.0	1.0	3.2	0.76	1.4	0.042
10,11-DiHDPE	1.2‡	0.059	2.1	0.20	2.0	0.072	1.9	0.19	2.4	0.25	2.3	0.22	2.3	0.10
8,9-DiHETrE	1.2	0.061	1.6	0.15	1.7	0.12	1.6	0.08	1.9	0.19	1.6	0.20	2.2*	0.14
5,6-DiHETE	< 0.25	-	< 0.25	-	1.0	0.15	< 0.25	-	< 0.25	-	< 0.25	-	< 0.25	-
7,8-DiHDPE	1.1*	0.038	1.6	0.11	1.9	0.10	1.6	0.10	2.0*	0.21	1.7	0.13	1.9	0.099
5,6-DiHETrE	1.0	0.049	1.2	0.077	2.1‡	0.10	1.6*	0.12	1.8†	0.078	1.5	0.058	2.2‡	0.14
4,5-DiHDPE	6.1†	0.66	13	0.86	22‡	1.2	15	1.4	15	1.2	15	0.75	26‡	2.4
9,10-Dihydroxy-stearic acid	59	4.8	81	16	58	2.9	57	2.4	50	1.8	60	4.8	87	17

If analyte concentration is below the limit of quantification (LOQ), it is indicated as <. The given value represents the LOQ.

* p <0.05 Dunnetts test vs. LPS

† p <0.01 Dunnetts test vs. LPS

‡ p <0.001 Dunnetts test vs. LPS

Tab. 11.9: Oxylipin concentrations in liver tissue 24 h after LPS treatment.

COXi	-				Celecoxib				Genistein				Resveratrol				ε-viniferin	
LPS	-		+		+		+		+		+		+		+			
Analyte (fmol/mg)	Mean	SE	Mean	SE	Mean	SE	Mean	SE	Mean	SE	Mean	SE	Mean	SE	Mean	SE	Mean	SE
TXB_2	25	7.4	13	3.1	12	4.1	17	3.1	31	5.7	10	2.0	8.4	1.6				
$PGF_{2\alpha}$	65	21	40	9.8	17	4.9	26	3.8	57	7.4	37	7.7	12	2.0				
PGE_2	14	5.0	15	3.1	11	3.6	15	2.5	21	3.4	24	6.7	4.2	0.89				
6-keto-$PGF_{1\alpha}$	56	11	45	7.1	32	11	32	7.1	74	14	49	9.5	29	5.1				
$PGF_{2\alpha}$	65	21	40	9.8	17	4.9	26	3.8	57	7.4	37	7.7	12	2.0				
PGE_1	2.6	0.87	2.7	0.57	1.9	0.63	2.3	0.50	3.7	0.59	3.0	0.68	0.88	0.19				
PGD_1	1.7	0.38	1.3	0.21	0.87	0.16	1.2	0.23	2.3	0.37	1.3	0.21	0.91	0.077				
PGD_2	31	8.8	25	5.0	14	4.4	34	8.1	42	7.5	35	5.5	13	1.7				
5-iP$F_{2\alpha}$	1.2	0.086	1.3	0.13	1.5	0.13	1.1	0.067	< 1.0	-	< 1.0	-	2.3‡	0.28				
dihomo-$PGF_{2\alpha}$	3.7	1.3	3.6	0.86	1.8	0.68	3.6	0.73	5.3	1.0	4.1	0.97	1.0	0.27				
13,14-dihydro-15-keto-$PGF_{2\alpha}$	7.1	0.62	5.2	0.35	2.6*	0.22	7.0	1.3	8.2*	1.0	6.2	0.79	7.0	0.36				
TxB_3	1.6	0.45	2.3	0.49	0.96	0.24	0.89	0.12	1.2	0.14	0.80	0.11	< 0.05	-				
$PGF_{1\alpha}$	8.8	2.5	5.8	1.1	2.4	0.67	2.8	0.30	6.9	0.71	5.5	0.87	2.5	0.35				
13,14-dihydro-15-keto-PGE_1	0.63	0.050	0.38	0.042	0.31	0.070	0.57	0.23	0.61	0.078	0.53	0.050	0.62	0.13				
8-iP$F_{2\alpha}$	1.6	0.65	0.62	0.22	1.4	0.41	2.1	0.11	3.0*	0.52	2.2	0.71	< 0.10	-				
9-HOTrE	20†	2.5	11	1.3	9.0	0.93	8.1	1.1	9.9	1.3	9.3	1.0	5.0	0.58				
13-HOTrE	110	50	21	4.9	11	1.8	18	4.5	18	5.9	19	5.0	8.5	1.5				
20-HETE	< 2.6	-	5.3	0.67	4.5	0.67	7.2	2.2	6.3	1.7	4.1	0.18	< 2.6	-				
15-HEPE	11	3.3	4.2	0.82	2.2	0.25	3.4	0.86	4.0	1.0	3.2	0.52	1.7	0.27				
8-HEPE	1.2	0.17	0.99	0.048	0.84	0.094	0.98	0.23	1.2	0.089	1.0	0.16	< 0.60	-				
12-HEPE	85	28	40	9.2	19	2.7	27	11	39	6.1	19	4.9	6.8	1.1				
5-HEPE	3.0	0.28	3.0	0.42	4.6	0.72	2.8	0.80	2.7	0.37	2.3	0.18	1.2	0.087				
13-HODE	1400	550	500	72	300	29	370	79	530	98	520	48	230	15				

Tab. 11.9 continued

COXi	-				Celecoxib				Apigenin				Genistein				Resveratrol				ε-viniferin	
LPS	-		+		+				+				+				+				+	
Analyte (fmol/mg)	Mean	SE	Mean	SE	Mean	SE			Mean	SE			Mean	SE			Mean	SE			Mean	SE
9-HODE	600	79	480	58	300	36			370	64			550	85			540	38			250	16
15-HETE	42	9.0	32	3.5	26	2.1			31	6.0			40	5.4			34	4.5			14	0.86
11-HETE	24	5.8	21	3.0	13	2.2			21	4.0			35	5.1			23	3.3			7.0	0.93
8-HETE	13	2.7	8.2	0.79	7.4	0.86			8.5	1.9			10	1.4			8.2	1.6			4.2	0.33
12-HETE	430*	122	140	29	98	15			120	50			150	21			69	17			32	6.0
9-HETE	4.3	0.54	4.5	0.41	6.2	0.71			5.2	1.1			6.2	0.84			6.3	0.91			2.9	0.12
15-HETrE	18	4.1	11	1.1	8.9	0.98			9.0	1.4			14	1.4			11	1.2			5.2	0.37
5-HETE	3.0	0.28	3.0	0.42	4.6†	0.72			2.8	0.80			2.7	0.37			2.3	0.18			1.2	0.087
20-HEPE	18	2.1	25	1.8	5.9‡	0.72			15	2.4			22	5.8			16	3.2			4.1‡	0.51
18-HEPE	3.4	0.50	3.3	0.20	3.1	0.25			3.3	0.73			4.6	0.53			4.1	0.26			1.6	0.17
20-HDHA	13	1.5	18	1.2	20	1.4			22	3.5			27*	2.7			22	1.7			9.1*	0.83
16-HDHA	4.2	0.50	5.0	0.35	5.2	0.70			6.0	1.1			8.1*	0.80			6.3	0.74			2.4	0.25
13-HDHA	7.8	1.2	8.5	0.82	8.3	0.84			10	2.1			16†	2.0			10	1.2			3.8	0.48
17-HDHA	49	14	22	3.4	18	2.4			21	4.9			25	4.4			19	2.7			9.0	0.90
10-HDHA	6.3	1.0	5.1	0.48	5.5	0.59			5.7	1.3			7.6	0.56			4.9	0.58			2.2	0.15
14-HDHA	240*	73	70	14	60	8.0			68	21			97	13			48	9.4			18	2.9
11-HDHA	4.0	0.47	4.4	0.39	7.0	1.1			5.5	0.94			7.0	0.82			5.0	0.46			2.8	0.31
7-HDHA	2.4	0.28	2.8	0.26	5.6‡	0.50			3.2	0.64			4.4	0.64			2.7	0.37			1.7	0.15
8-HDHA	12	1.2	15	1.1	24*	3.3			20	3.6			25*	2.9			18	1.2			9.0	0.93
4-HDHA	7.6	0.92	10	0.83	18†	1.7			12	2.7			14	1.4			13	1.4			6.8	0.65
9,12,13-TriHOME	230	48	190	39	77	16			41	3.0			64	11			300	63			110	26
9,10,13-TriHOME	26	3.3	27	5.5	9.2*	1.1			6.4*	0.76			8.6*	1.1			46	8.0			16	3.5
13-oxo-ODE	13	2.7	17	2.2	12	1.7			16	2.2			20	3.2			23	1.5			9.4	0.86

Tab. 11.9 continued

COXi	-		-		Celecoxib		Apigenin		Genistein		Resveratrol		ε-viniferin	
LPS	-		+		+		+		+		+		+	
Analyte (fmol/mg)	Mean	SE	Mean	SE	Mean	SE	Mean	SE	Mean	SE	Mean	SE	Mean	SE
15-oxo-ETE	3.3	0.65	4.2	0.18	6.8	0.89	4.0	1.4	5.8	0.96	5.5	1.1	2.8	0.23
9-oxo-ODE	82	18	120	15	66	12	120	14	160	26	150	8.5	53	3.9
5-oxo-ETE	13	2.2	11	0.53	35	2.8	15	2.6	19	3.46	17	2.8	14	2.4
EKODE	40	11	45	3.7	70	16	28	9.5	40	6.78	53	6.0	34	4.9
9(10)-EpODE	8.2	1.5	10	1.0	15	1.7	11	2.7	12	1.81	12	1.1	9.2	0.70
17(18)-EpETE	3.6	0.43	3.8	0.37	5.0	0.37	4.2	0.77	4.6	0.44	4.8	0.45	3.2	0.30
12(13)-EpODE	3.9	0.69	4.9	0.46	6.2	0.73	5.0	1.1	5.7	1.01	5.8	0.48	3.9	0.49
14(15)-EpETE	2.2	0.32	2.5	0.18	3.5	0.30	3.1	0.56	3.3	0.3	3.2	0.32	1.8	0.25
11(12)-EpETE	2.3	0.33	2.8	0.23	3.3	0.35	4.4	0.55	5.1†	0.47	4.6*	0.46	2.0	0.20
8(9)-EpETE	1.5	0.23	1.5	0.17	2.5*	0.26	2.1	0.34	2.5	0.21	2.3	0.32	1.5	0.12
19(20)-EpDPE	22	2.4	25	1.8	47‡	5.3	33	3.9	40*	1.9	33	3.8	17	1.8
12(13)-EpOME	68	9.7	82	8.3	120	14	99	12	110	12	110	16	72	3.3
14(15)-EpETrE	26	3.8	26	2.1	51†	6.5	38	4.3	44*	4.4	33	5.3	21	2.0
9(10)-EpOME	82	12	97	9.3	140	16	120	17	130	15	120	12	84	5.7
16(17)-EpDPE	14	1.8	16	1.3	31‡	4.2	23	3.0	27*	1.3	23	2.8	11	1.4
13(14)-EpDPE	14	1.9	16	1.3	32‡	4.0	24	2.9	27*	1.4	23	3.0	12	1.6
10(11)-EpDPE	17	2.3	20	1.7	40‡	5.1	30	3.8	33*	1.8	28	3.4	15	1.9
11(12)-EpETrE	34	4.6	32	2.4	58†	6.3	47	7.0	51	5.3	39	6.3	27	2.9
8(9)-EpETrE	13	2.0	13	1.0	25†	2.8	20	2.8	20	2.3	14	1.8	9.8	0.91
5(6)-EpETrE	59	9.0	59	3.2	120†	13	97	16	90	12	64	7.8	45	4.3
15(16)-EpODE	14	1.9	16	1.3	32	4.0	24	2.9	27	1.4	23	3.0	12	1.6
9(10)-Epoxy-stearic acid	61	4.6	61	3.4	75	10	86	9.4	82	6.1	84	11	66	8.6
15,16-DiHODE	150	18	120	23	47*	7.1	49	7.6	63	13	49	6.9	17†	1.7

Tab. 11.9 continued

COXi	-		-		Celecoxib		Apigenin		Genistein		Resveratrol		ε-viniferin	
LPS	-		+		+		+		+		+		+	
Analyte (fmol/mg)	Mean	SE	Mean	SE	Mean	SE	Mean	SE	Mean	SE	Mean	SE	Mean	SE
8,15-DiHETE	3.8	1.9	< 0.80	-	< 0.80	-	< 0.80	-	0.88	0.067	< 0.80	-	< 0.80	-
9,10-DiHODE	13	1.6	10	1.8	4.4	0.58	8.6	2.3	7.6	1.3	6.1	1.4	3.9	0.55
12,13-DiHODE	20	3.2	13	3.5	3.2	0.56	5.7	1.4	5.7	1.3	6.1	1.5	< 2.0	-
17,18-DiHETE	22	2.2	23	1.5	9.4†	0.81	15	2.3	19	4.0	18	3.3	5.6‡	0.54
14,15-DiHETE	12	1.1	10	0.51	2.6‡	0.18	7.4	1.2	8.6	2.1	8.1	2.0	2.1‡	0.21
11,12-DiHETE	3.6	0.34	3.0	0.19	1.2*	0.078	2.9	0.67	2.9	0.62	2.9	0.75	1.0*	0.11
12,13-DiHOME	370	32	340	31	70‡	8.3	140†	17	210	60	200	53	45‡	2.6
8,9-DiHETE	2.8	0.33	2.4	0.15	1.4	0.13	2.3	0.70	2.6	0.52	2.4	0.48	1.2	0.13
9,10-DiHOME	93	6.9	95	7.6	40†	2.8	69	16	82	16	79	17	43*	4.6
19,20-DiHDPE	150	22	200	15	55†	5.9	110	18	170	49	140	35	17‡	3.6
14,15-DiHETrE	71	9.9	67	4.5	23†	1.4	43	6.9	62	14	47	11	12‡	1.1
16,17-DiHDPE	32	3.5	38	2.4	8.0‡	0.55	22	4.1	35	9.9	27	6.4	3.0‡	0.36
11,12-DiHETrE	26	3.8	24	1.8	11*	0.53	18	3.5	22	4.3	17	4.0	5.5†	0.68
13,14-DiHDPE	11	1.4	15	1.1	4.4†	0.28	11	2.0	15	3.8	11	2.2	1.6‡	0.20
10,11-DiHDPE	8.2	1.2	10	0.87	4.8*	0.37	9.8	2.1	11	2.3	7.8	1.4	2.2†	0.27
8,9-DiHETrE	12	1.8	11	0.96	7.9	0.51	10	2.8	12	2.3	8.7	1.8	4.4	0.56
5,6-DiHETE	< 0.30	-	< 0.30	-	0.99	0.21	< 0.30	-	< 0.30	-	< 0.30	-	< 0.30	-
7,8-DiHDPE	4.8	0.62	5.2	0.47	3.8	0.33	5.2	1.2	6.3	1.0	4.5	0.73	1.9	0.23
5,6-DiHETrE	4.2	0.72	3.9	0.32	4.9	0.42	5.1	1.5	6.3	1.1	4.0	0.73	1.9	0.16
4,5-DiHDPE	44	12	57	6.8	76	7.9	74	18	64	11	70	5.8	20	4.6
9,10-Dihydroxy-stearic acid	140	19	160	36	65	2.8	53	2.2	64	3.7	260	28	170	21

If analyte concentration is below the limit of quantification (LOQ), it is indicated as <. The given value represents the LOQ.
* p <0.05 Dunnetts test vs. LPS; † p <0.01 Dunnetts test vs. LPS; ‡ p <0.001 Dunnetts test vs. LPS

Abbreviations

AA	arachidonic acid
ACN	acetonitrile
AKI	acute kidney injury
ALT	alanine transaminase
AMPP	N-(4-aminomethylphenyl) pyridinium
AST	aspartate transaminase
BCA	bicinchoninic acid
BHT	butylated hydroxytoluene
BSA	bovine serum albumin
CAD	collisionally activated dissociation
CE	collision energy
CLP	cecal puncture ligation
COX	cyclooxygenase
Ctrl.	control
CXP	collision exit potential
CYP	cytochrome P450 monooxygenase
DAI	disease activity index
DHA	docosahexaenoic acid
DiHDPE	dihydroxy docosopentaenoic acid
DiHETE	dihydroxy eicosatetraenoic acid
DiHETrE	dihydroxy eicosatrienoic acid
DiHODE	dihydroxy octadecadienoic acid
DiHOME	dihydroxy octadecenoic acid
DMEM	Dulbecco’s Modified Eagle Medium

DMSO	dimethyl sulfoxide
DP	declustering potential
DSS	dextran sulfate sodium
Dyn. range	dynamic range
EDTA	ethylenediaminetetraacetic acid
EET	epoxy-AA
EIA	enzyme immune assay
EKODE	epoxy-keto-octadecenoic acid
EP	entrance potential
EPA	eicosapentaenoic acid
EpDPE	epoxy docosapentaenoic acid
EpETE	epoxy eicosatetraenoic acid
EpETrE	epoxy eicosatrienoic acid
EpODE	epoxy octadecadienoic acid
EpOME	epoxy octadecenoic acid
ESI	electrospray ionization
FA	fatty acid
FBS	fetal bovine serum
FCS	fetal calf serum
FWHM	full width at half maximum
GUS	glucuronidase
HAc	acetic acid
HDHA	hydroxy docosahexaenoic acid
HEPE	hydroxy eicosapentaenoic acid
HEPES	4-(2-hydroxyethyl)-1-piperazineethanesulfonic acid
HETE	hydroxy eicosatetraenoic acid
HETrE	hydroxyl eicosatrienoic acid
HLM	human liver microsomes
HODE	hydroxy octadecadienoic acid
HOTrE	hydroxy octadecatrienoic acid

HpETE	hydroperoxyeicosatetraenoic acid; hydroperoxy-AA
HRMS	high resolution MS
IL	interleukin
iP	isoprostane
IS	internal standard
LC	liquid chromatography
LDH	lactate dehydrogenase
LLE	liquid liquid extraction
LLOQ	lower limit of quantification
LOD	limit of detection
LOQ	limit of quantification
LOX	lipoxygenase
LPS	lipopolysaccharide
LT	leukotriene
LY	lucifer yellow
m/z	mass to charge ratio
MeOH	methanol
mPGES	mircosomal prostaglandin E synthase
MRM	multiple reaction monitoring
MS	mass spectrometry
n.d.	not detected
NSAID	non-steroidal anti-inflammatory drug
PAGE	polyacrylamide gel electrophoresis
P_{app}	apparent permeability coefficient
PBS	phosphate buffered saline
PFB	pentafluorobenzyl
PG	prostaglandin
PUFA	polyunsaturated fatty acid
RIPA	radioimmunoprecipitation assay buffer
RLM	rat liver microsomes

RPMI	Roswell Park Memorial Institute medium
SD	standard deviation
SDS	sodium dodecyl sulfate
SE	standard error mean
sEH	soluble epoxide hydrolase
SOP	standard operating procedure
SPE	solid phase extraction
SRM	selected reaction monitoring
TBST	tris buffered saline tween
TEER	trans-epithelial electrical resistance
TNF	tumor nekrose factor
TRIS	tris(hydroxymethyl)aminomethane
Tx	thromboxane
TxAS	thromboxane A synthase
UC	ulcerative colitis
UDP	uridine 5’-diphosphate
UDPGA	uridine 5’-diphosphoglucuronic acid
UGT	UDP-glucuronosyltransferase
ULOQ	Upper limit of quantification
UV	ultraviolet absorbance detection

Acknowledgement

This work was carried out from January 2012 to May 2015 at the Institute for Food Toxicology and Chemical Analysis (University of Veterinary Medicine Hannover) in the research group of Dr. Nils Helge Schebb.

First of all, I would like to thank my supervisor Dr. Nils Helge Schebb for the opportunity to work with him on this interesting topic which allowed me to combine the field of analytics with biological questions. Furthermore, I thank him for supporting and encouraging me the whole time and for the opportunity to present my results at so many national and international conferences.

I would like to thank Prof. Dr. Pablo Steinberg for the opportunity to use the lab and equipment of his group which allowed me to carry out all of the cell culture work. Moreover, his support and scientific advices throughout my whole time at the Institute were very helpful.

I would like to thank the Fonds der Chemischen Industrie (Frankfurt/Main) for the financial support in form of a Kekulé Ph.D. fellowship.

As the list of the different coauthors demonstrates, this thesis is based on the collaboration with other researchers. I would like to grateful acknowledge everyone who contributed to the research of this thesis.

I thank Prof. Dr. Faikah Güler for the successful cooperation in the sepsis experiments. Our collaboration allowed me to use murine sepsis model experiments and she taught me how to interpret the clinical aspects of the *in vivo* experiments. Moreover, I would like to thank Faikah´s team, especially Nelli Shushakova, Song Rong, Mi-Sun Jang, Martina Ackermann and Herle Chlebusch for the friendly and uncomplicated cooperation.

Furthermore, I would like to thank Maria Michael and Anna K. Meschede who worked with me as part of their master thesis´. I thank Jasmin Wonik, she contributed to some experiments of this thesis as a research student.

I thank Anne von Keutz for her help with the DSS experiment. Without your practical skills and help we would have not been able to carry out this experiment.

Moreover, I thank Maren von Köckritz-Blickwede and her colleagues for teaching us how to isolate monocytes.

I thank all members of the Institute for the pleasant working atmosphere and for helping me with all small and bigger problems occurring during three years of Ph.D. studies.

A special thank goes to Annika Ostermann. She was a wonderful colleague and friend right from the day on she joined the group. Thank you for all of your help - either scientifically or as a friend.

Furthermore, I thank Michael Empl, for introducing me to work with cells, for the endless discussions (about science and beyond…) and last but not least for the supply with ice cream. You took care of all the social events within the group and you often brought good mood to our lunch or coffee breaks.

Mein letzter, aber zugleich wichtigster Dank, richtet sich an meine Familie und Freunde. Euch allen danke ich für die wundervolle Zeit abseits des Arbeitsalltages. Insbesondere danke ich meinen Eltern, Conni sowie meiner Schwester für die bedingungslose Unterstützung und unerschöpfliche Geduld während der letzten Jahre. DANKE.

Curriculum Vitae

Der Lebenslauf ist in der Online-Version aus Gründen des Datenschutzes nicht enthalten.

Der Lebenslauf ist in der Online-Version aus Gründen des Datenschutzes nicht enthalten.

List of Publications

PUBLICATIONS IN PEER-REVIEWED JOURNALS

WITHIN THE SCOPE OF THIS THESIS

I. Willenberg, A.K. Meschede, F. Güler, M.S. Jang, N. Shushakova and N. H. Schebb (**2015**) Food polyphenols fail to cause a biological relevant reduction of COX-2 activity. *In preparation*

I. Willenberg, S. Rong, N. Shushakova, F. Güler and N.H. Schebb (**2015**) Characterization of changes in plasma and tissue oxylipin levels in LPS and CLP induced murine sepsis. *Submitted for publication*

I. Willenberg, A.I. Ostermann, A. v. Keutz, P. Steinberg and N.H. Schebb (**2015**) Effect of acute and chronic DSS induced colitis on plasma eicosanoid and oxylipin levels in the rat. Prostag Oth Lipid M *10.1016/j.prostaglandins.2015.04.002*

I. Willenberg, A.K. Meschede and N.H. Schebb (**2015**) Determining COX-2 activity in three different test systems utilizing online-solid phase extraction-liquid chromatography-mass spectrometry for parallel quantification of prostaglandin E2, D2 and thromboxane B2. J Chromatogr A, 1391, 40-48

I. Willenberg, A.I. Ostermann and N.H. Schebb (**2015**) Targeted metabolomics of the arachidonic acid cascade - Current state and challenges of LC-MS analysis of oxylipins. Anal Bioanal Chem, 407, 2675–2683.

I. Willenberg, M. Michael, J. Wonik, L.C. Bartel, M.T. Empl and N.H.Schebb (**2015**) Investigation of the absorption of resveratrol oligomers in the Caco-2 cellular model of intestinal absorption. Food Chem. 167, 245–250.

I. Willenberg, W. Brauer, M.T. Empl and N.H. Schebb (**2012**) Development of a rapid LC-UV Method for the Investigation of chemical and metabolic Stability of Resveratrol Oligomers. J Agric Food Chem. 60 (32), 7844–7850.

FURTHER PUBLICATIONS

I. Willenberg, M. Michael, J. Wonik and N.H.Schebb (**2015**) Investigation of the effects of soluble fibers on the absorption of resveratrol and of 2-amino-1-methyl-6-phenylimidazo[4,5-b]pyridine (PHIP) in the Caco-2 cellular model of intestinal absorption. *Submitted for publication.*

A. I. Ostermann, J. Herbers, I.Willenberg, R. Chen, S. H. Hwang,R. Greite, C. Morisseau, F. Gueler, B. D. Hammock and N. H. Schebb (**2015**) Oral treatment of rodents with soluble epoxide hydrolase inhibitor 1-trifluoromethoxyphenyl-3-(1-propionylpiperidin-4-yl) urea (TPPU): bioavailability, resulting drug levels and modulation of oxylipin pattern. *Submitted for publication.*

P. Nicken, A. v. Keutz, I. Willenberg, A. Ostermann, N.H. Schebb, O. Kershawb, S. Giovanninib, G. Breves and P. Steinberg (**2015**) Dextran sodium sulphate-induced colitis does not impact the intestinal transport of PhIP in the Fischer 344 rat. *Submitted for publication.*

P. Nicken, I. Willenberg, A. v. Keutz, L. v. Elsner, G. Hamscher, L. Vanhaecke, B. Schröder, G. Breves, N.H. Schebb and P. Steinberg (**2015**) Intestinal absorption and cell transforming potential of PhIP-M1, a bacterial metabolite of the heterocyclic aromatic amine 2-amino-1-methyl-6-phenylimidazo[4,5-b]pyridine (PhIP). Toxicology Letters, 234, 92-98.

I. Willenberg, L. v. Elsner, P. Steinberg and N.H. Schebb (**2015**) Development of an online-SPE-LC-MS method for the investigation of the intestinal absorption of 2-amino-1-methyl-6-phenylimidazo[4,5-b]pyridine (PHIP) and its bacterial metabolite PHIP-M1 in a Caco-2 Transwell system. Food Chem. 166, 537–543.

A.I. Ostermann, I. Willenberg and N.H. Schebb (**2015**) Comparison of sample preparation methods for the quantitative analysis of eicosanoids and other oxylipins in plasma by means of LC-MS/MS. Anal Bioanal Chem, 407(5),1403-1414.

A.I. Ostermann, I. Willenberg, K.W. Weylandt and N.H. Schebb (**2015**) Development of an online-SPE-LC-MS/MS method for 26 hydroxylated polyunsaturated fatty acids as rapid targeted metabolomics approach for the LOX, CYP and autoxidation pathways of the arachidonic acid cascade. Chromatographia, 78(5), 415-428.

M.T. Empl, P. Kammeyer, R. Ulrich, J.F. Joseph, M.K. Parr, I. Willenberg, N.H. Schebb, W. Baumgärtner, E. Röhrdanz, C. Steffen and P. Steinberg (**2014**) The influence of L-carnitine on the formation of preneoplastic and atherosclerotic lesions in the colon and aorta of male F-344 rats. Arch Toxicol. DOI 10.1007/s00204-014-1341-4.

A.I. Ostermann, M. Müller, I. Willenberg and N.H. Schebb (**2014**) Determining the fatty acid composition in plasma and tissues as fatty acid methyl esters by gas chromatography – A comparison of different derivatization and extraction procedures. Prostag Leukotr Ess. 91, 235-241.

J.P. Schuchardt, I. Schneider, I. Willenberg, J. Yang, B.D. Hammock, A. Hahn and N.H. Schebb (**2014**) Increase of EPA-derived hydroxy, epoxy and dihydroxy fatty acid levels in human plasma after a single dose of long-chain omega-3 PUFAs. Prostag Oth Lipid M. 109-111, 23–31.

J.P. Schuchardt, S. Schmidt, G. Kressel, H. Dong, I. Willenberg, B.D. Hammock, A. Hahn and N.H. Schebb (**2014**) Modulation of blood oxylipin levels by long-chain omega-3 fatty acid supplementation in hyper- and normolipidemic men. Prostag Leukotr Ess. 90, 27-37.

S. Stolte, S. Steudte, I. Willenberg, N.H. Schebb and P. Stepnowski (**2013**) Ecotoxicity of artificial sweeteners and stevioside. Environ Int. 60, 123-127.

J.P. Schuchardt, S. Schmidt, G. Kressel, H. Dong, I. Willenberg, B.D. Hammock, A. Hahn and N.H. Schebb (**2013**) Comparison of free serum oxylipin concentrations in hyper- vs. normolipidemic men. Prostag Leukotr Ess. 89, 19-29.

T. Heinrich, I. Willenberg and M.A. Glomb, (**2012**) Chemistry of color formation during rooibos fermentation. J Agric Food Chem 60(20):5221-5228.

ORAL PRESENTATIONS

I. Willenberg, L. v. Elsner, P. Steinberg and N.H. Schebb (**2014**) Entwicklung einer online-SPE-LC-ESI-MS Methode zur Charakterisierung der intestinalen Aufnahme des heterocyclischen Amins PHIP und dessen bakteriellen Metaboliten (PHIP-M1) 24th Doktorandenseminar des Arbeitskreises Separation Sciene der Fachgruppe Analytische Chemie der GDCh, Hohenroda, Germany

I. Willenberg, A.K. Meschede and N.H. Schebb (**2014**) Untersuchungen zum Einfluss von Lebensmittelinhaltsstoffen auf die Cyclooxygenase-2 Aktivität. Regionaltagung-Nord Lebensmittelchemische Gesellschaft in Hamburg, Germany

POSTER PRESENTATIONS

A. I. Ostermann, I. Willenberg and N. H. Schebb (**2015)** Comparison of Solid Phase Extraction Protocols for LC-MS based Analysis of Oxylipins. Anakon in Graz, Austria.

M. Krohn, I. Willenberg, M. T. Empl, S. Hellhake, S. Meckelmann und N.H. Schebb (**2015**) Analysis of stability, intestinal absorption food polyphenols by means of LC-UV. Anakon in Graz, Austria.

M. Krohn, I. Willenberg, M. T. Empl, S. Hellhake, S. Meckelmann und N.H. Schebb (**2015**) Bestimmung der chemischen und metabolischen Stabilität von Polyphenolen. Regionaltagung-West Lebensmittelchemische Gesellschaft in Düsseldorf, Germany

I. Willenberg, A. Meschede, A. Ostermann, N.H. Schebb (**2014**) Investigation of COX-2 inhibition *in vitro* – A comparison of different test systems. 5th European Workshop on Lipid Mediators in Istanbul, Turkey.

A. I. Ostermann, I. Willenberg and N. H. Schebb (**2014**) Comparison of Solid Phase Extraction Protocols for LC-MS based Analysis of Oxylipins. 5th European Workshop on Lipid Mediators in Istanbul, Turkey.

A.I. Ostermann, M. Müller, I. Willenberg, N.H. Schebb (**2014**) Quantifizierung von Fettsäuren in Plasma und Gewebe. Deutscher Lebensmittelchemikertag in Gießen, Germany.

I. Willenberg, A. Meschede, A. Ostermann, N.H. Schebb (**2014**) Untersuchung zum Einfluss von Lebensmittelinhaltsstoffen auf die COX-2 Aktivität. Deutscher Lebensmittelchemikertag in Gießen, Germany.

P. Waindok, A.I. Ostermann, I. Willenberg, U. Kassner, E. Steinhagen-Thiessen, K.H. Weylandt and N.H. Schebb (**2014**) Effect of statin treatment on the plasma oxylipin pattern and its modulation by fish oil supplementation. Deutscher Lebensmittelchemikertag in Gießen, Germany.

J.P. Schuchardt, I. Willenberg, A. Hahn, N.H. Schebb (**2014**) Wirkung von Nahrungsergänzung mit omega-3 Fettsäuren auf die Verteilung von Eicosanoiden und anderen Oxylipinen im Blut. Deutscher Lebensmittelchemikertag in Gießen, Germany.

A.I. Ostermann, M. Müller, I. Willenberg, N.H. Schebb (**2014**) Targeting the precursors of eicosanoids and other oxlipins – Quantitative analysis of polyunsaturated fatty acids by means of GC-FID. International School of Pharmacology in Erice, Italy.

A.I. Ostermann, I. Willenberg, N.H. Schebb (**2014**) Comparison of Solid Phase Extraction Protocols for LC-MS based Analysis of Oxylipins. International School of Pharmacology in Erice, Italy.

J.P. Schuchardt, I. Willenberg, B.D. Hammock, A. Hahn and N.H. Schebb (**2014**) A single dose of long-chain n-3 PUFAs induces significant changes in oxylipin patterns of human plasma. ISSFAL Congressin Stockholm, Sweden.

I. Willenberg, A. Meschede and N.H. Schebb (**2014**) Modulation of COX-2-activity by food polyphenols. ISSFAL Congress in Stockholm, Sweden.

J.P. Schuchardt, I. Willenberg, S. Schmidt, A. Hahn and N.H. Schebb (**2014**) Modulation des Oxylipinmusters im Blut durch Fischölsupplementation. Regionaltagung-Nord Lebensmittelchemische Gesellschaft in Hamburg, Germany.

I. Willenberg, L. von Elsner, P. Steinberg and N.H. Schebb (**2014**) Characterization of the intestinal absorption of the heterocyclic amine PHIP and its bacterial metabolite PHIP-M1 in the Caco-2-Transwell-system. DGPT-Jahrestagung 2014 in Hannover, Germany.

A. Ostermann, I. Willenberg and N.H. Schebb (**2014**) Investigation of N-Glucuronidation of the Carbanilide Triclocarban. DGPT-Jahrestagung 2014 in Hannover, Germany.

I. Willenberg, A. Meschede and N.H. Schebb (**2014**) A comprehensive analysis of the effects of naturally occuring resveratrol oligomers on COX-2 activity. 15th Winter Eicosanoid Conference (WEC) in Baltimore, MD, USA.

I. Willenberg, L. von Elsner, A. Ostermann, A. von Keutz, P. Steinberg and N.H. Schebb (**2013**) Charakterisierung der intestinalen Aufnahme von 2-amino-1-methyl-6-phenylimidazo-[4,5-b]pyridine (PHIP) und dessen bakteriellem Metaboliten (PHIP-M1) im Caco-2-Transwell-System. Deutscher Lebensmittelchemikertag 2013 in Braunschweig, Germany.

A. Ostermann, I. Willenberg, N.H. Schebb (**2013**) Untersuchung zur N-Glucuronidierung von Triclocarban in Zellkultur. Deutscher Lebensmittelchemikertag 2013 in Braunschweig, Germany.

I. Willenberg, M. Michael, J. Wonik, M.T. Empl and N.H. Schebb (**2013**) Untersuchung der intestinalen Aufnahme von Resveratrol und seinen Oligomeren sowie ihrer chemischen und metabolischen Stabilität mittels neuer LC-UV Methoden. Anakon in Essen, Germany.

I. Willenberg, M. Empl and N.H. Schebb (**2012**) Hopeaphenol shows a unique chemical and metabolic stability among resveratrol and its oligomers. Deutscher Lebensmittelchemikertag 2012 in Münster, Germany.

M. Michael, I. Willenberg and N.H. Schebb (**2012**) Development of an online solid phase extraction (SPE) liquid chromatography method for the analysis of resveratrol, ε-Viniferin and hopeaphenol in complex biological samples. Deutscher Lebensmittelchemikertag 2012 in Münster, Germany.

.